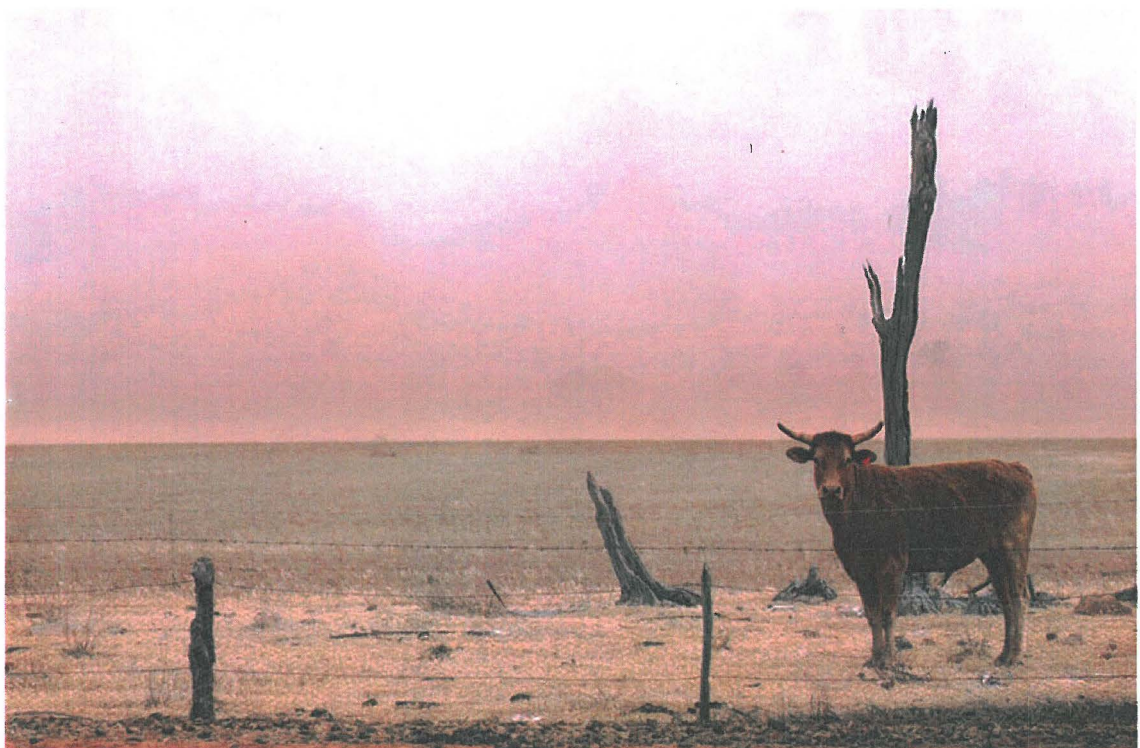


Dust and Terrestrial Salt (NaCl) in SE Australia: Implications for Aeolian Co-Transportation and Co- Deposition

by

Yuki Shiga



Submitted in partial fulfilment of the requirements for the degree of

Master of Geographical Sciences

of the Australian National University

February 2009



THE AUSTRALIAN NATIONAL UNIVERSITY

Acknowledgements

This project was made possible through funds from the Australian Institute of Nuclear Science and Engineering and Dr. Frank Valzano, and wide range of supporters. This part of the research could not have been completed without their devoted support and encouragement.

I would like to express my deepest gratitude to my two supervisors: Dr. Richard Greene, at the Fenner School of Environment and Society, ANU and Mr. Keith Scott, at the Research School of Earth Sciences, ANU. Thank you for your friendly, but strict supervision and support. Nothing would have been possible without your effort and dedication.

Dr. Richard Cresswell and Mr. John Dighton (CSIRO Land and Water), thank you for sharing and sending the samples, they are really a fundamental part of this research.

Dr. David Cohen, Mr. Eduard Stelcer and Mr. Michael Prior (ANSTO), thank you for all things ion beam analysis and your devoted technical support. Your hospitality was warm, and your response was always quick and accurate.

Dr. Frank Brink (ANU Electron Microscopy Unit), thank you for your considerable patience and support in SEM. Everything morphologic I owe to you.

I would also like to thank Dr. Brian Murphy and Ms. Madeleine Rankin, at the NSW Department of Environment and Climate Change, for sharing their thoughtful ideas and invaluable samples. Your samples are important components of this research.

I am also indebt to Dr. Emlyn Williams, at the Statistical Consulting Unit, ANU, for his valuable statistical advice and guidance.

Dr. Sue Holzknecht (the Fenner School of Environment and Society, ANU), I am grateful for all your time and efforts in reviewing this paper. I am grateful for your support and encouragement throughout this research.

In addition, I would like to gratefully acknowledge the NOAA Air Resources Laboratory for the provision of the HYSPLIT transport and dispersion model and/or READY website (<http://www.arl.noaa.gov/ready.html>) used in this publication.

Finally, to all of the staff of the Fenner School of Environment and Society and my friends in room F1.08B, thank you.

Abstract

Aeolian dust exerts major effects across the Australian continent in terms of soil-landscape processes and impacts on human society. It not only has serious health implications, but is also thought to be an insidious carrier of terrestrial salts, which when deposited cause salinisation and/or sodification of the soil. However, this argument is still controversial and especially lacks information regarding co-transportation and co-deposition of terrestrial soil and terrestrial salt (NaCl) from their presumed source — enclosed inland drainage systems in South Australia. Therefore, the purpose of this research is to overcome this lack of information, with a special focus on the potential role of aeolian dust to co-transport and co-deposit with terrestrial salt.

One hundred and fifteen dust samples, each representing one month's deposition, were acquired from samplers located in 16 different sites across Australia, mainly covering the south-eastern region. These samples were subjected to several analyses to reveal their properties. The analyses included ion beam analysis (IBA) to determine their chemical characteristics. Subsequently, sets of equations were applied to the IBA analyses to reveal the contributions from soil, salt (both terrestrial and oceanic) and smoke to the dust samples. Principal Component Analysis (PCA) was also applied to the IBA results to detect the important components of the dust samples. Scanning electron microscope (SEM) and back trajectory analyses, plus rainfall records, were then applied to selected samples to determine differences in their morphology and aeolian dust dispersion routes, respectively.

Careful study of the results has revealed the following findings:

- (i) Despite limitations due to errors arising in some of the calculations, the use of a combination of equations to determine the contribution of terrestrial NaCl to aeolian dust (i.e., terrestrial salt ratio), was able to discriminate between samples with extreme or no terrestrial salt influence;
- (ii) The use of principal component analysis (PCA) gave similar results to terrestrial salt ratios and validated the use of these ratios;
- (iii) Back trajectory plots, along with rainfall records (at the site and along the trajectory), appeared overall to be consistent with high and zero values of the terrestrial salt ratios calculated from IBA results;
- (iv) The SEM images appeared to indicate that dust samples which had high terrestrial salt ratios have smaller particle size. Two samples out of five which had a high terrestrial salt ratio had a conspicuously smaller particle size. This implied that these samples were influenced to a greater extent by the distant source(s) compared to other samples. However, overall, morphological traits were unclear;
- (v) The above features suggest that there is evidence for the existence of terrestrial salt dispersion associated with aeolian dust from the presumed source — the inland salt lake regions of South Australia; and
- (vi) An influence of terrestrial salt appeared to be dependent on only one or two events, of no more than six hours duration within a monthly collection period.

Table of Contents

Candidate's Declaration.....	ii
Acknowledgements.....	iii
Abstract.....	iv
Table of Contents	v
List of Figures.....	vii
List of Tables	viii
List of Equations	viii
List of Acronyms and Abbreviations	ix
List of Chemical Symbols.....	x
1. Introduction.....	1
1.1. Aeolian Dust in Australia	1
1.2. Position of the Research	1
1.3. Project Timeline.....	2
1.4. Research Question.....	3
1.6. Objectives	3
1.7. Thesis Structure	4
1.8. Summary	4
2. Literature Review	6
2.1. Introduction — What is Aeolian Dust?	6
2.2. Characteristics of Australian Dust.....	6
2.3. Causes of Aeolian Dust	9
2.3.1. Surface Soil Conditions.....	9
2.3.2. Geographical and Meteorological Conditions.....	11
2.4. Deposition of Aeolian Dust.....	16
2.5. Impacts and Consequences of Aeolian Dust.....	17
2.5.1. Soil Erosion and Development.....	18
2.5.2. Damage to Health.....	20
2.5.3. Salinisation and Sodification	22
2.5.4. Climate Change.....	25
2.6. Summary	27
3. Methods	28
3.1. Introduction.....	28
3.2. Sample Collection	28
3.3. Summary of Evaluated Samples used in this Research.....	31
3.4. Procedures.....	34
3.5. Analysis.....	35
3.5.1. Ion Beam Analysis	35
3.5.1.1. Calculation of Sea-Salt, Non-Sea-Salt and Terrestrial Salt Fractions	37
3.5.1.2. Soil, Salt and Smoke Contribution.....	38
3.5.1.2.1. Soil Contribution	38
3.5.1.2.2. Salt Contribution	39
3.5.1.2.3. Smoke Contribution.....	39
3.5.1.3. Total Weight.....	39
3.5.2. Principal Component Analysis	40
3.5.3. Back Trajectory Analysis	40
3.5.4. Scanning Electron Microscopy Analysis	42
3.6. Summary	42
4. Results.....	43
4.1. Introduction.....	43
4.2. Ion Beam Analysis.....	43

4.2.1. CSIRO Samples — Soluble and Insoluble Materials.....	43
4.2.2. CSIRO Samples — Insoluble Materials	44
4.2.3. Cowra Samples — Pellets.....	45
4.2.4. Cowra Samples — Filters.....	46
4.3. Principal Component Analysis.....	47
4.4. Back Trajectory Analysis.....	50
4.4.1. CSIRO Samples.....	52
4.4.2. Cowra Samples	57
4.5. Scanning Electron Microscopy Analysis	61
4.5.1. CSIRO Samples — Soluble and Insoluble Materials.....	61
4.5.2. Cowra Samples	64
5. Discussion.....	67
5.1. Introduction.....	67
5.2. Chemical Features of Dust	67
5.2.1. Ion Beam Analysis	67
5.2.2. Principal Component Analysis	68
5.3. Physical Features of Dust.....	69
5.4. Verification of Dust Source	70
6. Conclusions and Directions for Future Work.....	74
6.1. Conclusions	74
6.1.1. Answer to the Research Question.....	75
6.2. Directions for Future Work	76
References	77
Appendix A-1: IBA Results 1	89
Appendix A-2: IBA Results 2	104
Appendix A-3: IBA Results 3	110
Appendix A-4: IBA Results 4	112
Appendix B: Back Trajectories	113
Appendix C: SEM Images	173

List of Figures

Figure 1-1: The protocol of this research.....	2
Figure 1-2: Project timeline	3
Figure 2-1: Dust storm in eastern Australia (October 23, 2002).....	7
Figure 2-2: Spatial distribution of dust activity in Australia (1960 - 1999) using the Dust Storm Index.....	11
Figure 2-3: Synoptic chart for 1800 UTC 22 OCT 2002	14
Figure 2-4: Synoptic chart for 1200 UTC 22 OCT 2002	14
Figure 2-5: Australian dust transportation route	15
Figure 2-6: Schematic diagram of Australian dust transportation	24
Figure 2-7: Satellite image of dust blown from Lake Eyre.....	25
Figure 3-1: The location of 16 sampling sites associated with this research consisting of the CLW project and CRS project.....	28
Figure 3-2: CLW sampling device and an example of placement at a CSIRO sampling site.....	29
Figure 3-3: An example of CSIRO sample.....	30
Figure 3-4: CRS sampling device, and an example of a dried sample sent from CRS in a plastic container	31
Figure 4-1: A trajectory with rainfall (mm hour ⁻¹) record of Wagga Wagga December 21 st at 20hrs	54
Figure 4-2: A trajectory with rainfall (mm hour ⁻¹) record of Melbourne November 3 rd at 16hrs	55
Figure 4-3: A trajectory with rainfall (mm hour ⁻¹) record of Melbourne November 3 rd at 18hrs	55
Figure 4-4: A trajectory with rainfall (mm hour ⁻¹) record of Adelaide February 19 th at 10hrs...	56
Figure 4-5: A trajectory with rainfall (mm hour ⁻¹) record of Adelaide February 19 th at 12hrs...	56
Figure 4-6: A trajectory with rainfall (mm hour ⁻¹) record of Adelaide February 19 th at 14hrs...	57
Figure 4-7: A trajectory with rainfall (mm hour ⁻¹) record of Cowra March 24 th at 16hrs	59
Figure 4-8: Trajectories with rainfall (mm hour ⁻¹) record of Cowra May 29 th at 16, 18 and 20hrs	59
Figure 4-9: A trajectory with rainfall (mm hour ⁻¹) record of Cowra June 5 th at 00hrs.....	60
Figure 4-10: A trajectory with rainfall (mm hour ⁻¹) record of Cowra June 5 th at 02hrs.....	60
Figure 4-11: A trajectory with rainfall (mm hour ⁻¹) record of Cowra June 5 th at 04hrs.....	61
Figure 4-12: SEM image of Wagga Wagga December 2007 sample	62
Figure 4-13: SEM image of Melbourne April 2008 sample	63
Figure 4-14: SEM image of Adelaide February 2008 sample	63
Figure 4-15: SEM image of Melbourne November 2007 sample	64
Figure 4-16: SEM image of Cowra March 2007 sample	65
Figure 4-17: SEM image of Cowra June 2007 sample	65

List of Tables

Table 2-1: Impacts and Consequences of dust events.....	18
Table 3-2: The analysis procedures for CSIRO samples	35
Table 3-3: The analysis procedures for Cowra samples	35
Table 3-4: Major soil elements and their assumed oxide forms	40
Table 4-1: Various calculated values using the IBA results for CSIRO samples for which both soluble and insoluble materials had been analysed	44
Table 4-2: Values calculated using IBA results for Cowra samples in pellets	46
Table 4-3: Components and factor loading values.....	48
Table 4-4: Component scores of CSIRO samples for which both soluble and insoluble materials had been analysed.....	49
Table 4-5: A list of CSIRO samples with back trajectory analysis and SEM applied.....	51
Table 4-6: A list of Cowra samples with back trajectory analysis and SEM applied	51
Table 4-7: The dates for which back trajectory analysis was applied to the CSIRO samples	53
Table 4-8: The dates for which back trajectory analysis was applied to the Cowra samples	58
Table 5-1: Summary of the interpretations of the back trajectory analysis with rainfall records	70

List of Equations

Equation 3-1: Equation for ssNa.....	37
Equation 3-2: Equation for nssCa	37
Equation 3-3: Equation for ssCa and Na.....	37
Equation 3-4: Equation for tsNa	38
Equation 3-5: Equation for minNa.....	38
Equation 3-6: Soil contribution to aeolian dust	38
Equation 3-7: Sea-salt contribution to aeolian dust	39
Equation 3-8: Terrestrial salt contribution to aeolian dust.....	39
Equation 3-9: Smoke contribution to aeolian dust.....	39
Equation 3-10: Equation for total weight.....	40

1. Introduction

1.1. Aeolian Dust in Australia

Aeolian dust plays a critical role within Australia, in terms of soil-landscape processes and its impacts on human society. For example, millions of dollars are lost annually in Australia due to the loss of soil by wind erosion (Williams and Young, 1999; Forward *et al.*, 2004). Considering the poor nutritional condition of Australian soils, the loss of nutrients from the soil has severe consequences for the economy and the society. Furthermore, salinity and sodicity are major issues in the Australian landscape that can have serious impacts not only on industries such as agriculture and pastoralism, but also on the biodiversity of the environment (Wong *et al.*, 2008; DEWHA, 2008). Aeolian dust is also thought to be an insidious carrier of terrestrial salts and to be partially responsible for causing salinity and sodicity (Acworth *et al.*, 1997; Jankowski and Acworth, 1997; Acworth and Jankowski, 2001; Melis and Acworth, 2001; Smithson, 2004; Greene *et al.*, 2004; Bierwirth and Brodie, 2008; Cattle *et al.*, in press). Vast arid regions with saline deposits, which are potentially susceptible to wind erosion, occur in northern South Australia (Hesse and McTainsh, 2003). For example, up to 700 million tonnes of sodium chloride occur in Lake Eyre North, which is one of the possible sources (Bonython, 1956). These salts are assumed to be carried by the wind and induce salinisation and sodification in the leeward landscape when deposited; however, this proposition is still controversial due to the lack of research on this topic in an Australian context (Hesse and McTainsh, 2003; Hesse, 2004). For example, Hesse (2004) points to the lack of quantitative data that would confirm the link between aeolian dust transportation and consequent salinisation, such as evidence for co-transportation and co-deposition of terrestrial soil and terrestrial salts from inland saline basins. This link is not easily discerned, because the aeolian characteristics of the salts are quickly lost once dust is deposited onto the ground and the soluble salts are easily leached out from the landscape (McPherson, 2003) and mineral dusts are quickly integrated into the in-situ landscape (Cattle *et al.*, in press). Therefore, the purpose of this study is to provide quantitative data that will contribute to the research on the link between saline sources such as enclosed inland drainage systems in South Australia and aeolian deposition in south-east Australia.

1.2. Position of the Research

The research presented in this thesis is linked to two other ongoing projects on aeolian dust by: (i) CSIRO Land and Water (CLW); and, (ii) Department of Environment and Climate Change, NSW at the Cowra Research Station (CRS). The research based at the Australian National University (ANU) is also carried out in collaboration with ANSTO (Australian

Nuclear Science and Technology Organisation). Figure 1-1 shows how these various organisations are involved.

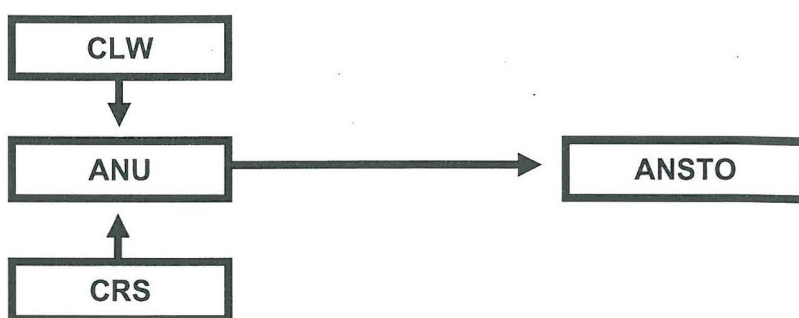


Figure 1-1: The protocol of this research; arrows indicate sample input/output flows

The CLW project, lead by Dr. Richard Cresswell, involves analysing rainfall chemistry and isotopic composition. It focuses on gaining an understanding of the accumulation of salt in the Murray Darling Basin, in particular the origins, mobilisation and transport of salt in the Australian regolith and response times related to salinity. The CLW project maintains 20 sample collectors across the Australian continent (Cresswell *et al.*, 2006). In this research, samples from 15 collectors, mainly within south-east Australia, are used (Table 3-1). About 50 ml of the samples are initially sub-sampled for the CLW project on rainfall chemistry and isotopic composition, and the remaining portions of the samples are sent to the ANU for the purpose of this research. The samples from the CLW project comprise the majority of the samples studied in this research.

The CRS project involves dust collection and monitoring. CRS is a field research station operated by the NSW Department of Environment and Climate Change of NSW, located in Cowra, NSW, approximately 300 km west of Sydney.

The collaboration with ANSTO staff involves the chemical analysis of dust samples. The samples are initially sent to ANU from the two projects cited above and then sent to ANSTO where they are subjected to detailed quantitative chemistry analysis by ion beam analysis (IBA), utilising the STAR accelerator as part of an AINSE (Australian Institute of Nuclear Science and Engineering) grant.

1.3. Project Timeline

The current research reported in this thesis was carried out from July 2007 to January 2009; the various stages involved are outlined in Figure 1-2. Phase 1 had its main focus on the establishment of techniques for collection and processing of dust samples. The extensive examination of samples was conducted in phase 2. The final phase 3 concentrated on establishing a hypothesis based on the acquired results and integrating every part of the research into the final output. The results from the current research will contribute to the understanding

of the potential role of aeolian dust as an important carrier of terrestrial salt from the source area in the salt lake regions of South Australia.

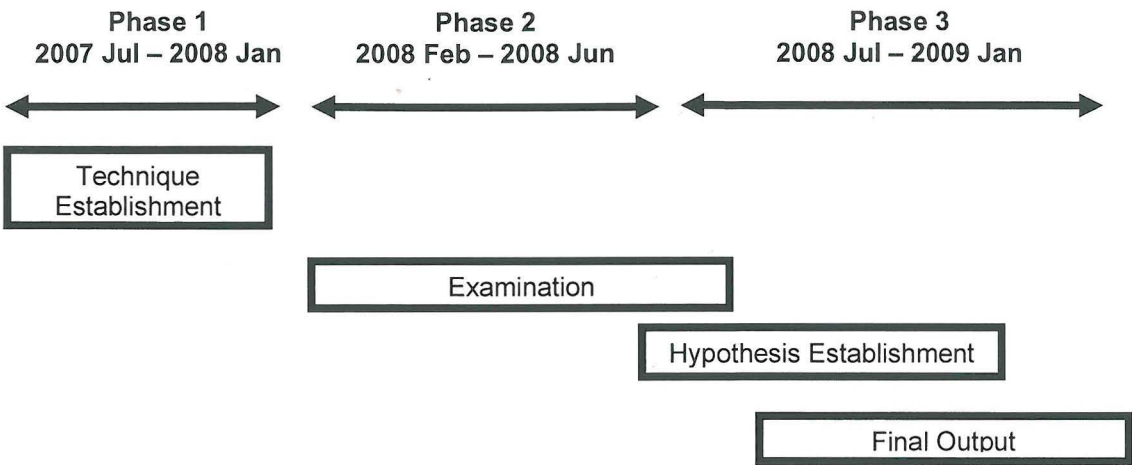


Figure 1-2: Project timeline

1.4. Research Question

The main question posed in this research is:

Do the aeolian processes contribute to the deposition of terrestrial salts (NaCl), particularly in south-east Australia?

In order to answer the above question, the following aim and objectives are set up.

1.5. Aim of Research

The aim of this research is to investigate the aeolian co-transportation and co-deposition of dust and terrestrial salt (NaCl) in south-east Australia.

1.6. Objectives

To achieve the above aim, the following objectives are pursued:

- (i) Validate the use of a set of equations to determine the component of terrestrial salt (NaCl) in the aeolian dust;
- (ii) Characterise dust deposited at various sites across south-east Australia; and
- (iii) Confirm the presumed source of dust that is deposited across south-eastern Australia with a high terrestrial salt influence.

1.7. Thesis Structure

This thesis is comprised of six chapters, references and three appendices. The outline of the chapters is as follows:

- Chapter 1: Defines the scope of the thesis and describes the purpose of the study with regards to the relevant background information (this chapter).
- Chapter 2: Relevant past and recent literature is reviewed with a focus on the causes, deposition and impacts of aeolian dust. The causes of the dust are explored in two parts: (i) geographical and meteorological conditions, and; (ii) surface soil conditions. The impacts of the dust are described in four parts: (i) soil erosion and development; (ii) damage to human health; (iii) salinisation and sodification; and, (iv) climate change.
- Chapter 3: The locations of the sampling sites used in this research and how the samples were collected are described. The analytical methods and procedures taken are also described. Four main analytical methods are applied in this research. These were: (i) IBA; (ii) PCA (principal component analysis); (iii) back trajectory analyses; and, (iv) SEM (scanning electron microscopy).
- Chapter 4: The results of the analyses undertaken are presented.
- Chapter 5: The results presented in the previous chapter are discussed.
- Chapter 6: Conclusions and the limitations of the current research are outlined and suggestions for future work are made.
- References: List of 178 references.
- Appendix A: Complete results from IBA.
- Appendix B: Complete results from back trajectory analysis.
- Appendix C: Complete results from SEM.

1.8. Summary

This chapter has described the position and timeline and set out the research question, aims and objectives of this research. Aeolian dust is thought to be an insidious carrier of terrestrial salts; however, this proposition is still controversial due to the lack of research on this topic in an Australian context. Therefore, the aim of this research (conducted in collaboration with CLW, CRS and ANSTO) is to reveal the characteristics of aeolian dust associated with terrestrial salt transportation in terms of chemistry and morphology, particularly in south-east Australia. Samples are obtained through CLW and CRS projects and they are subsequently analysed at ANSTO and ANU.

The following chapter examines and assembles available information from past research on aeolian dust to establish an overall understanding of the dust, particularly those in relation to the Australian context.

2. Literature Review

2.1. Introduction — What is Aeolian Dust?

Aeolian dust consists of fine-grain particles that become suspended in the atmosphere by the action of strong surface winds. Therefore, unlike fluvial transport, aeolian transport is much less constrained by topographic parameters such as slopes and channels (Pell *et al.*, 2000; McTainsh and Strong, 2007). Because of this unique characteristic, aeolian dust has the potential to travel thousands of kilometres and affect wide and remote areas (Grousset *et al.*, 2002). Thus, aeolian dust has been an important factor in the development of the Australian soil landscape (Greene *et al.*, 2001; McTainsh and Strong, 2007).

Aeolian dust is a consequence of a wide range of atmospheric and ground conditions (McTainsh and Strong, 2007). Wind direction and speed, soil particle size and moisture level and precipitation are just some of the major factors influencing a dust event (Brookfield, 1970; Gatehouse *et al.*, 2001; Ekström *et al.*, 2004; Greene *et al.*, 2004; SCDSI, 2005). The effects of aeolian dust are also diverse (McTainsh and Strong, 2007). For instance, soil-landscape processes, aspects of the health of human society and even global climate change are heavily affected by aeolian dust (Chartes *et al.*, 1988; Cattle *et al.*, 2002; SCDSI, 2005; Tanaka and Chiba, 2006; Forster *et al.*, 2007; Tate *et al.*, 2007; Bierwirth and Brodie, 2008; Rotstayn *et al.*, 2008).

This literature review outlines the characteristics of aeolian dust in Australia and covers the conditions under which dust events occur, the transportation and deposition mechanisms of dust, and its impacts on society. The potential role of aeolian dust in transporting salts and hence leading to salinity will also be addressed.

2.2. Characteristics of Australian Dust

The Australian continent is one of the major areas of the world prone to aeolian dust (Pye, 1989; Tanaka and Chiba, 2006). Although the total dust emissions in Australia, which amount to 106 Mt yr⁻¹ (Tanaka and Chiba, 2006: 93), might not be as large as other dust source areas, such as North Africa (1,087 Mt yr⁻¹) (Tanaka and Chiba, 2006:93), aeolian dust from the Australian continent is important because it is the dominant source of dust in the southern hemisphere (Tanaka and Chiba, 2006). The dust emission of Australia is roughly equivalent to that of the total emission from two other major dust source regions in the southern hemisphere; i.e., South America (44 Mt yr⁻¹) and South Africa (63 Mt yr⁻¹) (Tanaka and Chiba, 2006: 93). McTainsh and Lynch (1996) have found the dust deposition rate to be 31.4 to 43.8 t km⁻² yr⁻¹ in rural areas in eastern Australia. The dust is even capable of being transported outside the Australia continent, to areas such as New Zealand and Antarctica (McGowan *et al.*, 2000; McGowan *et al.*, 2005; Revel-Rolland *et al.*, 2006; Tanaka and Chiba, 2006; Marx *et al.*, 2008).

Therefore, within the context of the southern hemisphere, the role of Australian dust is critical and its impacts are significant (Figure 2-1). In addition, the amount of dust deposition in and around Australia was larger during the Last Glacial Maximum (25.0 – 21.7 ka), compared to that of the Holocene period (Hesse and McTainsh, 1999; Petherick *et al.*, in press). Less vegetation cover over the source regions due to more stressful environmental conditions is assumed to be the reason (Hesse and McTainsh, 1999). This phenomenon is discussed in Section 2.3.1.

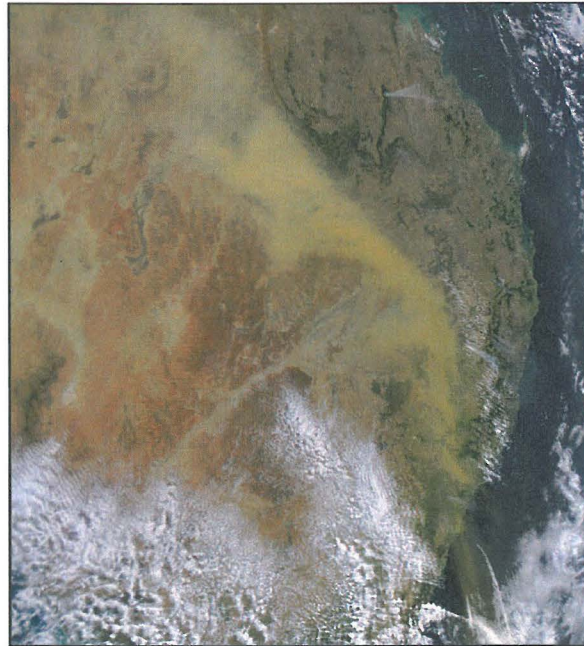


Figure 2-1: Dust storm in eastern Australia (October 23, 2002)
(Source: Earth Observatory, 2002)

Historically, aeolian dust deposited in Australia has been referred to as ‘*parna*’, a term introduced by Butler (1956) in the early days of dust research in Australia. Parna is an Aboriginal word which refers to a ‘sandy and dusty ground’ (Butler, 1956: 147). Parna is usually transported as stable silt or sand size aggregates, which are composed of calcareous clay covering the larger sand or silt size mineral grains, such as quartz and feldspar, in the centre (Butler, 1956; McIntyre, 1976; Dare-Edwards, 1984; Kiefert *et al.*, 1996). These aggregates have been referred to as ‘pellets’ (Dare-Edwards, 1984; Greene *et al.* 2006). Therefore, when the pellets are dis-aggregated after deposition, they often present a unique bimodal particle size distribution — one mode in the clay size range and another in either silt or sand size range (Dare-Edwards, 1984; Munday *et al.*, 2000). However, other studies have reported that the dust aggregates have high resistance to dispersion (McIntyre, 1976; Mays *et al.*, 2003). This stability is assumed to derive from the unique face-to-face orientation of the particles within the aggregates (Greene *et al.*, 1978). This close contact increases the van der Waals attraction forces between the particles, and hence improves the stability of the aggregates (Greene *et al.*, 1978; Quirk, 1994; Mays *et al.*, 2003).

Another conspicuous characteristic of parna is its high clay content; normally between 30 to 70%, and varies with the distance from the source areas (Butler, 1956; Butler and Hutton, 1956; Greene *et al.*, 2001). In addition, parna covers the landscape uniformly and homogeneously without any conspicuous stratifications, regardless of the underlying soils or topography (Butler, 1956; Beattie, 1969; Dare-Edwards, 1984).

Aeolian dust in Australia is also known for its high organic content (Boon *et al.*, 1998; Leys and McTainsh, 1999). Boon *et al.* (1998) have reported a significantly high organic matter content in dust collected in four monitoring sites in rural areas of NSW. In general, Australian soils are extremely low in organic content (Spain *et al.*, 1983; Boon *et al.*, 1998; McTainsh and Strong, 2007). The work by Spain *et al.* (1983) suggests that 75% of Australian soils have less than 1% of organic carbon content in the surface and rarely does it exceed 5%. For instance, dust source soils in the semi-arid and arid areas generally contain less than 1% of organic matter content (McTainsh and Strong, 2007). Therefore, the values of 31% and 34% mean organic matter content measured in the suspended and deposited dusts, respectively, by Boon *et al.* (1998), was a notable finding. Organic matter content of 7.98% reported by Leys and McTainsh (1999) in the upper Namoi River region was smaller than the figures reported by Boon *et al.* (1998), however it was still conspicuously higher than the proportions of organic matter generally found in Australian soils (Spain *et al.*, 1983). Boon *et al.* (1998) pointed out some possible sources of the organic matter, such as fragments of plants and soil biological crust, burnt plant materials from bushfires and pollens. In addition, a winnowing effect of wind is conjectured to be the possible concentration mechanism for organic matter (Leys and McTainsh, 1994; Boon *et al.*, 1998).

Loess is a term which refers to terrestrial materials transported and deposited by wind. These materials are predominated by silt-size minerals, such as quartz and feldspars (Pye, 1987). Although parna has similarities to loess, which occurs in other parts of the world such as in North America and China, the reason why a different term was proposed for aeolian dust in Australia is because of the conspicuous disparities between the two types of dust in their production mechanism (Smalley and Krinsley, 1978; Pye, 1987; Wright, 2001). The production mechanism of parna had been considered to be significantly low compared to that of loess (Smalley and Krinsley, 1978; Pye, 1987; Wright, 2001). For example, loess deposition found in the Loess Plateau in China could be as thick 300 m in some areas, whereas a parna layer rarely exceeds 3 m (Butler, 1956; Huang *et al.*, 2002). In addition, no efficient mechanisms for producing large amount of silt-size material were known except glacial grinding which had only a minimal contribution in Australia (Smalley and Krinsley, 1978; Wright, 2001; Smalley, 2008). For example, Smalley and Krinsley (1978: 63) concluded that 'glacial grinding is the only natural process which efficiently converts sand-sized quartz particles totally into a silt-sized product'.

However, what had been known as loess is becoming more accepted as a cold or glacial loess, a sub-set of the new loess terminology, while the dust deposition in Australia is becoming more accepted as a hot or desert loess, rather than as parna, as the production mechanism of desert loess becomes more recognised as an effective mechanism for generating a large quantity of silt-size minerals found widely around the world (Dare-Edwards, 1984; Pye, 1984; Pye, 1989; Wright, 2001; Hesse and McTainsh, 2003; Mays *et al.*, 2003; Smalley, 2008). Three reasons have been suggested to explain why the accumulation of dust is so thin in Australia, even though there is an effective mechanism for producing fine material: (i) Australia's low-relief landscape is inefficient in producing fine material compared to areas such as Central Asia where high and steep mountains occur; (ii) wind energy in dust source areas in Australia is lower compared to that of other areas, such as the Gobi and Taklamakan Deserts, for aeolian transportation; and, (iii) only minimal vegetation cover is available to effectively trap aeolian materials on the ground (Pye, 1987; Tsoar and Pye, 1987).

2.3. Causes of Aeolian Dust

Attributing causes to the aeolian dust in Australia is not simple; many factors are involved, making it a complicated phenomenon. This section will explain this from two perspectives. Section 2.3.1. discusses the relationship between the surface soil conditions and aeolian dust, that is, the conditions leading to the formation of dust. Section 2.3.2. will describe the phenomenon from a macro perspective, that is, from the geographical and meteorological aspects (where it occurs, how the dust is entrained in the atmosphere and how it is transported) utilising the extreme manifestation of aeolian dust — the dust storm.

2.3.1. Surface Soil Conditions

Surface soil conditions are strongly related to the occurrence and degree of impact of aeolian dust (Goudie and Middleton, 1992; Ekström *et al.*, 2004; Greene *et al.*, 2004; SCDSI, 2005; Reynolds *et al.*, 2007; Bullard *et al.*, 2008); this is particularly the case in the Australian context (Hesse, 2004). While wind strength is important and increases the degree of wind erosion, it is estimated from past records that this has been constant in Australia, at least throughout the Quaternary period. Therefore, for a long time in Australia, aeolian dust has been fundamentally controlled by the surface soil conditions (Hesse, 2004).

Several conditions of the surface soil are relevant to dust formation and wind erosion. Vegetation cover, aggregate stability, moisture level and particle size are the principal factors to be taken into account (Potter, 1990; Pye, 1987; McTainsh *et al.*, 1998; Gatehouse *et al.*, 2001; Greene *et al.*, 2004; SCDSI, 2005; Batjargal *et al.*, 2006). Some of these factors might be inherent characteristics of the landscape, at least to a certain degree, but others are closely related to human activities.

Protective vegetation cover and aggregate stability strongly influence the erosion of soils and hence dust events (Pye, 1987; Raupach *et al.*, 1994; Greene *et al.*, 2004; Okin *et al.*, 2006). In the Australian context, records exist of the increase in soil erosion which has resulted from the depletion of the vegetation and destabilisation of soil caused by not only the prolonged droughts, but by also over-grazing and inadequate farming practices as well (Raupach *et al.*, 1994; Greene *et al.*, 2004; SOEC, 2006). For example, studies by Greene *et al.* (1998) in the rangelands of central New South Wales point out the negative effects of high-intensity grazing by feral goats (4.0 goats ha⁻¹) on the vegetation cover and aggregate stability of the soil. This over-grazing has made the landscape more vulnerable to wind erosion by breaking up the soil surface into fine materials and catalysing the amount of dust emission. Other herbivores, such as introduced rabbits and native kangaroos, are also responsible for the unfavourable impacts that can lead to wind erosion by means of vegetation depletion and break up of soil stability (Greene *et al.*, 2004). In addition, the mobility of the source dust is presumed to have been more extensive during the Last Glacial Maximum due to less protective vegetation cover as a consequence of an extreme aridity (Hesse and McTainsh, 1999; McGowan *et al.*, 2008; Petherick *et al.*, in press).

Along with physical soil crusts, past research has revealed the importance of biological soil crusts, which comprise micro-organisms such as cyanobacteria, bacteria, fungi, lichens, mosses and liverworts, in determining the extent of wind erosion (Eldridge and Greene, 1994; Leys and Eldridge, 1998; Eldridge and Rosentreter, 1999). Leys and Eldridge (1998) evaluated the effectiveness of biological crusts in controlling the wind erosion on both loamy and sandy Australian rangeland soils using a portable field wind tunnel. Biological crusts become particularly important in the context of Australian dust, because they are often the only biological soil cover, especially during dry periods, in the arid and semi-arid rangelands where most dust originates (Eldridge and Greene, 1994).

The moisture level of the soil is also an important factor to consider in respect of dust events (Goudie and Middleton, 1992; McTainsh *et al.*, 1999). A strong correlation between aridity and the strength of dust activity, at least since the Last Glacial Maximum, has been recognized from the past (Goudie and Middleton, 1992; McGowan *et al.*, 2008; Petherick *et al.*, in press). Goudie and Middleton (1992) argue that difficulties in detecting a consistent trend in the frequency of Australian dust storms are due to Australia's variable climate in terms of precipitation. However, the correlation is not always simple. Low intensity rains (less than 10 mm) in the Channel Country of western Queensland were found to increase the erodibility of particular soils which catalysed aeolian dust emission (McTainsh *et al.*, 1999). In addition, a correlation between El Niño and consequent droughts in Australia has been recorded; this can lead to increased future dust emission (Manins *et al.*, 2001).

Particle size is also an important factor in aeolian dust. Whether dust can be suspended in the atmosphere depends on particle size as well (Pye, 1987; Potter, 1990). According to Pye

(1987), in moderate windstorm conditions, only dust particles less than 70 μm in size can be suspended and those capable of travelling long distances are even smaller (less than 20 μm). However, these smaller dust particles have the potential to travel significant distances (Pye, 1987). For instance, dust found by Grousset *et al.* (2002) in the French Alps is assumed to have come from China, across the Pacific Ocean, North America and the Atlantic Ocean. Australian dust is found extensively in New Zealand and Antarctica (McGowan *et al.*, 2000; McGowan *et al.*, 2005; Revel-Rolland *et al.*, 2006; Marx *et al.*, 2008). For example, the depositions of Australian soils on New Zealand, which is 3,000 km away to the east, are often reported as ‘red rain or snow’ (McGowan *et al.*, 2000). In addition, McGowan and Clark (2008) have indicated, by using HYSPLIT program (Section 3.5.3.), the possibility that Australian dust could also be affecting Indonesia, Papua New Guinea and even the southern Philippines, including a vast area of tropical rainforests and coral reefs in this region.

2.3.2. Geographical and Meteorological Conditions

Dust storms in the Australian continent appear to originate mainly in the arid inland drainage basins (Prospero *et al.*, 2002; Hesse and McTainsh, 2003; Greene *et al.*, 2004). Figure 2-2 depicts the spatial pattern of dust entrainment in Australia, using the Dust Storm Index, an index of both frequency and intensity of dust entrainment (Hesse and McTainsh, 2003; Mackie *et al.*, 2008).

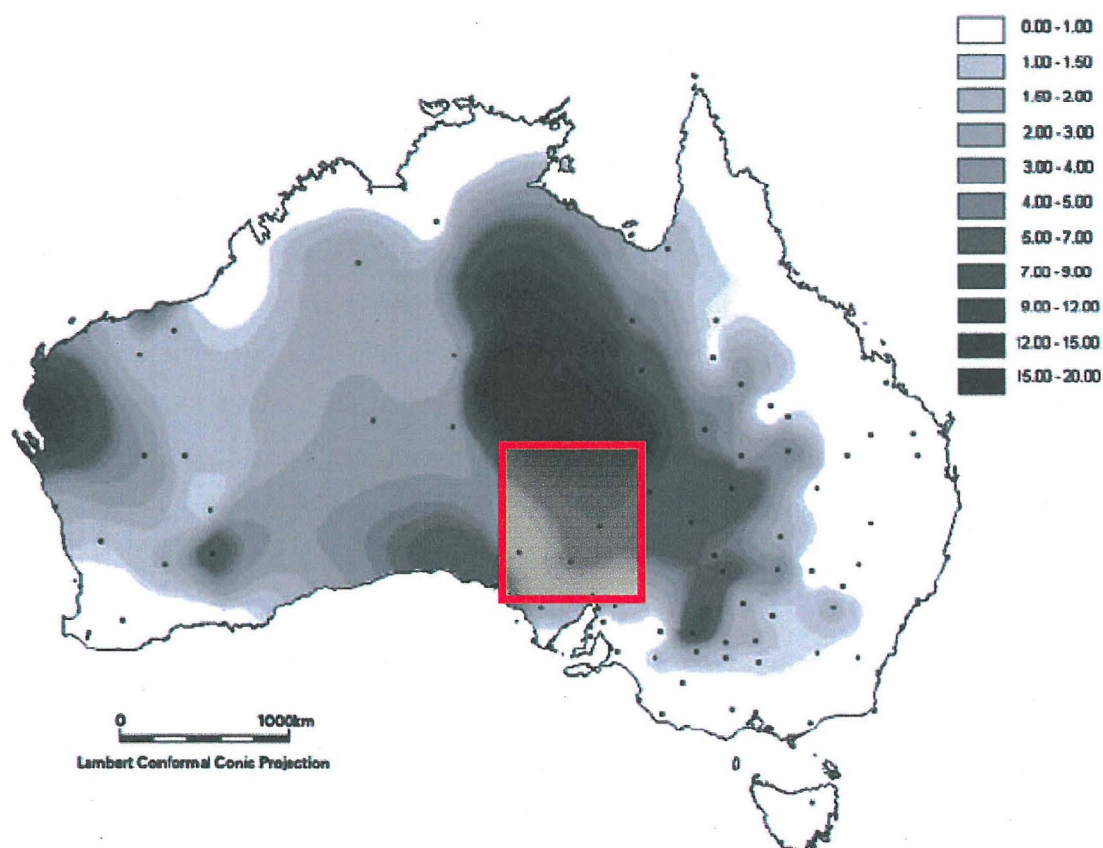


Figure 2-2: Spatial distribution of dust activity in Australia (1960 - 1999) using the Dust Storm Index; the region shown in the red box is the presumed source of the terrestrial salt (Source: Hesse and McTainsh, 2003)

The major dust source areas are the Simpson Desert-Channel Country in southwest Queensland, the Strzelecki Desert in South Australia, areas extending from western New South Wales to the Mallee region in northwest Victoria and the Carnarvon region in Western Australia. Most of these areas lie within the lower parts of major drainage basins, which are also extremely arid. Such basins are the Lake Eyre Basin and the Murray Darling Basin, where the sediments and materials for a dust source are more easily gathered by existing alluvial processes and hence develop the potential for contributing to the formation of aeolian dust and dust storms (Kiefert *et al.*, 1996; Hesse and McTainsh, 2003; Hesse, 2004). This is particularly the case in the Lake Eyre drainage which is enclosed with no regular outflow to the ocean, and hence the accumulation of sediments and salts is significantly high (Bonython, 1956; Gunn and Fleming, 1984). The centres of such enclosed inland drainage systems, such as the Bodélé Depression in Western Africa and Tarim Basin in Central Asia, are typical of the topography most prone to dust entrainment around the world in general (McTainsh, 1985; Tungsheng *et al.*, 1985; Prospero *et al.*, 2002; Yang *et al.* 2002; Zender *et al.*, 2003). Moreover, Lake Eyre, which is situated in the centre of the basin, where it is mostly occupied by endorheic dry lakes, playas and claypans, and is dry most of the time and water is filled only in decadal episodic flooding events (Bullard *et al.*, 2008). Between episodic inundations, the lake is often dry and is covered by either a saliniferous mud or thick halite crust (Williams, 2002). In such harsh environments, typically that of playas (salt flats), the ground cover is extremely low and sparse and thus highly vulnerable to winds, thus making these regions highly prone to dust entrainment (Pye, 1987). Furthermore, salt weathering, a common phenomenon in such regions, enhances disintegration of dust particles to even looser and finer ones, and hence, makes them even more susceptible to the wind actions (Pye 1984; Pye, 1987; Pye 1989). In fact, from long term observations by satellite, the areas around the centre of the Lake Eyre Basin are conjectured to be the dustiest location in Australia (Prospero *et al.*, 2002; Washington *et al.*, 2003). In addition, it has been predicted that future precipitation in this region will be shorter, but more intense and of larger volume, which may lead to an accelerated accumulation rate of fine sediments in the centres of the basins (Williams, 2002). Importantly, Tegan *et al.* (2004) have estimated that dust emissions from the Australian continent will increase in decadal time-scale. However, it must be noted that although dust is more easily entrained in the atmosphere in the centre of the basin, in terms of absolute volume, dust may originate more from other sources such as dunes, dry lake margins, and flood plains. This is because even though these source areas may not release dust as easily as the centre of the basin, their areas are much more extensive (Bullard *et al.*, 2008).

Within these source areas, surface dust is entrained in the atmosphere by meteorological circumstances (McGowan *et al.*, 1996; Ekström *et al.*, 2004; Leslie and Speer, 2006). Even in the world's largest single dust source, the Bodélé Depression, dusts cannot be entrained in the atmosphere unless winds of sufficient velocity exist (Washington *et al.*, 2006; Warren *et al.*, 2007). McGowan *et al.* (1996), have revealed the essential role of foehn winds, which are

typically warm, dry and gusty, amongst the dust entrainment processes in Lake Tekapo, New Zealand. In Australia, cold fronts, which are typically dry, shallow and become more intense at night, play a fundamental role in this context (Smith *et al.*, 1995). Strong surface winds, often induced either ahead of or behind these cold fronts, are capable of entraining large quantities of dust from the ground (Pye 1987). Therefore, the conditions for strong ground winds are entangled and complex.

Figures 2-3 (McTainsh *et al.*, 2005) and 2-4 (Leslie and Speer, 2006) are synoptic charts of the October 2002 dust storm, which is said to have been the largest in eastern Australia in at least 40 years (McTainsh *et al.*, 2005). Figure 2-3 is a macro synoptic chart of the whole continent and illustrates the distribution of the high and low pressures and related cold front which stretch from a cyclone in the south of Tasmania. This is one of the most typical synoptic distributions causing dust events in Australia (Ekström *et al.*, 2004). Figure 2-4 focuses on the south eastern areas of the continent, but is also a synoptic chart of the same dust storm; it depicts the meteorological environment just six hours before the event depicted in Figure 2-3. The typical surface wind directions associated with cold fronts are shown in Figure 2-4 as pre-frontal north winds and post-frontal west winds (McTainsh *et al.*, 1998). These surface winds are the major cause of dust entrainment in the atmosphere; however, the amount of dust entrained depends heavily on the speed of the winds. Brookfield (1970) found that 4.63 m sec^{-1} was the minimum wind speed to cause dust movement and 9.79 m sec^{-1} for a significant dust movement in central Australia. However, these figures can fluctuate depending on the ground conditions, such as soil moisture and topography. For instance, McTainsh *et al.* (1999) set 6 m sec^{-1} as the threshold that would cause dust entrainment in the Channel Country of western Queensland.

Despite the importance of wind in entraining dust into the atmosphere, it must be noted that the existence of abrading materials also has a significant role in this respect, especially in supply-limited environments, including Australia (Section 2.3.1.) (Houser and Nickling, 2001; Bullard *et al.*, 2008). The abrading materials are generally larger than the dust particles, which are capable of travelling a long distance, and they can only bounce or roll across the ground surface (saltation) and are usually contained within the local landscape (Leys and McTainsh, 1994). However, the bombardment of these particles plays a pivotal role in generating finer dust particles, which could travel much longer distances; without such a mechanism, even a strong wind could not entrain dust into the atmosphere (Houser and Nickling, 2001).

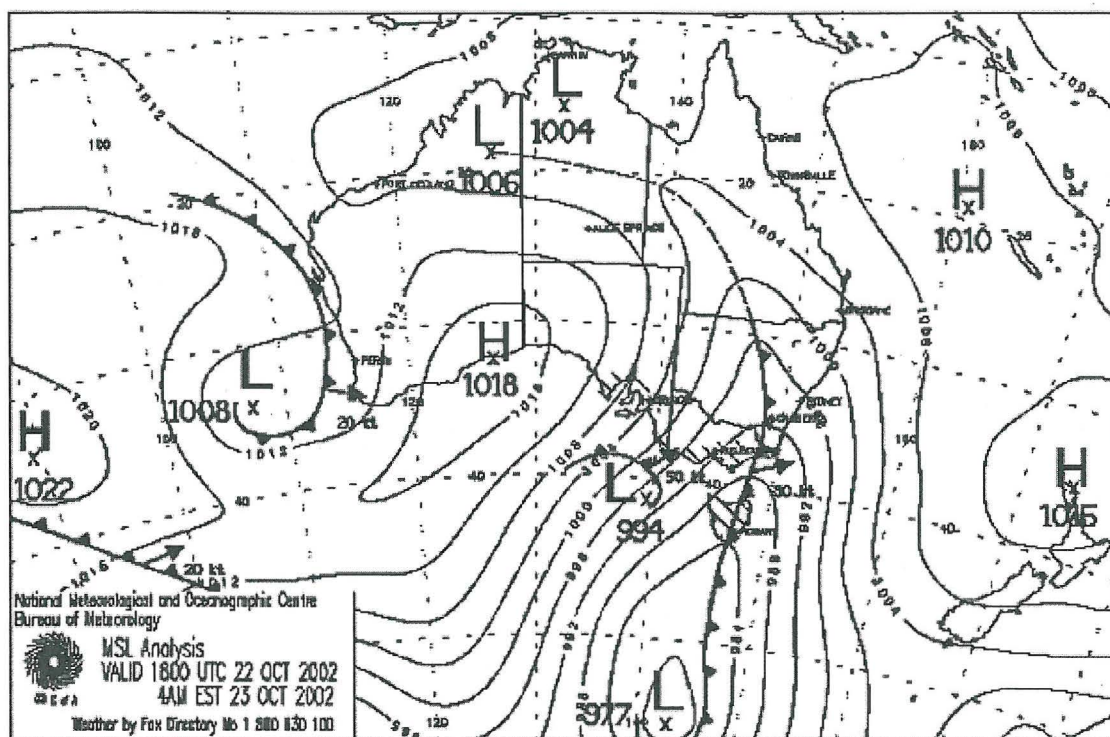


Figure 2-3: Synoptic chart for 1800 UTC 22 OCT 2002
(Source: McTainsh *et al.*, 2005)

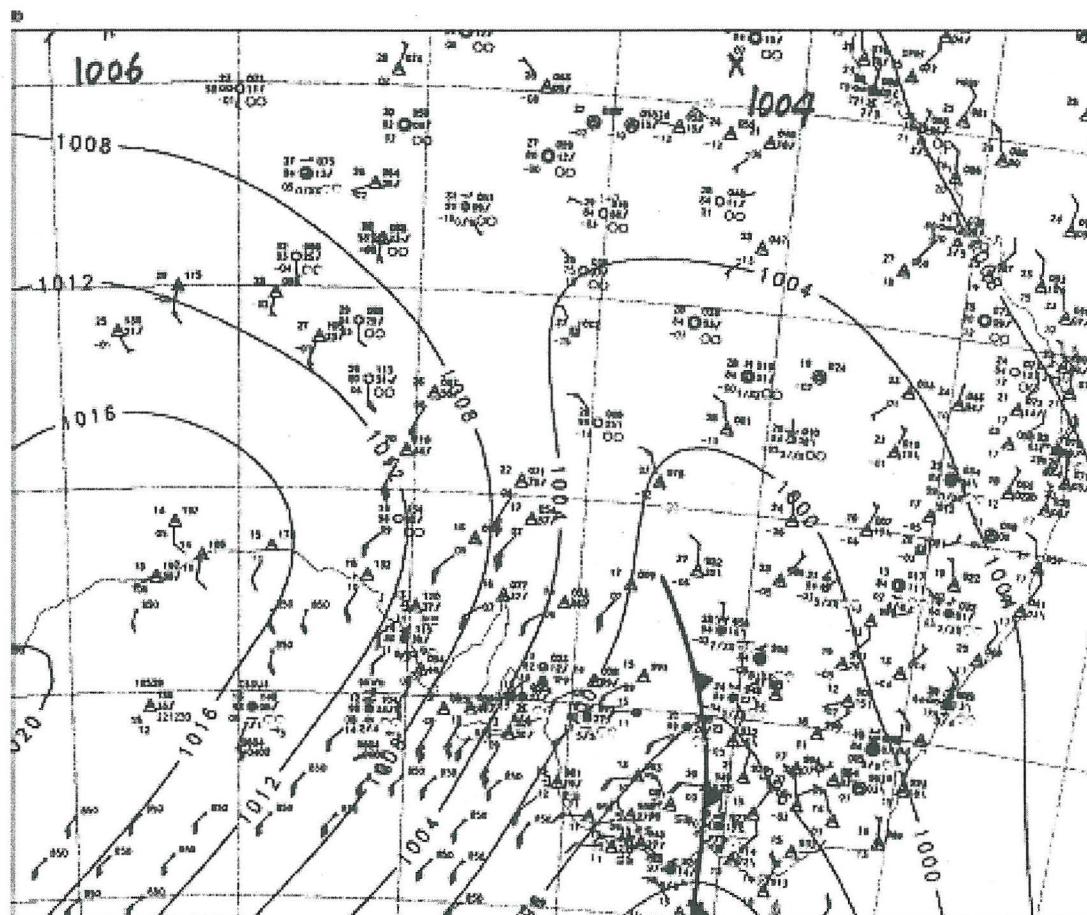


Figure 2-4: Synoptic chart for 1200 UTC 22 OCT 2002
(Source: Leslie and Speer, 2006)

After the entrainment of the dust in the atmosphere, the aeolian particles are carried and transferred not only by the surface winds, but also by the above-surface winds, such as jet streams (Pye, 1987). Once the dust is suspended by the surface winds, the height to which the dust can be carried is up to several kilometres above the ground (McTainsh *et al.*, 2005; SCDSI, 2005). Therefore, after the dust is entrained in the atmosphere, it is essential to consider not only the surface wind, but also the wind much higher above the ground.

Figure 2-5 represents an outline of Australian dust transportation paths. It depicts wind paths passing the source areas, such as the Lake Eyre and the Murray Darling Basins and the two major transportation paths, one over the south-east of the Tasman Sea associated with zonal westerly winds and the other over the north-west of the Indian Ocean associated with south-easterly trade winds (Bowler, 1976; McTainsh and Lynch, 1996; Kiefert *et al.*, 1996). The impacts of the aeolian dust in the south-east are the more critical of the two and attract more interest from both the public and researchers because of the relatively high population density and the consequent social and economic importance of this region (Hesse and McTainsh, 2003). The impacts and consequences of dust events are discussed in Section 2.5.

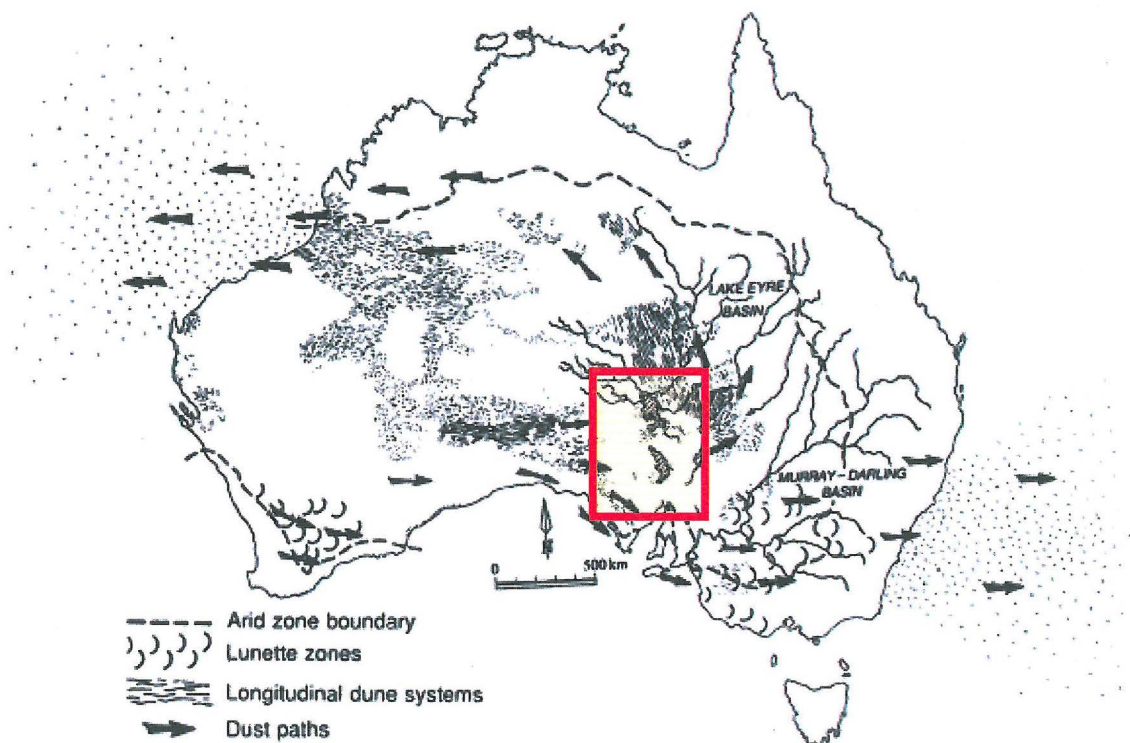


Figure 2-5: Australian dust transportation route; the region shown in the red box is the presumed source of the terrestrial salt
(Source: Hesse and McTainsh, 2003)

2.4. Deposition of Aeolian Dust

Having outlined the properties and processes of dust formation and transport, it is now necessary to discuss the deposition of dust. Similar to its production, the deposition of aeolian dust is controlled by a range of geographical and meteorological conditions, in addition to gravity. Particular landscapes or topography, such as mountains with high elevations, can effectively intercept dust transported in the atmosphere and cause it to become deposited. A good example in Australia in this respect is the eastern ranges (Walker and Costin, 1971). Walker and Costin (1971) assert that the much lower dust deposition rate observed in Canberra compared to that of Mount Kosciuszko, which is higher in altitude and is located south south-west of Canberra, is a result of this interception mechanism, that is, aeolian dust originating in the arid inland is intercepted as it moves to the east. Not just macro landscapes such as mountain, but also smaller scale landscapes, such as forests, have an effect on dust deposition. Pye (1984) and Tiller *et al.* (1987) have found conspicuously more dust fallout under tree foliage than in adjacent open areas — nearly double the amount of fallout was observed under the foliage. Tsoar and Pye (1987) assert that rough topography, such as forests, is effective in terms of reducing the wind velocity which is an important energy source maintaining the suspension of dust particles in the atmosphere, and hence effectively trapping dust back to the ground.

Particle size is another important factor which determines the deposition of dust (Pye, 1987; Cattle *et al.*, in press). In general, the finer the particle, the further it travels from the source. Alternatively, the larger the particles, the closer they are deposited to the source. Therefore, dust deposition often creates graduation or *thinning* of particle size — larger to smaller — depending on the distance from the source. In Australia, Cattle *et al.* (in press) have described this thinning effect of dust along the south-east transportation route (Section 2.3.2.).

Meteorological conditions are also an important factor in dust deposition mechanisms. Wind speed, which provides the fundamental energy for suspension, is critical; precipitation also has a considerable influence on dust deposition (wet deposition) (Arimoto *et al.*, 1985; Zhang *et al.*, 1993). However, the proportion of wet and dry depositions against the amount of total deposition depends on the conditions of each particular environment. In the Loess Plateau in China, dry deposition was found to be much higher than wet deposition (Zhang *et al.*, 1993). The amount of wet deposition of Fe was found to be only 4.3% of total deposition (Zhang *et al.*, 1993). In contrast, in Enewetak Atoll in the Pacific Ocean, Fe was found at levels 3.3 times higher in wet deposition compared to dry deposition (Arimoto *et al.*, 1985).

Past research has shown that dry deposition is relatively more effective in removing larger (thus heavier) particles, but ineffective for removing smaller size particles (Pye, 1987; Hesse and McTainsh, 1999; Woodward, 2001). In terms of global means, Woodward (2001) found the highest proportion of wet deposition in the 0.316 – 1.0 μm range while dry deposition had its peak in the 10.0 – 31.6 μm . Results from Hesse and McTainsh's (1999) research in Brisbane

and Charleville in eastern Australia are consistent with the above trend; larger particles were always found more in dry deposition. A model by Zender *et al.* (2003) predicts a larger quantity of wet depositions in eastern Australia, although dry deposition seems to predominate in most other regions. However the model is inconsistent with the observation made by Leys and McTainsh (1999) in the upper Namoi River region, north-east NSW. Although the deposition rate was higher in the wet deposition, as a total, contribution from the dry deposition was higher; 67% of the total deposition was observed during dry periods (Leys and McTainsh, 1999). In addition, according to a model devised by Tanaka and Chiba (2006), dry deposition which constitutes 61% of total deposition weight is larger than that of wet deposition which constitutes the remaining 39% in Australia as a whole. Research conducted in an area near Adelaide by Tiller *et al.* (1987), alludes to a possible correlation between the amount of precipitation and dust fallout in the region; however, this hypothesis has not been confirmed. As seen above, the contribution of wet and dry depositions in Australia still remains largely uncertain and requires further study, especially at a finer scale.

2.5. Impacts and Consequences of Aeolian Dust

The impacts and consequences of aeolian dust cannot be ignored, especially those arising from the extreme events of dust storms. For example, in terms of the economy, damage from the worst-ever recorded Asian dust storm in China (May 1993) is estimated to have cost 560 million RMB (Renminbi), which is equivalent to 73 million AUD (Australian dollars) (SCDSI, 2005). This loss was caused by just a single dust storm event. China's average annual dust storm damage is estimated to be around 1.5 billion RMB (ca. 200 million AUD) (Yang and Lu, 2001). In South Korea, calculations by Kang (2004) estimate a loss of approximately 4 trillion won (ca. 400 million AUD) per annum due to dust damage.

In Australia, a partial estimate suggests an annual loss of millions of Australian dollars (AUD) due to dust events (Forward *et al.*, 2004). For instance, a single dust storm which struck Melbourne in 1983 is estimated to have caused damage of more than 4 million AUD, just in terms of soil nutrient loss from the source areas (Raupach *et al.*, 1994). Visibility was reduced to less than 100 m and consequently, airports were closed (Lourensz and Abe, 1983).

Therefore, damage due to aeolian dust is severe. Major aeolian dust impacts and consequences are summarized in Table 2-1.

Table 2-1: Impacts and Consequences of dust events

Impacts and Consequences	Source
Soil erosion and development	Butler, 1956; Butler and Hutton, 1956; Chartres, 1982; Chartres, 1983; Pye, 1987; Swap <i>et al.</i> , 1992; Leys and McTainsh, 1994; Knight <i>et al.</i> , 1995; Stoorvogel <i>et al.</i> , 1997; Leys and McTainsh, 1999; Johnston, 2001; Squires, 2001; Kurtz <i>et al.</i> , 2001; Garrison <i>et al.</i> , 2003; Forward <i>et al.</i> , 2004; Greene <i>et al.</i> , 2004; McTainsh, 2005; McTainsh and Strong, 2007; Cattle <i>et al.</i> , in press
Damage to human, animal and vegetation health	Williamson and Johnson, 1981; Pye, 1987; Herr <i>et al.</i> , 1996; Chiarandia <i>et al.</i> , 1997; Wray, 1998; Williams and Young, 1999; Squires, 2001; Garrison <i>et al.</i> , 2003; Kang, 2004; Greene <i>et al.</i> , 2004; SCDSI, 2005; CSEM, 2006; Kellogg and Griffin, 2006; Batjargal <i>et al.</i> , 2006; Bollhöfer <i>et al.</i> , 2006; Derbyshire, 2007; Moreno <i>et al.</i> , 2007; Marx <i>et al.</i> , 2008
Salinisation and/or sodification	Acworth <i>et al.</i> , 1997; Jankowski and Acworth, 1997; Munday <i>et al.</i> , 2000; Acworth and Jankowski, 2001; Melis and Acworth, 2001; Orlovsky and Orlovsky, 2001; Pillans and Bourman, 2001; Smithson, 2004; Abuduwaili <i>et al.</i> , 2008; Bierwirth and Brodie, 2008
Climate change	Jickells <i>et al.</i> , 1998; Schollaert and Merrill, 1998; Woodward, 2001; Garrison <i>et al.</i> , 2003; SCDSI, 2005; Jickells <i>et al.</i> , 2005; Yan <i>et al.</i> , 2005; Tanaka and Chiba, 2006; Sivakumar, 2007; McTainsh and Strong, 2007; Boyd <i>et al.</i> , 2007; Forster <i>et al.</i> , 2007; Mackie <i>et al.</i> , 2008
Nutrient gain	Swap <i>et al.</i> , 1992; Stoorvogel <i>et al.</i> , 1997; Leys and McTainsh, 1999; Kurtz <i>et al.</i> , 2001; Poulton and Raiswell, 2002; Garrison <i>et al.</i> , 2003; Hesse, 2004; SCDSI, 2005; McTainsh and Strong, 2007
Damage to infrastructure and households	Pye, 1987; Leys and McTainsh, 1994; Leys and McTainsh, 2004; Williams and Young, 1999; Squires, 2001; SCDSI, 2005

2.5.1. Soil Erosion and Development

Soil erosion is an important consequence of dust events around the world. For instance, the dust storm in China in 1993 carried away 10 to 30 cm of topsoil (SCDSI, 2005). In the Australian context, soil erosion is especially significant. This is due to the natural characteristics of its soil: it is generally shallow, nutrient-poor and vulnerable to erosion. For these reasons, soil and nutrient losses due to erosion are particularly important in Australia. From past research, the average aeolian dust load in Australia seems to exceed even that of fluvial sediment on a per capita base (Knight *et al.*, 1995; McTainsh and Strong, 2007). In the case of a noticeable dust event, such as the 23rd October 2002 dust storm in eastern Australia, McTainsh *et al.* (2005)

estimate a loss of 3.35 to 4.85 million tonnes of soil. As a consequence of the event, 3.5 and 12.0 kilotonnes of dust depositions were measured in Sydney and Brisbane, respectively (Chan *et al.*, 2005). During another noticeable dust storm that hit Melbourne on 8 February 1983, it is estimated that 2 ± 1 million tonnes of dust along with nitrogen worth 3.9 million AUD and phosphorus worth 0.4 million AUD were lost (Raupach *et al.*, 1994). In addition, not only do wind events deplete soil, they also degrade its properties (Leys and McTainsh, 1994). Leys and McTainsh (1994) have found approximately only half of the cation exchange and available water-holding capacities in the soil affected by the wind, compared to those unaffected in south-west NSW.

However, the eroded soils which are carried away by winds can also have positive consequences. For instance, not only does the aeolian dust provide soil, but it may also provide essential nutrients to a particular environment (Leys and McTainsh, 1999; Garrison *et al.*, 2003). For example, Kurtz *et al.* (2001) detected a significant amount of aeolian dust input from Asia in Hawaiian soils; this was found to be an important factor in the nutrient budget of the soils in these isolated islands (particularly Si and P). In addition, dust from the Sahara and/or Sahel is not only assumed to be an important source of nutrients in the coastal forest zone along the Gulf of Guinea, it is also presumed to be providing fundamental nutrients that are critical in sustaining the Amazon rainforest ecosystem (Swap *et al.*, 1992; Stoorvogel *et al.*, 1997). In Australia, past research has revealed a significant contribution of aeolian materials to the development of soils, particularly in the south-east (Butler, 1956; Butler and Hutton, 1956; Chartres, 1982; Chartres, 1983; McTainsh and Strong, 2007; Cattle *et al.*, in press). For example, Johnston (2001) has found a substantial amount of aeolian dust input into the alpine soils in the Kosciuszko National Park. Even in such a remote region, the dust accession rate was calculated to be up to $11.3 \text{ g m}^{-2} \text{ year}^{-1}$ (Johnston, 2001). Furthermore, Leys and McTainsh (1999) have found significant enrichment of organic matter and nutrients in aeolian materials which could be contributing to fertility in particular regions in Australia (Section 2.2.). The concentration of organic matter and N were 8 times and P concentration was 3 times higher in aeolian-derived dust than that of soils found around the sampling sites in rural eastern Australia (Leys and McTainsh, 1999). This concentration is a consequence of the selective erosion of lighter organic matter and finer soil particles, which generally contain a larger portion of nutrients (Leys and McTainsh, 1994).

Aeolian dust can also enhance the productivity of micro-organisms in oceans which are often limited by the availability of Fe (Garrison *et al.*, 2003; SCDSI, 2005; McTainsh and Strong, 2007). Although the global aeolian input of Fe to the oceans is relatively low (16 Mt yr^{-1}) compared to that by other means such as fluvial ($626 \text{ to } 963 \text{ Mt yr}^{-1}$) or glacial transportations ($34 \text{ to } 211 \text{ Mt yr}^{-1}$), the aeolian input becomes especially important in remote seas where Fe inputs from other sources are low (Section 2.5.4.) (Poulton and Raiswell, 2002; Jickells *et al.*, 2005). For example, the contribution from aeolian dust is found to be up to 80%

of total sediments on some ocean floors (Pye, 1987). In the Australian context, Australian dust is generally high in Fe content and this can be carried over to the Southern Ocean, where it can act as an essential fertilizer for micro-organisms (Boyd *et al.*, 2004). However, it must be noted that these nutrient inputs are the consequences of soil depletion in the source areas.

2.5.2. Damage to Health

The impacts of aeolian dust on the health of humans, livestock and flora are another important issue. For example, Batjargal *et al.* (2006) assert that the loss of biodiversity in dust affected regions is due to the increased stress on habitats. The nature and properties of dust particles themselves are responsible for severe damage to health, which is estimated to be affecting millions of people around the globe (SCDSI, 2005; Derbyshire, 2007). Finer dust particles are reported by Derbyshire (2007) to be especially responsible for this. Dust particles larger than 10 μm are relatively safer for the human body since they remain in the upper respiratory tract and are ejected by expectoration, even though they are inhaled (Pye, 1987; Derbyshire, 2007). In contrast, finer dust particles, 4 μm or smaller, are more serious for human bodies, because they penetrate more easily into the deeper parts of the lungs, and as a consequence can induce severe health issues such as silicosis, asbestosis and even lung cancer (Pye, 1987; Derbyshire, 2007).

However, combined with other particles that dust entrains during their transportation, the problem becomes even worse (SCDSI, 2005; CSEM, 2006; Kellogg and Griffin, 2006). Some of the most harmful particles found in dust are chemical contaminants, bacteria, fungi and viruses (Pye, 1987; Garrison *et al.*, 2003; SCDSI, 2005; CSEM, 2006). For example, dust from Africa that was collected above the Caribbean region in 2001 contained 170 colonies of bacteria, about 75 colonies of fungi and many viruses (CSEM, 2006). Nearly one third of the bacteria were pathogens which affect humans, animals and flora (CSEM, 2006). Also, aeolian dusts can carry toxic chemical contaminants, depending on their origin and the route of transportation (Chiarandia *et al.*, 1997; SCDSI, 2005; Marx *et al.*, 2008). For instance, Asian dust is assumed to entrain agrichemicals and pollutant chemicals, in addition to bacteria and fungi, while crossing agricultural land and industrial zones, respectively (SCDSI, 2005). In South Korea, research conducted by Kwon *et al.* (2002) has found a clear 2.2% increase in deaths of people aged 65 and over during and in the three days following a dust storm. In addition, an increase in the number of patients with respiratory, cardiovascular and eye complaints was reported (Kang, 2004). In the Australian context, Chiarandia *et al.* (1997) using isotopic analysis, have found a significant Pb contribution from leaded gasoline and the local copper smelting industry to dust collected in roof cavities in the Illawarra region, NSW. On a larger scale, Marx *et al.* (2008) have found a significant amount of pollutants on the west coast of New Zealand which derived from industrial and populated areas of eastern Australia.

Along with the harmful particles discussed above, heavy metals from mine sites and contaminated radionuclides may also be mobilised (Williamson and Johnson, 1981; Herr *et al.*, 1996; Greene *et al.*, 2004). For example, in an abandoned gold mine in Rodalquilar, Spain, which closed after approximately 20 years of operation in 1966, toxic elements such as Sb, As and Pb, which can cause severe health problems in humans, were found to be extremely susceptible to the aeolian processes and dispersion (Wray, 1998; Moreno *et al.*, 2007; National Research Council Canada, 2008). In Australia, where mining operations are intense and commonly located in the arid regions prone to dust entrainment, toxic materials associated with aeolian dust are especially important (Pye, 1987; Bollhöfer *et al.*, 2006). Ground conditions, particularly vegetation cover and soil moisture level, are two of the most important factors controlling the susceptibility to aeolian dispersion, as described in the previous section (Greene *et al.*, 2004; SCDSI, 2005; Batjargal *et al.*, 2006). Historically, in Australia, an extensive mining operation would deplete the vegetation cover and in an arid climate, the moisture level of the soil is lowered leading to enhanced aeolian dispersion. Even today, the legacy of past poor mining practices has on-going consequences. For example, the Ranger uranium mine in Northern Territory was found to be influencing the surrounding environment by aeolian means (Bollhöfer *et al.*, 2006). One dust event in Canberra in 2005 contained significant amounts of Pb which may have come from Broken Hill (CSEM, 2006). Fortunately, the dust event was rather small, thus it did not have serious health impacts, but it could have been dangerous if the dust event had been as large as the October 2002 dust storm (Figure 2-1) (CSEM, 2006; DEWR, 2007).

Therefore, local populations have serious concerns about mining activities and the influence from them through aeolian means. For example, just after Northparkes Mine, 27 km north north-northwest of Parkes, NSW, commenced an open-cut mining operation in May 1994, 226 out of approximately 600 cattle in a property just 7.5 km north of the mine died (Reid, 1996; Bourke and Ottaway, 1998). Heavy metals blown out from the mine were suspected to be responsible for the incident (Brooks and Gillan, 1996; Bourke and Ottaway, 1998). Furthermore, in 1995, thousands of migratory and non-migratory waterbirds died from a high cyanide level in the tailing dams of Northparkes Mine which had resulted from 'a poor understanding of cyanide chemistry, and inappropriate analytical procedures and interpretation of monitoring data' (Environment Australia, 2003: 6). However, in the former case, it was found that an excessive amount of fluoride from fertiliser was the cause of the deaths and the incident was in no way related to the mining operations (Reid, 1996; Brooks and Gillan, 1996; Bourke and Ottaway, 1998). In the latter case, the conditions quickly recovered after appropriate countermeasures had been taken (Environment Australia, 2003: 6). Nevertheless, these cases illustrate the local population's high concerns about mining activities in Australia.

Contaminated radionuclides (plutonium and americium) have been recorded in one of the most dust-storm-prone regions in Australia, Maralinga, South Australia (Greene *et al.*, 2004).

The radionuclides were found to be confined and stabilised in the upper layer of the soil owing to the presence of micro-organisms and biological crusts (Section 2.3.1.); entrainment risk has been investigated and assessed as low (Greene *et al.*, 2004). However, the ingestion risk of these radionuclides must be recognized since the area lies within one of the windward regions of the dust events (Figure 2-5).

2.5.3. Salinisation and Sodification

Whereas salinity refers to the amount of soluble salt in a soil, sodicity refers to the amount of sodium ions adsorbed onto soil particles (Irvine and Doughton, 2001). Increases in salinity and sodicity are defined as salinisation and sodification, respectively. In general, both phenomena have adverse effects on the landscape. Sodicity has a strong influence over the soil structure (Irvine and Doughton, 2001). Sodic soils are easily dispersed when wet and in contrast, scalded when dry (Irvine and Doughton, 2001). Therefore, they are highly prone to water erosion and cause problems in the penetration of water and plant roots at the same time (Irvine and Doughton, 2001). On the other hand, salinity has a direct effect on plant growth due to reduced osmotic pressure and increased toxicity (Irvine and Doughton, 2001).

A link between salinisation and sodification, and aeolian dust in Australia is possible but has not yet been conclusively established. Some past research supports this hypothesis (Acworth *et al.*, 1997; Jankowski and Acworth, 1997; Acworth and Jankowski, 2001; Melis and Acworth, 2001; McPherson, 2003; Smithson, 2004; Bierwirth and Brodie, 2008; Cattle *et al.*, in press). Figure 2-6 is a schematic diagram of typical aeolian dust transportation in Australia. As explained in Section 2.3.2., inland basins are considered to be the sites of origin of major dust events. These basins effectively collect sediments, including salts, by fluvial processes from the surrounding source areas. This is especially the case in the Lake Eyre Catchment, as it is an enclosed drainage system with no water-way connecting it to the ocean, and thus has a high potential for the accumulation of salts (Bonython, 1956). For example, Bonython (1956) calculated that there were approximately 700 million tonnes of sodium chloride in Lake Eyre North and an average 20 cm of salt crust covering the surface. In terms of accession rate, Gunn and Fleming (1984) estimated a deposition of 478 thousand tonnes of sodium chloride into the lake during flooding in the early 1970s. From a study conducted in Diamond Lake in Wyoming, Greene *et al.*, (2004) postulate that dry saline lakebeds, often found in such regions, are effective in terms of developing salt-rich dust particles which can be easily entrained in the atmosphere. In Australia, a possible influence from such regions through aeolian transportation was reported by Hingston and Gailitis (1976) over Western Australia and by Blackburn and McLeod (1983) over the Murray Darling Basin. Though influence from sea spray exceeded that from terrestrial sources, substantial amount of terrestrial salt was found in considerable numbers of sites in both cases (Hingston and Gailitis, 1976; Blackburn and McLeod, 1983).

Some researchers argue that these salts are/were an important source of the salinisation and sodification experienced in the eastern regions, at least to some extent. For example, Bierwirth and Brodie (2008), using a gamma-ray remote sensing technique, put forward the possibility that the soils of the western slopes of the Great Dividing Range are largely influenced by aeolian salt deposits. Melis and Acworth (2001) noted, based on the particle size distributions of the soils, the possible influence that aeolian dust and associated salt have on landscape formation and salinisation in the upper reaches of the Dicks Creek catchment, near Yass, NSW. The grain sizes of most soils found in the catchment were consistent with those of aeolian dust (phi scale value of 6 - 8) (Melis and Acworth, 2001).

Acworth and Jankowski (2001) assert that the salinity in the Jinchille site at Dicks Creek, NSW is strongly influenced by aeolian dust in terms of salt input into the landscape. The soils of the Jinchille site, which is only 2 km from the catchment divide, have a high level of salinity; however, the level of salinity varies across the site (Acworth and Jankowski, 2001). The source of the high concentration of salt found in the site is unlikely to be the underlying bedrocks, sea-spray or other catchments (Acworth and Jankowski, 2001). This is because, first, the salt concentration of the aquifer of the bedrock, which comprises Ordovician marine sediments, is low and thus could not be the source of the salinity (Acworth and Jankowski, 2001). Second, sea-salt is unlikely to be the source as well, because the sea-salt transported and deposited by means of wind and precipitation is more likely to be distributed uniformly across the landscape, unlike the highly variable distribution actually observed in the site (Acworth and Jankowski, 2001). In addition, the salt is unlikely to have come from other catchments, considering that the site is only 2 km from both a groundwater and a surface water divide (Acworth and Jankowski, 2001). Therefore, according to Acworth and Jankowski (2001), salt-rich aeolian dust deposition is most likely responsible for the salinity reported in the region.

Furthermore, Smithson (2004) concluded that clay-rich, unconsolidated, sedimentary units, which have derived from aeolian deposition during the glacial periods of the Quaternary, are responsible for salinity and sodicity around the Snake Gully Catchment in central NSW. Smithson (2004) asserts that the sodium chloride salt associated with this aeolian deposition is the pivotal contributor to such phenomena. She has calculated that every erosion event of these sediments of 20m × 20m and 2m thickness will provide 772 kg of salt to the surface water system (Smithson, 2004).

However, a consensus on this conclusion has not been reached (Hesse and McTainsh, 2003; Greene *et al.*, 2004; Hesse, 2004; Greene *et al.*, in press). For example, Hesse (2004) cites the lack of quantitative data to confirm the link between aeolian dust depositions and the consequent salinisation, such as the evidence for co-transportation and co-deposition of terrestrial soil and terrestrial salts from inland saline basins. The evidence for these phenomena is not easily discerned, since the soluble salts are easily leached out from the landscape once the dust is deposited onto the ground (McPherson, 2003) and mineral dusts are quickly integrated

into the in-situ landscape (Cattle *et al.*, in press). For example, McPherson (2003) has reported an interesting contrast of salt accumulation between those of high and low relief environments in the very same Upper Billabong Creek Catchment of NSW. Despite the similar deposition rate of salt in these environments, the low relief environment accumulated markedly more salt through a leaching process from the surrounding areas, compared to the high relief environment (McPherson, 2003).

Sources and Sinks of Aeolian Dust

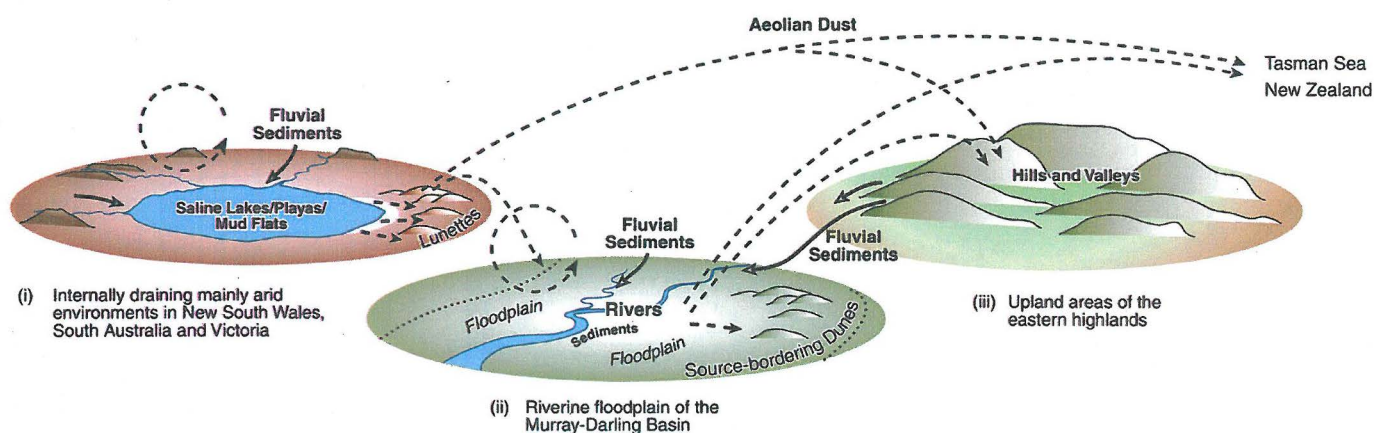


Figure 2-6: Schematic diagram of Australian dust transportation
(Source: Greene *et al.*, in press)

Despite the controversy in Australia, a clear relationship between aeolian dust and salinisation has been claimed in other parts of the world. In Central Asia, a wide range of adverse influences caused by salt-rich *white* dust from the bottom of the dried-up Aral Sea, and a sharp increase in salinisation around the region, has been reported (Orlovsky and Orlovsky; 2001; Mees and Singer, 2006). The white dust could contain more than 90% salt and its deposition rate is reported to be up to 150 kg ha^{-1} in parts (Mees and Singer, 2006). Similarly, Abuduwaii *et al.* (2008) have concluded that salinisation around the western Junggar Basin in northwest China is at least partially a consequence of salt dispersion associated with dust from the lakebed of dried-up Lake Ebinur. They calculated that up to 25% of the total dust deposition around the region was soluble salts (Abuduwaii *et al.*, 2008). In addition, a study of the salt lakes in Texas and the sabkha near Abu Dhabi in the United Arab Emirates shows clear decreases in the salt accumulation ratio with increased distance from the lakes (Wood and Sanford, 1995). However, further evidence is needed to establish this relationship for Australia. Considering the significant effect of salts in the Australian soil-landscape, further research on the role of dust in transporting salts is warranted (McTainsh and Strong, 2007; Greene *et al.*, in press).

Some evidence of a terrestrial source of salt in Australia is captured in the satellite image of an aeolian dust event in Figure 2-7. In this event, the dust is clearly originating from the centre of the Lake Eyre Basin, including salt rich playas and dried lakes. Thus, there is a

potential for aeolian dust to transport salt to other regions in Australia. This aeolian dust may contribute to salinisation and sodification in other sites as well.

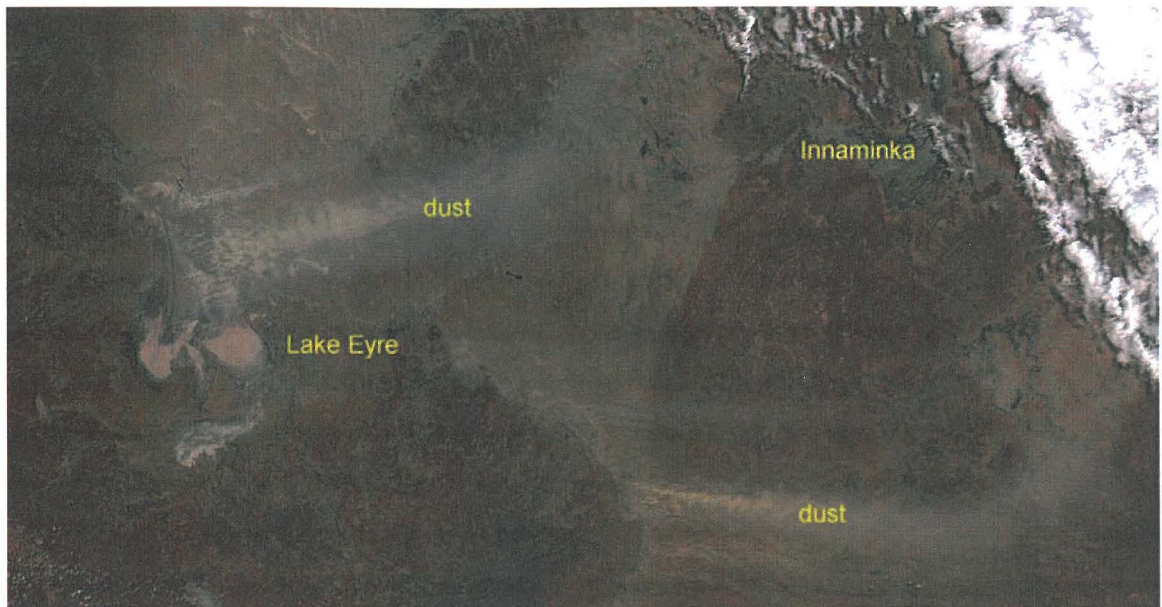


Figure 2-7: Satellite image (MODIS) of dust blown from Lake Eyre on 28 October, 2002 (Source: Dust Watch, 2002 cited in R. Greene, email. comm., 21 October 2007)

2.5.4. Climate Change

Not only is aeolian dust one of the consequences of climate, that is meteorological conditions as explained in Section 2.3.2., but aeolian dust has a potential to influence the global climate as well. Aeolian dust has a potential to both influence and be influenced by, the climate (Pye, 1987; Rotstayn *et al.*, 2008). However, the whole mechanism is yet to be investigated (SCDSI, 2005; McTainsh and Strong, 2007). For example, soil is known to be a significant carbon sink; this carbon, if released into the atmosphere by adverse anthropogenic activities, will enhance global warming (Arimitsu, 1997; Matsunaka, 2003). Yan *et al.* (2005) estimate the annual global soil organic carbon input to the atmosphere by soil wind erosion to be around 1.0 PgC, based on the results from Smith *et al.* (2001).

In addition, aeolian dust exerts a significant impact on the global temperature through its negative (cooling) as well as positive (warming) radiative effect (Schollaert and Merrill, 1998; Woodward, 2001; Forster *et al.*, 2007; Sivakumar, 2007). According to Woodward's (2001) calculations, aeolian dust has the potential to increase annual mean direct forcing by 0.07 W m^{-2} globally at the top of the atmosphere and to decrease 0.82 W m^{-2} at the surface only by its direct effect, because aeolian dust reflects the sunlight back to space, preventing the energy that warms the Earth from reaching the ground (Sivakumar, 2007). Forster *et al.* (2007) estimate an up to 0.2 W m^{-2} decrease (average estimate: 0.1 W m^{-2} decrease) in radiative forcing caused by the direct influence of anthropogenic dust. However, the impact of the indirect effect of the aerosols, which include dust, by means of cloud albedo (a measure for reflectivity of

electromagnetic radiation) forcing, since dust particles are excellent condensation nuclei for cloud formation (Pye, 1987), is estimated to be up to 1.8 W m^{-2} decrease (average estimate: 0.7 W m^{-2} decrease). Interestingly, this figure is comparable to that of the greenhouse gas effect induced by CO_2 , which is an increase of 1.83 W m^{-2} at the maximum estimation (average estimate: 1.66 W m^{-2} increase). Therefore, aeolian dust is assumed to have the potential to offset, at least partially, the warming effect from greenhouse gases (Forster *et al.*, 2007; Rotstayn *et al.*, 2008). However, there still remain large uncertainties in the degree of radiative forcing by aerosols (Mitchell *et al.*, 2006; Forster *et al.*, 2007; Rotstayn *et al.*, 2008).

In contrast to the above findings on negative radiative forcing by aeolian dust, research by Tanaka and Chiba (2006) points out that dust storms originating in Australia have the possibility of influencing global warming by their positive radiative effect when deposited on snow and ice in Antarctica, even though the total amount of emissions from the continent is not large compared to other regions of the world (the amount of dust emissions in Australia is only about 10% of that in North Africa). There are two reasons suggested for this. First, the dust of Australian origin is the most dominant dust in the atmosphere across the southern hemisphere, including Antarctica (Tanaka and Chiba, 2006). The dust emissions from Australia are roughly equivalent to the total emissions from South America and South Africa (Tanaka and Chiba, 2006). Second, impurities caused by dust deposition on the surface of the snow are among the major causes of reduction of albedo (Aoki *et al.*, 2003). Therefore, Australian dust is not just a domestic issue, but a global problem as well, since Australian dust can reduce albedo by covering the snow surface of Antarctica, which as a consequence induces global temperature fluctuations.

In addition to the above impacts on the global climate through both positive and negative radiative effects, aeolian dust influences global climate through micro-organisms, such as phytoplanktons in the ocean as well (Mackie *et al.*, 2008). Dust deposits in marine environments act as a fertilizer, and increased phytoplankton growth has been observed in several parts of the world as a result (Garrison *et al.*, 2003; SCDSI, 2005). In particular, Fe is assumed to be an important source of nutrients for micro-organisms in remote seas such as the Southern Ocean (Section 2.5.1.) (McTainsh and Strong, 2007). The enhancement of productivity by Fe can occur by catalysing a more efficient use of macronutrients such as N, P and Si, and/or by catalysing a more efficient nitrogen fixation function of the organisms (Jickells *et al.*, 2005). However, the availability of Fe in the surface water of the seas is often the limiting factor for the micro-organisms' production, since the demand for Fe is high and the upwelling of Fe from the deep sea is not enough to meet this demand (Jickells *et al.*, 2005). Since fluvial (626 to 963 Mt yr^{-1}) or glacial Fe inputs (34 to 211 Mt yr^{-1}) are not available in the remote seas, and the hydrothermal and authigenic Fe inputs, which are available, are only 14 and 5 Mt yr^{-1} , respectively, 16 Mt yr^{-1} of aeolian input constitutes a large proportion of the total input in remote seas (Poulton and Raiswell, 2002; Jickells *et al.*, 2005). Therefore, Fe input into remote

seas by means of long-distance aeolian dust transportation from the land is highly significant for the productivity of micro-organisms in these waters (Jickells *et al.*, 2005).

These micro-organisms are also capable of uptaking a significant amount of CO₂ and acting as an immense carbon sink by exporting carbon to deep water by means of a particulate-matter and/or dissolved-matter form, which in turn influences the global climate (Jickells *et al.*, 1998; Mackie *et al.*, 2008). However, the productivity of the micro-organisms is more complex than a simple Fe restriction; phytoplankton is constrained by other factors as well, depending on the conditions of the water (Jickells *et al.*, 2005; Mackie *et al.*, 2008). In *low-nitrate low-chlorophyll* water, P, CO₂, N and P can be a limiting factor, while in *high-nitrate low-chlorophyll* water, availability of sunlight and Si can limit the productivity (Boyd *et al.*, 2007; Mackie *et al.*, 2008). The interaction among sea water conditions, aeolian dust input and the productivity of the micro-organisms is complex and much more research is needed in this area.

Interestingly, as discussed in the beginning of this section, terrestrial soils are a very important source of carbon sinks (Yan *et al.*, 2005). However, on the other hand, aeolian dust, which is actually one of the consequences of soil erosion, is an important fertiliser for micro-organisms in the oceans, which also act as immense carbon sinks (Jickells *et al.*, 2005). Therefore, to evaluate the complexity of the impacts of dust on global climate change, a more coherent and holistic understanding of the whole system is needed (Jickells *et al.*, 2005).

2.6. Summary

This literature review has examined a wide range of past research associated with aeolian dust. Overall characteristics of the aeolian dust in Australia, its causes, deposition and consequent effects have been outlined. Although its significance might have declined since the last glacial maximum, terrestrial salt dispersion associated with dust from ephemeral lakes and brackish playas could exist even today. This might be insidiously inducing various adverse effects, including salinisation and sodification, on the leeward regions, that is in the agricultural zones in the southeast. However, further research on this topic is needed to confirm this possibility — co-transportation and co-deposition of dust and terrestrial salt.

The next chapter describes the protocol for sample collection and analysis designed for this study, through which it is hoped to reach a better understanding of these important phenomena.

3. Methods

3.1. Introduction

This chapter initially outlines the sites from which the various dust samples used in the study were collected. The analysis protocols for the CLW and CRS projects (CSIRO and Cowra samples, respectively) are then described, including the IBA carried at ANSTO. An outline of the calculations used to determine the various salt fractions and the total sample weight, is then provided. Finally the procedures are described for principal component analysis (PCA), back trajectory analysis, and scanning electron microscopy (SEM), all of which were used to determine the likely origins of the dust and hence its relationship to know salt source.

3.2. Sample Collection

The samples of aeolian dust examined in this research were provided through two independent projects. These projects are co-ordinated by the CSIRO Land and Water (CLW) and the NSW Department of Environment and Climate Change, Cowra Research Station (CRS). The 16 sampling locations are shown in Figure 3-1. Circles represent the CLW sampling sites and a rectangle represents the sampling site at CRS. These numbers are used as identification for each site in Table 3-1 (Section 3.3.).



Figure 3-1: The location of 16 sampling sites associated with this research consisting of the CLW project (1 – 15) (circles) and CRS project (16) (rectangle)
(Source: Geoscience Australia, 2008)

(i) CLW project (CSIRO samples)

The majority of the samples examined for this project were obtained through the CLW project. This project specifically documents ion chemistry and the stable isotopes of atmospheric precipitation, and hence, initially, samples are collected as rainfall through devices especially designed for that purpose (Cresswell *et al.*, 2006). Most of these devices are maintained by the Australian Bureau of Meteorology (BoM); however, some are managed by local agencies such as CSIRO and the Queensland Department of Natural Resources, Mines and Water (Cresswell *et al.*, 2006). In total, 20 sample collectors have been installed across Australia (Cresswell *et al.*, 2006). An image of a CLW sampling device and an example of its placement at a sampling site are presented in Figure 3-2. The sample collection area of the device (i.e., size of the funnel) was 314 cm² for most of the sites, but there were some with only 78.5 cm² collection area.



Figure 3-2: CLW sampling device and an example of placement at a CSIRO sampling site
(Source: Cresswell *et al.*, 2006)

The samples from the CLW project (subsequently referred to as CSIRO samples) are collected on a monthly basis. However, there are some exceptions when they are sampled over a 0.5 or 2 month period. The samples are first sent to the CLW in Adelaide and sub-sampled for ion chemistry and stable isotope analysis. However, because the samples are collected through rainfall collectors, samples are not available for those months in which precipitation has not occurred. The analyses done in CLW only require approximately 50 ml of rainwater (F. Leaney, e-mail comm., 9 May 2008). If there is still rainwater left after this amount has been sub-

sampled, samples are subsequently sent to ANU in a plastic bottle (Figure 3-3). As the focus of the current research was on south-east Australia, 15 different CLW sampling sites across this region were investigated in this research (sites 1 – 15 in Figure 3-1). The samples studied were collected from May 2007 to April 2008 (Table 3-1).



Figure 3-3: An example of CSIRO sample. Note the deposition of solid material (dust) on the bottom of the bottle in the right image.
(Photo by: Y. Shiga, 14 May 2008)

(ii) CRS project (Cowra samples)

Only a minor portion of the samples used for the purpose of this research came from Cowra Research Station (CRS) in Cowra, NSW (Site 16 in Figure 3-1). The sampling device is depicted in Figure 3-4. The sample collection area of the device, i.e., $1,131 \text{ cm}^2$, was much larger than that of CSIRO samplers, i.e., 78.5 or 314 cm^2 . Samples from CRS (hereafter referred to as Cowra samples) were also collected on a monthly basis — one exception was a January – February 2008 sample that had been collected over a two month period. The samples studied were collected from October 2006 to June 2008, as either wet or dry deposition events, which covered the entire collection period for CSIRO samples (Table 3-1). The Cowra samples were collected in suspension using distilled water to wash out the dust from the samplers at the end of each collection term. Therefore, the availability of the samples was not affected by the amount of precipitation, unlike the CSIRO samples. Collected samples were placed in a vial and dried in an oven. Thus, the samples were in a dried form and were not suspended in water or coated on a filter when they were sent to ANU (Figure 3-4).

List of Acronyms and Abbreviations

AINSE	Australian Institute of Nuclear Science and Engineering
ANSTO	Australian Nuclear Science and Technology Organisation
ANU	Australian National University
AUD	Australian dollars
BoM	Bureau of Meteorology
CLW	CSIRO Land and Water
CRS	Cowra Research Station
CSEM	Centre for Science and Engineering of Materials
DEWHA	Department of the Environment, Water, Heritage and the Arts, Australia
DEWR	Department of the Environment and Water Resources, Australia
ERDC	Energy Research and Development Corporation
GDAS	Global Data Assimilation System
HYSPLIT	HYbrid Single-Particle Lagrangian Integrated Trajectory
IBA	Ion Beam Analysis
ka	thousand years ago
min	mineral
NASA	National Aeronautics and Space Administration
nss	non-sea-salt
OMI	Ozone Monitoring Instrument
PCA	Principal Component Analysis
RMB	Renminbi
SCDSI	Special Committee on Dust and Sandstorm Issues
SEM	Scanning Electron Microscopy
SOEC	2006 Australian State of the Environment Committee
ss	sea-salt
ts	terrestrial SALT

List of Chemical Symbols

C	Carbon
N	Nitrogen
O	Oxygen
F	Fluorine
Na	Sodium
Mg	Magnesium
Al	Aluminium
Si	Silicon
P	Phosphorus
S	Sulphur
Cl	Chlorine
K	Potassium
Ca	Calcium
Ti	Titanium
V	Vanadium
Cr	Chromium
Mn	Manganese
Fe	Iron
Co	Cobalt
Ni	Nickel
Cu	Copper
Zn	Zinc
As	Arsenic
Br	Bromine
Rb	Rubidium
Sr	Strontium
Y	Yttrium
Zr	Zirconium
Sb	Antimony
Pb	Lead



Figure 3-4: CRS sampling device (top right and top left), and an example of a dried sample sent from CRS in a plastic container (bottom)
 (Photo by: top left: R. Greene, 22 May 2008; top right and bottom: Y. Shiga, 22 May 2008)

3.3. Summary of Evaluated Samples used in this Research

Samples were collected by the 15 CLW dust collectors and at the CRS (Figure 3-1). These sites were mainly located in south-eastern Australia; most samples were collected on a monthly basis from May 2007 to April 2008. In addition, samples were not always collected exactly from the first day of the month to the last: the start and the end date of most of the samples varied by a few days. However, some samples were not available for the purpose of this research due to reasons such as a lack of rainfall or an insufficient amount of dust. The samples evaluated in this research are listed in Table 3-1.

For some of the CSIRO samples, only insoluble components were evaluated; however, for the majority of the CSIRO samples, both insoluble and soluble materials were evaluated (Section 3.4).

Table 3-1: List of CSIRO and Cowra samples evaluated in this research; for the CSIRO samples, '✓' indicates that only the insoluble materials for these samples were analysed, whereas '✓✓' indicates both insoluble and soluble materials were analysed for these samples. For Cowra samples, '✓' indicates analysis done on Teflon filters, whereas '✓✓' indicates analysis done in pellets. Note that some samples are collected over a 2-month period (e.g., Cowra January – February, 2008) or sampled twice (the first and second halves of the month) in the same month (e.g., Townsville January). A blank indicates no sample was available. (1/2)

	ID	Lat	Long	2007.5	2007.6	2007.7	2007.8	2007.9	2007.10	2007.11	2007.12	2008.1	2008.2	2008.3	2008.4
Cobar	1	-31.4840	145.8294		✓✓	✓✓		✓	✓	✓	✓	✓	✓	✓	✓✓
Sydney	2	-33.9411	151.1725	✓✓		✓✓		✓	✓	✓✓	✓	✓	✓✓	✓✓	✓✓
Wagga Wagga	3	-35.1583	147.4573		✓			✓	✓	✓	✓✓	✓✓	✓✓	✓✓	✓✓
Melbourne	4	-37.6632	144.8337		✓✓	✓✓		✓	✓	✓✓	✓	✓	✓✓	✓✓	✓✓
Mildura	5	-34.2306	142.0839		✓✓	✓✓	✓	✓		✓	✓	✓✓		✓✓	✓✓
Cape Grim	6	-40.6822	144.6883	✓✓	✓✓			✓	✓	✓✓	✓		✓✓	✓✓	✓✓
Adelaide	7	-34.9524	138.5204					✓	✓	✓	✓	✓	✓✓	✓✓	✓✓
Woomera	8	-31.1558	136.8054		✓✓		✓✓	✓	✓	✓✓	✓✓	✓		✓	✓✓
Alice Springs	9	-23.7951	133.8890		✓✓		✓✓		✓✓	✓✓	✓✓	✓✓	✓✓		✓✓
Darwin	10	-12.4239	130.8925									✓✓			

Table 3-1 continued (2/2)

	ID	Lat	Long	2007.5	2007.6	2007.7	2007.8	2007.9	2007.10	2007.11	2007.12	2008.1	2008.2	2008.3	2008.4
Halls Creek	11	-18.2292	127.6636						✓✓		✓✓	✓✓			
Brisbane	12	-27.3917	153.1292									✓✓			
Charleville	13	-26.4156	146.2542									✓✓			
Townsville	14	-19.2483	146.7661						✓✓		✓✓	✓✓			
Mount Isa	15	-20.6778	139.4875						✓✓		✓✓				
				2006.10	2006.11	2006.12	2007.1	2007.2	2007.3	2007.4	2007.5	2007.6	2007.7	2007.8	2007.9
Cowra	16	-33.8100	148.7058	✓✓	✓✓	✓	✓✓	✓✓	✓✓	✓✓	✓✓	✓✓	✓✓	✓✓	✓
				2007.10	2007.11	2007.12	2008.1	2008.2	2008.3	2008.4	2008.5	2008.6			
Cowra	16	-33.8100	148.7058	✓	✓✓	✓✓	✓✓		✓	✓	✓	✓			

3.4. Procedures

Both the CSIRO and Cowra samples were initially sent to ANU for processing and then sent onto ANSTO for IBA (ion beam analysis). Subsequently, these samples were sent back to ANU, where the samples were subjected to further SEM examination, depending on the IBA results (Tables 3-2 and 3-3).

Ninety five aqueous dust/rainfall samples from CLW were first filtered at ANU before sending them to ANSTO, since IBA (and also SEM) is not suitable for analysing samples suspended in water. The filtration procedure is summarised in Figure 3-5. ADVANTEC filters, 47 mm in diameter, and made of polycarbonate, with 0.4 μm pores, were used for this purpose. In addition to the insoluble materials being collected by the filtration, the filtrate of 60 samples (approximately two thirds of the total rainfall samples) was also evaluated. In this case, the filtrate was collected in a petri dish by using another ADVANTEC filter over the bottom of the dish (Figure 3-5). The filters were then placed in an oven (ca. 50 °C) at ANU for drying before being sent to ANSTO. These filters were sent back to ANU after IBA had been completed at ANSTO.

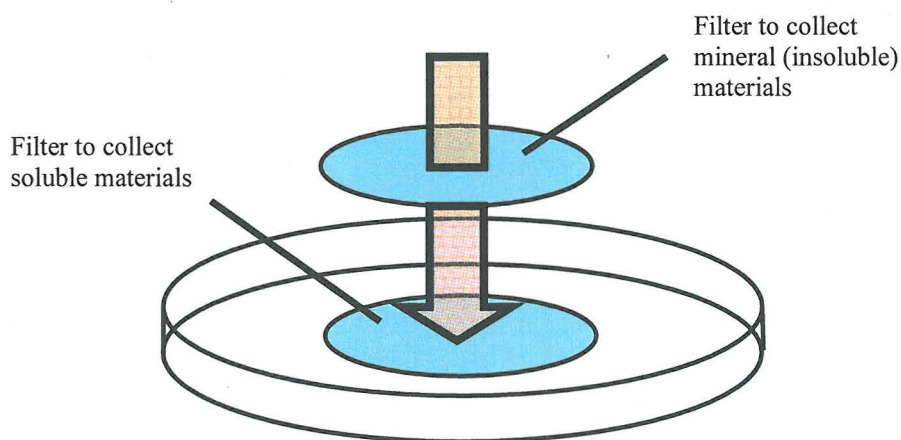


Figure 3-5: A schematic diagram of the filtration procedure. The orange arrow indicates the flow of the rainfall sample. Both soluble and insoluble materials were collected for the most of samples using two sets of filters and a petri dish; however, only the insoluble portion was collected for approximately one third of the samples.

The dried Cowra samples sent to ANU in vials were first divided into two parts: one part was kept for SEM and the other was sent onto ANSTO for IBA. This was because while CSIRO samples coated on the filters could be utilised later for SEM analysis after IBA, the preparation method for IBA of the Cowra samples prevents this (Section 3.5.1.). Therefore, Cowra samples had to be divided into two before being sent to ANSTO. The analysis procedures used for the CSIRO and Cowra samples are summarised in Tables 3-2 and 3-3, respectively.

Table 3-2: The analysis procedures for CSIRO samples

Procedures		Location
1	Samples are sent to CLW	15 sampling sites
2	Samples are sent to ANU as rainwater in a bottle	CLW
3	Filtration	ANU
4	Samples coated on the filters, insoluble plus some with corresponding soluble materials, are sent to ANSTO	ANU
5	IBA	ANSTO
6	Samples are sent back to ANU	ANSTO
7	SEM are applied as necessary	ANU

Table 3-3: The analysis procedures for Cowra samples

Procedures		Location
1	Samples are sent to ANU as pure dust form in a container	CRS
2	Samples divided into two: one for IBA and one for SEM	ANU
3	Samples for IBA are sent to ANSTO	ANU
4	Preparation for IBA	ANSTO
5	IBA	ANSTO
6	SEM are applied as necessary	ANU

3.5. Analysis

3.5.1. Ion Beam Analysis

Samples were sent to ANSTO for IBA using the STAR Accelerator. For the samples on the filters, the ion beam analysis (IBA) gave the weight per unit area ($\mu\text{g per cm}^2$) for 21 different elements (F, Na, Al, Si, P, S, Cl, K, Ca, Ti, V, Cr, Mn, Fe, Co, Ni, Cu, Zn, Br, Sr, and Pb). For Cowra samples in pellets, IBA gave the weight per unit weight (mg per kg) for 24 different elements (the aforementioned 21 elements plus Rb, Y and Zr). IBA is well known for its high sensitivity and effectiveness, in terms of analysing small-size samples, including aeolian dust (Cohen, 1998; Cohen, 1999; Cohen *et al.*, 2002; Cohen, 2004; Cohen *et al.*, 2004c; Cohen *et al.*, 2007). IBA is also capable of analysing a wide range of chemical elements in a non-destructive manner (Cohen *et al.*, 2004a; Cohen *et al.*, 2004b; Cohen *et al.*, 2004d). Therefore, the results from IBA were considered as the most fundamental data in this research.

However, it must be noted that the IBA results might not exactly reflect the chemical properties of the original sources of dust. This is due to chemical reactions between the elements during transportation. For example, Cl deficit in the aerosols due to acid displacement or catalysis is known (Ayers *et al.*, 1999; Newberg *et al.*, 2005). While this deficit is linked to nitric acids in larger particles (Newberg *et al.*, 2005), that of smaller sub-micron particles is mainly controlled by the sulphuric acid (Ayers *et al.*, 1999). However, the deficits are contained to within a few percentages points in either size (Ayers *et al.*, 1999; Newberg *et al.*, 2005).

IBA was applied to all CSIRO samples (both soluble and insoluble materials) which were on filter backings. As these filters contain impurities, the contribution from these filters was later cancelled out by subtracting the values of blank filters. In contrast, dry Cowra dust samples in a dried form required special preparation before IBA was applied (procedure number 4 of

Table 3-3). If the volumes of the samples were enough to fill the pellets (approximately 235 mm³), then the samples were packed in these pellets and analysed. However, if the volume was not sufficient to fill the pellets, they were filtered instead, utilising an air suction device before applying IBA in ANSTO. The filter used in this latter process was a 25 mm diameter stretched Teflon filter with 4 µm mesh. The chemical composition of the filter was 76% Teflon and 24% carbon. The elements associated with this Teflon filter had no influence over the elements analysed, therefore subtraction was not necessary, unlike the CSIRO samples. The filter was coated with Apiezon grease to minimise the rebound of dust particles during the air filtration procedure. However, rebound could not be completely prevented. The larger particles are especially easily bounced off the filter. Thus, considering the fact that the chemical composition of dust particles may vary according to their particle size, the IBA results for these air-filtered samples are not completely reliable. For example, Si is more likely to be found in a larger size particle, because of this compound's high tolerance to weathering, and hence Si content may be lowered in the IBA results.

The weights of the elements in the dust samples detected by the IBA were further subjected to various calculations to reveal their origins. The process of the calculations is summarised in Figure 3-6. IBA results were first analysed in a set of equations to reveal sea-salt, non-sea-salt and/or terrestrial salt fractions of Na and along with Ca (Section 3.5.1.1.). The results from the calculations were subsequently subjected to further calculations in order to depict the contribution from the salt of terrestrial origin. This was done by two independent means — the calculation of the terrestrial salt contribution ratio (Section 3.5.1.1) and principal component analysis (PCA) (Section 3.5.2). The ratio of terrestrial salt contribution was calculated using the estimated total weight of the samples (Section 3.5.1.3.), in order to compare the level of contribution between the samples.

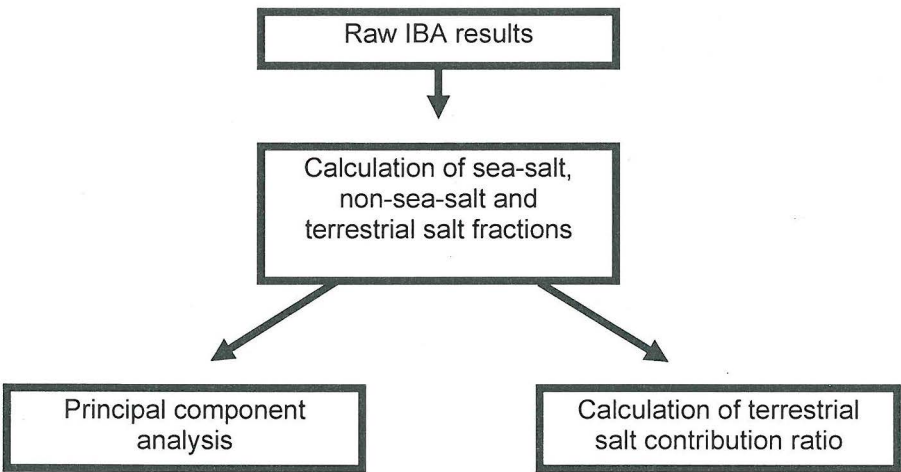


Figure 3-6: The calculation process of IBA results

3.5.1.1. Calculation of Sea-Salt, Non-Sea-Salt and Terrestrial Salt Fractions

The commonly occurring element of aeolian dust and also the important indicator of terrestrial salt, Na, can contain contributions from both oceanic (sea-salt) and terrestrial (non-sea-salt) sources. Therefore, the values for sea-salt (ss) and non-sea-salt (nss) fractions of Na, acquired through IBA, were calculated (i.e., ssNa and nssNa). In doing so, ss and nss fractions of another commonly occurring element of aeolian dust, Ca, were also calculated (i.e., ssCa and nssCa). These fractions were calculated by utilising the two equations below (Equations 3-1 and 3-2) (Benassai *et al.*, 2005).

$$\begin{aligned}\text{Since } nssNa/nssCa &= (Na/Ca)_{\text{crust}} \\ ssNa &= Na - nssNa \\ &= Na - nssCa (Na/Ca)_{\text{crust}}\end{aligned}$$

Equation 3-1: Equation for ssNa

$$\begin{aligned}\text{Since } ssCa/ssNa &= (Ca/Na)_{\text{sea water}} \\ nssCa &= Ca - ssCa \\ &= Ca - ssNa (Ca/Na)_{\text{sea water}}\end{aligned}$$

Equation 3-2: Equation for nssCa

Na and Ca in Equations 3-1 and 3-2 are the value of each element acquired by IBA, whereas $(Na/Ca)_{\text{crust}}$ and $(Ca/Na)_{\text{sea water}}$ represent the average ratio between the two elements in the earth's crust and in sea water, respectively. According to Bowen (1979), $(Na/Ca)_{\text{crust}}$ is 0.560 and $(Ca/Na)_{\text{sea water}}$ is 0.038. It is important to note that because the materials comprising the earth's crust are highly heterogeneous, the composition of materials entrained by wind will reflect this. But in the absence of accurate values for various materials present in the earth's crust and sea water the current values for these ratios are considered to be reasonable estimates. Therefore, Equation 3-3 was set out by substituting Equation 3-1 in Equation 3-2.

$$\begin{aligned}nssCa &= Ca - \{ Na - nssCa (Na/Ca)_{\text{crust}} \} (Ca/Na)_{\text{sea water}} \\ &= (Ca - 0.038 Na) / 0.97872\end{aligned}$$

Equation 3-3: Equation for ssCa and Na

If the calculated nssCa value was larger than the Ca, nssCa was assumed to equal the Ca value detected by IBA. In contrast, if the calculated nssCa value was smaller than 0, the nssCa value was assumed to be 0. The other three values (ssCa, ssNa and nssNa) were then calculated by utilizing Equations 3-1 and 3-2 after nssCa had been determined.

Subsequently, the terrestrial salt (sodium chloride, hereafter referred to as *ts*) and mineral (hereafter referred to as *min*) fractions of nssNa were estimated. In this current research, nssNa was assumed to have two possible compound forms: a soluble form consisting of NaCl (*tsNa*),

which is the main contributor to salinity and sodification, and an insoluble mineral form consisting of Na₂O (minNa), which is less likely to cause these phenomena. Therefore, the Na contribution from the insoluble minNa has to be subtracted from nssNa to reveal the contributions from the terrestrial salt (NaCl), tsNa. Thus, tsNa was calculated by utilising Equations 3-4 and 3-5.

$$\text{tsNa} = \text{nssNa} - \text{minNa}$$

Equation 3-4: Equation for tsNa

$$\text{minNa} = \text{Fe} (\text{Na/Fe})_{\text{mineral dust}}$$

Equation 3-5: Equation for minNa

The value for (Na/Fe)_{mineral dust} used in this research was set as 0.353. This value was calculated from the known composition of Fe₂O₃ and Na₂O in aeolian dust around the world (Pye, 1987). If minNa was larger than nssNa, then tsNa was assumed to be 0. As with the ratios for (Na/Ca)_{crust} and (Ca/Na)_{sea water}, it is recognised that the composition of aeolian dust is highly variable and hence the (Na/Fe)_{mineral dust} ratio will also be highly variable. However, a value of 0.353 is considered to be a reasonable estimate.

3.5.1.2. Soil, Salt and Smoke Contribution

The weights of the elements in the dust samples were further subjected to calculations to determine the respective contributions from soil, salt and smoke.

3.5.1.2.1. Soil Contribution

The amount of soil contribution to dust samples can be calculated by using the five elements which typically dominate soil: Al, Si, nssCa, Ti and Fe (Malm *et al.*, 1994; ERDC, 1995) (Equation 3-6). The oxides of these five elements account for more than 85% of the total weight of the soil contribution of aeolian dust (ERDC, 1995). There are still other elements associated with soil found in aeolian dust such as Mg and K; however, Equation 3-6 already includes the weight contribution from these elements by using a multiplicative factor (ERDC, 1995). In this research, only those samples in which all five elements were present were assumed to be influenced by soil and used to calculate the soil contribution.

$$\text{Soil} = 2.20[\text{Al}] + 2.49[\text{Si}] + 1.63[\text{nssCa}] + 1.94[\text{Ti}] + 2.42[\text{Fe}]$$

Equation 3-6: Soil contribution to aeolian dust

3.5.1.2.2. Salt Contribution

The amounts of both sea and terrestrial salt (sodium chloride) contributions in aeolian dust can be calculated by Equations 3-7 and 3-8 (Malm *et al.*, 1994; ERDC, 1995). In this research, only those samples in which both ssNa (or tsNa) and Cl were present were used to calculate the contribution from salt. However, Cl was not used in these equations since its abundance could be affected by industrial activities, which would increase Cl (ERDC, 1995) and acid displacement or catalysis, which would decrease Cl (Section 3.5.1.).

$$\text{Sea-salt} = 2.54[\text{ssNa}]$$

Equation 3-7: Sea-salt contribution to aeolian dust

$$\text{Terrestrial-salt} = 2.54[\text{tsNa}]$$

Equation 3-8: Terrestrial salt contribution to aeolian dust

3.5.1.2.3. Smoke Contribution

Smoke from a particular activity or incident such as a bush fire can be indicated by the presence of K. However, since K is also found in soil, the calculation of the smoke contribution to total aeolian dust requires the subtraction of this portion of K. Therefore, utilising the general K/Fe ratio in soils of 0.6 (± 0.2), the total weight of K associated with smoke is calculated by Equation 3-9 (Malm *et al.*, 1994; ERDC, 1995). Again, as with the other elemental ratios, the K/Fe ratio in soils will vary according to location. However, 0.6 is considered to be a reasonable estimate. In this research, only samples in which a value of more than 0 after Equation 3-9 was applied were recognised as being influenced by smoke.

$$\text{Smoke} = [\text{K}] - 0.6[\text{Fe}]$$

Equation 3-9: Smoke contribution to aeolian dust

3.5.1.3. Total Weight

The ratios of contribution from soil, salt (both sea-salt and terrestrial salt) and smoke were calculated against the estimated total weight of the dust samples. However, oxygen, which is one of the major elements of dust, was not analysed by the IBA (Bowen, 1979; Pye, 1987; Rodriguez and Dabdub, 2004). Therefore, the weights of the major elements — minNa, Al, Si, K, nssCa, Ti and Fe — which are usually found in their oxide forms in dust, were converted to their oxide forms to estimate the total weight of each dust sample. This was carried out by assuming that these elements were in the oxide compound forms listed in Table 3-4 (Malm *et al.*, 1994; ERDC, 1995). Thus, all the weights for minNa, Al, Si, nssCa and Ti measured by the IBA were assumed to be in the common forms found in aeolian dust of Na₂O, Al₂O₃, SiO₂, CaO and TiO₂, respectively (Pye, 1987). Fifty percent of measured Fe was assumed to be in Fe₂O₃ form

and the remaining half to be in FeO form (ERDC, 1995). Only 60% of K measured by IBA was calculated in its oxide weight because the remaining 40% was considered to derive from smoke and not from the soil (Section 3.5.1.2.3.) (Malm *et al.*, 1994; ERDC, 1995).

Table 3-4: Major soil elements and their assumed oxide forms

Elements	Assumed Compound Form(s)
minNa	Na ₂ O
Al	Al ₂ O ₃
Si	SiO ₂
K	K ₂ O
nssCa	CaO
Ti	TiO ₂
Fe	Fe ₂ O ₃ (50%) and FeO (50%)

Presuming the above contribution from oxygen, the total weight of the samples was estimated using Equation 3-10.

$$\text{Total Weight} = \text{minNa}_2\text{O} + \text{Al}_2\text{O}_3 + \text{SiO}_2 + \text{K}_2\text{O} + \text{CaO} + \text{TiO}_2 + \text{Fe}_2\text{O}_3 / \text{FeO} + \sum \text{remaining elements}$$

Equation 3-10: Equation for total weight

3.5.2. Principal Component Analysis

Principal component analysis (PCA) was applied to the elemental values measured by IBA (Section 3.5.1.). However, for the elements Ca and Na, the sea-salt, non-sea-salt, terrestrial salt and mineral values (i.e., ssCa, ssNa, nssCa, tsNa and minNa) calculated as per the previous equations (Section 3.5.1.1.) were used, instead of using the values measured by IBA. In addition, a correlation matrix was used to normalise the input variables in order to have variance equal to one.

3.5.3. Back Trajectory Analysis

The characteristics of aeolian dust in terms of its spatial distribution can be analysed by utilising a back trajectory analysis (Boyd *et al.*, 2004; McGowan *et al.*, 2005; Wai and Tanner, 2005; Cohen *et al.*, 2006; Cohen *et al.*, 2007; Olmo *et al.*, 2008; Mackie *et al.*, 2008; McGowan and Clark, 2008). In this research, this was done through the web-based HYSPLIT (HYbrid Single-Particle Lagrangian Integrated Trajectory) program, which uses wind speed and direction data to calculate the likely origin of a certain atmospheric environment (Draxler and Hess, 1998; Draxler and Rolph, 2003; Rolph, 2003).

Since the duration of sample collection was long (approximately one month), dates and time of the day had to be carefully chosen to effectively apply the back trajectory analysis. In

order to achieve this, two independent approaches were used: aerosol observation from the satellite and the records of precipitation.

First, aerosol OMI (Ozone Monitoring Instrument) Level 3 data were used. The OMI Level 3 data is a dataset compiled from satellite observations on a daily basis by the National Aeronautics and Space Administration (NASA) (NASA, 2008). The data-set contains information on the abundance of aerosols, if any, in 1 degree latitude by 1.00 degree longitude zones, which cover the Earth (NASA, 2008). Back trajectory analysis was applied to the dates on which the aerosols were detected in the nearest grid according to the OMI Level 3 dataset. However, it must be noted here that the OMI sensor has important limitations regarding this research: although the detection does cover the Earth daily, a particular location is sensed only on a certain time of the day and is not continuously monitored (NASA, 2008). In addition, it is not good at detecting near-surface aerosols (NASA, 2008). Therefore, dust could be undetected because of these temporal and depth constraints.

In addition to the satellite observation, daily records of precipitation were used for selecting the dates. Although the contribution of wet and dry depositions in Australia, especially at a finer scale still remains largely uncertain, smaller particles which have a potential to travel significant distance are more likely, in general, to be washed out and deposited onto the ground by a process of wet deposition (Section 2.4.). Therefore, precipitation was considered as a potential indication of mass dust deposition and hence the back trajectories were applied on those dates when precipitation occurred. However, only when the rainfall was greater than 1.0 mm day⁻¹ was it regarded as effective in washing out the dust. The rainfall records, ultimately derived from the Australian Bureau of Meteorology, were obtained from The Weather Co. (2008).

Twelve back trajectories were calculated for dates which aerosols or precipitation had been recorded. The back trajectories were calculated every two hours from 00hrs until 22hrs of the same day, for those dates on which aerosols had been detected. For the dates on which precipitation has been recorded, the back trajectories were calculated every two hours from 10hrs of the previous day to 08hrs of the following day. This is because the 24 hour rainfall record used in this research was measured from 09hrs of the previous day to 09hrs of the following day (The Weather Co., 2008). Each trajectory was tracked back 48 hours from each start time. The back trajectories were calculated from 500 m above the sampling sites utilising a GDAS (Global Data Assimilation System) dataset. GDAS is a global dataset whose resolution is 3 hours temporally and 1 degree latitude/longitude spatially (NASA, 2008). The final image of the trajectory was plotted on a map with each node representing an interval of 6 hours of a day from 00hrs (i.e., 00hrs, 06hrs, 12hrs and 18hrs).

The influence of precipitation from the presumed source of the terrestrial salt — the salt lake regions of South Australia including Lake Eyre which is the largest inland salt lake in Australia (Figures 2-2 and 2-5) — to the sampling site along the trajectories was further

examined for the trajectories which showed an influence from the source. Dust could have been washed out, if rain had occurred before reaching the site. That is, it is unlikely that the trajectory has transported the dust associated with salt, even though it might have crossed the presumed source region, if the trajectory encountered heavy rain before reaching the site. The precipitation data (mm per hour) between the source and the sampling site were obtained from HYSPLIT program. In addition, the amount of precipitation (mm per hour) at the sampling site at the time when the trajectory reached the site was investigated. This is because the finer particles, which could travel thousands of kilometres, are more effectively deposited with the wet deposition mechanism. An hourly precipitation record was obtained from The Weather Co. (2008) for this purpose. The nearest rainfall record, which was usually taken from no further than several kilometres from a sampling site, was generally used; rainfall was measured at the sampling site for most of the samples. However, for those dust events whose amount was large enough to be detected by the OMI sensor, they might have needed less assistance from rain for deposition to occur.

3.5.4. Scanning Electron Microscopy Analysis

A JEOL JSM-6400 was utilised for SEM (scanning electron microscopy) examination of the morphological features of the CSIRO and Cowra dust samples. These samples were mounted on a round stub (ca. 13 mm in diameter) in order to carry out this analysis. Therefore, the CSIRO samples, which were deposited on filters with a diameter greater than 13 mm, had to be cut to fit the area and shape of the stub. The cut samples were fixed on the stub with double-sided carbon tape. In contrast to the CSIRO samples, pure dust samples from CRS were directly mounted on the stub without any special preparation. After being mounted on the stubs, both the CSIRO and Cowra samples were gold-coated in order for them to acquire a sufficient level of electrical conductivity for SEM examination.

3.6. Summary

This chapter has provided a comprehensive description of sample collection and pre-treatment of the dust samples from the 16 depositional samplers across south-east Australia (15 CLW and 1 CRS) prior to their analysis. Following this, the analysis protocols for both CSIRO and Cowra samples were then outlined. This included IBA (and calculations using that data), PCA, SEM and back trajectory analysis which are used to determine the likely origins of the dust and hence its relationship to known salt sources.

The following chapter presents the results from the set of analyses explained in this chapter.

4. Results

4.1. Introduction

This chapter presents the results from the various analyses explained in Section 3. These are: ion beam analysis (IBA); principal component analysis (PCA); back trajectory analysis; and, scanning electron microscopy (SEM).

4.2. Ion Beam Analysis

The ion beam analysis (IBA) results are presented in four sections: (i) CSIRO samples analysed for both soluble and insoluble materials; (ii) CSIRO samples analysed for only insoluble materials; (iii) Cowra samples analysed in pellets; and (iv) Cowra samples analysed on stretched Teflon filters.

4.2.1. CSIRO Samples — Soluble and Insoluble Materials

Both soluble and insoluble materials for 60 CSIRO samples were examined. Table 4-1 shows only the results which are directly related to the further discussion in this report, while Appendix A-1 shows the results for all 60 samples including the initial soluble and insoluble fractions of the samples. Twenty-one elements were analysed in total. These were: F, Na, Al, Si, P, S, Cl, K, Ca, Ti, V, Cr, Mn, Fe, Co, Ni, Cu, Zn, Br, Sr, and Pb. The unit of analysis was micrograms of the element per square centimetre ($\mu\text{g cm}^{-2}$) on the filter (Section 3.5.1.). Any measurable influence from the filter backing had already been subtracted from the results, thus the values represent only the properties of the dust samples. In addition, it should be noted that the values have been rounded to three decimal places. Therefore, the value 0.000 could denote either that the value is smaller than the minimum detection level and/or that the value is < 0.0005 . Furthermore, 0.000 for the soil, ts, ss and smoke ratios, denotes that the values are actually 0, unless otherwise indicated.

Both the initial measured values and the various calculated values are given in Table 4-1 and Appendix A-1. Mineral (min), terrestrial salt (ts) and the sea-salt (ss) fractions of Na and sea-salt (ss) and the non-sea-salt (nss) fractions of Ca were calculated using Equations 3-1 – 3-5. The soil contributions were estimated using Equation 3-6. Furthermore, salt (ts and ss) contributions were estimated by utilising Equations 3-7 and 3-8. Equation 3-9 was used to estimate smoke contributions. The contributions from the oxide forms of the major soil elements were incorporated into the total sample weight using Equation 3-10. The ratios of soil, salt (ts and ss), and smoke were then obtained relative to the estimated total weight of each sample. These calculated ratios should be larger than the actual ratios. This is because IBA lacks some major dust contributors, such as Mg, O and organic matter, and therefore the calculated total sample weight is underestimated. Even though the total weight sum incorporates the

weight of the oxide forms for some elements, the extrapolation was limited to some extent (Section 3.5.1.3.). However, the ratios can be used to examine the approximate relative difference between the samples.

Of the total 60 samples, 41 showed no contributions from terrestrial salt (i.e., ts ratio = 0). However, of the remaining 19 samples that were determined to contain some terrestrial salt (i.e., ts ratio > 0), several did show a significant amount. Among these, the Adelaide February 2008 sample clearly had the highest terrestrial salt ratio (0.225). Other samples which have shown a high contribution from terrestrial salt were the Melbourne April 2008 (0.114) and the Wagga Wagga December 2008 (0.122) samples.

Table 4-1: Various calculated values using the IBA results for CSIRO samples for which both soluble and insoluble materials had been analysed (1/2)

Element			Unit	Wagga Wagga	Wagga Wagga	Wagga Wagga	Wagga Wagga	Wagga Wagga	Adelaide
				2007.12	2008.1	2008.2	2008.3	2008.4	2008.2
Na	nssNa	minNa	$\mu\text{g cm}^{-2}$	0.185	0.000	0.000	0.772	1.868	4.906
		tsNa	$\mu\text{g cm}^{-2}$	1.017	0.000	0.000	0.000	0.000	132.838
	ssNa		$\mu\text{g cm}^{-2}$	0.448	0.000	0.000	0.193	0.000	152.260
Total			$\mu\text{g cm}^{-2}$	21.255	6.415	10.780	294.649	114.783	1498.201
Soil			$\mu\text{g cm}^{-2}$	14.178	4.222	0.000	347.511	118.369	554.059
Soil			ratio	0.667	0.658	0.000	1.179	1.031	0.370
ts			$\mu\text{g cm}^{-2}$	2.583	0.000	0.000	0.000	0.000	337.408
ts			ratio	0.122	0.000	0.000	0.000	0.000	0.225

Table 4-1: continued (2/2)

Element			Unit	Melbourne	Melbourne	Melbourne	Melbourne	Melbourne	Melbourne
				2007.6	2007.7	2007.11	2008.2	2008.3	2008.4
Na	nssNa	minNa	$\mu\text{g cm}^{-2}$	0.404	0.315	0.000	0.385	6.297	2.870
		tsNa	$\mu\text{g cm}^{-2}$	0.086	1.599	0.000	7.267	0.000	8.444
	ssNa		$\mu\text{g cm}^{-2}$	43.574	29.756	0.000	64.467	15.887	9.586
Total			$\mu\text{g cm}^{-2}$	115.001	84.308	26.111	235.653	243.140	188.126
Soil			$\mu\text{g cm}^{-2}$	11.195	14.727	23.134	48.656	209.533	129.704
Soil			ratio	0.097	0.175	0.886	0.206	0.862	0.689
ts			$\mu\text{g cm}^{-2}$	0.218	4.061	0.000	18.457	0.000	21.448
ts			ratio	0.002	0.048	0.000	0.078	0.000	0.114

4.2.2. CSIRO Samples — Insoluble Materials

For 35 of the CSIRO samples, only the insoluble portions were examined. As explained in Section 4.2.1., a total of 21 elements was analysed. These were: F, Na, Al, Si, P, S, Cl, K, Ca, Ti, V, Cr, Mn, Fe, Co, Ni, Cu, Zn, Br, Sr, and Pb. The unit of analysis was micrograms of the element per square centimetre ($\mu\text{g cm}^{-2}$) on the filter (Section 3.5.1.). The influence from the filter backing had already been subtracted from the values presented in the table. All results are shown in Appendix A-2.

As with the results for the CSIRO samples which had been analysed for both soluble and insoluble portions, various calculations were carried out on the results for the CSIRO samples

whose only insoluble portions had been analysed. However, the results were not useable for the purpose of this research since in none of the samples was a terrestrial salt contribution detected. This lack of terrestrial salt detection could be explained by the high solubility of Na and Cl in the samples. The evidence for this can be seen in Appendix A-1. For example, whereas Cl was detected in 40 out of 60 soluble portions of the CSIRO samples which had been analysed for both soluble and insoluble contributions, it was detected in only six samples in the insoluble portions. Furthermore, the smaller sea-salt values compared to the CSIRO samples analysed for both soluble and insoluble materials (Appendices A-1 and A-2) can also be explained by the Na and Cl leaching through the filters.

4.2.3. Cowra Samples — Pellets

Thirteen Cowra samples from Cowra Research Station (CRS) were examined in pellets. Twenty-four elements were analysed in total. These were: F, Na, Al, Si, P, S, Cl, K, Ca, Ti, V, Cr, Mn, Fe, Co, Ni, Cu, Zn, Br, Rb, Sr, Y, Zr and Pb. The unit of analysis was milligrams of the element per kilogram (mg kg^{-1}) of dust sample contained in the pellets (Section 3.5.1.). The results are shown in Tables 4-2 and Appendix A-3. Table 4-2 shows only the results which are directly related to the further discussions in this report, while Appendix A-3 shows the results for the rest of the samples.

Mineral (min), terrestrial salt (ts) and the sea-salt (ss) fractions of Na, sea-salt (ss) and the non-sea-salt (nss) fractions of Ca, soil, salt (ts and ss) and smoke contributions and the total sample weights using the oxide forms of the major soil elements were calculated using a method similar to those described in Section 4.2.1. In addition, it should be noted that the value 0 denotes not only that the value is smaller than 1, but also the possibility that the value is smaller than the minimum detection level and/or error.

The ratios of soil, salts (ts and ss) and smoke were expected to be more accurate in comparison to those of the other three types of samples (i.e., both types of CSIRO samples and the Cowra samples on Teflon filters). This was because the unit of analysis was mg kg^{-1} and the estimation of the total weight was not needed to calculate the ratios, thus avoiding any errors which could have incurred during such an estimation. However, soil ratios were conspicuously high in most of the samples. For instance, the November 2006 and February 2007 samples had a soil ratio of 1.713 and 1.568, respectively (Table 4-2), which indicated that the amount of soil is more than the total amount of dust sample. This raised doubts as to the accuracy of the soil ratios and the use of Equation 3-6 that was used to calculate the soil contribution to Aeolian dust.

However, the terrestrial salt ratios seemed to be much more reliable. As a comparison, the ts ratios were also calculated using the estimated total sample weight, similar to the calculation used with the other three types of samples. Even though terrestrial salt was only detected in three of the samples (i.e., the March, June and December 2007 samples), the ratios calculated using the two methods appeared to correspond well. Interestingly, all the terrestrial salt ratios

calculated using the estimated total weights were larger than those calculated without using it. The December 2007 sample showed the most extreme difference, with the ratio calculated using the estimated total sample weight (0.012) being approximately 30% larger than the ratio calculated without using an estimated total sample weight (0.009).

The average ts ratio was 0.003 (ranging from 0.000 to 0.018) calculated without estimating the total sample weight and 0.004 (ranging from 0.000 to 0.022) calculated using the estimated total sample weight (Appendix A-3). This ratio was markedly lower compared to the CSIRO samples which had been analysed for both soluble and insoluble materials (Section 4.2.2.). The average ts ratio for CSIRO samples which had been analysed for both soluble and insoluble materials was 0.020 (ranging from 0.000 to 0.225) (Appendix A-1).

Table 4-2: Values calculated using IBA results for Cowra samples in pellets

Element			Unit	Month						
				2006.11	2007.1	2007.2	2007.3	2007.6	2007.12	2008.1 – 2008.2
Na	nssNa	minNa	mg kg ⁻¹	3370	4290	6059	9833	6123	6005	6543
		tsNa	mg kg ⁻¹	0	0	0	4383	7060	3549	0
	ssNa		mg kg ⁻¹	3860	4625	8215	6284	0	27959	6138
Total			mg kg ⁻¹	1492039	928834	1392050	906128	806876	764586	1095404
Soil			mg kg ⁻¹	1713152	0	1568252	0	0	0	1231810
Soil *1			ratio	1.713	0.000	1.568	0.000	0.000	0.000	1.232
ts			mg kg ⁻¹	0	0	0	11132	17932	9015	0
ts *1			ratio	0.000	0.000	0.000	0.011	0.018	0.009	0.000
ts *2			ratio	0.000	0.000	0.000	0.012	0.022	0.012	0.000

*1: Ratios calculated without using estimated total sample weight

*2: Ratios calculated using estimated total weight

4.2.4. Cowra Samples — Filters

Seven Cowra samples were examined on stretched Teflon filters. Twenty-one elements were analysed in total. These were: F, Na, Al, Si, P, S, Cl, K, Ca, Ti, V, Cr, Mn, Fe, Co, Ni, Cu, Zn, Br, Sr, and Pb. The unit of the analysis was micrograms of the element per square centimetre ($\mu\text{g cm}^{-2}$) of the element on the filter (Section 3.5.1.). The results are shown in Appendix A-4.

As with the results for the CSIRO samples which had been analysed for both soluble and insoluble portions, various calculations were carried out for the IBA results for the Cowra samples analysed on the filters. However, the results were not useable for the purpose of this research since the terrestrial salt component was only detected in the September 2007 sample (Appendix A-4). This lack of terrestrial salt detection can be explained by the rebound of dust particles due to preparation procedure (Section 3.5.1.).

In addition, the soil ratio was extremely low compared to that of the Cowra samples in pellets. The average soil ratio was 0.410 (ranging from 0.242 to 0.558) for the samples analysed on Teflon filters, whereas the average for the Cowra samples analysed in pellets was 0.870 (ranging from 0.000 to 1.713) (Appendix A-3). This could be an also effect of rebound of dust

particles during the air-filtration procedure causing particles to be lost, as discussed in Section 3.5.1. Despite the use of Apiezon grease to prevent the particles from rebounding from the filter, some loss could have occurred, especially with the larger particles.

4.3. Principal Component Analysis

The principal component analysis (PCA) results are shown in Tables 4-3 and 4-4. PCA was only applied to the CSIRO samples whose soluble and insoluble materials had both been analysed. This is because the numbers of samples were the largest and the terrestrial salt values — the main focus of this research — were clearly detected in this set. Thus, it was expected that the results would sufficiently depict the important components controlling the terrestrial salt dispersion.

All elements analysed by IBA were used as input variables for PCA, except for Na and Ca, for which derived components (i.e., minNa, tsNa, ssNa, nssCa and ssCa) were used instead (Section 3.5.2.). Therefore, the total number of input variables was 24 elements: F, minNa, tsNa, ssNa, Al, Si, P, S, Cl, K, Ti, nssCa, ssCa, V, Cr, Mn, Fe, Co, Ni, Cu, Zn, Br, Sr and Pb. In addition, the ratios of the various elements to the estimated total sum of the weights were calculated and used in the analysis. This was because the amount of filtrate produced during the filtration was not recorded and hence absolute abundance could not be determined (Section 3.4.).

The factor loading values of the seven defined components are presented in Table 4-3. These seven components, in total, explained 76.7% of the total variations. Since the first component had large factor loading values for sea-salt components, i.e., ssNa, S, Cl, ssCa and Br, and also showed substantial influence from the known sea-salt elements, i.e., S and Br, the factor was labelled 'sea-salt' (c.f., Bowen, 1979). This component explained 24.9% of the total variation. In contrast, the second component had the highest factor loading values in several soil-related elements, i.e., Si, P and Zn and substantially large values for Mn and Ni. Therefore it was defined as 'soil'. This component accounted for 14.3% of the total variation. The third component accounted for 10.7% of the total variation and was labelled 'industry 1', because it was characterised by high factor loading values for Cr, Fe and Ni. The fourth component, explaining 10.1% of the variation, was the only component which had a positive value for both tsNa and Cl besides the first component, which was already labelled 'sea-salt', and so this fourth component was labelled 'terrestrial salt'. However, the loading factors for S, K and Mn were also high. The fifth component was dominated by nssCa and Sr and is probably related to carbonate (c.f., Dart *et al.*, 2007). The sixth and seventh components were difficult to interpret; however since they had large values of industry-related components, such as Co, Cu and Pb, they were labelled 'industry 2 and 3', respectively. The contributions of these components to the total variation were 16.7% in total. Table 4-4 presents the component scores of 60 samples analysed against the seven defined components.

Table 4-3: Components and factor loading values

	Components and Proportions (%)						
	1 st component	2 nd component	3 rd component	4 th component	5 th component	6 th component	7 th component
	Sea-salt	Soil	Industry 1	Terrestrial salt	Carbonate	Industry 2	Industry 3
Element	24.9	14.3	10.7	10.1	6.9	5.3	4.5
F	0.061	0.351	-0.176	-0.574	0.020	-0.225	0.008
tsNa	0.324	-0.203	-0.242	0.335	0.042	-0.366	0.404
minNa	-0.194	-0.412	-0.021	0.258	0.031	-0.469	-0.114
ssNa	0.742	-0.527	0.219	-0.139	-0.189	0.120	-0.135
Al	-0.833	-0.194	-0.151	0.083	-0.219	-0.130	-0.006
Si	-0.794	0.329	-0.219	0.004	-0.242	0.030	0.125
P	0.051	0.564	-0.113	0.222	-0.262	0.422	-0.447
S	0.194	0.272	-0.297	0.573	0.089	0.343	0.191
Cl	0.795	-0.484	0.075	0.122	-0.148	0.045	-0.066
K	-0.368	0.014	-0.333	0.463	-0.399	-0.152	-0.082
nssCa	-0.012	-0.003	-0.316	0.268	0.853	0.046	-0.005
ssCa	0.743	-0.528	0.220	-0.138	-0.187	0.115	-0.131
Ti	-0.798	-0.297	-0.064	-0.090	-0.157	-0.051	0.091
V	-0.574	-0.296	-0.018	-0.036	-0.061	-0.147	-0.448
Cr	-0.015	0.323	0.830	0.105	0.135	-0.131	0.002
Mn	-0.194	0.313	0.189	0.650	0.018	0.132	-0.235
Fe	-0.626	0.177	0.707	0.025	0.039	-0.093	0.057
Co	-0.651	-0.503	0.079	-0.229	0.127	0.165	-0.169
Ni	-0.056	0.381	0.783	0.075	0.110	-0.060	0.087
Cu	-0.621	-0.343	0.183	-0.106	-0.156	0.256	0.128
Zn	0.073	0.626	-0.226	-0.490	-0.009	0.057	-0.057
Br	0.116	0.433	-0.201	-0.608	0.052	-0.147	-0.096
Sr	-0.450	-0.422	-0.091	-0.130	0.624	0.152	-0.272
Pb	-0.396	-0.301	0.065	-0.245	-0.027	0.538	0.452

Table 4-4: Component scores of CSIRO samples for which both soluble and insoluble materials had been analysed (1/2)

Sample		Sea-salt	Soil	Industry 1	Terrestrial salt	Carbonate	Industry 2	Industry 3
Cobar	2007.6	0.133	-0.088	-1.248	1.487	-0.098	-1.686	1.005
Cobar	2007.7	-0.429	1.116	0.959	1.441	-0.003	-0.426	-0.463
Cobar	2008.4	-0.050	0.145	-1.094	2.683	0.085	-1.332	0.360
Sydney	2007.5 – 2007.6	3.122	-0.667	1.495	-0.829	0.014	-0.317	-0.275
Sydney	2007.7	-2.522	-0.105	-0.725	-0.743	1.170	-0.415	-0.163
Sydney	2007.11	0.756	2.098	1.069	1.967	-0.098	1.102	-0.620
Sydney	2008.2	-1.230	1.439	-0.112	-0.809	-0.559	-0.296	0.977
Sydney	2008.3	2.292	-1.401	0.153	-0.463	-0.390	-0.108	0.365
Sydney	2008.4	2.915	0.501	-0.692	1.073	-2.491	1.888	-2.696
Wagga Wagga	2007.12	0.446	-0.298	-1.335	1.528	-0.673	-1.413	1.606
Wagga Wagga	2008.1	0.499	1.775	-0.794	-2.538	-0.014	-1.243	0.567
Wagga Wagga	2008.2	-2.278	0.766	0.290	-0.199	-1.593	0.628	1.084
Wagga Wagga	2008.3	-3.533	-0.193	0.284	0.056	-1.032	-0.763	-0.567
Wagga Wagga	2008.4	-1.465	0.401	-0.468	1.348	-0.469	-0.861	-0.578
Melbourne	2007.6	3.820	-1.823	0.649	-0.858	-0.745	0.588	-0.443
Melbourne	2007.7	3.565	-1.823	0.379	-0.463	-0.525	0.634	0.193
Melbourne	2007.11	-0.184	2.693	-0.618	2.740	-0.657	2.126	-1.060
Melbourne	2008.2	3.572	-1.404	0.119	-0.081	-0.206	0.129	0.289
Melbourne	2008.3	-1.170	-1.778	-0.102	-0.109	-0.158	-0.845	-0.254
Melbourne	2008.4	1.186	-0.286	-1.430	2.219	0.548	-0.782	1.371
Mildura	2007.6	0.879	1.492	0.448	-0.316	1.455	-0.045	0.706
Mildura	2007.7	-1.997	0.773	1.584	-0.235	0.253	-0.809	0.634
Mildura	2008.1	0.406	-1.335	-0.869	0.844	-0.494	-1.716	0.679
Mildura	2008.3	-2.194	-1.231	-0.763	0.168	1.415	-1.210	-0.683
Mildura	2008.4	0.133	-0.742	-1.804	0.060	7.663	1.102	-1.237
Cape Grim	2007.5	3.127	-2.054	0.803	-1.107	-0.555	0.996	-0.400
Cape Grim	2007.6	-3.065	-4.415	1.561	-2.607	1.316	3.143	0.810
Cape Grim	2007.11	1.779	-1.720	0.318	0.040	0.132	-0.118	-0.450
Cape Grim	2008.2	-0.109	-1.096	0.975	0.740	0.031	-0.069	-1.412
Cape Grim	2008.3	1.849	-1.834	0.537	-0.546	-0.260	-0.032	-0.432
Cape Grim	2008.4	3.482	-1.457	0.366	-0.272	-0.599	0.488	-0.472
Adelaide	2008.2	3.002	-1.124	-1.172	1.272	1.637	-0.862	1.642
Adelaide	2008.3	3.761	-1.544	0.184	-0.339	-0.371	0.184	0.110
Adelaide	2008.4	3.204	-0.756	-0.470	0.625	0.054	0.215	0.730
Woomera	2007.6	-1.049	4.095	8.926	1.737	1.331	-0.521	0.350
Woomera	2007.8	-1.345	1.354	-1.607	1.612	-1.795	-0.014	0.084
Woomera	2007.11	1.058	-0.903	-0.491	0.863	-0.147	-1.299	0.151
Woomera	2007.12	-4.061	-1.304	-0.410	-0.895	-0.473	-0.276	-0.513
Woomera	2008.4	-0.751	-1.305	-0.267	0.568	-0.278	-1.594	-0.802

Table 4-4 continued (2/2)

Sample		Sea-salt	Soil	Industry 1	Terrestrial salt	Carbonate	Industry 2	Industry 3
Alice Springs	2007.6	-3.035	0.086	-0.266	0.413	-0.607	-0.461	-0.942
Alice Springs	2007.8	-2.509	-0.384	-0.165	0.727	0.406	-0.597	-0.977
Alice Springs	2007.10	-4.235	-1.482	0.176	-0.677	-0.110	-0.405	-0.675
Alice Springs	2007.11	0.917	1.592	-1.866	2.894	1.872	1.345	0.815
Alice Springs	2007.12	-4.168	-1.585	-0.192	-0.631	-0.294	-0.412	-0.632
Alice Springs	2008.1	-0.996	0.902	-1.145	1.195	0.188	0.182	-0.124
Alice Springs	2008.2	-5.685	-2.762	0.387	-0.781	-0.185	0.378	-2.896
Alice Springs	2008.3 – 2008.4	-0.763	2.878	-1.219	2.903	-0.894	2.222	-1.033
Darwin	2008.1	1.947	0.346	4.121	-0.527	0.530	-1.014	-0.231
Halls Creek	2007.10	-3.255	-0.341	0.303	-1.156	-0.770	-0.439	0.952
Halls Creek	2007.12	-1.111	1.096	-0.690	-0.229	0.084	0.087	1.194
Halls Creek	2008.1	0.363	-0.825	-0.643	0.697	-0.726	-1.484	0.443
Brisbane	2008.1	1.441	3.870	-1.597	-5.328	0.521	-1.622	-0.257
Charleville	2008.1 (1/2)	0.990	4.890	-1.929	-4.807	-0.091	-0.364	-0.825
Charleville	2008.1 (2/2)	0.792	3.106	-1.474	-0.094	0.983	1.484	-0.076
Townsville	2007.10	3.961	-1.624	0.479	-0.831	-0.729	0.451	-0.381
Townsville	2007.12	0.599	3.735	-1.569	-1.598	-0.863	1.035	-0.766
Townsville	2008.1 (1/2)	-0.130	2.956	2.184	-0.775	0.118	-0.032	0.671
Townsville	2008.2 (2/2)	3.667	-0.980	0.652	-1.170	-0.394	0.404	-0.320
Mt Isa	2007.10	-2.944	-0.567	0.132	-0.547	-0.600	2.566	2.933
Mt Isa	2007.12	-3.402	-0.871	-0.308	-1.341	-0.862	2.504	2.936

Despite some uncertainty about the significance of other features (especially Mn loading factors) in component 4, “terrestrial salt” component scores and terrestrial salt (ts) ratios correlate and appear to reflect the contribution from the terrestrial salt input, as seen in samples such as the Adelaide February 2008 (ts ratio: 0.225; 4th component score: 1.272), the Melbourne April 2008 (ts ratio: 0.114; 4th component score: 2.219) and the Wagga Wagga December 2007 (ts ratio: 0.122; 4th component score: 1.528). PCA results also seem to provide additional information on other contributions to the dust. However more extensive use of the PCA results was difficult because PCA was only applicable to the CSIRO samples whose soluble and insoluble properties had both been analysed. Moreover, use of PCA relies upon large coherent data sets and is not as robust as ts ratios which can be calculated even for single samples and so PCA is assigned a secondary role in further discussion.

4.4. Back Trajectory Analysis

Back trajectory analysis was applied to selected samples to determine the differences in their aeolian dust dispersion route. The samples were selected in relation to their degree of terrestrial salt contribution (Section 4.2.1.). The CSIRO samples selected had had both their soluble and insoluble materials measured, and the selected Cowra samples had been measured in pellets.

The Wagga Wagga December 2007 and Melbourne April 2008 samples were selected because of their conspicuously high terrestrial salt ratios, that is 0.122 and 0.114, respectively. Similarly, the Cowra March and June 2007 samples were chosen because of their terrestrial salt ratios, that is 0.011 and 0.018, respectively. As a comparison to these samples containing a high terrestrial salt influence, samples collected in the same locations, but showing no terrestrial salt influence, were also chosen. Therefore, Wagga Wagga January, February, March and April 2008 samples and Melbourne November 2007 and March 2008 samples were chosen for the CSIRO samples. Since there were quite a few Cowra samples in pellets which showed no influence from terrestrial salt, the comparative samples had to be chosen carefully for the Cowra samples. Because December to February are known to be the months for maximum dust activity in Australia (Prospero *et al.*, 2002), samples collected during these months were chosen for this purpose. That is, the three selected Cowra samples were: January and February 2007 and January – February 2008.

In addition, back trajectory analysis was also applied to the Adelaide February 2008 sample due to its extremely high terrestrial salt ratio (0.225). However, no Adelaide sample could be found having a zero terrestrial salt ratio that could be used as a comparison. Tables 4-5 and 4-6 summarise those CSIRO and Cowra samples respectively which had back trajectory analysis applied to them. SEM was also applied to this same set of CSIRO and Cowra samples (Section 4.5.).

Table 4-5: A list of CSIRO samples with back trajectory analysis and SEM applied

Sample		ts ratio
Wagga Wagga	2007.12	0.122
Wagga Wagga	2008.1	0.000
Wagga Wagga	2008.2	0.000
Wagga Wagga	2008.3	0.000
Wagga Wagga	2008.4	0.000
Melbourne	2008.4	0.114
Melbourne	2007.11	0.000
Melbourne	2008.3	0.000
Adelaide	2008.2	0.225

Table 4-6: A list of Cowra samples with back trajectory analysis and SEM applied

Sample		ts ratio
Cowra	2007.3	0.011
Cowra	2007.6	0.018
Cowra	2007.1	0.000
Cowra	2007.2	0.000
Cowra	2008.1 – 2008.2	0.000

4.4.1. CSIRO Samples

The samples chosen for back trajectory analysis represented material that was collected in the samplers over a period of approximately one month. However, it was decided to carry out back trajectory analysis only on certain days in that monthly period. Thus, back trajectory analysis was applied to dates which either: (i) had aerosols detected according to the aerosol OMI Level 3 from NASA (2008); or, (ii) had recorded 1.0 mm day⁻¹ or more rain (Section 3.5.3.). If the trajectory showed an influence from the presumed terrestrial salt source area (i.e., if the trajectory crossed over regions with playas and dried lakes in South Australia) (Figures 2-2 and 2-5), it was further examined to see whether rain had occurred at the time when the potential dust had reached the sampling site or not and the influence of the rain between the presumed source and the sampling site (Section 3.5.3.). No further examination was carried out, if the trajectory did not show any influence from the presumed source region. The results are summarised in Table 4-7.

Table 4-7: The dates for which back trajectory analysis was applied to the CSIRO samples. Back trajectory analysis was applied based on either satellite detection or daily rainfall records, both indicated by '✓' in the column 'Reason for back trajectory analysis'. In the column 'Trajectory influenced by terrestrial salt source', 'X' indicates the trajectory was not influenced by the terrestrial salt source; if the trajectory has shown an influence from the presumed terrestrial salt source, the date, time and corresponding figure (in brackets) were given (trajectories for 'X' are in Appendix B). '✓✓' indicates that the trajectory encountered heavy rain (5 mm hour⁻¹ or more) at the site or along its trajectory. '✓' indicates that the trajectory encountered moderate rain (less than 5 mm hour⁻¹) at the site or along its trajectory before reaching the site.

Sample		ts ratio	Date	Reason for back trajectory analysis		Trajectory influenced by terrestrial salt source	Rain	
				Satellite	Rainfall		Along trajectory	At sampling site
Wagga Wagga	2007.12	0.122	8		✓	X	---	---
			14	✓		X	---	---
			16		✓	X	---	---
			17		✓	X	---	---
			20		✓	X	---	---
			21		✓	X	---	---
			22		✓	21st 20hrs (Figure 4-1)	✓	✓✓
			23		✓	X	---	---
Wagga Wagga	2008.1	0.000	5	✓		X	---	---
			13	✓		X	---	---
			19		✓	X	---	---
			20		✓	X	---	---
			21		✓	X	---	---
			22		✓	X	---	---
			29	✓		X	---	---
			Feb 1		✓	X	---	---
Wagga Wagga	2008.2	0.000	4		✓	X	---	---
			5		✓	X	---	---
			6		✓	X	---	---
			12		✓	X	---	---
			13		✓	X	---	---
			14	✓		X	---	---
Wagga Wagga	2008.3	0.000	1	✓		X	---	---
			17	✓		X	---	---
			23		✓	X	---	---
			25		✓	X	---	---
			26		✓	X	---	---
			Apr 3		✓	X	---	---
Wagga Wagga	2008.4	0.000	18	✓		X	---	---
			28		✓	X	---	---
Melbourne	2008.4	0.114	23	✓		X	---	---
			27		✓	X	---	---
Melbourne	2007.11	0.000	2		✓	X	---	---
			4		✓	3rd 16hrs (Figure 4-2) 3rd 18hrs (Figure 4-3)	✓ ✓✓	0 0
			5		✓	X	---	---
			10		✓	X	---	---
			18		✓	X	---	---
			21		✓	X	---	---
			22		✓	X	---	---
			Dec 3		✓	X	---	---
			8		✓	X	---	---
Melbourne	2008.3	0.000	15	✓		X	---	---
			22	✓		X	---	---
			25		✓	X	---	---
			27		✓	X	---	---
			28		✓	X	---	---
			30		✓	X	---	---
			Apr 7	✓		X	---	---
Adelaide	2008.2	0.225	20		✓	19th 10hrs (Figure 4-4) 19th 12hrs (Figure 4-5) 19th 14hrs (Figure 4-6)	0 0 0	0 0 0
			23		✓	X	---	---

None of the trajectories plotted due to aerosol detection by the OMI sensor showed any influence from the presumed terrestrial salt source. In contrast, one trajectory of the Wagga Wagga December 2007 sample (21st at 20hrs), two trajectories of the Melbourne November 2007 sample (3rd at 16hrs and 18hrs) and three trajectories of the Adelaide February 2008 sample (19th at 10hrs, 12hrs and 14hrs) which were plotted due to having a record of precipitation at the site, appeared to have come from the presumed terrestrial salt source region. However, all trajectories of the Adelaide February 2008 and all trajectory of the Melbourne November 3rd 2008 did not have any precipitation at the sampling site at the time when they reached the site. Furthermore, the November 3rd 18hrs trajectory of Melbourne had already encountered heavy rain ($\geq 5 \text{ mm hour}^{-1}$) along the trajectory before reaching the site. In contrast, the trajectory of Wagga Wagga December 21st 20hrs had encountered only minimal rain along the trajectory, but had had heavy rain at the site.

The trajectories of Wagga Wagga December 22nd 2007 (one trajectory), Melbourne November 4th 2007 (two trajectories) and Adelaide February 20th 2008 (three trajectories) are presented in Figure 4-1, Figures 4-2 and 4-3 and Figures 4-4, 4-5 and 4-6, respectively. These trajectories are extended up to 168 hours to effectively present the influence from the presumed terrestrial salt source regions. Note that rainfall records are also shown in the figures (time increases from right to left). All the other trajectories are to be found in Appendix B.

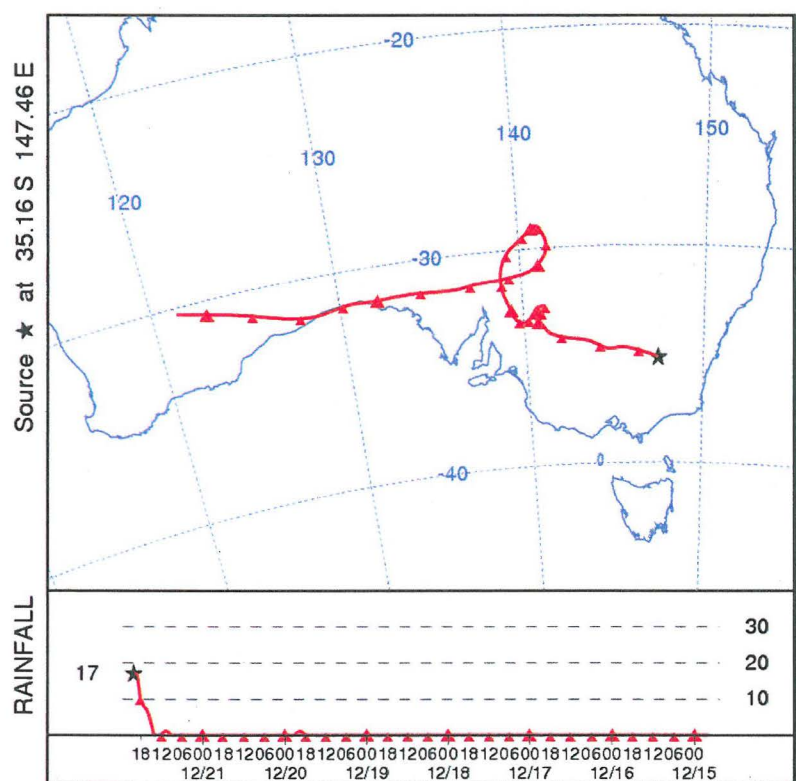


Figure 4-1: A trajectory with rainfall (mm hour^{-1}) record of Wagga Wagga December 21st at 20hrs

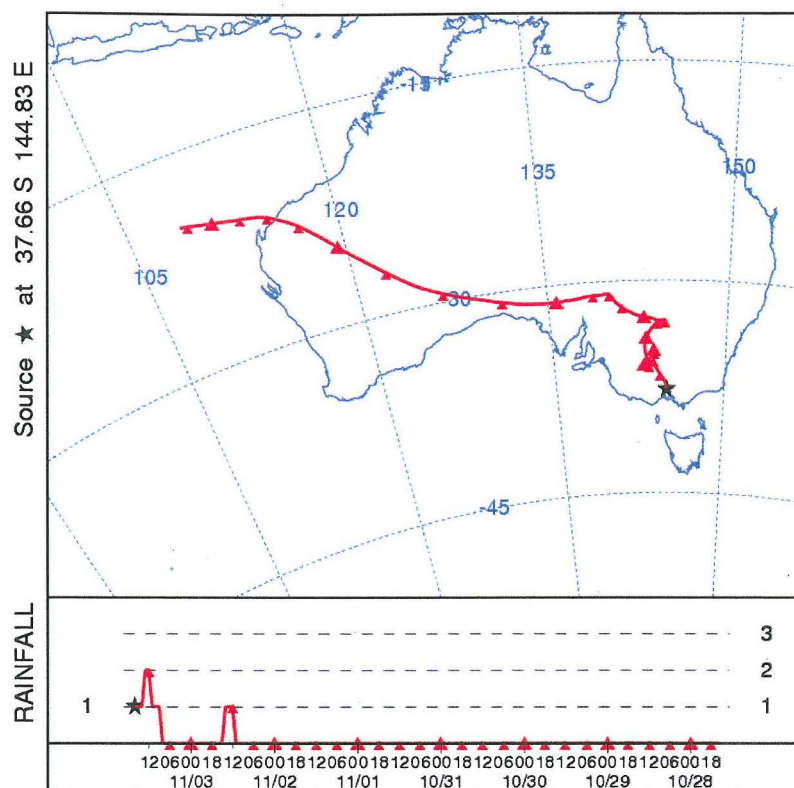


Figure 4-2: A trajectory with rainfall (mm hour^{-1}) record of Melbourne November 3rd at 16hrs

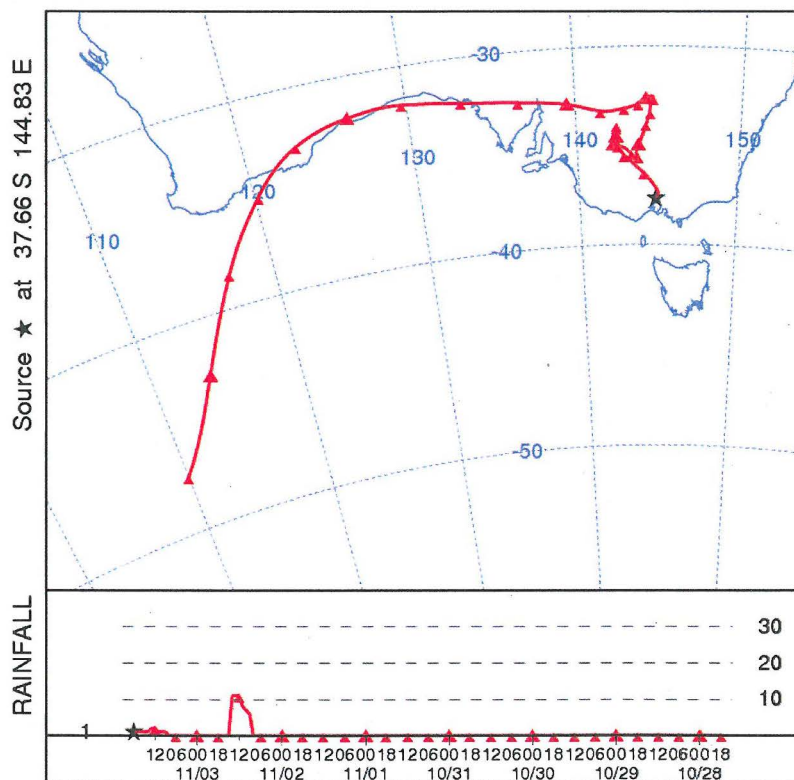


Figure 4-3: A trajectory with rainfall (mm hour^{-1}) record of Melbourne November 3rd at 18hrs

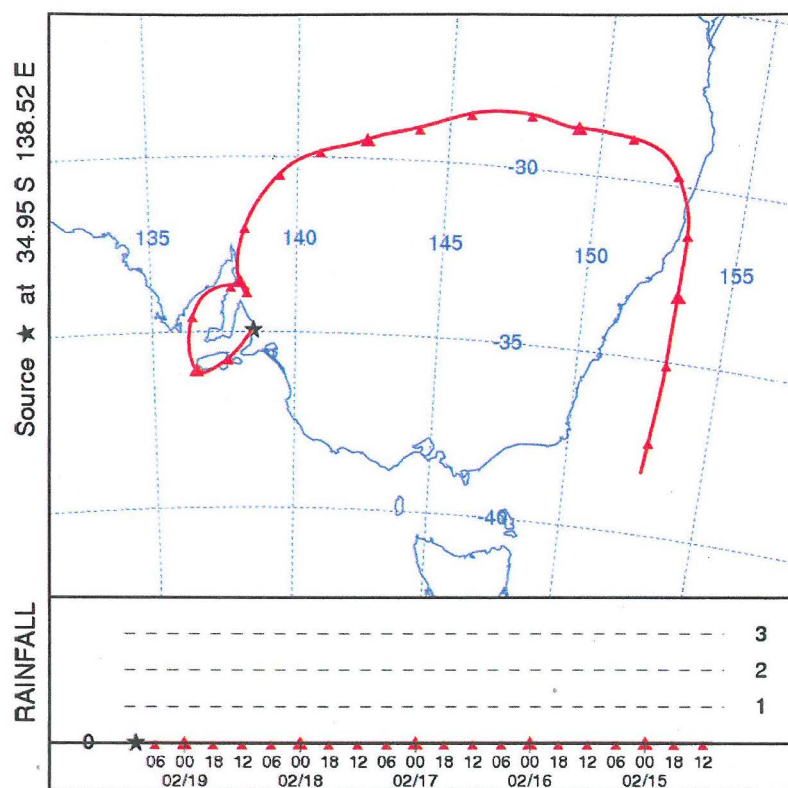


Figure 4-4: A trajectory with rainfall (mm hour^{-1}) record of Adelaide February 19th at 10hrs

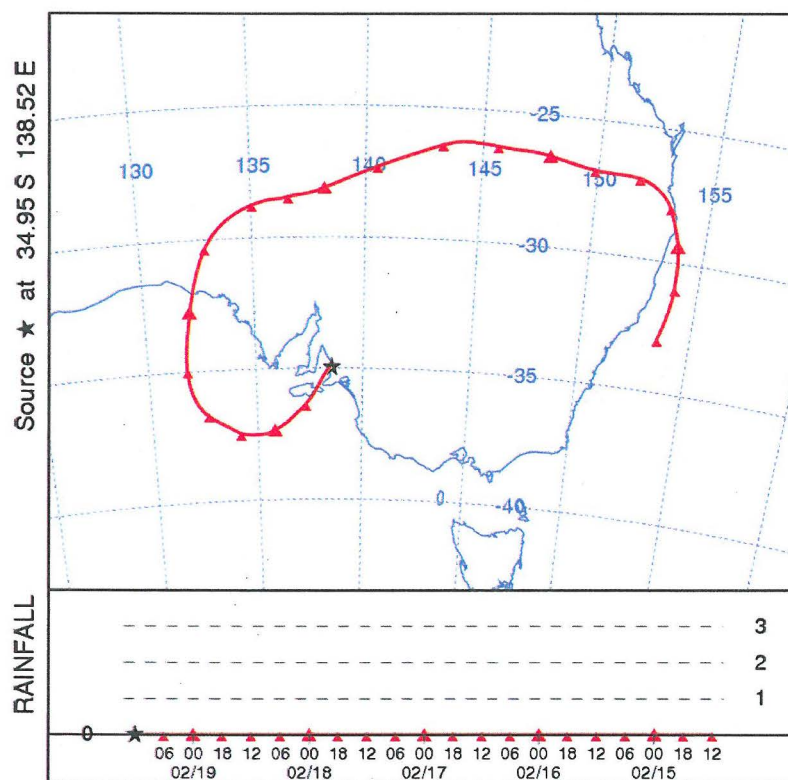


Figure 4-5: A trajectory with rainfall (mm hour^{-1}) record of Adelaide February 19th at 12hrs

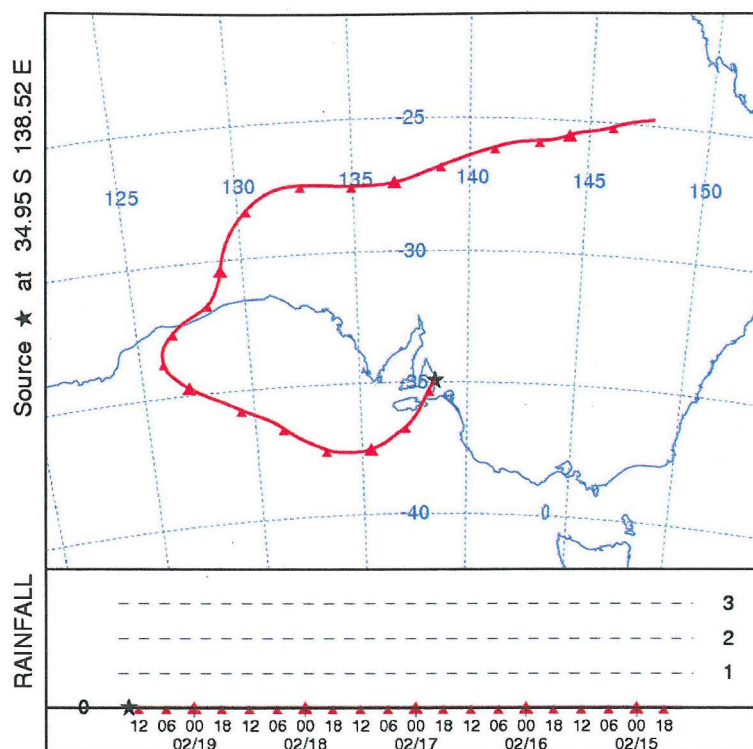


Figure 4-6: A trajectory with rainfall (mm hour^{-1}) record of Adelaide February 19th at 14hrs

4.4.2. Cowra Samples

The back trajectory analysis was applied to two Cowra samples which clearly had a significant terrestrial salt ratio and, as a comparison, to the three Cowra samples which had a zero terrestrial salt ratio. Due to the large number of samples having a zero ratio, the representative samples were selected from the months between December to February, when the dust activity is at its maximum amplitude (Prospero *et al.*, 2002). The back trajectory analysis was applied to these Cowra samples and the results were interpreted using rainfall records in a similar manner to the CSIRO samples (Section 4.4.1.). The results are summarised in Table 4-8.

Table 4-8: The dates for which back trajectory analysis was applied to the Cowra samples. Back trajectory analysis was applied based on either satellite detection or daily rainfall records, both indicated by '✓' in the column 'Reason for back trajectory analysis'. In the column 'Trajectory influenced by terrestrial salt source', 'X' indicates trajectory was not influenced by terrestrial salt source; if the trajectory has shown an influence from the presumed terrestrial salt source, the date, time and corresponding figure (in brackets) were given (trajectories for 'X' are in Appendix B). '✓✓' indicates that the trajectory encountered heavy rain (5 mm hour⁻¹ or more) at the site or along its trajectory. '✓' indicates that the trajectory encountered moderate rain (less than 5 mm hour⁻¹) at the site or along its trajectory before reaching the site.

Sample		ts ratio	Date	Reason for back trajectory analysis		Trajectory influenced by terrestrial salt source	Rain	
				Satellite	Rainfall		Along trajectory	At sampling site
Cowra	2007.3	0.011	25		✓	24th 16hrs (Figure 4-7)	✓	✓✓
Cowra	2007.6	0.018	May 30		✓	29th 16hrs (Figure 4-8)	✓✓	0
						29th 18hrs (Figure 4-8)	✓	✓
						29th 20hrs (Figure 4-8)	✓	✓✓
						5th 00hrs (Figure 4-9)	0	0
			5	✓		5th 02hrs (Figure 4-10)	0	0
						5th 04hrs (Figure 4-11)	0	0
Cowra	2007.1	0.000	8		✓	X	---	---
			20		✓	X	---	---
			18		✓	X	---	---
			Feb 2		✓	X	---	---
Cowra	2007.2	0.000	Feb 3		✓	X	---	---
			10		✓	X	---	---
			22		✓	X	---	---
			23		✓	X	---	---
			25		✓	X	---	---
			27		✓	X	---	---
			28		✓	X	---	---
Cowra	2008.1 –2008.2	0.000	Mar 5		✓	X	---	---
			Jan 13		✓	X	---	---
			Jan 17		✓	X	---	---
			Jan 19		✓	X	---	---
			Jan 20		✓	X	---	---
			Feb 12		✓	X	---	---
			Feb 13		✓	X	---	---

Three trajectories plotted due to aerosol detection by the OMI sensor (June 5th 00hrs to 04hrs) and four trajectories plotted due to precipitation record (March 24th 16hrs and May 29th 16hrs to 20hrs) appeared to have crossed the presumed terrestrial salt source. Although rain did not occur along the trajectories or during the time when the trajectories reached Cowra on June 5th 2007, dust could still have been deposited into the samples due to the dry deposition mechanism (Section 2.4.), considering that the amount of dust was large enough to be detected by the satellite. Two trajectories, of March 24th 16hrs and May 29th 20hrs, appear to be responsible for the terrestrial salt input to their corresponding samples; although they encountered moderate rainfall (< 5 mm hour⁻¹) before reaching the sampling site, they experienced much heavier rain (≥ 5 mm hour⁻¹) at Cowra.

The trajectories of March 25th 2007, May 30th 2007 and June 5th 2007 are presented in Figure 4-7, Figure 4-8 and Figures 4-9, 4-10 and 4-11, respectively. These trajectories were extended up to 168 hours to effectively present the influence from the source regions. Note that in the rainfall records in all figures, time increases from right to left. All the other trajectories are to be found in Appendix B.

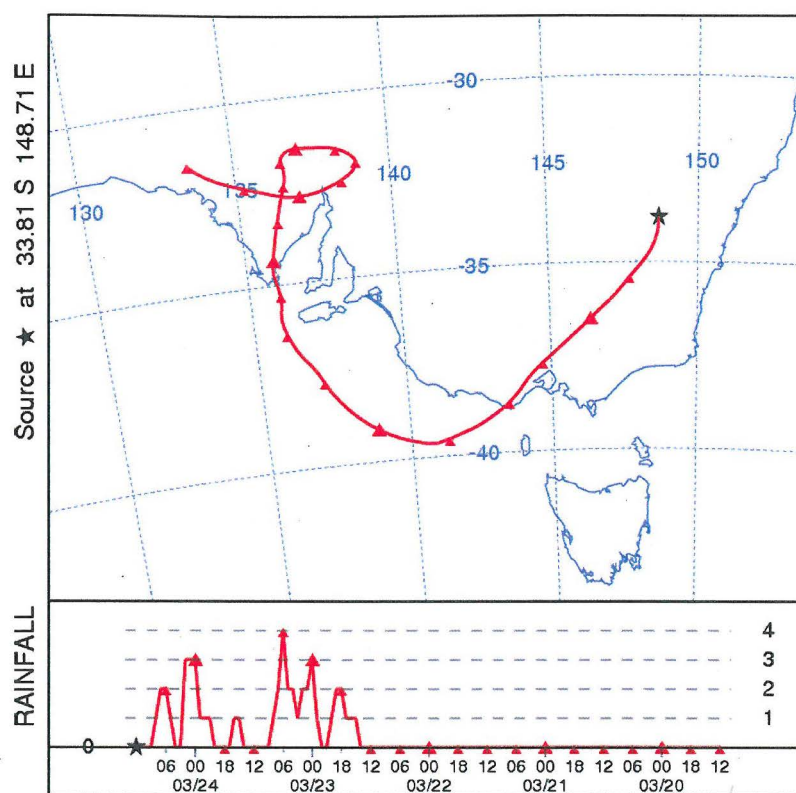


Figure 4-7: A trajectory with rainfall (mm hour^{-1}) record of Cowra March 24th at 16hrs

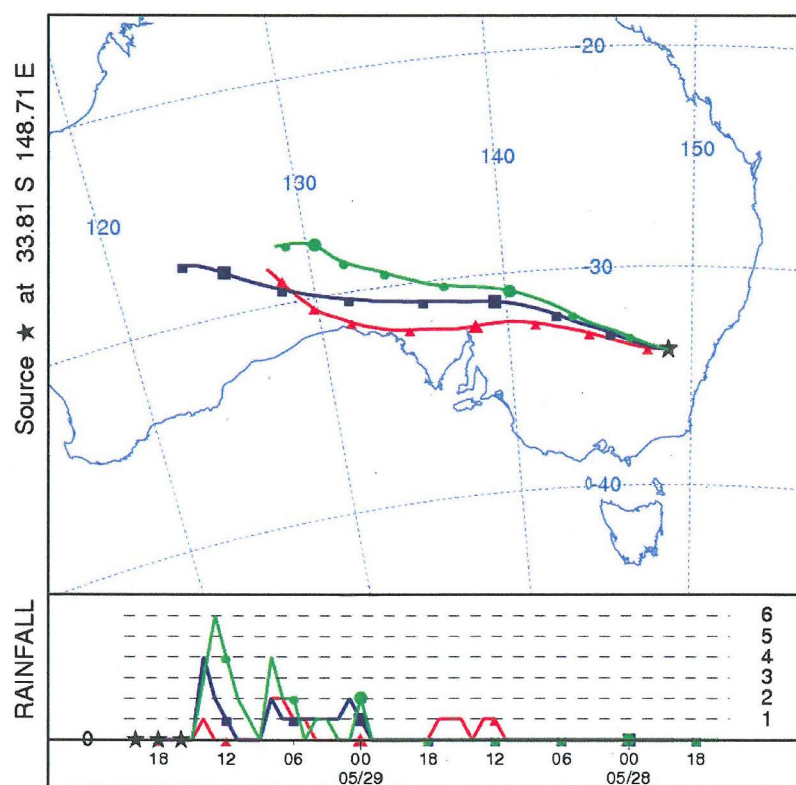


Figure 4-8: Trajectories with rainfall (mm hour^{-1}) record of Cowra May 29th at 16, 18 and 20hrs

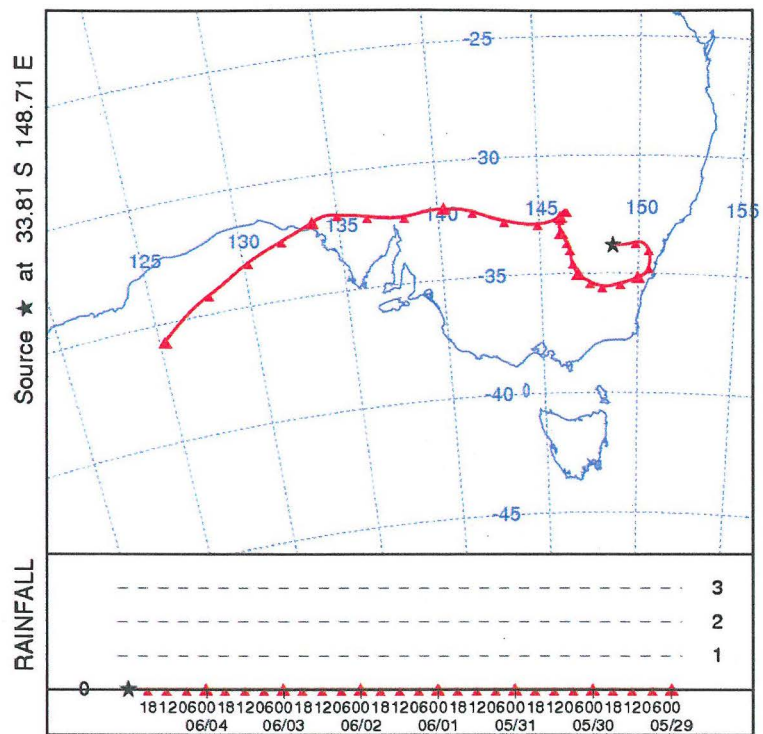


Figure 4-9: A trajectory with rainfall (mm hour^{-1}) record of Cowra June 5th at 00hrs

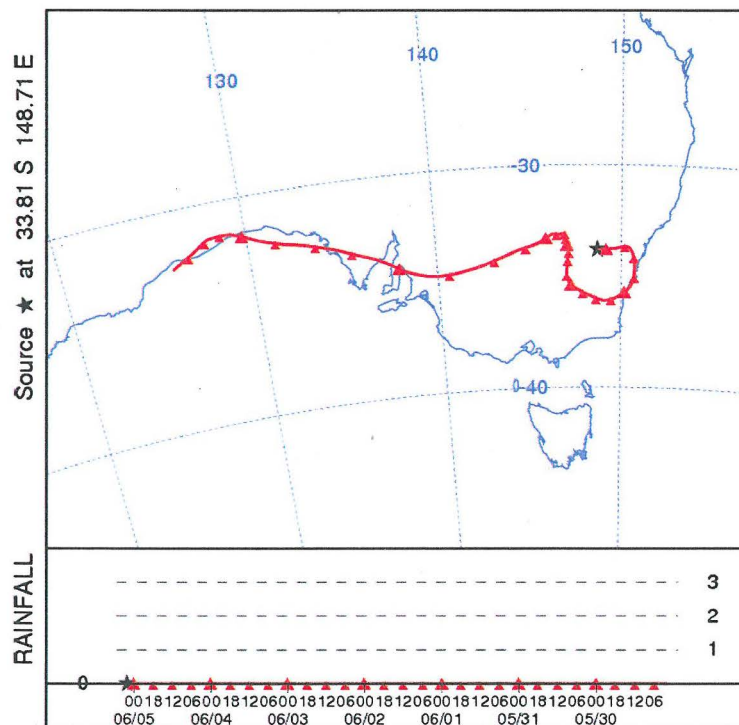


Figure 4-10: A trajectory with rainfall (mm hour^{-1}) record of Cowra June 5th at 02hrs

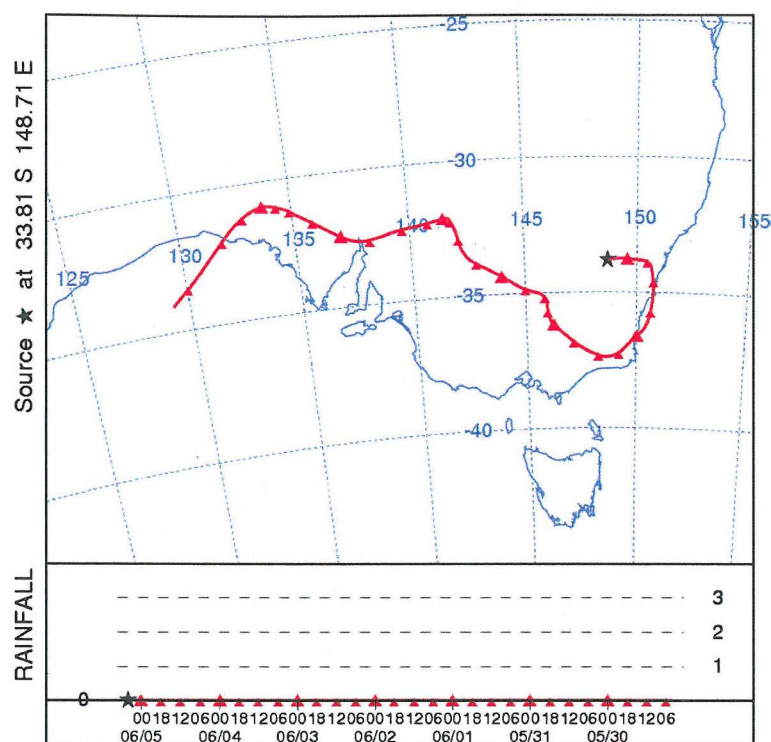


Figure 4-11: A trajectory with rainfall (mm hour^{-1}) record of Cowra June 5th at 04hrs

4.5. Scanning Electron Microscopy Analysis

Scanning electron microscopy (SEM) analysis was applied to selected samples to determine the differences in their terrestrial salt contributions. These samples were chosen for the same reasons that these samples were chosen for back trajectory analysis — a conspicuously high or none terrestrial salt influence (Section 4.4.). Therefore, SEM was applied to the same set of samples to which back trajectory analysis had been applied (Tables 4-5 and 4-6). The SEM images were taken for the following CSIRO samples: Wagga Wagga December 2007 and Wagga Wagga January, February, March and April 2008; Melbourne November 2007 and Melbourne March and April 2008; and, Adelaide February 2008. In addition, SEM images of the following Cowra samples were obtained as well: January, February, March and June 2007 and January – February 2008.

4.5.1. CSIRO Samples — Soluble and Insoluble Materials

SEM images for samples which had a high terrestrial salt ratio are shown in Figures 4-12 – 4-14. These are the Wagga Wagga December 2007, Melbourne April 2008 and Adelaide February 2008 samples, respectively. An SEM image for the Melbourne November 2007 sample which did not show a contribution from terrestrial salt is shown for comparison (Figure 4-15). The other SEM images are found in Appendix C. While large particles were found in the Wagga Wagga December 2007 sample (Figure 4-12), there was a predominance of small

particles, less than 1 μm in diameter, in samples from Melbourne April 2007 (Figure 4-13) and from Adelaide February 2008 samples (Figure 4-14). The Adelaide February 2008 (Figure 4-14) was particularly dominated by the small particles — not even one particle clearly larger than 10 μm in diameter was found. In contrast, the SEM image of the Melbourne November 2007 (Figure 4-15) showed a predominance of larger particles, some even larger than 30 μm in diameter, possibly indicating that the dust had not travelled far compared to the dust of the aforementioned samples. However, overall, the morphological trend of dust particles in the samples was difficult to interpret from the images. In addition, it must be noted that the morphology of the samples was affected by their suspension in rainwater during collection (Section 3.2.).

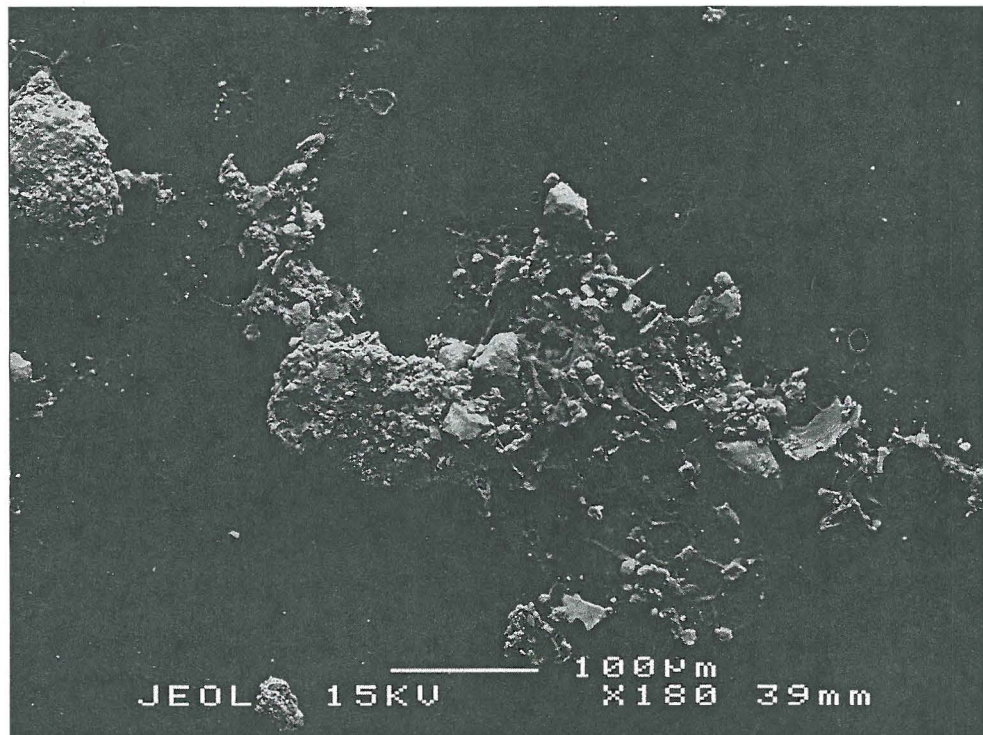


Figure 4-12: SEM image of Wagga Wagga December 2007 sample

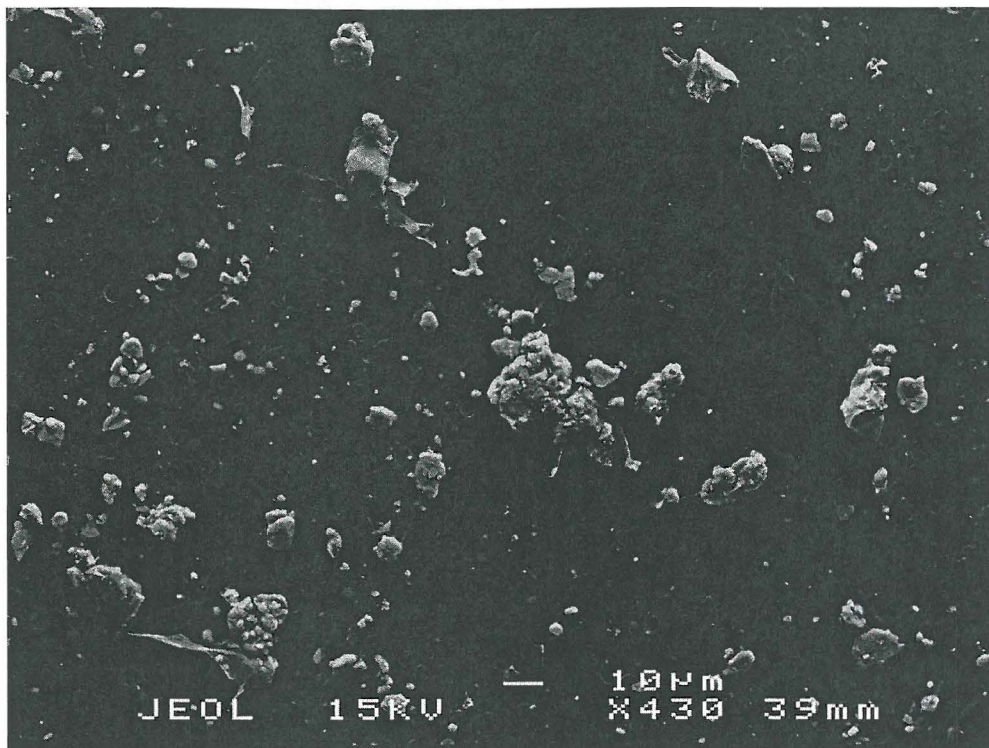


Figure 4-13: SEM image of Melbourne April 2008 sample

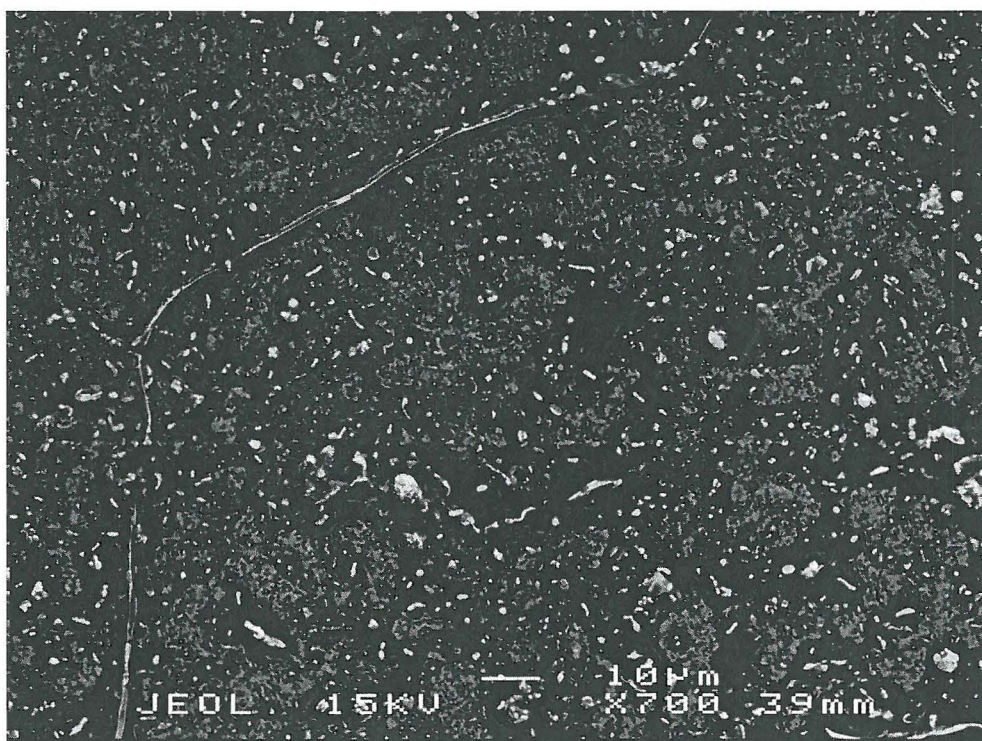


Figure 4-14: SEM image of Adelaide February 2008 sample

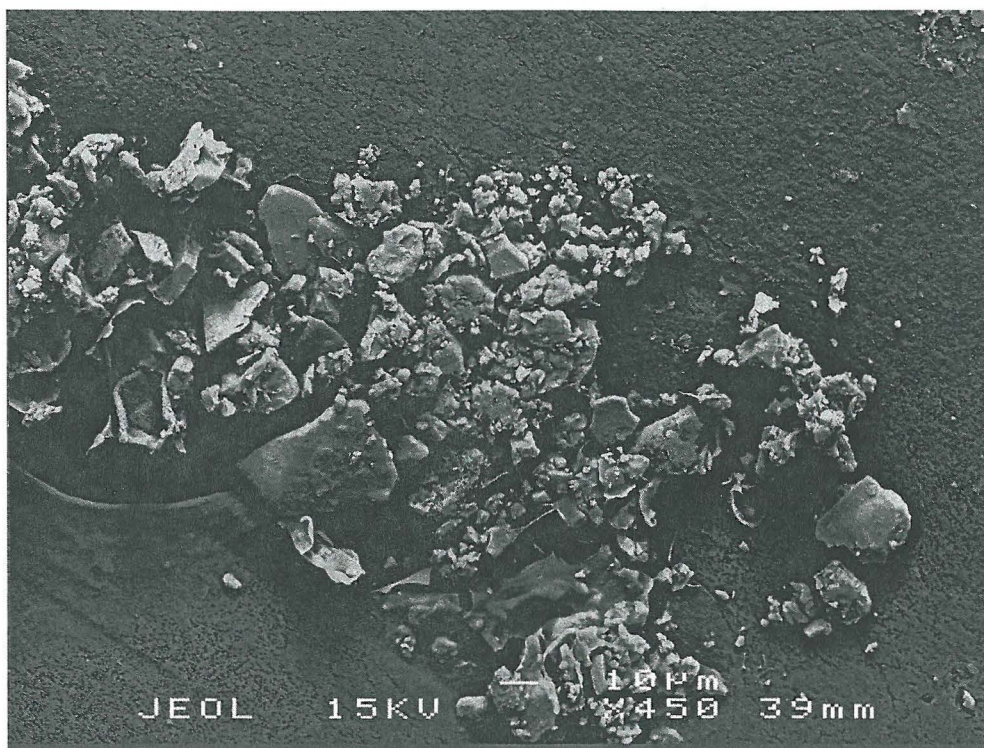


Figure 4-15: SEM image of Melbourne November 2007 sample

4.5.2. Cowra Samples

The SEM images of the Cowra March 2007 and June 2007 samples, which had a high terrestrial salt ratio (Table 4-6), are shown as Figures 4-16 and 4-17, respectively. SEM images for the samples which did not show a contribution from terrestrial salt, in comparison to Figures 4-16 and 4-17, are presented in Appendix C.

The morphological traits of the original dust seem to have been completely lost due to the procedures of water suspension and subsequent oven drying during collection (Section 3.2.). The dust crusts formed by this procedure completely dominated the samples, and thus it was not possible to determine the original morphological traits of the dust particles (Figures 4-16 and 4-17 and Appendix C).

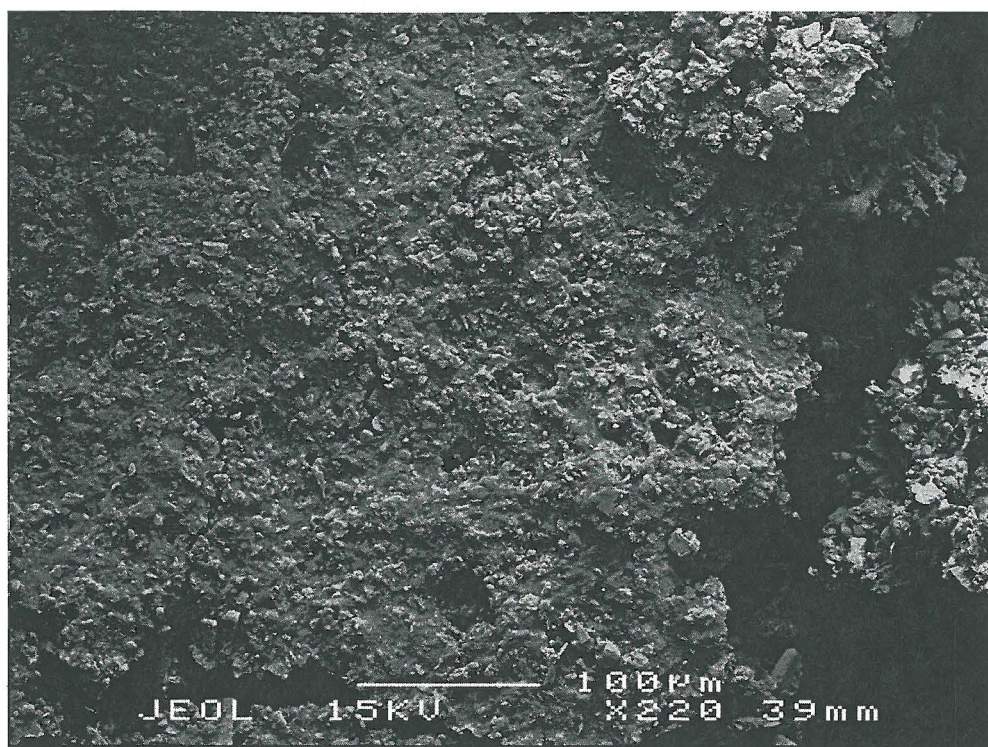


Figure 4-16: SEM image of Cowra March 2007 sample

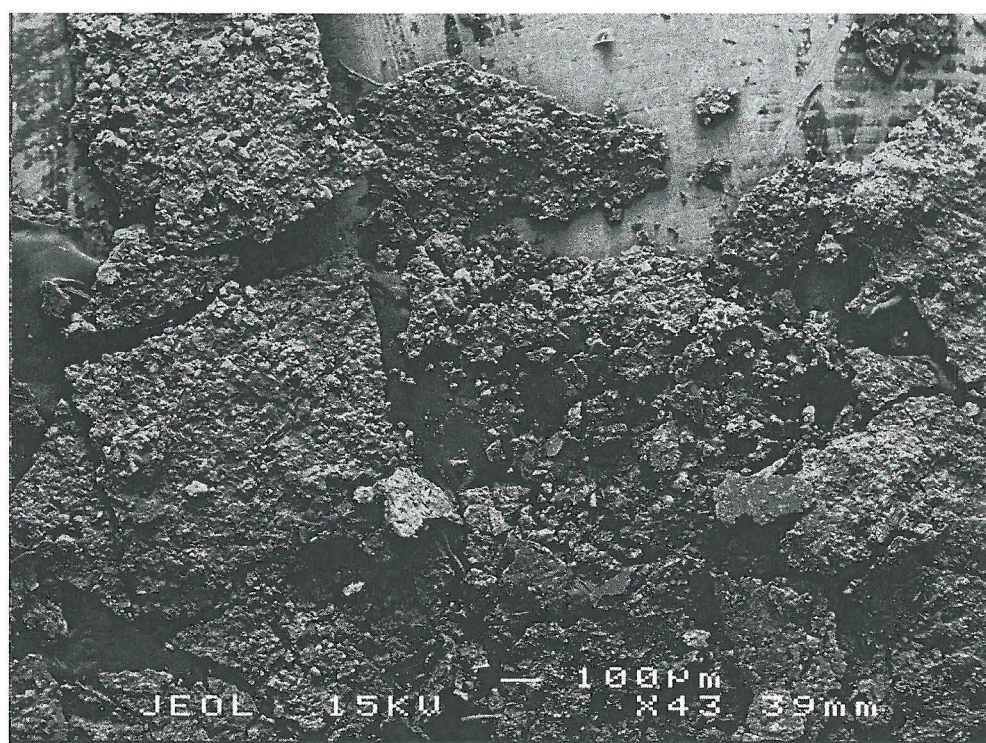


Figure 4-17: SEM image of Cowra June 2007 sample

4.6. Summary

This chapter has presented comprehensive results from IBA for 115 samples from 16 different sites. Among these samples, PCA were applied to 60 CSIRO samples for which both soluble and insoluble materials were analysed. Back trajectory analysis and SEM were applied to five samples which clearly showed a high terrestrial salt ratio and also as a comparison to nine corresponding samples which had a zero terrestrial salt ratio.

The following chapter discusses these results and presents possible implications.

5. Discussion

5.1. Introduction

This chapter discusses the various results presented in Chapter 4 and implications from them. This chapter documents the chemical and physical features of dust samples and considers whether suggested sources of terrestrial salt (NaCl) can be confirmed.

5.2. Chemical Features of Dust

5.2.1. Ion Beam Analysis

The terrestrial salt (ts) ratios calculated from the results of the ion beam analysis (IBA) varied substantially depending on how the samples were prepared prior to analysis (Tables 4-1 and 4-2 and Appendices A-1 – A-4). An indication of terrestrial salt was found in three out of four types of samples; i.e., the CSIRO sample for which both soluble and insoluble materials had been analysed and both types of Cowra samples. No indication of terrestrial salt (NaCl) was found in any of the CSIRO samples for which only the insoluble materials were analysed. This was due to NaCl leaching through the filters (Section 4.2.2.). In addition, an indication of terrestrial salt was found in only one of the Cowra samples collected using the Teflon filters (Appendix A-4). The reason for this is probably the rebound of dust particles during sample preparation (Section 3.5.1.).

The errors were not limited to the sample preparation methods; they were also associated with the various calculations carried out on the IBA results. For instance, the error between the two terrestrial ratios of the Cowra samples in pellets (calculated with and without estimated total weight) came from an error intrinsic to the estimation of total weights using Equation 3-10. Ideally, estimated total weights of the Cowra samples in pellets should be less than 1,000,000 mg kg⁻¹. This lower amount would be due to the IBA not including some of the important elements in dust such as Mg and organic matter. In fact, some weights were low, up to 764,586 mg kg⁻¹ (December 2007); however, on the other hand, there were weights up to 1,492,039 mg kg⁻¹ (November 2006) (Table 4-2).

After considering these potential errors (arising from both the preparation methods and the calculations), the terrestrial salt ratios calculated using these estimated weights were used only to determine the samples with extreme differences in the ts ratios, and were not used to identify the subtle differences between the samples.

In contrast to their relatively low terrestrial salt ratios, which ranged from 0.000 to 0.018, (without using the estimated total weight), the soil ratios of the Cowra samples in pellets were markedly high. Even without using the estimated total weight, the soil ratios were up to 1.713 (November 2006) and some of the total soil weights were even larger than the estimated total

weights (Table 4-2 and Appendix A-3). These results raised doubts as to the accuracy of the soil ratios and the use of Equation 3-6.

Another interesting finding was that the terrestrial salt ratios of the CSIRO samples were generally much larger than those of the Cowra samples, even after considering possible error from the estimation of the total sample weights (Tables 4-1 and 4-2 and Appendices A-1 and A-3). An identification of the reason for this is beyond the scope of this research; however some possible explanations might be:

- (i) Simply due to its location; Cowra is located relatively distant from the presumed terrestrial salt source in South Australia. That is, the low ratios of Cowra might be simply reflecting the low inputs of terrestrial salt into the region; and/or
- (ii) An effect of collection methods and/or devices. For example, the sample collection area was 1,131 cm² for the Cowra samples; however it was 314 or 78.5 cm² for the CSIRO samples (Section 3.2.).

Therefore, any direct comparison of the ratios between the two types of samples was regarded as difficult in this research.

Some samples had a clearly larger terrestrial salt ratio than other samples; for example, Wagga Wagga December 2007 (0.122), Melbourne April 2008 (0.114) and Adelaide February 2008 (0.225) of the CSIRO samples and March 2007 (0.011) and June 2007 (0.018) of the Cowra samples. Since these ratios were extreme amongst sample types, these samples were considered to have had a substantial influence from the terrestrial salt, even considering the possible errors discussed above.

5.2.2. Principal Component Analysis

Considering the number of samples required for reliable results, the principal component analysis (PCA) was only applicable to the CSIRO samples for which soluble and insoluble materials were both analysed and for which there was the largest numbers of samples (60 samples). Seven components, which in total explained 76.7% of variations, were found (Table 4-3). Terrestrial salt component scores and terrestrial salt ratios appeared to correlate to some extent, such as the Adelaide February sample (ts ratio: 0.225; 4th component score: 1.272). These results validated the use of terrestrial salt ratios. However the latter are more versatile because they can be calculated for very small groups of samples rather than relying upon the large coherent data sets necessary for PCA.

However, the PCA results seemed to be of limited value for this research. This is because PCA could only be applied to the CSIRO samples for which soluble and insoluble properties had both been analysed and not for the other types of samples. In addition to this, a significant influence of contamination from the elements other than those related to terrestrial salt (NaCl) was found, such as S (0.573), K (0.463) and Mn (0.650), while those of tsNa and Cl were only

0.335 and 0.122, respectively. Therefore, the PCA results were found to be inadequate for the purpose of this research. The reasons for the contamination could be:

- (i) The terrestrial salt contribution to the aeolian dust is too minor to be revealed by the major principal components; and
- (ii) High diversity of sampling sites. There were 15 CSIRO sampling sites in total and the environments of the sampling sites varied substantially. Some were in or near large cities which could have influenced the samples by their anthropogenic activities, and in contrast, some were in remote regions, where such influence is minimal. Some were located along the coast, where they could be highly affected by sea-salt and, in contrast, some were located inland (Figure 3-1). Therefore, considering this high environmental diversity amongst the 15 sampling sites of this research, 60 samples in total might not have been a large enough number to clearly distinguish the underlying components.

5.3. Physical Features of Dust

Scanning electron microscopy (SEM) images were obtained for the CSIRO and Cowra samples (Tables 4-5 and 4-6, respectively) to compare the disparities in morphological traits, such as size and shape, between dust samples which had high values of terrestrial salt ratio and samples which had no terrestrial salt (Tables 4-5 and 4-6). There was a total of 14 selected samples: five with a high terrestrial salt contribution, and nine with no terrestrial salt contribution. It was expected that dust particles containing relatively large amounts of terrestrial salt and which had come from the presumed salt sources would have different morphologies to dust particles containing no terrestrial salt and which had come from a different source area.

However, the results from the SEM images were inconclusive. Overall, the images of both the CSIRO and Cowra samples did not show clear trends in morphology with regards to terrestrial salt ratios. In particular, artificially coherent dust crusts of dried dust particles dominated the Cowra samples, causing the original structure of individual dust particles to be completely lost in all five Cowra samples (Figures 4-16 and 4-17 and Appendix C). The crust would have resulted from the water suspension of the dust particles and subsequent oven drying during the sample collection (Section 3.2.).

Even though the CSIRO samples were also suspended in rainwater and then separated onto filter papers during their collection (Section 3.2.), they appear to have kept their original morphological traits better than the Cowra samples. The formation of an artificial crust was not as common in the CSIRO samples. The Wagga Wagga December 2007 (Figure 4-12) and Adelaide February 2008 (Figure 4-14) samples seemed to be predominantly composed of smaller particles, less than 1 μm in diameter, compared to the other seven CSIRO samples. The Adelaide February 2008 sample (Figure 4-14) was especially dominated by the small particles — not even one particle clearly larger than 10 μm in diameter was found. As discussed in

Section 2.3.1., in general, smaller particles are entrained in the atmosphere more easily and travel longer distances than larger particles (Pye, 1987). Therefore, it seemed reasonable to interpret from these images that the Wagga Wagga December 2007 sample, and especially the Adelaide February 2008 sample, had experienced relatively more influence from distant source(s) compared to the other samples. However, overall, the morphological trends of samples were difficult to interpret from the images and it was not possible to conclude anything definite about the origin of the samples.

5.4. Verification of Dust Source

Back trajectory analysis was applied to selected CSIRO and Cowra dust samples, in relation to their degree of terrestrial salt (ts) contributions, to reveal any disparities in the aeolian dust dispersion route (Tables 4-5 and 4-6). Therefore, back trajectory analysis was applied to the same samples which had been exposed to SEM (Section 5.3.). The back trajectory plots combined with the rainfall records demonstrated a strong disparity between the two extremes: i.e., the samples with a high terrestrial salt contribution, and samples with no terrestrial salt contribution, in relation to the influence from the presumed terrestrial salt source. A summary of the interpretation of the combined results from the CSIRO and Cowra samples of the back trajectory plots with rainfall records along the trajectory and at the site is shown in Table 5-1.

Table 5-1: Summary of the interpretations of the back trajectory analysis with rainfall records. (CSIRO and Cowra samples combined)

	Influence from the presumed source	No Influence from the presumed source
High ts ratio samples	3 / 5	2 / 5
Zero ts ratio samples	0 / 9	9 / 9

Amongst the samples with no influence from the presumed source, there was an excellent agreement. None of the nine samples which had no indication of terrestrial salt appeared to be influenced by the presumed source (Table 5-1) (Section 2.3.2.). Most of the trajectories of these samples seemed to come from elsewhere; if the trajectories had come from such regions, either the content had been significantly washed out before reaching the site owing to heavy rainfall or the deposition onto the site was doubtful because of the lack of rainfall at the time they reached the site (Tables 4-7 and 4-8). For example, the Melbourne November 2007 sample had eight possible dates which might have had dust deposition influenced from the presumed source based on satellite detection or recorded rainfall (Table 4-7). However, the trajectories of seven of these dates did not come from the presumed source region. Two trajectories of 16hrs and

18hrs of the 3rd had come from the source region, yet both trajectories did not have rainfall at the site, meaning that the deposition was less likely (Table 4-7). In addition, the trajectory of 16hrs had encountered moderate rain ($< 5 \text{ mm hour}^{-1}$) before reaching the Melbourne site (Figure 4-2), whilst the trajectory of 18hrs had even encountered heavy rain ($\geq 5 \text{ mm hour}^{-1}$) before reaching the Melbourne site (Figure 4-3). Considering the above facts, it appears reasonable to argue that the Melbourne November 2007 sample is unlikely to have been influenced by the presumed source regions. This accords with the sample not having a terrestrial salt contribution.

In contrast, three out of five samples which had a high terrestrial ratio seemed to have been influenced by the presumed source (Tables 5-1). These three were: the Wagga Wagga December 2007 sample, and the Cowra March and June 2007 samples. For example, the trajectory from Cowra at 20hrs on May 29th 2007 had crossed such a region and while the trajectory did encounter moderate rainfall before reaching Cowra, it encountered much heavier precipitation when it reached the site (Figure 4-8). Therefore, it is reasonable to argue that the dust deposition with substantial amount of terrestrial salt did occur at the site at the time. In addition, the trajectories from Cowra which were investigated due to aerosol detected by satellite on June 5th 2007, seemed to have come from the presumed source since all three trajectories on that date, at 00hrs, 02hrs and 04hrs, had come from that region (Figures 4-9, 4-10 and 4-11, respectively). No rainfall was recorded en route for all three trajectories, and although rainfall was also not recorded during the time when these trajectories reached Cowra, dust could have been deposited into the sampler due to a dry deposition mechanism (Section 2.4.), considering that the amount of dust was large enough to be detected by the satellite. In addition, interestingly, the high contributions of terrestrial salt appeared to depend only on one or two dust events, no longer than six hours, in all three samples, whose back trajectories along with rainfall records agreed with their high terrestrial salt ratios.

However, it must be noted that the Adelaide February 2008 and Melbourne April 2008 samples, which also had a conspicuously high terrestrial salt ratio, could not be effectively explained by their back trajectories and precipitation records at the site and along the trajectories (Tables 4-7 and 5-1). Three trajectories of the Adelaide February 2008 sample crossed the presumed terrestrial salt source region and although they did not encounter any rain before reaching the site, sufficient rain for deposition was also not recorded at the site at the time these trajectories reached there (Figures 4-4 – 4-6) (Table 4-7). As for the Melbourne April 2008 sample, its two trajectories did not even cross the presumed source region (Table 4-7). This incompleteness might be explained by the limitations of the approach taken in this research. These were:

- (i) Wind conditions can change drastically on a scale of minutes (Raupach *et al.*, 1994). Therefore, an important trajectory(s) could have been missed by the analysis

-
- due to the 3 hour GDAS temporal resolution (NASA, 2008) and/or 2 hour intervals set in this research (Section 3.5.3.);
- (ii) The one degree latitude and longitude resolution of GDAS data (NASA, 2008) might have been too coarse;
 - (iii) Aerosol OMI Level 3 data has limitation in the detection (Section 3.5.3.) of aerosol. Therefore, samples which might have been influenced by dust may not have been sensed by the satellite;
 - (iv) The presumed source region of the terrestrial salt was limited to the salt lake regions of South Australia in this research (Section 3.5.3.). There could be other possible sources, such as saline deposits in arid regions within the Murray Darling drainage system;
 - (v) Surface soil and meteorological conditions of the possible source area were not considered. As discussed in Section 2.3.1 and 2.3.2., these are important factors to be considered in the entrainment of the dust into the atmosphere;
 - (vi) Except for rainfall, other metrological conditions between the possible source area and the deposition site were not considered in interpreting the results from the back trajectory analysis. For example, wind speed might have been of an insufficient level to carry dust along the trajectory; and
 - (vii) Topographical conditions in the deposition sites were not considered. As discussed in Section 2.4., these are important factors to be considered in dust deposition.

Despite these inconsistencies in some of the data, considering the complexity of the mechanism for aeolian dust transportation, the combination of back trajectory analysis and precipitation record at the site and along the trajectory path, appears to imply the existence of terrestrial salt dispersion from the presumed source, at least to some extent. These presumed sources are regions with brackish endorheic dry salt lakes and/or playas which contain immense amounts of fragile dust and soil with a conspicuously high proportion of terrestrial salt (Bonython, 1956; Gunn and Fleming, 1984; Greene *et al.*, 2004). Hence, the dust from these regions could cause dispersion of salt in association with aeolian dust which might, as a consequence, cause problems such as salinisation and/or sodification in leeward regions (Sections 2.3.2. and 2.5.2.) (Acworth *et al.*, 1997; Jankowski and Acworth, 1997; Acworth and Jankowski, 2001; Melis and Acworth, 2001; Smithson, 2004).

Although the absolute amount of terrestrial salt deposition could not be calculated for the CSIRO samples, since the amount of rainwater used for filtration was not recorded during the sample preparation procedure (Section 3.4.), some terrestrial salt ratios, such as the Adelaide February sample (0.225), are significant. These values imply potentially high rates or potential dispersion of terrestrial salt associated with aeolian dust to distant regions. On the other hand,

the Cowra samples were weighed and this allowed rates of salt deposition to be calculated. The two highest terrestrial salt ratios of the Cowra samples were recorded in the June 2007 (0.018) and March 2007 (0.011) samples. Since the collection area of the Cowra sampler was 1,131 cm² (Section 3.2.), and the weight of the June dust sample collected over 27 days was 0.0537 g, the terrestrial salt deposition rate per month (30 days) around Cowra at the time this dust sample was collected can be estimated to be approximately 95 g ha⁻¹ month⁻¹. Furthermore, since the March sample had more dust deposition (0.2679 g) over 20 days, the deposition rate of the terrestrial salt per month (31 days) can be estimated to be approximately 404 g ha⁻¹ month⁻¹. This is approximately four times the salt deposition rate in March. Over an extended period, these terrestrial salt inputs by means of aeolian transportation could add significantly to the problems of soil salinisation at Cowra; however, further research is necessary to confirm this hypothesis.

6. Conclusions and Directions for Future Work

6.1. Conclusions

Terrestrial salt derived from ephemeral salt lakes and playas within the inland drainage system of South Australia appears to be associated with dust deposited in south-east Australia.

This research indicated that:

- (i) Despite limitations due to errors arising in some of the calculations, the use of a combination of equations to determine the contribution of terrestrial NaCl to aeolian dust (i.e., terrestrial salt ratio), was able to discriminate between samples with extreme or no terrestrial salt influence;
- (ii) The use of PCA gave similar results to terrestrial salt ratios and validated the use of these ratios. However, PCA relies on large coherent data sets and hence is not as robust a method as terrestrial salt ratios;
- (iii) Back trajectory plots, along with rainfall records (at the site and along the trajectory), appeared overall to be consistent with high and zero values of the terrestrial salt ratios calculated from IBA results (Tables 4-7, 4-8 and 5-1);
- (iv) The SEM images appeared to indicate that dust samples which had high terrestrial salt ratios have smaller particle size. Two samples out of five which had a high terrestrial salt ratio (Figures 4-13 and 4-14) had a conspicuously smaller particle size. This implied that these samples were influenced to a greater extent by the distant source(s) compared to other samples. However, overall, morphological traits were unclear;
- (v) The above features suggest that there is evidence for the existence of terrestrial salt dispersion associated with aeolian dust from the presumed source — the inland salt lake regions of South Australia; and
- (vi) An influence of terrestrial salt appeared to be dependent on only one or two events, of no more than six hours duration within a monthly collection period.

Following on from the above conclusions, it is necessary to outline limitations in the research. These were:

- (i) The major limitation of the research was the lack of a systematic uncertainty analysis, which limited the qualitative significance of the results. However, as noted in Chapter 3 there was a lack of data on the variability of the elemental composition of the dust samples, and hence the various elemental ratios used in the calculations. Therefore, calculations of standard uncertainty values were not possible;

-
- (ii) The presumed source region of the terrestrial salt was postulated to the salt lake regions of South Australia in this research (Section 3.5.3.). There could also be other possible sources;
 - (iii) The fourth component calculated by PCA was labelled ‘terrestrial salt’ due to its positive factor loading values for both tsNa and Cl (Table 4-3). However, the factor loading values of these elements were lower than those of elements not related to the terrestrial salt, such as S, K and Mn, indicating the possibly of the fourth factor also being affected by other factor(s) other than terrestrial salt;
 - (iv) SEM analysis of the dust samples was difficult because the morphological traits of the original dust samples could have been affected due to suspension in water and subsequent drying during the sampling process (Sections 3.2. and 3.4.);
 - (v) Particle sizes presented in this research were only inferences made from the SEM images and were not quantitative;
 - (vi) Wind conditions can change drastically on a scale of minutes (Raupach *et al.*, 1994); therefore, an important trajectory(s) could have been missed by the analysis due to the 3 hour GDAS temporal resolution (NASA, 2008) and/or 2 hour intervals set in this research (Section 3.5.3.);
 - (vii) The one degree latitude and longitude resolution of GDAS data (NASA, 2008) might have been too coarse;
 - (viii) Aerosol OMI Level 3 data had its limitation in detection (Section 3.5.3.);
 - (ix) Surface soil and meteorological conditions of the possible source area were not considered;
 - (x) Except for rainfall, other meteorological conditions between the possible source area and the deposition site were not considered in interpreting the results from the back trajectory analysis; and
 - (xi) Topographical conditions in the deposition sites were not considered.

6.1.1. Answer to the Research Question

All three objectives (Section 1.6.) and the aim (Section 1.5.) of this research have been fulfilled. The main question was: ‘Do the aeolian processes contribute to the deposition of terrestrial salts, particularly in south-east Australia?’ (Section 1.4.). Given the wide range of evidence found in this research, it is likely that the dust deposited in south-eastern Australia may contain substantial amounts of terrestrial salt. This further implies that the input of terrestrial salt to the distant areas, including the Murray Darling Basin, which is valuable for agricultural purposes, could be significant. However, given the above limitations (Section 6.1.), this conclusion should be regarded as somewhat tentative, with more work needed using the strategy outlined below.

6.2. Directions for Future Work

Given the findings and limitations of this research, the following suggestions are presented for future work:

- (i) Increase the number of samples to cover a greater time – one year is too short to reach general conclusions;
- (ii) The analysis with mg kg^{-1} unit (e.g., analysis using pellets) is strongly recommended to avoid any possible errors. However, analysis with ug cm^{-2} unit (e.g., analysis using filters) was confirmed to also be viable, at least to some extent; it could be expected to be more accurate if the amount of rainwater used for the filtration process (Section 3.4.) was recorded or fixed to a certain amount throughout the samples;
- (iii) The collection area of sampling devices should be consistent across the devices and sufficiently large to lower the risk of possible errors;
- (iv) More work is required to document natural variability in the composition of crustal materials that influence dust, and hence improve the estimation of the various elemental ratios used in the calculations;
- (v) Consider additional possible source(s) of the terrestrial salt other than the salt lake regions of South Australia presumed in this research;
- (vi) Increase the resolution of the sampling period — one month is too long. This is because the high terrestrial salt ratios of the samples appeared to be dependent on only one or two short events during the month. Daily collection is recommended, but weekly or fortnightly collection can still be expected to give better results;
- (vii) Improve on the SEM images used for morphology, quantitative particle size data should be obtained by utilising instruments such as the Multisizer;
- (viii) Acquire information on surface soil and meteorological conditions of the possible source area;
- (ix) Acquire data on metrological conditions from the possible source area to the deposition site; and
- (x) Acquire meteorological and topographical conditions of the deposition sites.

References

- Abuduwaili, J., Gabchenko, M. V. and Junrong, X., 2008. Eolian transport of salts – a case study in the area of Lake Ebinur (Xinjian, Northwest China), *Journal of Arid Environment*, 72(10): 1843-1852.
- Acworth, R. I. and Jankowski, J., 2001. Salt source for dryland salinity-evidence from an upland catchment on the Southern Tablelands of New South Wales, *Australian Journal of Soil Research*, 39(1): 39-59.
- Acworth, R. I., Broughton, A. and Jankowski, J., 1997. The role of debris-flow deposits in the development of dryland salinity in the Yass Catchment, New South Wales, Australia, *Hydrogeology Journal*, 5(1): 22-36.
- Aoki, T., Hachikubo, A. and Hori, M., 2003. Effects of snow physical parameters on shortwave broadband albedos, *Journal of Geophysical Research*, 108(D19): ACL 13-1, CiteID 4616, DOI 10.1029/2003JD003506.
- Arimitsu, K., 1997. Chapter 8 Forest soils, in *The Latest Soil Science*, eds K. Kyuma, Asakura, Tokyo, pp.119-133.
- Arimoto, R., Duce, R. A., Ray, B. J. and Unni, C. K., 1985. Atmospheric trace elements at Enewetak Atoll: 2. Transport to the ocean by wet and dry deposition, *Journal of Geophysical Research*, 90(D1): 2391-2408.
- Ayers, G. P., Gillett, R. W., Caine, J. M. and Dick, A. L., 1999. Chloride and bromide loss from sea-salt particles in Southern Ocean air, *Journal of Atmospheric Chemistry*, 33(3): 299-319.
- Batjargal, Z., Dulam, J. and Chung, Y. S., 2006. Dust storms are an indication of an unhealthy environment in east Asia, *Environmental Monitoring and Assessment*, 114(1-3): 447-460.
- Beattie, J. A., 1969. Peculiar features of soil development in parna deposits in the eastern Riverina, N.S.W., *Australian Journal of Soil Research*, 8(2): 145-156.
- Benassai, S., Becagli, S., Gragnani, R., Magand, O., Proposito, M., Fattori, I., Traversi, R. and Udisti, R., 2005. Sea-spray deposition in Antarctic coastal and plateau areas from ITASE traverses, *Annals of Glaciology*, 41(1): 32-40.
- Bierwirth, P. N. and Brodie, R. S., 2008. Gamma-ray remote sensing of aeolian salt sources in the Murray-Darling Basin, Australia, *Remote Sensing of Environment*, 112(2): 550-559.
- Blackburn, G. and McLeod, S., 1983. Salinity of atmospheric precipitation in the Murray-Darling Drainage Division, Australia, *Australian Journal of Soil Research*, 21(4): 411-434.
- Bollhöfer, A., Honeybun, R., Rosman, K. and Martin, P., 2006. The lead isotopic composition of dust in the vicinity of a uranium mine in northern Australia and its use for radiation dose assessment, *Science of the Total Environment*, 366(2-3): 579-589.
- Bonython, C. W., 1956. The salt of Lake Eyre – Its occurrence in Madigan Gulf and its possible origin, *Transactions of the Royal Society of South Australia*, 79: 66-92.
- Boon, K., Kiefert, L. and McTainsh, G. H., 1998. Organic matter content of rural dusts in Australia, *Atmospheric Environment*, 32(16): 2817-2823.

-
- Bourke, C. and Ottaway, S., 1998. Chronic gypsum fertiliser ingestion as a significant contributor to a multifactorial cattle mortality, *Australian Veterinary Journal*, 76(8): 565-569.
- Bowen, H. J. M., 1979. *Environmental Chemistry of the Elements*, Academic Press, London.
- Bowler, J. M., 1976. Aridity in Australia: Age, origins and expression in aeolian landforms and sediments, *Earth-Science Review*, 12(2-3): 279-310.
- Boyd, P. W., McTainsh, G., Serlock, V., Richardson, K., Nichol, S., Ellwood, M. and Frew, R., 2004. Episodic enhancement of phytoplankton stocks in New Zealand subantarctic waters: contribution of atmospheric and oceanic iron supply, *Global Biogeochemical Cycles*, 18, GB1029, doi:10.1029/2002GB002020.
- Brooks, K. and Gillan, S., 1996. *Results of Analysis of Soil, Sediment and Water Samples from Three Properties in the Goonumbla Area*, Department of Mineral Resources, Lidcombe, New South Wales.
- Brookfield, M., 1970. Dune trends and wind regime in central Australia, *Zeitschrift für Geomorphologie N.F. Supplementband*, 10: 151-153.
- Bullard, J., Baddock, M., McTainsh, G. H. and Leys, J. F., 2008. Sub-basin scale dust source geomorphology detected using MODIS, *Geophysical Research Letters*, 35, L15404, doi:10.1029/2008GL033928.
- Butler, B. E., 1956. Parna – an aeolian clay, *The Australian Journal of Science*, 18: 145-151.
- Butler, B. E. and Hutton, J. T., 1956. Parna in the riverine plain of south-eastern Australia and the soils thereon, *Australian Journal of Agricultural Research*, 7: 536-553.
- Cattle, S. R., Greene, R. S. B. and McPherson, A. A., (in press) The role of local regolith-landscape processes in determining the pedological characteristics of aeolian dust deposits across south-eastern Australia, *Quaternary International*.
- Cattle, S. R., McTainsh, G. H. and Wagner, S., 2002. Aeolian dust contributions to soil of the Namoi Valley, northern NSW, Australia, *Catena*, 47(3): 245-264.
- Chan, Y., McTainsh, G. H., Leys, J., McGowan, H. and Tews, K., 2005. Influence of the 23 October 2002 dust storm on the air quality of four Australian cities, *Water, Air, and Soil Pollution*, 164(1-4): 329-348.
- Chartres, C. J., 1982. The pedogenesis of desert loam soils in the Barrier Range, Western New South Wales. I. Soil parent materials, *Australian Journal of Soil Research*, 20(4): 269-281.
- Chartres, C. J., 1983. The pedogenesis of desert loam soils in the Barrier Range, western New South Wales. II. Weathering and soil formation, *Australian Journal of Soil Research*, 21(1): 1-13.
- Chartres, C. J., Chivas, A. R. and Walker, P. H., 1988. The effect of aeolian accessions on soil development on granitic rocks in south-eastern Australia. II. Oxygen-isotope, mineralogical and geochemical evidence for aeolian deposition, *Australian Journal of Soil Research*, 26(1): 17-31.
- Chiarandia, M., Chenhall, B. E., Depers, A. M., Gulson, B. L. and Jones, B. G., 1997. Identification of historical lead sources in roof dusts and recent lake sediments from an industrialized area: indications from lead isotopes, *The Science of the Total Environment*, 205(2-3): 107-128.

-
- Cohen, D. D., 1998. Characterisation of atmospheric fine particles using IBA techniques, *Nuclear Instruments and Methods in Physics Research B*, 136-138: 14-22.
- Cohen, D. D., 1999. *Simultaneous X-ray and γ -ray Ion Beam Methods for Fine Particle Analysis*, Physics Division, ANSTO, Menai, NSW.
- Cohen, D. D., 2004. Over a decade of fine soil measurements at selected Australian and Asian sites by ANSTO, *Proceedings of Wind-blown Dust Workshop*, 8-10 November 2004, Melbourne, CSIRO Marine and Atmospheric Research, Melbourne, pp.40-44.
- Cohen, D. D., Stelcer, E. and Bac, V. T., 2007. Quantification of Fine Particle Composition, Sources and Transboundary Transport in Hanoi, Vietnam from 2001-06, ANSTO, Sydney.
- Cohen, D. D., Stelcer, E. and Garton, D., 2002. Ion beam methods to determine trace heavy metals concentrations and source in urban airsheds, *Nuclear Instruments and Methods in Physics Research B*, 190(1): 466-470.
- Cohen, D. D., Garton, D., Stelcer, E. and Hawas, O., 2004a. Accelerator based studies of atmospheric pollution processes, *Radiation Physics and Chemistry*, 71(3-4):759-767.
- Cohen, D. D., Stelcer, E., Hawas, O. and Garton, D., 2004b. IBA methods for characterisation of fine particulate atmospheric pollution: a local, regional and global research problem, *Nuclear Instruments and Methods in Physics Research B*, 219-220:145-152.
- Cohen, D. D., Garton, D., Stelcer, E., Hawas, O. and Zahorowski, W., 2004c. Long range transport of fine particulate soil, sulphate and black carbon across the east asian region and beyond during 2001-03, *13th World Clean Air and Environmental Protection Congress*, 22-27 August 2004, London, UK.
- Cohen, D. D., Stelcer, E., Hawas, O., Garton, D., Santos, F. and Bac, V. T., 2006. Fine particle characterisation and source apportionment in Manila and Hanoi from 2001-2005 using nuclear techniques, *Proceeding of 5th Better Air Quality Symposium*, 13-16 December 2006, Yogyakarta, Indonesia, pp.10-16.
- Cohen, D. D., Garton, D., Stelcer, E., Hawas, O., Wang, T., Poon, S., Kim, J., Choi, B. C., Oh, S. N., Shin, H-J, Ko, M. Y. and Uematsu, M., 2004d. Multielemental analysis and characterization of fine aerosols at several key ACE-Asia sites, *Journal of Geophysical Research*, 109, D19S12, doi:10.1029/2003JD003569.
- Cresswell, R., Dighton, J., Herczeg, A., Turner, J., Walder, G. and Gillett, R., 2006. MD311: Australia-wide network to measure rainfall chemistry and isotopic composition, CSIRO Land and Water.
- CSEM (Centre for Science and Engineering of Materials), 2006. Fingerprinting dust, *Materials Monthly* (August 2006).
- Dare-Edwards, A. J., 1984. Aeolian clay deposits of south-eastern Australia: parna or loessic clay?, *Transactions of the Institute of British Geographers*, 9(3): 337-344.
- Dart, R. C., Barovich, K. M., Chittleborough, D. J. and Hill, S. M., 2007. Calcium in regolith carbonates of central and southern Australia: its source and implications for the global carbon cycle, *Palaeogeography, Palaeoclimatology, Palaeoecology*, 249(3-4): 322-334.
- Derbyshire, E., 2007. Natural minerogenic dust and human health, *Ambio*, 36(1): 73-77.
-

DEWHA (Department of the Environment, Water, Heritage and the Arts, Australia), 2008. *Salinity*. Available from:
<http://www.environment.gov.au/land/pressures/index.html>
(Accessed 8 October 2008).

DEWR (Department of the Environment and Water Resources, Australia), 2007. Substance fact sheets. Available from:
<http://www.npi.gov.au/database/substance-info/profiles/index.html>
(Accessed 1 September 2008).

Draxler, R. R. and Hess, G. D., 1998. An overview of the HYSPLIT_4 modelling system for trajectories, dispersion and deposition, *Australian Meteorological Magazine*, 47: 295-308.

Draxler, R. R. and Rolph, G. D., 2003. HYSPLIT (HYbrid Single-Particle Lagrangian Integrated Trajectory) Model, NOAA Air Resources Laboratory, Silver Spring, MD. Available from:
<http://www.arl.noaa.gov/ready/hysplit4.html>
(Accessed 13 October 2008).

Earth Observatory, 2002. Dust storm over Eastern Australia. Available from:
http://earthobservatory.nasa.gov/NaturalHazards/shownh.php3?img_id=5199
(Accessed 1 September 2008).

Ekström, M., McTainsh, G. H. and Chappell, A., 2004. Australian dust storms: temporal trends and relationships with synoptic pressure distributions (1960-99), *International Journal of Climatology*, 24(12): 1581-1599.

Eldridge, D. J. and Greene, R. S. B., 1994. Microbiotic soil crusts: a review of their roles in soil and ecological processes in the rangelands of Australia, *Australian Journal of Soil Research*, 32(3): 389-415.

Eldridge, D. J. and Rosentreter, R., 1999. Morphological group: a framework for monitoring microphytic crusts in arid landscapes, *Journal of Arid Environments*, 41(1): 11-25.

Environment Australia, 2003. *Cyanide Management*, Environment Australia, Canberra.

ERDC (Energy Research and Development Corporation), 1995. *Final Report Vol I*, ANSTO, NSW Environmental Protection Agency, University of NSW and Macquarie University, Sydney.

Forster, P., Ramaswamy, V., Artaxo, P., Berntsen, T., Betts, T., Fahey, D. W., Haywood, J., Lean, J., Lowe, D. C., Myhre, G., Nganga, J., Prinn, R., Raga, G., Schulz, M. and van Dorland, R., 2007. Changes in Atmospheric Constituents and in Radiative Forcing, in *Climate Change 2007: The Physical Science Basis. Contribution of Working Group I to the Fourth Assessment Report of the Intergovernmental Panel on Climate Change*, eds Solomon, S., Qin, D., Manning, M., Chen, Z., Marquis, M., Averyt, K. B., Tignor, M. and Miller H. L., Cambridge University Press, Cambridge and New York.

Forward, G., Payne, R. and Bright, M., 2004. The estimated cost of wind erosion in South Australia's agricultural lands, *Proceedings of Wind-blown Dust Workshop*, 8-10 November 2004, Melbourne, CSIRO Marine and Atmospheric Research, Melbourne, pp.93-97.

Garrison, V. H., Shinn, E. A., Foreman, T., Griffin, D. W., Holmes, C. W., Kellogg, C. A., Majewski, M. s., Richardson, L. L., Ritchie, K. B. and Smith, G. W., 2003. African and Asian dust: From desert soils to coral reefs, *BioScience*, 53(5): 469-480.

Gatehouse, R. D., Williams, I. S. and Pillans, B. J., 2001. Fingerprinting windblown dust in south-eastern Australian soils by uranium-lead dating of detrital zircon, *Australian Journal of Soil Research*, 39(1): 7-12.

Geoscience Australia, 2008. Maps of Australia. Available from:
<http://www.ga.gov.au/map/>
(Accessed 4 September 2008).

Goudie, A. S. and Middleton, N. J., 1992. The changing frequency of dust storms through time, *Climate Change*, 20(3): 197-225.

Greene, R. S. B., Cattle, S. R. and McPherson, A. A., (in press) The role of aeolian dust deposits in landscape development and soil degradation in southeastern Australia, *Australian Journal of Earth Sciences*.

Greene, R. S. B., Joeckel, R. M. and Mason, J. A., 2006. Dry saline lakebeds as potential source areas of aeolian dust: studies from the central Great Plains of the USA and SE Australia, *Regolith 2006: Consolidation and Dispersion of Ideas, Proceedings of the CRCLEME Regolith Symposium*, November 2006, Hahndorf Resort, South Australia, eds Fitzpatrick, R. W. and Shand, P., Cooperative Research Centre for Landscape Environments and Mineral Exploration, Western Australia, pp.113-117.

Greene, R. S. B., Posner, A. M. and Quirk, J. P., 1978. Section 1 Chapter 4 A study of the coagulation of montmorillonite and illite suspensions by calcium chloride using the electron microscope, in *Modification of Soil Structure*, eds Emerson, W. W., Bond, R. D. and Dexter, A. R., John Wiley & Sons, New York, pp.35-40.

Greene, R. S. B., Gatehouse, R., Scott, K. and Chen, X. Y., 2001. Symposium report: Aeolian dust – implications for Australian mineral exploration and environmental management, *Australian Journal of Soil Research*, 39: 1-6.

Greene, R. S. B., McPherson, A. Eldridge, D. Murphy, B. and Rankin, M., 2004. Recent aeolian dust activity in Australia: implications of land management for dust sources and their control, *Proceeding of Wind-blown Dust Workshop*, 8-10 November 2004, Melbourne, CSIRO Marine and Atmospheric Research, Melbourne, pp.57-63.

Greene, R. S. B., Nettleton, W. D., Chartres, C. J., Leys, J. F. and Cunningham, R. B., 1998. Runoff and micromorphological properties of grazed haplargids, near Cobar, N.S.W., Australia, *Australian Journal of Soil Research*, 36(1): 87-108.

Grousset, F. E., Ginoux, P., Bory, A. and Biscaye, P. E., 2003, Case study of a Chinese dust plume reaching the French Alps, *Geophysical Research Letters*, 30(6): 1277, doi:10.1029/2002GL016833

Gunn, R. H. and Fleming, P. M., 1984. The estimated store of soluble salts in Lake Eyre Catchment in Queensland and their possible transport in streamflow to the lake, *Australian Journal of Soil Research*, 22: 119-134.

Herr, C., O'Neill, C. and Gray, N. F., 1996. Metal contamination from open-cast copper and sulphur mining in southeast Ireland, *Land Degradation & Development*, 7(2): 161-174.

Hesse, P. P., 2004. The late Quaternary records of dust in Australia: source area controls – downstream impacts, *Proceedings of Wind-blown Dust Workshop*, 8-10 November 2004, Melbourne, CSIRO Marine and Atmospheric Research, Melbourne, pp.76-80.

-
- Hesse, P. P. and McTainsh, G. H., 1999. Last Glacial Maximum to early Holocene wind strength in the mid-latitudes of the southern hemisphere from aeolian dust in the Tasman Sea, *Quaternary Research*, 52(3): 343-349.
- Hesse, P. P. and McTainsh, G. H., 2003. Australian dust deposits: modern processes and the Quaternary record, *Quaternary Science Reviews*, 22(18-19): 2007-2035.
- Hingston, F. J. and Gailitis, V., 1976. The geographic variation of salt precipitated over Western Australia, *Australian Journal of Soil Research*, 14(3): 319-335.
- Houser, C. A. and Nickling, W. C., The emission and vertical flux of particulate matter <10 µm from a disturbed clay-crust surface, *Sedimentology*, 48(2): 255-267.
- Huang, C. C., Pang, J. and Li, P., 2002. Abruptly increased climatic aridity and its social impact on the Loess Plateau of China at 3100 a B.P., *Journal of Arid Environments*, 52(1): 87-99.
- Irvine, S. A. and Doughton, J. A., 2001. Salinity and sodicity, implications for farmers in Central Queensland, *Proceeding of the 10th Australian Agronomy Conference*, Hobart, January 29th – February 1st 2001. Available from: <http://www.regional.org.au/au/asa/2001/index.htm> (Accessed 1 January 2009).
- Jankowski, J. and Acworth, R. I., 1997. Impact of debris-flow deposits on hydrogeochemical processes and the development of dryland salinity in the Yass River Catchment, New South Wales, Australia, *Hydrogeology Journal*, 5(4): 71-88.
- Jickells, T. D., Dorling, S., Deuser, W. G., Church, T. M., Arimoto, R. and Prospero, J. M., 1998. Air-borne dust fluxes to a deep water sediment trap in the Sargasso Sea, *Global Biogeochemical Cycles*, 12(2): 311-320.
- Jickells, T. D., An, Z. S., Andersen, K. K., Baker, A. R., Bergametti, G., Brooks, N., Cao, J. J., Boyd, P. W., Duce, R. A., Hunter, K. A., Kawahata, H., Kubilay, N., laRoche, J., Liss, P. S., Mahowald, N., prospero, J. M., Ridgweel, A. J., Tegan, I. and Torres, R., 2005. Global iron connections between desert dust, ocean biogeochemistry, and climate, *Science*, 308(5718): 67-71.
- Johnston, S. W., 2001. The influence of aeolian dust deposits on alpine soils in south-eastern Australia, *Australian Journal of Soil Research*, 39(1): 81-88.
- Kang, K., 2004. DSS damage types and quantitative estimation in Korea, *International Workshop on Quantitative Analysis and Reduction Measures of DSS Damage in North-east Asia*, 19 November 2004, Seoul, Korea Environmental Institute, Seoul, pp.46-56.
- Kiefert, L., McTainsh, G. H. and Nickling, W. G., 1996. Sedimentological characteristics of Saharan and Australian dusts, in *The Impact of Desert Dust Across the Mediterranean*, eds Guerzoni, S. and Chester, R., Kluwer, Dordrecht, Netherlands, pp.183-190.
- Kellogg, C. A. and Griffin, D. W., 2006. Aerobiology and the global transport of desert dust, *TRENDS in Ecology and Evolution*, 21(11): 638-644.
- Knight, A. W., McTainsh, G. H. and Simpson, R. W., 1995. Sediment loads in an Australian dust storm: Implications for present and past dust processes, *Catena*, 24(3): 195-213.
- Kurtz, A. C., Derry, L. A. and Chadwick, O. A., 2001. Accretion of Asian dust to Hawaiian soils: Isotopic, elemental, and mineral mass balances, *Geochimica et Cosmochimica Acta*, 65(12): 1971-1983.
-

-
- Kwon, H.-J., Cho, S.-H., Chun, Y., Lagarde, F. and Pershagen, G., 2002. effects of the Asian dust effects of the Asian dust events on daily mortality in Seoul, Korea, *Environmental Research*, 90 (1): 1-5.
- Leslie, L. M. and Speer, M. S., 2006. Modelling dust transport over central eastern Australia, *Meteorological Applications*, 13(2): 141-167.
- Leys, J. F. and Eldridge, D. J., 1998. Influence of cryptogamic crust disturbance to wind erosion on sand and loam rangeland soils, *Earth Surface Processes and Landforms*, 23(11): 963-974.
- Leys, J. F. and McTainsh, G. H., 1994. Soil loss and nutrient decline by wind erosion – cause for concern, *Australian Journal of Soil and Water Conservation*, 7(3): 30-35.
- Leys, J. F. and McTainsh, G. H., 1999. Dust and nutrient deposition to riverine environments of south-eastern Australia, *Zeitschrift für Geomorphologie N.F. Supplementband*, 116: 59-76.
- Lourensz, R. S. and Abe, K., A dust storm over Melbourne, *Weather*, 38: 272-274.
- Mackie, D. S., Boyd, P. W., McTainsh, G. H., Tindale, N. W., Westberry, T. B. and Hunter, K. A., 2008. Biogeochemistry of iron in Australian dust: From eolian uplift to marine uptake, *Geochemistry Geophysics Geosystems*, 9(3): Q03Q08, doi:10.1029/2007GC001813.
- Malm, W. C., Silsler, J. F., Huffman, D., Eldred, R. A. and Cahill, T. A., 1994. Spatial and seasonal trends in particle concentration and optical extinction in the United States, *Journal of Geophysical Research*, 99(D1): 1347-1370.
- Manins, P., Holper, P., Suppiah, R., Allan, R., Walsh, K., Fraser, P. and Beer, T., 2001. Part 3a Climate variability and change, in *Australia State of the Environment Report 2001 – Atmosphere Theme Report*, CSIRO Publishing on behalf of Department of the Environment and Heritage, Collingwood, Australia. Available from: <http://www.environment.gov.au/soe/2001/publications/theme-reports/atmosphere/> (Accessed 1 September 2008).
- Marx, S. K., Kamber, B. S. And McGowan, H. A., 2008. Scavenging of atmospheric trace metal pollutants by mineral dusts: Inter-regional transport of Australian trace metal pollution to New Zealand, *Atmospheric Environment*, 42(10): 2460-2478.
- Matsunaka, T., 2003. Chapter 3 The contributions of organic matters on development of soils, in *Principles of Soil Science*, Rural Culture Association, Tokyo, pp.41-50.
- Mays, M. D., Nettleton, W. D., Greene, R. S. B. and Mason, J. A., 2003. Dispersibility of glacial loess in particle size analysis, USA, *Australian Journal of Soil Research*, 41(2): 229-244.
- McGowan, H. A. and Clark, A., 2008. Identification of dust transport pathways from Lake Eyre, Australia using Hysplit, *Atmospheric Environment*, 42(29): 6915-6925.
- McGowan, H. A., Sturman, A. P. and Owens, I. F., 1996. Aeolian dust transport and deposition by foehn winds in an alpine environment, Lake Tekapo, New Zealand, *Geomorphology*, 15(2): 135-146.
- McGowan, H. A., Petherick, L. M. and Kamber, B. S., 2008. Aeolian sedimentation and climate variability during the late Quaternary in southeast Queensland, Australia, *Palaeogeography, Palaeoclimatology, Palaeoecology*, 265(5): 171-181.
- McGowan, H. A., Kamber, B., McTainsh, G. H. and Marx, S. M., 2005. High resolution provenancing of long travelled dust deposited on the Southern Alps, New Zealand, *Geomorphology*, 69(1-4): 208-221.
-

-
- McGowan, H. A., McTainsh, G. H., Zawar-Reza, P. and Sturman, A. P., 2000. Identifying regional dust transport pathways: application of kinematic trajectory modelling to trans-Tasman case, *Earth Surface Processes and Landforms*, 25(6): 633-647.
- McIntyre, D. S., 1976. Subplasticity in Australian soils. I. Description, occurrence, and some properties, *Australian Journal of Soil Research*, 14(3): 227-136.
- McPherson, A., 2003. Salt source and development of the regolith salt store in the upper Billabong Creek Catchment, S.E. NSW, in *Advances in Regolith: Proceedings of the CRC LEME Regional Regolith Symposia, 2003*, eds Roach, I. C., Cooperative Research Centre for Landscape Environments and Mineral Exploration, Bentley, pp.292-295.
- McTainsh, 1985. Dust processes in Australia and West Africa: a comparison, *Search*, 16(3-4): 104-106.
- McTainsh, G. H. and Lynch, A. W., 1996. Quantitative estimates of the effect of climate change on dust storm activity in Australia during the Last Glacial Maximum, *Geomorphology*, 17(1-3): 263-271.
- McTainsh, G. H. and Strong, C., 2007. The role of aeolian dust in ecosystems, *Geomorphology*, 89(1-2): 39-54.
- McTainsh, G. H., Leys, J. F. and Nickling, W. G., 1999. Wind erodibility of arid lands in the Channel Country of western Queensland, Australia, *Zeitschrift für Geomorphologie N.F.*, 116: 113-130.
- McTainsh, G. H., Lynch, A. W. and Tews, E. K., 1998. Climatic controls upon dust storm occurrence in eastern Australia, *Journal of Arid Environments*, 39(3): 457-466.
- McTainsh, G. H., Chan, Y., McGowan, H. Leys, J. and Tews, K., 2005. The 23rd October 2002 dust storm in eastern Australia: characteristics and meteorological conditions, *Atmospheric Environment*, 39(7): 1227-1236.
- Mees, F. and Singer, A., 2006. Surface crust on soils/sediments of the southern Aral Sea basin, Uzbekistan, *Geoderma*, 136(1-2): 152-159.
- Melis, M. I. and Acworth, R. I., 2001. An aeolian component in Pleistocene and Holocene valley aggradation: evidence from Dicks Creek catchment, Yass, New South Wales, *Australian Journal of Soil Research*, 39(1): 13-38.
- Mitchell, R. M., O'Brien, D. M. and Campbell, S. K., 2006. Characteristics and radiative impact of the aerosol generated by the Canberra firestorm of January 2003, *Journal of Geophysical Research*, 111, D02204, doi:10.1029/2005JD006304.
- Moreno, T., Oldroyd, A., McDonald, I. and Gibbons, W., 2007. Preferential fractionation of trace metals – metalloids into PM₁₀ resuspended from contaminated gold mine tailings at Rodalquilar, Spain, *Water, Air and Soil Pollution*, 179(1-4): 93-105.
- Munday, T. J., Reilly, N. S., Glover, M., Lawrie, K. C., Scott, T., Chartres, C. J. and Evans, W. R., 2000. Petrophysical characterisation of parna using ground and downhole geophysics at Marinna, central New South Wales, *Exploration Geophysics*, 31(2): 260-266.
- NASA (National Aeronautics and Space Administration), 2008. Measurement of Atmospheric Composition in the Ultraviolet Region. Available from: <http://macuv.gsfc.nasa.gov/OMIAerosol.md> (Accessed 15 October 2008).
-

-
- National Research Council Canada, 2008. Periodic Table of the Elements. Available from: <http://www.nrc-cnrc.gc.ca/eng/education/elements/index.html#tphp> (Accessed 28 August 2008).
- Newberg, J. T., Matthew, B. M. and Anastasio, C., 2005. Chloride and bromide depletions in sea-salt particles over the northeastern Pacific Ocean, *Journal of Geophysical Research*, 110, D06209, doi:10.1029/2004JD005446.
- Okin, G. S., Gillette, D. A. and Herrick, 2006. Multi-scale controls on and consequences of aeolian processes in landscape change in arid and semi-arid environments, *Journal of Arid Environment*, 65(2): 253-275.
- Olmo, F. J., Quirantes, A., Lara, V., Lyamani, H. and Aldos-Arboleda, L., 2008. Aerosol optical properties assessed by an inversion method using the solar principal plane for non-spherical particles, *Journal of Quantitative Spectroscopy & Radiative Transfer*, 109(8): 1504-1516.
- Orlovsky, N. and Orlovsky, L., 2001. Part IV Chapter 8 White sandstorms in Central Asia, in *Global alarm: Dust and sandstorms from the World's drylands*, eds Youlin, Y., Squires, V. and Qi, L., United Nations, Bangkok, pp.169-201. Available from: <http://www.unccd.int/publicinfo/duststorms/globalAlarm-eng.pdf> (Accessed 1 September 2008).
- Pell, S. D., Chivas, A. R. and Williams, I. S., 2000. The Simpson, Strzelecki and Tirari Deserts: development and sand provenance, *Sedimentary Geology*, 130(1-2): 107-130.
- Petherick, L. M., McGowan, H. A. and Kamber, B. S., (in press) Reconstructing transport pathways for late Quaternary dust from eastern Australia using the composition of trace elements of long travelled dust, *Geomorphology*, doi:10.1016/j.geomorph.2007.12.015
- Pilans, B. and Bourman, R., 2001. Mid Pleistocene arid shift in southern Australia, dated by magnetostratigraphy, *Australian Journal of Soil Research*, 39(1): 89-98.
- Potter, K. N., 1990. Estimating wind-erodible materials on newly crusted soils, *Soil Science*, 150(5), 771-776.
- Poulton, S. W. and Raiswell, R., 2002. The low-temperature geochemical cycle of iron: from continental fluxes to marine sediment deposition, *American Journal of Science*, 302(9): 774-805.
- Prospero, J. M., Ginoux, P., Torres, O., Nicholson, S. E. and Gill, T. E., 2002. Environmental characterization of global sources of atmospheric soil dust identified with the NIMBUS 7 Total Ozone Mapping Spectrometer (TOMS) absorbing aerosol product, *Reviews of Geophysics*, 40(1): 1002, doi:10.1029/2000RG000095.
- Pye, K., 1984. Loess, *Progress in Physical Geography*, 8(2): 176-217.
- Pye, K., 1987. *Aeolian Dust and Dust Deposits*, Academic Press, London.
- Pye, K., 1989. Processes of fine particle formation, dust source regions, and climatic changes, in *Paleoclimatology and Paleometeorology: Modern and Past Patterns of Global Atmospheric Transport*, eds Leinen, M. and Sarnthein, M., Kluwer Academic Publisher, Dordrecht, Netherlands, pp.3-30.
- Quirk, J. P., 1994. Interparticle forces: a basis for the interpretation of soil physical behaviour, *Advances in Agronomy*, 53: 121-183.
- Raupach, M., McTainsh, G. H. and Leys, J. F., 1994. Estimates of dust mass in recent major Australian dust storms, *Australian Journal of Soil and Water Conservation*, 7(3): 20-24.
-

-
- Reid, A. , 1996. *Investigation into Heavy Metal Content of Soil and Dust within the Goonumbla Region*, The North Group, Melbourne.
- Revel-Rolland, M., De Deckker, P., Delmonte, B., Hesse, P. P., Magee, J. W., Basile-Doelsch, I., Grousset, F. and Bosch, D., 2006. Eastern Australia: A possible source of dust in East Antarctica interglacial ice, *Earth and Planetary Science Letters*, 249(1-2): 1-13.
- Reynolds, R. L., Yount, J. C., Reheis, M., Goldstein, H., Chavez, P. Jr., Fulton, R., Whitney, J., Fuller, C. and Forester, R. M., 2007. Dust emission from wet and dry playas in the Mojave Desert, USA, *Earth Surface Processes and Landforms*, 32(12): 1811-1827.
- Rodriguez, M. A. and Dabdub, D., 2004. IMAGES-SCAPE2: A modeling study of size- and chemically resolved aerosol thermodynamics in a global chemical transport model, *Journal of Geophysical Research*, 109, D02203, doi:10.1029/2003JD003639.
- Rolph, G. D., 2003. Real-time Environmental Applications and Display sYstem (READY) Website, NOAA Air Resources Laboratory, Silver Spring, MD. Available from: <http://www.arl.noaa.gov/ready/hysplit4.html> (Accessed 13 October 2008).
- Rotstayn, L. D., Keywood, M. D., Forgan, B. W., Gabric, A. J., Galbally, I. E., Gras, J. L., Luhar, A. K., McTainsh, G. H., Mitchell, R. M. and Young, S. A., 2008. Possible impacts of anthropogenic and natural aerosols on Australian climate: a review, *International Journal of Climatology*, DOI: 10.1002/joc.1729.
- SCDSI (Special Committee on Dust and Sandstorm Issues), 2005. *The Special Committee Report on Dust and Sandstorm Issues*. Available from: <http://www.env.go.jp/earth/dss/report/02/index.html> (Accessed 1 September 2008).
- Schollaert, S. E. and Merrill, J. T., 1998. Cooler sea surface west of the Sahara Desert correlated to dust events, *Geophysical Research Letters*, 25(18): 3529-3532.
- Sivakumar, M. V. K., 2007. Interactions between climate and desertification, *Agricultural and Forest Meteorology*, 142(2-4): 143-155.
- Smalley, I. 2008. A call for Australian loess: discussion and commentary, *Area*, 40(1): 131-134.
- Smalley, I. J. and Krinsley, D. H., 1978. Loess deposits associated with deserts, *Catena*, 5: 53-66.
- Smith, R. K., Reeder, M. J. and Tapper, N. J., 1995. Central Australian cold fronts, *Monthly Weather Review*, 123(1): 16-38.
- Smith, S. V., Renwick, W. H., Buddemeier, R. W. and Crossland, C. J., 2001, Budgets of soil erosion and deposition for sediments and sedimentary organic carbon across the conterminous United States, *Global Biogeochemical Cycles*, 15(3): 697-707.
- Smithson, A., 2004. Evidence of aeolian Quaternary sediments as a salt source for dryland salinity in Central New South Wales, *The 9th Murray-Darling Basin Groundwater Workshop*, 17-19 February 2004, Bendigo.
- SOEC (2006 Australian State of the Environment Committee), 2006. Section 8.2 Land condition, in *Australia State of the Environment 2006*. Available from: <http://www.environment.gov.au/soe/2006/publications/report/land-2.html#soil-loss> (Accessed 1 September 2008).
-

Spain, A. V., Isbell, R. F. and Probert, M. E., 1983. Chapter 34: Soil organic matter, in *Soils: an Australian Viewpoint*, CSIRO/Academic Press, Melbourne/London, pp.551-563.

Squires, V., 2001. Part III Chapter 7 Dust storms and dust devils in South Australia: The driest province of the driest continent on Earth, in *Global Alarm: Dust and sandstorms from the World's drylands*, eds Youlin, Y., Squires, V. and Qi, L., United Nations, Bangkok, pp.155-166. Available from:

<http://www.unccd.int/publicinfo/duststorms/globalAlarm-eng.pdf>

(Accessed 1 September 2008).

Stoorvogel, J. J., van Breemen, N. And Janssen, B. H., 1997. The nutrient input by Harmattan dust to a forest ecosystem in Côte d'Ivoire, Africa, *Biogeochemistry*, 37(2): 145-157.

Swap, R., Garstang, M. and Greco, S., 1992. Saharan dust in the Amazon Basin, *Tellus*, 44B: 133-149.

Tanaka, T. Y. and Chiba, M., 2006. A numerical study of the contributions of dust source regions to the global dust budget, *Global and Planetary Change*, 52(1-4): 88-104.

Tate, S. E., Greene, R. S. B., Scott, K. M. and McQueen, K. G., 2007. Recognition and characterisation of the aeolian component in soils in the Girilambone Region, north western New South Wales, Australia, *Catena*, 69(2): 122-133.

Tegan, I., Werner, M., Harrison, S. P. and Kohfeld, K. E., 2004. Relative importance of climate and land use in determining present and future global soil dust emission, *Geophysical Research Letter*, 31, L05105, doi:10.1029/2003GL019216.

The Weather Co., 2008. Weather forecast – Australia and world weather – live BoM radar. Available from: <http://www.weatherzone.com.au/> (Accessed 23 December 2008).

Tiller, K. G., Smith, L. H. and Merry, R. H., 1987. Accessions of atmospheric dust east of Adelaide, South Australia and the implications for pedogenesis, *Australian Journal of Soil Research*, 25(1): 43-54.

Tsoar, H. and Pye, K., 1987. Dust transport and the question of desert loess formation, *Sedimentology*, 34(1): 139-153.

Tungsheng, L, Zhisheng, A., Baoyin, Y. and Jiamao, H., 1985. The loess-paleosol sequence in China and climatic history, *Episodes*, 8(1): 21-28.

Wai, K. M. and Tanner, P. A., 2005. Case studies of Asian Dust Storm impacts on a coastal site: Implication of a good dust storm tracer, *Water, Air, and Soil Pollution*, 168(1-4): 59-70.

Walker, P. H. and Costin, A. B., 1971. Atmospheric dust accession in south-eastern Australia, *Australian Journal of Soil Research*, 9: 1-5.

Warren, A., Chappell, A., Todd, M. C., Bristow, C., Drake, N., Engelstaedter, S., Martins, V., M'bgainayel, S. and Washington, R., 2007. Dust-raising in the dustiest place on earth, *Geomorphology*, 92(1-2): 25-37.

Washington, R., Todd, M., Middleton, N. J. and Goudie, A. S., 2003. Dust-storm source areas determined by the Total Ozone Monitoring Spectrometer and surface observations, *Annals of the Association of American Geographers*, 93(2): 297-313.

Washington, R., Todd, M. C., Lizcano, G., Tegan, I., Flamant, C., Koren, I., Ginoux, P., Engelstaedter, S., Bristow, C. S., Zender, C. S., Goudie, A. S., Warren, A. and Prospero, J. M., 2006. Links between topography, wind, deflation, lakes and dust: The case of the Bodélé Depression, Chad, *Geophysical Research Letters*, 33: L09401, doi:10.1029/2006GL025827

Williams, P. and Young, M., 1999. Costing dust – How much does wind erosion cost the people of South Australia? Available from:
http://www.clw.csiro.au/publications/consultancy/1999/costing_dust.pdf
(Accessed 1 September 2008).

Williams, W. D., 2002. Environmental threats to salt lakes and the likely status of inland saline ecosystems in 2025, *Environmental Conservation*, 29(2): 154-167.

Williamson, A. and Johnson, M. S., 1981. Chapter 6 Reclamation of metalliferous mine wastes, in *Effect of Heavy Metal Pollution on Plants – Volume 2: Metals in the Environment*, eds Lepp, N. W., Applied Science Publishers, London and New Jersey.

Wong, V. N. L., Murphy, B. W., Koen, T. B., Greene, R. S. B. and Dalal, R. C., 2008. Soil organic carbon stocks in saline and sodic landscapes, *Australian Journal of Soil Research*, 46(4): 378-389.

Wood, W. W. and Sanford, W. E., 1995. Eolian transport, saline lake basins, and groundwater solutes, *Water Resources Research*, 31(12): 3121-3129.

Woodward, S., 2001. Modeling the atmospheric life cycle and radiative impact of mineral dust in the Hadley Centre climate model, *Journal of Geophysical Research*, 106(D16): 18,155-18,166.

Wray, D. S., 1998. The impact of unconfined mine tailings and anthropogenic pollution on a semi-arid environment – an initial study of the Rodalquilar mining district, south east Spain, *Environmental Geochemistry and Health*, 20(1): 29-38.

Wright, J. S., 2001. “Desert” loess versus “glacial” loess: quartz silt formation, source areas and sediment pathways in the formation of loess deposits, *Geomorphology*, 36(3-4): 231-256.

Yan, H., Wang, S., Wang, C., Zhang, G. and Patel, N., 2005. Losses of soil organic carbon under wind erosion in China, *Global Change Biology*, 11(5): 828-840.

Yang, Y. and Lu, Q., 2001. Part V Chapter 11 Dust-sandstorms: Inevitable consequences of desertification – A case study of desertification disaster in the Hexi Corridor, Northwest China, in *Global Alarm: Dust and sandstorms from the World's drylands*, eds Youlin, Y., Squires, V. and Qi, L., United Nations, Bangkok, pp.227-240. Available from:
<http://www.unccd.int/publicinfo/duststorms/globalAlarm-eng.pdf>
(Accessed 1 September 2008).

Yang, X., Zhu, Z., Jaekel, D., Owen, L. A. and Han, J., 2002. Late Quaternary palaeoenvironment change and landscape evolution along the Keria River, Xinjiang, China: the relationship between high mountain glaciation and landscape evolution in foreland desert regions, *Quaternary International*, 97-98: 155-166.

Zender, C. S., Bian, H. and Newman, D., 2003. The mineral dust entrainment and deposition (DEAD) model: Description and 1990s dust climatology, *Journal of Geophysical Research*, 108(D14): 4416, doi:10.1029/2002JD002775.

Zhang, Z., Arimoto, R., An, Z., Chen, T., Zhang, G., Zhu, G. and Wang, X., 1993. Atmospheric trace elements over source regions for Chinese dust: Concentrations, sources and atmospheric deposition on the Loess Plateau, *Atmospheric Environment*, 27A(13): 2051-1067.

Appendix A-1: IBA Results 1

IBA results for CSIRO samples which had been analysed soluble and insoluble materials.

			Cobar	Cobar	Cobar	Sydney	Sydney	Sydney
Element	Unit		2007.6	2007.7	2008.4	2007.5 – 2007.6	2007.7	2007.11
F	Ins	$\mu\text{g cm}^{-2}$	0.122	0.000	0.039	0.030	0.015	0.000
	Sol	$\mu\text{g cm}^{-2}$	0.000	0.000	0.000	1.800	0.000	0.000
Na	Ins	$\mu\text{g cm}^{-2}$	0.000	0.000	0.072	0.000	0.118	0.000
	Sol	$\mu\text{g cm}^{-2}$	6.950	1.450	9.800	12.900	0.000	0.000
Al	Ins	$\mu\text{g cm}^{-2}$	5.124	1.368	5.256	0.000	0.600	0.257
	Sol	$\mu\text{g cm}^{-2}$	0.000	0.000	0.000	0.000	0.000	0.000
Si	Ins	$\mu\text{g cm}^{-2}$	20.273	6.132	16.677	0.767	3.264	1.601
	Sol	$\mu\text{g cm}^{-2}$	10.600	12.150	10.100	0.900	0.000	2.600
P	Ins	$\mu\text{g cm}^{-2}$	0.000	0.202	0.103	0.000	0.000	0.053
	Sol	$\mu\text{g cm}^{-2}$	0.000	0.950	0.550	0.000	0.000	0.500
S	Ins	$\mu\text{g cm}^{-2}$	0.162	0.199	0.155	0.036	0.100	0.156
	Sol	$\mu\text{g cm}^{-2}$	3.050	1.650	4.750	0.900	0.000	0.900
Cl	Ins	$\mu\text{g cm}^{-2}$	0.000	0.000	0.000	0.000	0.000	0.000
	Sol	$\mu\text{g cm}^{-2}$	21.600	9.750	17.550	24.100	0.000	6.500
K	Ins	$\mu\text{g cm}^{-2}$	1.583	0.867	1.715	0.058	0.245	0.142
	Sol	$\mu\text{g cm}^{-2}$	4.700	0.400	5.200	0.000	0.000	0.300
Ca	Ins	$\mu\text{g cm}^{-2}$	0.186	0.168	0.353	0.026	0.535	0.084
	Sol	$\mu\text{g cm}^{-2}$	11.700	2.900	13.200	1.500	0.400	0.500
Ti	Ins	$\mu\text{g cm}^{-2}$	0.588	0.257	0.635	0.025	0.176	0.071
	Sol	$\mu\text{g cm}^{-2}$	0.000	0.000	0.000	0.000	0.000	0.000
V	Ins	$\mu\text{g cm}^{-2}$	0.023	0.009	0.021	0.000	0.000	0.000
	Sol	$\mu\text{g cm}^{-2}$	0.000	0.000	0.000	0.000	0.000	0.000
Cr	Ins	$\mu\text{g cm}^{-2}$	0.055	0.086	0.003	0.000	0.000	0.009
	Sol	$\mu\text{g cm}^{-2}$	0.000	0.500	0.000	0.750	0.000	0.250
Mn	Ins	$\mu\text{g cm}^{-2}$	0.070	0.027	0.048	0.000	0.023	0.018
	Sol	$\mu\text{g cm}^{-2}$	0.200	0.400	1.000	0.000	0.000	0.200
Fe	Ins	$\mu\text{g cm}^{-2}$	6.339	3.668	5.787	0.298	1.321	0.872
	Sol	$\mu\text{g cm}^{-2}$	0.000	7.100	1.950	3.200	0.000	1.450
Co	Ins	$\mu\text{g cm}^{-2}$	0.000	0.023	0.049	0.000	0.012	0.000
	Sol	$\mu\text{g cm}^{-2}$	0.000	0.000	0.000	0.000	0.000	0.000
Ni	Ins	$\mu\text{g cm}^{-2}$	0.057	0.028	0.012	0.000	0.000	0.000
	Sol	$\mu\text{g cm}^{-2}$	0.000	0.500	0.200	0.500	0.000	0.300
Cu	Ins	$\mu\text{g cm}^{-2}$	0.133	0.034	0.096	0.005	0.021	0.012
	Sol	$\mu\text{g cm}^{-2}$	0.000	0.150	0.000	0.000	0.000	0.000
Zn	Ins	$\mu\text{g cm}^{-2}$	0.084	0.050	0.047	0.007	0.066	0.008
	Sol	$\mu\text{g cm}^{-2}$	0.550	0.200	0.300	0.300	0.300	0.250
Br	Ins	$\mu\text{g cm}^{-2}$	0.000	0.002	0.002	0.000	0.001	0.000
	Sol	$\mu\text{g cm}^{-2}$	0.050	0.000	0.050	0.250	0.050	0.000
Sr	Ins	$\mu\text{g cm}^{-2}$	0.000	0.000	0.009	0.000	0.009	0.000
	Sol	$\mu\text{g cm}^{-2}$	0.000	0.000	0.000	0.000	0.000	0.000
Pb	Ins	$\mu\text{g cm}^{-2}$	0.018	0.000	0.017	0.000	0.008	0.000
	Sol	$\mu\text{g cm}^{-2}$	0.000	0.000	0.000	0.000	0.000	0.000

Note: An influence of the size of the petri dish on the soluble portion is corrected in the tables. Therefore, soluble and insoluble portions are directly comparable.

			Sydney	Sydney	Sydney	Wagga Wagga	Wagga Wagga	Wagga Wagga
Element	Unit		2008.2	2008.3	2008.4	2007.12	2008.1	2008.2
F	Ins	$\mu\text{g cm}^{-2}$	0.000	0.000	0.000	0.000	0.000	0.000
	Sol	$\mu\text{g cm}^{-2}$	0.000	0.600	0.000	0.000	2.900	0.000
Na	Ins	$\mu\text{g cm}^{-2}$	0.000	0.083	0.000	0.000	0.000	0.000
	Sol	$\mu\text{g cm}^{-2}$	0.000	8.900	100.150	1.650	0.000	0.000
Al	Ins	$\mu\text{g cm}^{-2}$	0.078	0.323	0.000	0.305	0.047	0.308
	Sol	$\mu\text{g cm}^{-2}$	0.000	0.000	0.000	0.000	0.000	0.000
Si	Ins	$\mu\text{g cm}^{-2}$	1.085	3.462	0.098	2.395	0.925	2.937
	Sol	$\mu\text{g cm}^{-2}$	0.050	0.650	6.750	1.050	0.350	0.850
P	Ins	$\mu\text{g cm}^{-2}$	0.000	0.035	0.312	0.015	0.015	0.094
	Sol	$\mu\text{g cm}^{-2}$	0.000	0.000	35.500	0.000	0.000	0.000
S	Ins	$\mu\text{g cm}^{-2}$	0.043	0.111	0.081	0.015	0.013	0.068
	Sol	$\mu\text{g cm}^{-2}$	0.000	0.400	6.100	0.400	0.000	0.000
Cl	Ins	$\mu\text{g cm}^{-2}$	0.000	0.000	0.000	0.000	0.000	0.000
	Sol	$\mu\text{g cm}^{-2}$	0.000	14.800	176.550	4.050	0.000	0.000
K	Ins	$\mu\text{g cm}^{-2}$	0.079	0.345	0.054	0.210	0.097	0.328
	Sol	$\mu\text{g cm}^{-2}$	0.000	0.000	44.900	1.850	0.000	0.000
Ca	Ins	$\mu\text{g cm}^{-2}$	0.056	0.136	0.000	0.014	0.011	0.000
	Sol	$\mu\text{g cm}^{-2}$	0.000	2.150	3.650	2.150	0.000	0.000
Ti	Ins	$\mu\text{g cm}^{-2}$	0.038	0.190	0.000	0.082	0.022	0.086
	Sol	$\mu\text{g cm}^{-2}$	0.000	0.000	0.000	0.000	0.000	0.000
V	Ins	$\mu\text{g cm}^{-2}$	0.000	0.000	0.000	0.000	0.000	0.000
	Sol	$\mu\text{g cm}^{-2}$	0.000	0.000	0.000	0.000	0.000	0.000
Cr	Ins	$\mu\text{g cm}^{-2}$	0.004	0.004	0.000	0.000	0.000	0.000
	Sol	$\mu\text{g cm}^{-2}$	0.000	0.000	0.000	0.000	0.000	0.000
Mn	Ins	$\mu\text{g cm}^{-2}$	0.000	0.006	0.005	0.000	0.000	0.005
	Sol	$\mu\text{g cm}^{-2}$	0.000	0.000	0.400	0.000	0.000	0.000
Fe	Ins	$\mu\text{g cm}^{-2}$	0.511	1.190	0.003	0.525	0.215	0.716
	Sol	$\mu\text{g cm}^{-2}$	0.050	0.000	0.250	0.000	0.150	0.050
Co	Ins	$\mu\text{g cm}^{-2}$	0.000	0.000	0.000	0.000	0.000	0.000
	Sol	$\mu\text{g cm}^{-2}$	0.000	0.000	0.000	0.000	0.000	0.000
Ni	Ins	$\mu\text{g cm}^{-2}$	0.000	0.000	0.000	0.000	0.000	0.000
	Sol	$\mu\text{g cm}^{-2}$	0.000	0.000	0.150	0.300	0.000	0.200
Cu	Ins	$\mu\text{g cm}^{-2}$	0.005	0.018	0.008	0.005	0.005	0.006
	Sol	$\mu\text{g cm}^{-2}$	0.000	0.300	0.000	0.200	0.000	0.150
Zn	Ins	$\mu\text{g cm}^{-2}$	0.005	0.019	0.020	0.012	0.005	0.008
	Sol	$\mu\text{g cm}^{-2}$	0.200	0.450	0.550	0.400	0.000	0.000
Br	Ins	$\mu\text{g cm}^{-2}$	0.000	0.000	0.000	0.000	0.000	0.001
	Sol	$\mu\text{g cm}^{-2}$	0.000	0.000	0.250	0.000	0.000	0.000
Sr	Ins	$\mu\text{g cm}^{-2}$	0.000	0.000	0.000	0.000	0.000	0.000
	Sol	$\mu\text{g cm}^{-2}$	0.000	0.000	0.000	0.000	0.000	0.000
Pb	Ins	$\mu\text{g cm}^{-2}$	0.000	0.000	0.000	0.000	0.000	0.000
	Sol	$\mu\text{g cm}^{-2}$	0.000	0.000	0.000	0.000	0.000	0.000

			Wagga Wagga	Wagga Wagga	Melbourne	Melbourne	Melbourne	Melbourne
Element		Unit	2008.3	2008.4	2007.6	2007.7	2007.11	2008.2
F	Ins	$\mu\text{g cm}^{-2}$	0.231	0.025	0.000	0.000	0.000	0.017
	Sol	$\mu\text{g cm}^{-2}$	0.000	0.000	1.200	0.000	0.000	0.700
Na	Ins	$\mu\text{g cm}^{-2}$	0.965	0.218	0.164	0.020	0.000	0.069
	Sol	$\mu\text{g cm}^{-2}$	0.000	1.650	43.900	31.650	0.000	72.050
Al	Ins	$\mu\text{g cm}^{-2}$	23.914	5.756	0.156	0.220	0.325	0.528
	Sol	$\mu\text{g cm}^{-2}$	0.000	0.000	0.000	0.000	0.000	0.000
Si	Ins	$\mu\text{g cm}^{-2}$	82.813	23.769	2.151	1.964	1.828	3.849
	Sol	$\mu\text{g cm}^{-2}$	3.100	4.600	0.400	0.550	4.100	5.050
P	Ins	$\mu\text{g cm}^{-2}$	0.000	0.126	0.000	0.000	0.249	0.085
	Sol	$\mu\text{g cm}^{-2}$	0.000	1.000	0.000	0.000	0.750	0.000
S	Ins	$\mu\text{g cm}^{-2}$	0.397	0.151	0.027	0.013	0.105	0.163
	Sol	$\mu\text{g cm}^{-2}$	0.350	1.000	2.050	3.000	1.400	5.100
Cl	Ins	$\mu\text{g cm}^{-2}$	0.000	0.000	0.074	0.000	0.000	0.000
	Sol	$\mu\text{g cm}^{-2}$	0.000	7.850	55.300	34.450	2.400	110.000
K	Ins	$\mu\text{g cm}^{-2}$	8.136	2.259	0.145	0.099	0.167	0.240
	Sol	$\mu\text{g cm}^{-2}$	0.000	2.500	0.900	0.500	1.050	1.650
Ca	Ins	$\mu\text{g cm}^{-2}$	0.686	0.200	0.131	0.099	0.088	0.214
	Sol	$\mu\text{g cm}^{-2}$	0.700	6.700	2.400	4.450	1.800	15.900
Ti	Ins	$\mu\text{g cm}^{-2}$	3.092	0.827	0.156	0.129	0.091	0.217
	Sol	$\mu\text{g cm}^{-2}$	0.000	0.000	0.000	0.000	0.000	0.000
V	Ins	$\mu\text{g cm}^{-2}$	0.351	0.021	0.000	0.000	0.000	0.000
	Sol	$\mu\text{g cm}^{-2}$	0.000	0.000	0.000	0.000	0.000	0.000
Cr	Ins	$\mu\text{g cm}^{-2}$	0.000	0.004	0.027	0.003	0.005	0.001
	Sol	$\mu\text{g cm}^{-2}$	1.250	0.000	0.000	0.000	0.000	0.000
Mn	Ins	$\mu\text{g cm}^{-2}$	0.460	0.055	0.006	0.000	0.010	0.008
	Sol	$\mu\text{g cm}^{-2}$	0.300	0.450	0.000	0.000	0.250	0.400
Fe	Ins	$\mu\text{g cm}^{-2}$	23.754	6.080	1.145	0.893	0.670	1.092
	Sol	$\mu\text{g cm}^{-2}$	6.300	3.100	0.000	0.000	1.150	0.000
Co	Ins	$\mu\text{g cm}^{-2}$	0.105	0.055	0.000	0.000	0.000	0.000
	Sol	$\mu\text{g cm}^{-2}$	0.000	0.000	0.000	0.000	0.000	0.000
Ni	Ins	$\mu\text{g cm}^{-2}$	0.470	0.034	0.010	0.026	0.004	0.000
	Sol	$\mu\text{g cm}^{-2}$	0.800	0.650	0.000	0.000	0.200	0.200
Cu	Ins	$\mu\text{g cm}^{-2}$	1.827	0.114	0.013	0.011	0.032	0.014
	Sol	$\mu\text{g cm}^{-2}$	0.000	0.000	0.200	0.600	0.100	0.350
Zn	Ins	$\mu\text{g cm}^{-2}$	0.356	0.049	0.010	0.007	0.008	0.044
	Sol	$\mu\text{g cm}^{-2}$	0.000	0.150	0.250	0.600	0.650	0.650
Br	Ins	$\mu\text{g cm}^{-2}$	0.000	0.000	0.000	0.000	0.000	0.005
	Sol	$\mu\text{g cm}^{-2}$	0.050	0.000	0.000	0.000	0.000	0.050
Sr	Ins	$\mu\text{g cm}^{-2}$	0.060	0.011	0.000	0.000	0.000	0.000
	Sol	$\mu\text{g cm}^{-2}$	0.000	0.000	0.000	0.000	0.000	0.000
Pb	Ins	$\mu\text{g cm}^{-2}$	0.123	0.015	0.000	0.000	0.000	0.000
	Sol	$\mu\text{g cm}^{-2}$	0.000	0.000	0.000	0.000	0.000	0.000

		Melbourne	Melbourne	Mildura	Mildura	Mildura	Mildura
Element	Unit	2008.3	2008.4	2007.6	2007.7	2008.1	2008.3
F	Ins $\mu\text{g cm}^{-2}$	0.385	0.137	0.000	0.069	0.213	0.211
	Sol $\mu\text{g cm}^{-2}$	0.000	0.000	0.000	0.000	0.900	1.100
Na	Ins $\mu\text{g cm}^{-2}$	1.684	0.250	0.000	0.102	0.393	0.770
	Sol $\mu\text{g cm}^{-2}$	20.500	20.650	0.000	0.000	33.300	2.550
Al	Ins $\mu\text{g cm}^{-2}$	10.549	2.395	0.000	1.028	8.945	8.447
	Sol $\mu\text{g cm}^{-2}$	0.000	0.000	0.000	0.000	0.000	0.000
Si	Ins $\mu\text{g cm}^{-2}$	45.832	14.153	0.179	4.705	31.809	29.741
	Sol $\mu\text{g cm}^{-2}$	1.600	13.850	3.650	0.000	2.050	0.600
P	Ins $\mu\text{g cm}^{-2}$	0.000	0.081	0.000	0.000	0.000	0.000
	Sol $\mu\text{g cm}^{-2}$	0.000	0.000	0.000	0.000	0.000	0.000
S	Ins $\mu\text{g cm}^{-2}$	0.597	0.304	0.023	0.092	0.300	0.127
	Sol $\mu\text{g cm}^{-2}$	3.050	14.250	0.350	0.000	0.850	0.450
Cl	Ins $\mu\text{g cm}^{-2}$	0.000	0.000	0.000	0.000	0.000	0.000
	Sol $\mu\text{g cm}^{-2}$	36.200	35.800	2.400	0.000	28.150	4.150
K	Ins $\mu\text{g cm}^{-2}$	3.662	2.115	0.012	0.476	3.136	3.167
	Sol $\mu\text{g cm}^{-2}$	2.600	5.450	0.000	0.000	9.250	0.550
Ca	Ins $\mu\text{g cm}^{-2}$	2.298	1.318	0.051	0.200	0.957	1.320
	Sol $\mu\text{g cm}^{-2}$	9.550	19.250	2.600	1.300	20.700	26.400
Ti	Ins $\mu\text{g cm}^{-2}$	2.555	1.083	0.000	0.250	1.144	1.061
	Sol $\mu\text{g cm}^{-2}$	0.000	0.000	0.000	0.000	0.000	0.000
V	Ins $\mu\text{g cm}^{-2}$	0.100	0.019	0.000	0.000	0.065	0.110
	Sol $\mu\text{g cm}^{-2}$	0.000	0.000	0.000	0.000	0.000	0.000
Cr	Ins $\mu\text{g cm}^{-2}$	0.121	0.025	0.027	0.278	0.030	0.036
	Sol $\mu\text{g cm}^{-2}$	0.000	0.000	0.000	0.000	0.000	0.000
Mn	Ins $\mu\text{g cm}^{-2}$	0.062	0.099	0.011	0.028	0.138	0.110
	Sol $\mu\text{g cm}^{-2}$	0.000	0.400	0.000	0.000	0.000	0.000
Fe	Ins $\mu\text{g cm}^{-2}$	18.568	8.130	0.181	4.403	10.090	10.306
	Sol $\mu\text{g cm}^{-2}$	0.000	0.000	1.550	0.000	0.000	0.050
Co	Ins $\mu\text{g cm}^{-2}$	0.467	0.062	0.000	0.034	0.153	0.262
	Sol $\mu\text{g cm}^{-2}$	0.000	0.000	0.000	0.000	0.000	0.000
Ni	Ins $\mu\text{g cm}^{-2}$	0.334	0.013	0.016	0.097	0.083	0.165
	Sol $\mu\text{g cm}^{-2}$	0.150	0.000	0.450	0.000	0.000	0.000
Cu	Ins $\mu\text{g cm}^{-2}$	1.181	0.131	0.000	0.022	0.365	0.590
	Sol $\mu\text{g cm}^{-2}$	0.300	0.000	0.000	0.000	0.550	0.000
Zn	Ins $\mu\text{g cm}^{-2}$	0.345	0.120	0.008	0.069	0.165	0.201
	Sol $\mu\text{g cm}^{-2}$	0.650	0.250	0.000	0.300	0.000	0.000
Br	Ins $\mu\text{g cm}^{-2}$	0.000	0.000	0.000	0.008	0.034	0.000
	Sol $\mu\text{g cm}^{-2}$	0.050	0.000	0.100	0.000	0.000	0.000
Sr	Ins $\mu\text{g cm}^{-2}$	0.057	0.022	0.000	0.000	0.000	0.054
	Sol $\mu\text{g cm}^{-2}$	0.000	0.000	0.000	0.000	0.000	0.000
Pb	Ins $\mu\text{g cm}^{-2}$	0.315	0.000	0.000	0.016	0.081	0.141
	Sol $\mu\text{g cm}^{-2}$	0.000	0.000	0.000	0.000	0.000	0.000

			Mildura	Cape Grim	Cape Grim	Cape Grim	Cape Grim	Cape Grim
Element		Unit	2008.4	2007.5	2007.6	2007.11	2008.2	2008.3
F	Ins	$\mu\text{g cm}^{-2}$	0.000	0.363	0.756	0.355	0.252	0.150
	Sol	$\mu\text{g cm}^{-2}$	1.450	0.000	4.100	0.000	0.000	2.300
Na	Ins	$\mu\text{g cm}^{-2}$	0.000	3.073	7.375	4.832	4.285	0.928
	Sol	$\mu\text{g cm}^{-2}$	0.000	666.150	96.150	207.950	55.650	59.600
Al	Ins	$\mu\text{g cm}^{-2}$	0.413	14.168	20.215	8.017	7.738	3.211
	Sol	$\mu\text{g cm}^{-2}$	0.000	0.000	0.000	0.000	0.000	0.000
Si	Ins	$\mu\text{g cm}^{-2}$	1.365	60.403	65.768	33.741	29.187	13.394
	Sol	$\mu\text{g cm}^{-2}$	6.200	2.700	4.250	30.750	9.150	2.600
P	Ins	$\mu\text{g cm}^{-2}$	0.067	0.000	0.000	0.031	0.244	0.026
	Sol	$\mu\text{g cm}^{-2}$	0.700	0.000	0.000	0.000	5.350	0.000
S	Ins	$\mu\text{g cm}^{-2}$	0.089	1.112	0.182	0.214	0.557	0.163
	Sol	$\mu\text{g cm}^{-2}$	2.900	27.350	4.400	34.450	0.950	2.350
Cl	Ins	$\mu\text{g cm}^{-2}$	0.000	0.000	0.000	0.021	1.550	0.000
	Sol	$\mu\text{g cm}^{-2}$	2.700	757.950	133.950	406.200	109.850	105.200
K	Ins	$\mu\text{g cm}^{-2}$	0.172	2.538	1.291	1.351	1.482	0.469
	Sol	$\mu\text{g cm}^{-2}$	0.000	9.500	2.500	10.100	6.400	3.500
Ca	Ins	$\mu\text{g cm}^{-2}$	0.172	5.783	12.154	10.546	7.710	2.480
	Sol	$\mu\text{g cm}^{-2}$	293.700	17.300	9.800	38.950	11.000	6.650
Ti	Ins	$\mu\text{g cm}^{-2}$	0.042	7.783	12.227	8.257	5.587	2.514
	Sol	$\mu\text{g cm}^{-2}$	0.000	0.000	0.000	0.000	0.000	0.000
V	Ins	$\mu\text{g cm}^{-2}$	0.000	0.000	0.000	0.061	0.043	0.000
	Sol	$\mu\text{g cm}^{-2}$	0.000	0.000	0.000	0.000	0.000	0.000
Cr	Ins	$\mu\text{g cm}^{-2}$	0.001	0.198	0.450	0.258	0.198	0.044
	Sol	$\mu\text{g cm}^{-2}$	0.000	0.000	0.000	0.000	0.000	0.000
Mn	Ins	$\mu\text{g cm}^{-2}$	0.029	0.469	0.117	0.508	0.580	0.070
	Sol	$\mu\text{g cm}^{-2}$	0.350	0.000	0.000	1.450	3.150	0.300
Fe	Ins	$\mu\text{g cm}^{-2}$	1.557	67.388	122.315	66.946	52.733	18.490
	Sol	$\mu\text{g cm}^{-2}$	0.150	0.000	0.000	0.000	14.050	0.050
Co	Ins	$\mu\text{g cm}^{-2}$	0.000	1.859	5.484	1.052	0.764	0.278
	Sol	$\mu\text{g cm}^{-2}$	0.500	0.000	0.000	0.000	0.000	0.000
Ni	Ins	$\mu\text{g cm}^{-2}$	0.015	1.499	5.723	0.802	0.477	0.092
	Sol	$\mu\text{g cm}^{-2}$	0.000	0.000	0.000	0.000	0.000	0.000
Cu	Ins	$\mu\text{g cm}^{-2}$	0.007	4.427	11.894	2.350	1.515	0.297
	Sol	$\mu\text{g cm}^{-2}$	0.000	0.000	0.150	0.000	0.000	0.250
Zn	Ins	$\mu\text{g cm}^{-2}$	0.006	0.515	1.287	0.285	0.359	0.075
	Sol	$\mu\text{g cm}^{-2}$	0.000	0.000	0.000	0.000	0.000	0.000
Br	Ins	$\mu\text{g cm}^{-2}$	0.000	0.391	0.776	0.000	0.000	0.031
	Sol	$\mu\text{g cm}^{-2}$	0.000	0.000	0.100	0.700	0.200	0.100
Sr	Ins	$\mu\text{g cm}^{-2}$	0.000	0.251	0.841	0.282	0.152	0.058
	Sol	$\mu\text{g cm}^{-2}$	0.750	0.100	0.000	0.000	0.000	0.000
Pb	Ins	$\mu\text{g cm}^{-2}$	0.000	2.513	10.379	0.423	0.148	0.207
	Sol	$\mu\text{g cm}^{-2}$	0.000	0.000	0.000	0.000	0.000	0.000

			Cape Grim	Adelaide	Adelaide	Adelaide	Woomera	Woomera
Element	Unit		2008.4	2008.2	2008.3	2008.4	2007.6	2007.8
F	Ins	$\mu\text{g cm}^{-2}$	0.000	0.054	0.032	0.027	0.000	0.000
	Sol	$\mu\text{g cm}^{-2}$	0.000	0.000	0.000	0.200	0.000	0.000
Na	Ins	$\mu\text{g cm}^{-2}$	0.429	0.303	0.042	0.081	0.000	0.015
	Sol	$\mu\text{g cm}^{-2}$	182.700	289.700	83.750	118.900	0.000	0.000
Al	Ins	$\mu\text{g cm}^{-2}$	1.059	3.077	0.275	2.820	0.000	1.867
	Sol	$\mu\text{g cm}^{-2}$	0.000	0.000	0.000	0.000	0.000	0.000
Si	Ins	$\mu\text{g cm}^{-2}$	4.861	12.456	1.625	10.347	0.828	6.601
	Sol	$\mu\text{g cm}^{-2}$	8.200	32.350	1.300	19.050	2.550	0.900
P	Ins	$\mu\text{g cm}^{-2}$	0.344	0.035	0.000	0.000	0.312	0.405
	Sol	$\mu\text{g cm}^{-2}$	0.000	0.000	0.000	0.000	0.550	0.000
S	Ins	$\mu\text{g cm}^{-2}$	0.191	0.415	0.043	0.190	0.159	0.304
	Sol	$\mu\text{g cm}^{-2}$	17.950	68.550	5.250	33.850	0.550	0.700
Cl	Ins	$\mu\text{g cm}^{-2}$	0.035	0.037	0.000	0.000	0.000	0.000
	Sol	$\mu\text{g cm}^{-2}$	308.650	644.250	150.450	251.100	0.350	1.100
K	Ins	$\mu\text{g cm}^{-2}$	0.294	1.860	0.197	1.163	0.076	0.649
	Sol	$\mu\text{g cm}^{-2}$	11.800	12.000	3.650	7.700	0.900	1.850
Ca	Ins	$\mu\text{g cm}^{-2}$	1.122	0.906	0.087	0.198	0.000	0.201
	Sol	$\mu\text{g cm}^{-2}$	12.200	250.850	14.000	38.350	0.400	0.600
Ti	Ins	$\mu\text{g cm}^{-2}$	1.127	0.598	0.071	0.403	0.000	0.195
	Sol	$\mu\text{g cm}^{-2}$	0.000	0.000	0.000	0.000	0.000	0.000
V	Ins	$\mu\text{g cm}^{-2}$	0.000	0.000	0.000	0.010	0.000	0.000
	Sol	$\mu\text{g cm}^{-2}$	0.000	0.000	0.000	0.000	0.000	0.000
Cr	Ins	$\mu\text{g cm}^{-2}$	0.016	0.092	0.003	0.050	0.000	0.042
	Sol	$\mu\text{g cm}^{-2}$	0.000	0.000	0.000	0.000	3.000	0.000
Mn	Ins	$\mu\text{g cm}^{-2}$	0.062	0.123	0.009	0.036	0.005	0.046
	Sol	$\mu\text{g cm}^{-2}$	0.900	2.450	0.000	0.850	0.650	0.000
Fe	Ins	$\mu\text{g cm}^{-2}$	5.788	5.647	0.764	3.955	0.117	1.509
	Sol	$\mu\text{g cm}^{-2}$	3.800	8.250	0.000	0.000	30.250	0.000
Co	Ins	$\mu\text{g cm}^{-2}$	0.052	0.025	0.000	0.022	0.000	0.000
	Sol	$\mu\text{g cm}^{-2}$	0.000	0.000	0.000	0.000	0.000	0.000
Ni	Ins	$\mu\text{g cm}^{-2}$	0.000	0.027	0.006	0.366	0.000	0.012
	Sol	$\mu\text{g cm}^{-2}$	0.000	0.000	0.150	0.200	9.050	0.000
Cu	Ins	$\mu\text{g cm}^{-2}$	0.017	0.093	0.009	0.129	0.000	0.022
	Sol	$\mu\text{g cm}^{-2}$	0.000	0.000	0.150	0.200	0.600	0.000
Zn	Ins	$\mu\text{g cm}^{-2}$	0.022	0.316	0.027	0.082	0.004	0.074
	Sol	$\mu\text{g cm}^{-2}$	0.000	1.100	0.250	3.300	0.000	0.000
Br	Ins	$\mu\text{g cm}^{-2}$	0.000	0.009	0.002	0.000	0.000	0.000
	Sol	$\mu\text{g cm}^{-2}$	0.650	0.700	0.000	0.750	0.000	0.050
Sr	Ins	$\mu\text{g cm}^{-2}$	0.024	0.000	0.000	0.000	0.000	0.000
	Sol	$\mu\text{g cm}^{-2}$	0.000	0.800	0.000	0.000	0.000	0.000
Pb	Ins	$\mu\text{g cm}^{-2}$	0.000	0.024	0.000	0.016	0.000	0.007
	Sol	$\mu\text{g cm}^{-2}$	0.000	0.000	0.000	0.000	0.000	0.000

			Woomera	Woomera	Woomera	Alice Springs	Alice Springs	Alice Springs
Element	Unit		2007.11	2007.12	2008.4	2007.6	2007.8	2007.10
F	Ins	$\mu\text{g cm}^{-2}$	0.094	0.337	0.318	0.280	0.564	0.690
	Sol	$\mu\text{g cm}^{-2}$	0.000	1.750	0.000	0.000	0.000	2.050
Na	Ins	$\mu\text{g cm}^{-2}$	0.134	0.636	0.715	0.865	1.850	1.503
	Sol	$\mu\text{g cm}^{-2}$	19.650	0.000	19.100	0.000	0.000	0.000
Al	Ins	$\mu\text{g cm}^{-2}$	4.370	14.186	12.271	8.408	6.404	13.755
	Sol	$\mu\text{g cm}^{-2}$	0.000	0.000	0.000	0.000	0.000	0.000
Si	Ins	$\mu\text{g cm}^{-2}$	15.903	47.731	39.533	26.504	24.091	41.430
	Sol	$\mu\text{g cm}^{-2}$	6.550	0.750	1.950	4.300	7.050	0.800
P	Ins	$\mu\text{g cm}^{-2}$	0.000	0.000	0.049	0.079	0.088	0.000
	Sol	$\mu\text{g cm}^{-2}$	0.000	0.000	0.000	0.950	0.650	0.000
S	Ins	$\mu\text{g cm}^{-2}$	0.098	0.411	1.276	0.139	0.446	0.196
	Sol	$\mu\text{g cm}^{-2}$	1.100	0.000	0.700	0.550	1.250	0.000
Cl	Ins	$\mu\text{g cm}^{-2}$	0.000	0.000	0.000	0.002	0.000	0.000
	Sol	$\mu\text{g cm}^{-2}$	37.850	0.000	40.750	0.000	4.900	0.000
K	Ins	$\mu\text{g cm}^{-2}$	1.553	4.457	5.049	4.431	4.602	6.484
	Sol	$\mu\text{g cm}^{-2}$	4.600	0.300	3.750	0.000	1.050	0.000
Ca	Ins	$\mu\text{g cm}^{-2}$	0.544	0.789	2.190	1.355	2.302	2.213
	Sol	$\mu\text{g cm}^{-2}$	11.100	1.600	10.250	1.450	7.750	0.850
Ti	Ins	$\mu\text{g cm}^{-2}$	0.593	1.902	1.651	1.142	1.347	2.097
	Sol	$\mu\text{g cm}^{-2}$	0.000	0.000	0.000	0.000	0.000	0.000
V	Ins	$\mu\text{g cm}^{-2}$	0.023	0.169	0.148	0.071	0.075	0.138
	Sol	$\mu\text{g cm}^{-2}$	0.000	0.000	0.000	0.000	0.000	0.000
Cr	Ins	$\mu\text{g cm}^{-2}$	0.046	0.000	0.055	0.099	0.116	0.162
	Sol	$\mu\text{g cm}^{-2}$	0.000	0.000	0.000	0.000	0.000	0.000
Mn	Ins	$\mu\text{g cm}^{-2}$	0.078	0.018	0.288	0.154	0.313	0.214
	Sol	$\mu\text{g cm}^{-2}$	0.350	0.000	0.150	0.250	0.200	0.000
Fe	Ins	$\mu\text{g cm}^{-2}$	7.303	14.910	19.027	13.780	19.265	26.159
	Sol	$\mu\text{g cm}^{-2}$	0.000	0.950	0.000	0.000	0.000	0.300
Co	Ins	$\mu\text{g cm}^{-2}$	0.030	0.389	0.104	0.165	0.247	0.630
	Sol	$\mu\text{g cm}^{-2}$	0.000	0.000	0.000	0.000	0.000	0.000
Ni	Ins	$\mu\text{g cm}^{-2}$	0.034	0.280	0.145	0.143	0.123	0.385
	Sol	$\mu\text{g cm}^{-2}$	0.000	0.000	0.000	0.100	0.000	0.150
Cu	Ins	$\mu\text{g cm}^{-2}$	0.124	0.975	0.769	0.375	0.329	1.064
	Sol	$\mu\text{g cm}^{-2}$	0.000	0.200	0.000	0.000	0.100	0.000
Zn	Ins	$\mu\text{g cm}^{-2}$	0.057	0.287	0.380	0.215	0.363	0.436
	Sol	$\mu\text{g cm}^{-2}$	0.000	0.200	0.100	1.150	0.150	0.100
Br	Ins	$\mu\text{g cm}^{-2}$	0.000	0.000	0.000	0.012	0.000	0.056
	Sol	$\mu\text{g cm}^{-2}$	0.100	0.000	0.100	0.050	0.000	0.000
Sr	Ins	$\mu\text{g cm}^{-2}$	0.015	0.073	0.054	0.035	0.063	0.086
	Sol	$\mu\text{g cm}^{-2}$	0.000	0.000	0.000	0.000	0.000	0.000
Pb	Ins	$\mu\text{g cm}^{-2}$	0.023	0.194	0.046	0.020	0.000	0.289
	Sol	$\mu\text{g cm}^{-2}$	0.000	0.000	0.000	0.000	0.000	0.000

			Alice Springs	Alice Springs	Alice Springs	Alice Springs	Alice Springs	Darwin
Element	Unit		2007.11	2007.12	2008.1	2008.2	2008.3 – 2008.4	2008.1
F	Ins	$\mu\text{g cm}^{-2}$	0.042	0.299	0.029	1.871	0.000	0.000
	Sol	$\mu\text{g cm}^{-2}$	0.000	0.000	0.000	0.000	0.000	0.000
Na	Ins	$\mu\text{g cm}^{-2}$	0.191	1.135	0.247	11.376	0.059	0.000
	Sol	$\mu\text{g cm}^{-2}$	1.700	0.600	0.000	0.000	0.000	1.800
Al	Ins	$\mu\text{g cm}^{-2}$	2.076	13.598	4.476	27.663	1.329	0.000
	Sol	$\mu\text{g cm}^{-2}$	0.000	0.000	0.000	0.000	0.000	0.000
Si	Ins	$\mu\text{g cm}^{-2}$	12.323	46.533	15.561	149.964	4.438	0.071
	Sol	$\mu\text{g cm}^{-2}$	17.700	2.100	6.950	4.600	3.900	0.350
P	Ins	$\mu\text{g cm}^{-2}$	0.107	0.000	0.100	0.241	0.187	0.025
	Sol	$\mu\text{g cm}^{-2}$	0.000	0.000	0.750	1.300	0.950	0.000
S	Ins	$\mu\text{g cm}^{-2}$	0.128	0.306	0.126	0.756	0.126	0.005
	Sol	$\mu\text{g cm}^{-2}$	27.650	0.450	2.400	0.850	1.600	0.050
Cl	Ins	$\mu\text{g cm}^{-2}$	0.000	0.000	0.000	0.000	0.000	0.015
	Sol	$\mu\text{g cm}^{-2}$	18.250	0.000	3.200	0.000	0.000	0.600
K	Ins	$\mu\text{g cm}^{-2}$	1.330	5.180	1.923	22.003	0.613	0.000
	Sol	$\mu\text{g cm}^{-2}$	4.850	0.400	1.700	0.000	0.000	0.000
Ca	Ins	$\mu\text{g cm}^{-2}$	0.224	1.296	0.575	5.988	0.112	0.000
	Sol	$\mu\text{g cm}^{-2}$	50.800	2.950	11.350	1.000	1.100	0.300
Ti	Ins	$\mu\text{g cm}^{-2}$	0.370	1.862	0.511	4.669	0.111	0.000
	Sol	$\mu\text{g cm}^{-2}$	0.000	0.000	0.000	0.000	0.000	0.000
V	Ins	$\mu\text{g cm}^{-2}$	0.013	0.174	0.016	1.655	0.000	0.000
	Sol	$\mu\text{g cm}^{-2}$	0.000	0.000	0.000	0.000	0.000	0.000
Cr	Ins	$\mu\text{g cm}^{-2}$	0.059	0.047	0.010	0.000	0.000	0.000
	Sol	$\mu\text{g cm}^{-2}$	0.000	0.000	0.000	0.000	0.000	0.200
Mn	Ins	$\mu\text{g cm}^{-2}$	0.051	0.071	0.073	1.104	0.019	0.000
	Sol	$\mu\text{g cm}^{-2}$	1.050	0.000	0.200	0.200	0.200	0.000
Fe	Ins	$\mu\text{g cm}^{-2}$	4.853	19.016	5.133	68.429	1.275	0.031
	Sol	$\mu\text{g cm}^{-2}$	0.000	0.000	0.000	1.700	0.000	1.650
Co	Ins	$\mu\text{g cm}^{-2}$	0.040	0.556	0.045	2.142	0.000	0.000
	Sol	$\mu\text{g cm}^{-2}$	0.000	0.000	0.000	0.000	0.000	0.000
Ni	Ins	$\mu\text{g cm}^{-2}$	0.024	0.575	0.015	2.688	0.000	0.000
	Sol	$\mu\text{g cm}^{-2}$	0.000	0.000	0.000	0.000	0.000	0.250
Cu	Ins	$\mu\text{g cm}^{-2}$	0.040	1.252	0.063	10.101	0.009	0.000
	Sol	$\mu\text{g cm}^{-2}$	0.150	0.000	0.000	0.000	0.000	0.000
Zn	Ins	$\mu\text{g cm}^{-2}$	0.039	0.308	0.059	0.742	0.012	0.003
	Sol	$\mu\text{g cm}^{-2}$	3.350	0.250	0.150	0.000	0.000	0.250
Br	Ins	$\mu\text{g cm}^{-2}$	0.003	0.000	0.001	0.000	0.000	0.000
	Sol	$\mu\text{g cm}^{-2}$	0.300	0.000	0.000	0.000	0.000	0.000
Sr	Ins	$\mu\text{g cm}^{-2}$	0.000	0.070	0.008	0.421	0.000	0.000
	Sol	$\mu\text{g cm}^{-2}$	0.000	0.000	0.000	0.000	0.000	0.000
Pb	Ins	$\mu\text{g cm}^{-2}$	0.000	0.272	0.000	0.897	0.009	0.000
	Sol	$\mu\text{g cm}^{-2}$	0.000	0.000	0.000	0.000	0.000	0.000

			Halls Creek	Halls Creek	Halls Creek	Brisbane	Charleville	Charleville
Element	Unit		2007.10	2007.12	2008.1	2008.1	2008.1 (1/2)	2008.1 (2/2)
F	Ins	$\mu\text{g cm}^{-2}$	0.118	0.000	0.005	0.000	0.045	0.002
	Sol	$\mu\text{g cm}^{-2}$	2.750	0.000	0.000	0.950	0.100	0.000
Na	Ins	$\mu\text{g cm}^{-2}$	0.062	0.000	0.000	0.000	0.000	0.000
	Sol	$\mu\text{g cm}^{-2}$	0.000	0.000	3.050	0.000	0.000	0.000
Al	Ins	$\mu\text{g cm}^{-2}$	6.512	0.617	0.565	0.000	0.000	0.000
	Sol	$\mu\text{g cm}^{-2}$	0.000	0.000	0.000	0.000	0.000	0.000
Si	Ins	$\mu\text{g cm}^{-2}$	16.443	3.257	3.106	0.068	0.071	0.419
	Sol	$\mu\text{g cm}^{-2}$	1.100	1.550	0.650	0.050	0.400	0.250
P	Ins	$\mu\text{g cm}^{-2}$	0.000	0.000	0.025	0.015	0.032	0.086
	Sol	$\mu\text{g cm}^{-2}$	0.000	0.000	0.000	0.000	0.000	0.000
S	Ins	$\mu\text{g cm}^{-2}$	0.027	0.034	0.066	0.012	0.005	0.021
	Sol	$\mu\text{g cm}^{-2}$	0.000	0.400	0.250	0.000	0.000	0.150
Cl	Ins	$\mu\text{g cm}^{-2}$	0.000	0.000	0.000	0.000	0.000	0.000
	Sol	$\mu\text{g cm}^{-2}$	0.000	0.000	3.450	0.000	0.000	0.000
K	Ins	$\mu\text{g cm}^{-2}$	0.553	0.145	0.199	0.010	0.012	0.047
	Sol	$\mu\text{g cm}^{-2}$	0.000	0.000	1.250	0.000	0.000	0.000
Ca	Ins	$\mu\text{g cm}^{-2}$	0.293	0.037	0.020	0.008	0.000	0.000
	Sol	$\mu\text{g cm}^{-2}$	0.800	1.200	1.700	0.000	0.000	0.550
Ti	Ins	$\mu\text{g cm}^{-2}$	1.378	0.167	0.192	0.006	0.000	0.006
	Sol	$\mu\text{g cm}^{-2}$	0.000	0.000	0.000	0.000	0.000	0.000
V	Ins	$\mu\text{g cm}^{-2}$	0.000	0.000	0.000	0.000	0.000	0.000
	Sol	$\mu\text{g cm}^{-2}$	0.000	0.000	0.000	0.000	0.000	0.000
Cr	Ins	$\mu\text{g cm}^{-2}$	0.023	0.000	0.000	0.004	0.002	0.009
	Sol	$\mu\text{g cm}^{-2}$	0.000	0.000	0.000	0.000	0.000	0.000
Mn	Ins	$\mu\text{g cm}^{-2}$	0.056	0.005	0.005	0.000	0.000	0.000
	Sol	$\mu\text{g cm}^{-2}$	0.000	0.000	0.000	0.000	0.000	0.000
Fe	Ins	$\mu\text{g cm}^{-2}$	11.901	1.561	1.487	0.052	0.049	0.144
	Sol	$\mu\text{g cm}^{-2}$	0.000	0.000	0.000	0.000	0.000	0.000
Co	Ins	$\mu\text{g cm}^{-2}$	0.159	0.000	0.000	0.000	0.000	0.000
	Sol	$\mu\text{g cm}^{-2}$	0.000	0.000	0.000	0.000	0.000	0.000
Ni	Ins	$\mu\text{g cm}^{-2}$	0.066	0.000	0.000	0.004	0.004	0.004
	Sol	$\mu\text{g cm}^{-2}$	0.000	0.000	0.100	0.000	0.000	0.000
Cu	Ins	$\mu\text{g cm}^{-2}$	0.193	0.007	0.005	0.000	0.000	0.000
	Sol	$\mu\text{g cm}^{-2}$	0.000	0.000	0.100	0.000	0.000	0.000
Zn	Ins	$\mu\text{g cm}^{-2}$	0.065	0.000	0.013	0.003	0.006	0.003
	Sol	$\mu\text{g cm}^{-2}$	0.000	0.400	0.500	0.200	0.300	0.400
Br	Ins	$\mu\text{g cm}^{-2}$	0.025	0.000	0.000	0.002	0.000	0.000
	Sol	$\mu\text{g cm}^{-2}$	0.000	0.000	0.000	0.050	0.050	0.000
Sr	Ins	$\mu\text{g cm}^{-2}$	0.000	0.000	0.000	0.000	0.000	0.000
	Sol	$\mu\text{g cm}^{-2}$	0.000	0.000	0.000	0.000	0.000	0.000
Pb	Ins	$\mu\text{g cm}^{-2}$	0.082	0.007	0.000	0.000	0.000	0.000
	Sol	$\mu\text{g cm}^{-2}$	0.000	0.000	0.000	0.000	0.000	0.000

			Townsville	Townsville	Townsville	Townsville	Mt Isa	Mt Isa
Element	Unit		2007.10	2007.12	2008.1 (1/2)	2008.2 (2/2)	2007.10	2007.12
F	Ins	$\mu\text{g cm}^{-2}$	0.000	0.001	0.000	0.000	0.092	0.059
	Sol	$\mu\text{g cm}^{-2}$	0.000	0.100	0.000	0.000	0.000	0.550
Na	Ins	$\mu\text{g cm}^{-2}$	0.000	0.000	0.000	0.000	0.221	0.123
	Sol	$\mu\text{g cm}^{-2}$	25.250	0.000	0.000	4.050	0.000	0.000
Al	Ins	$\mu\text{g cm}^{-2}$	0.000	0.000	0.000	0.000	2.034	2.204
	Sol	$\mu\text{g cm}^{-2}$	0.000	0.000	0.000	0.000	0.000	0.000
Si	Ins	$\mu\text{g cm}^{-2}$	0.413	0.085	0.039	0.068	10.874	11.654
	Sol	$\mu\text{g cm}^{-2}$	1.450	0.300	1.250	0.500	0.950	0.700
P	Ins	$\mu\text{g cm}^{-2}$	0.000	0.046	0.047	0.027	0.000	0.000
	Sol	$\mu\text{g cm}^{-2}$	0.000	0.000	0.000	0.000	0.000	0.000
S	Ins	$\mu\text{g cm}^{-2}$	0.010	0.018	0.011	0.011	1.102	0.525
	Sol	$\mu\text{g cm}^{-2}$	1.000	0.000	0.000	0.200	0.000	0.000
Cl	Ins	$\mu\text{g cm}^{-2}$	0.000	0.000	0.000	0.000	0.000	0.000
	Sol	$\mu\text{g cm}^{-2}$	29.850	0.000	0.000	5.450	0.000	0.000
K	Ins	$\mu\text{g cm}^{-2}$	0.053	0.029	0.018	0.016	1.183	0.944
	Sol	$\mu\text{g cm}^{-2}$	1.150	0.000	0.000	0.000	0.000	0.000
Ca	Ins	$\mu\text{g cm}^{-2}$	0.014	0.000	0.000	0.006	1.074	0.089
	Sol	$\mu\text{g cm}^{-2}$	1.950	0.000	0.000	0.350	1.350	0.000
Ti	Ins	$\mu\text{g cm}^{-2}$	0.006	0.000	0.000	0.000	0.312	0.394
	Sol	$\mu\text{g cm}^{-2}$	0.000	0.000	0.000	0.000	0.000	0.000
V	Ins	$\mu\text{g cm}^{-2}$	0.000	0.000	0.000	0.000	0.000	0.000
	Sol	$\mu\text{g cm}^{-2}$	0.000	0.000	0.000	0.000	0.000	0.000
Cr	Ins	$\mu\text{g cm}^{-2}$	0.000	0.000	0.000	0.004	0.009	0.004
	Sol	$\mu\text{g cm}^{-2}$	0.000	0.000	0.000	0.000	0.000	0.000
Mn	Ins	$\mu\text{g cm}^{-2}$	0.000	0.000	0.000	0.000	0.081	0.009
	Sol	$\mu\text{g cm}^{-2}$	0.000	0.000	0.000	0.000	0.000	0.000
Fe	Ins	$\mu\text{g cm}^{-2}$	0.088	0.032	0.017	0.071	5.419	2.770
	Sol	$\mu\text{g cm}^{-2}$	0.100	0.000	0.550	0.100	0.000	0.200
Co	Ins	$\mu\text{g cm}^{-2}$	0.000	0.000	0.000	0.000	0.053	0.028
	Sol	$\mu\text{g cm}^{-2}$	0.000	0.000	0.000	0.000	0.000	0.000
Ni	Ins	$\mu\text{g cm}^{-2}$	0.000	0.003	0.000	0.006	0.000	0.000
	Sol	$\mu\text{g cm}^{-2}$	0.200	0.000	0.300	0.200	0.000	0.000
Cu	Ins	$\mu\text{g cm}^{-2}$	0.000	0.000	0.000	0.000	0.484	0.396
	Sol	$\mu\text{g cm}^{-2}$	0.000	0.000	0.000	0.000	0.100	0.000
Zn	Ins	$\mu\text{g cm}^{-2}$	0.013	0.006	0.003	0.010	0.447	0.325
	Sol	$\mu\text{g cm}^{-2}$	0.700	0.200	0.200	0.500	0.100	0.000
Br	Ins	$\mu\text{g cm}^{-2}$	0.000	0.000	0.000	0.001	0.000	0.000
	Sol	$\mu\text{g cm}^{-2}$	0.100	0.000	0.000	0.050	0.000	0.000
Sr	Ins	$\mu\text{g cm}^{-2}$	0.000	0.000	0.000	0.000	0.000	0.011
	Sol	$\mu\text{g cm}^{-2}$	0.000	0.000	0.000	0.000	0.000	0.000
Pb	Ins	$\mu\text{g cm}^{-2}$	0.000	0.000	0.000	0.006	0.532	0.446
	Sol	$\mu\text{g cm}^{-2}$	0.000	0.000	0.000	0.000	0.000	0.000

Values calculated using IBA results for CSIRO samples whose soluble and insoluble materials had both been analysed

Element			Unit	Cobar	Cobar	Cobar	Sydney	Sydney	Sydney
				2007.6	2007.7	2008.4	2007.5 – 2007.6	2007.7	2007.11
Na	nssNa	minNa	$\mu\text{g cm}^{-2}$	2.238	1.450	2.731	0.593	0.118	0.000
		tsNa	$\mu\text{g cm}^{-2}$	4.412	0.000	4.809	0.000	0.000	0.000
	ssNa		$\mu\text{g cm}^{-2}$	0.300	0.000	2.332	12.307	0.000	0.000
Ca	nssCa		$\mu\text{g cm}^{-2}$	11.875	3.068	13.464	1.058	0.935	0.584
	ssCa		$\mu\text{g cm}^{-2}$	0.011	0.000	0.089	0.468	0.000	0.000
Total			$\mu\text{g cm}^{-2}$	143.012	79.234	141.394	52.160	12.562	23.227
Soil			$\mu\text{g cm}^{-2}$	123.983	80.090	120.140	0.000	14.510	17.735
Soil			ratio	0.867	1.011	0.850	0.000	1.155	0.764
ts			$\mu\text{g cm}^{-2}$	11.207	0.000	12.215	0.000	0.000	0.000
ts			ratio	0.078	0.000	0.086	0.000	0.000	0.000
ss			$\mu\text{g cm}^{-2}$	0.763	0.000	5.923	31.261	0.000	0.000
ss			ratio	0.005	0.000	0.042	0.599	0.000	0.000
Smoke			$\mu\text{g cm}^{-2}$	2.480	0.000	2.273	0.000	0.000	0.000
Smoke			ratio	0.017	0.000	0.016	0.000	0.000	0.000

Element			Unit	Sydney	Sydney	Sydney	Wagga Wagga	Wagga Wagga	Wagga Wagga
				2008.2	2008.3	2008.4	2007.12	2008.1	2008.2
Na	nssNa	minNa	$\mu\text{g cm}^{-2}$	0.000	0.420	0.000	0.185	0.000	0.000
		tsNa	$\mu\text{g cm}^{-2}$	0.000	0.693	0.000	1.017	0.000	0.000
	ssNa		$\mu\text{g cm}^{-2}$	0.000	7.870	100.150	0.448	0.000	0.000
Ca	nssCa		$\mu\text{g cm}^{-2}$	0.056	1.987	0.000	2.147	0.011	0.000
	ssCa		$\mu\text{g cm}^{-2}$	0.000	0.299	3.650	0.017	0.000	0.000
Total			$\mu\text{g cm}^{-2}$	3.828	40.694	389.230	21.255	6.415	10.780
Soil			$\mu\text{g cm}^{-2}$	4.520	17.437	0.000	14.178	4.222	0.000
Soil			ratio	1.181	0.428	0.000	0.667	0.658	0.000
ts			$\mu\text{g cm}^{-2}$	0.000	1.759	0.000	2.583	0.000	0.000
ts			ratio	0.000	0.043	0.000	0.122	0.000	0.000
ss			$\mu\text{g cm}^{-2}$	0.000	19.991	254.381	1.137	0.000	0.000
ss			ratio	0.000	0.491	0.654	0.053	0.000	0.000
Smoke			$\mu\text{g cm}^{-2}$	0.000	0.000	44.802	1.745	0.000	0.000
Smoke			ratio	0.000	0.000	0.115	0.082	0.000	0.000

Element			Unit	Wagga Wagga	Wagga Wagga	Melbourne	Melbourne	Melbourne	Melbourne
				2008.3	2008.4	2007.6	2007.7	2007.11	2008.2
Na	nssNa	minNa	$\mu\text{g cm}^{-2}$	0.772	1.868	0.404	0.315	0.000	0.385
		tsNa	$\mu\text{g cm}^{-2}$	0.000	0.000	0.086	1.599	0.000	7.267
	ssNa		$\mu\text{g cm}^{-2}$	0.193	0.000	43.574	29.756	0.000	64.467
Ca	nssCa		$\mu\text{g cm}^{-2}$	1.379	6.900	0.875	3.418	1.888	13.664
	ssCa		$\mu\text{g cm}^{-2}$	0.007	0.000	1.656	1.131	0.000	2.450
Total			$\mu\text{g cm}^{-2}$	294.649	114.783	115.001	84.308	26.111	235.653
Soil			$\mu\text{g cm}^{-2}$	347.511	118.369	11.195	14.727	23.134	48.656
Soil			ratio	1.179	1.031	0.097	0.175	0.886	0.206
ts			$\mu\text{g cm}^{-2}$	0.000	0.000	0.218	4.061	0.000	18.457
ts			ratio	0.000	0.000	0.002	0.048	0.000	0.078
ss			$\mu\text{g cm}^{-2}$	0.000	0.000	110.678	75.580	0.000	163.746
ss			ratio	0.000	0.000	0.962	0.896	0.000	0.695
Smoke			$\mu\text{g cm}^{-2}$	0.000	0.000	0.358	0.063	0.125	1.235
Smoke			ratio	0.000	0.000	0.003	0.001	0.005	0.005

Element			Unit	Melbourne	Melbourne	Mildura	Mildura	Mildura	Mildura
				2008.3	2008.4	2007.6	2007.7	2008.1	2008.3
Na	nssNa	minNa	$\mu\text{g cm}^{-2}$	6.297	2.870	0.000	0.102	3.562	3.320
		tsNa	$\mu\text{g cm}^{-2}$	0.000	8.444	0.000	0.000	8.097	0.000
	ssNa		$\mu\text{g cm}^{-2}$	15.887	9.586	0.000	0.000	22.034	0.000
Ca	nssCa		$\mu\text{g cm}^{-2}$	11.244	20.204	2.651	1.500	20.820	27.720
	ssCa		$\mu\text{g cm}^{-2}$	0.604	0.364	0.000	0.000	0.837	0.000
Total			$\mu\text{g cm}^{-2}$	243.140	188.126	17.664	22.201	215.956	151.959
Soil			$\mu\text{g cm}^{-2}$	209.533	129.704	0.000	27.562	164.561	166.436
Soil			ratio	0.862	0.689	0.000	1.241	0.762	1.095
ts			$\mu\text{g cm}^{-2}$	0.000	21.448	0.000	0.000	20.567	0.000
ts			ratio	0.000	0.114	0.000	0.000	0.095	0.000
ss			$\mu\text{g cm}^{-2}$	40.353	24.348	0.000	0.000	55.966	0.000
ss			ratio	0.166	0.129	0.000	0.000	0.259	0.000
Smoke			$\mu\text{g cm}^{-2}$	0.000	2.687	0.000	0.000	6.332	0.000
Smoke			ratio	0.000	0.014	0.000	0.000	0.029	0.000

Element			Unit	Mildura	Cape Grim	Cape Grim	Cape Grim	Cape Grim	Cape Grim
				2008.4	2007.5	2007.6	2007.11	2008.2	2008.3
Na	nssNa	minNa	$\mu\text{g cm}^{-2}$	0.000	0.000	10.311	23.632	9.402	3.908
		tsNa	$\mu\text{g cm}^{-2}$	0.000	0.000	0.000	0.062	0.000	0.000
	ssNa		$\mu\text{g cm}^{-2}$	0.000	669.223	93.214	189.088	50.533	56.620
Ca	nssCa		$\mu\text{g cm}^{-2}$	293.872	0.000	18.412	42.311	16.790	6.978
	ssCa		$\mu\text{g cm}^{-2}$	0.000	23.083	3.542	7.185	1.920	2.152
Total			$\mu\text{g cm}^{-2}$	440.555	1771.232	695.876	1007.680	420.535	259.947
Soil			$\mu\text{g cm}^{-2}$	502.969	0.000	568.552	425.214	312.304	108.008
Soil			ratio	1.142	0.000	0.817	0.422	0.743	0.416
ts			$\mu\text{g cm}^{-2}$	0.000	0.000	0.000	0.158	0.000	0.000
ts			ratio	0.000	0.000	0.000	0.000*	0.000	0.000
ss			$\mu\text{g cm}^{-2}$	0.000	1699.826	236.764	480.284	128.353	143.815
ss			ratio	0.000	0.960	0.340	0.477	0.305	0.553
Smoke			$\mu\text{g cm}^{-2}$	0.000	0.000	0.000	0.000	0.000	0.000
Smoke			ratio	0.000	0.000	0.000	0.000	0.000	0.000

*: actual value is 0.0002

Element			Unit	Cape Grim	Adelaide	Adelaide	Adelaide	Woomera	Woomera
				2008.4	2008.2	2008.3	2008.4	2007.6	2007.8
Na	nssNa	minNa	$\mu\text{g cm}^{-2}$	3.385	4.906	0.270	1.396	0.000	0.015
		tsNa	$\mu\text{g cm}^{-2}$	0.256	132.838	5.969	18.073	0.000	0.000
	ssNa		$\mu\text{g cm}^{-2}$	179.488	152.260	77.554	99.512	0.000	0.000
Ca	nssCa		$\mu\text{g cm}^{-2}$	6.501	245.970	11.140	34.767	0.400	0.801
	ssCa		$\mu\text{g cm}^{-2}$	6.821	5.786	2.947	3.781	0.000	0.000
Total			$\mu\text{g cm}^{-2}$	587.603	1498.201	271.073	547.612	65.337	28.683
Soil			$\mu\text{g cm}^{-2}$	70.838	554.059	28.033	146.425	0.000	28.121
Soil			ratio	0.121	0.370	0.103	0.267	0.000	0.980
ts			$\mu\text{g cm}^{-2}$	0.651	337.408	15.160	45.906	0.000	0.000
ts			ratio	0.001	0.225	0.056	0.084	0.000	0.000
ss			$\mu\text{g cm}^{-2}$	455.900	386.740	196.986	252.760	0.000	0.000
ss			ratio	0.776	0.258	0.727	0.462	0.000	0.000
Smoke			$\mu\text{g cm}^{-2}$	6.341	5.522	3.389	6.490	0.000	1.594
Smoke			ratio	0.011	0.004	0.013	0.012	0.000	0.056

Element			Unit	Woomera	Woomera	Woomera	Alice Springs	Alice Springs	Alice Springs
				2007.11	2007.12	2008.4	2007.6	2007.8	2007.10
Na	nssNa	minNa	$\mu\text{g cm}^{-2}$	2.578	0.636	6.687	0.865	1.850	1.503
		tsNa	$\mu\text{g cm}^{-2}$	3.654	0.000	0.000	0.000	0.000	0.000
	ssNa		$\mu\text{g cm}^{-2}$	13.552	0.000	13.128	0.000	0.000	0.000
Ca	nssCa		$\mu\text{g cm}^{-2}$	11.129	2.389	11.941	2.805	10.052	3.063
	ssCa		$\mu\text{g cm}^{-2}$	0.515	0.000	0.499	0.000	0.000	0.000
Total			$\mu\text{g cm}^{-2}$	150.976	170.205	235.316	117.403	140.108	176.120
Soil			$\mu\text{g cm}^{-2}$	102.486	197.892	199.001	135.335	157.249	208.505
Soil			ratio	0.679	1.163	0.846	1.153	1.122	1.184
ts			$\mu\text{g cm}^{-2}$	9.282	0.000	0.000	0.000	0.000	0.000
ts			ratio	0.061	0.000	0.000	0.000	0.000	0.000
ss			$\mu\text{g cm}^{-2}$	34.421	0.000	33.345	0.000	0.000	0.000
ss			ratio	0.228	0.000	0.142	0.000	0.000	0.000
Smoke			$\mu\text{g cm}^{-2}$	1.771	0.000	0.000	0.000	0.000	0.000
Smoke			ratio	0.012	0.000	0.000	0.000	0.000	0.000

Element			Unit	Alice Springs	Alice Springs	Alice Springs	Alice Springs	Alice Springs	Darwin
				2007.11	2007.12	2008.1	2008.2	2008.3 – 2008.4	2008.1
Na	nssNa	minNa	$\mu\text{g cm}^{-2}$	1.713	1.735	0.247	3.751	0.059	0.133
		tsNa	$\mu\text{g cm}^{-2}$	0.178	0.000	0.000	0.000	0.000	0.000
	ssNa		$\mu\text{g cm}^{-2}$	0.000	0.000	0.000	7.625	0.000	1.667
Ca	nssCa		$\mu\text{g cm}^{-2}$	51.024	4.246	11.925	6.698	1.212	0.237
	ssCa		$\mu\text{g cm}^{-2}$	0.000	0.000	0.000	0.290	0.000	0.063
Total			$\mu\text{g cm}^{-2}$	207.616	177.989	92.852	558.445	27.870	6.822
Soil			$\mu\text{g cm}^{-2}$	174.956	207.564	98.751	635.411	28.962	0.000
Soil			ratio	0.843	1.166	1.064	1.138	1.039	0.000
ts			$\mu\text{g cm}^{-2}$	0.452	0.000	0.000	0.000	0.000	0.000
ts			ratio	0.002	0.000	0.000	0.000	0.000	0.000
ss			$\mu\text{g cm}^{-2}$	0.000	0.000	0.000	0.000	0.000	4.235
ss			ratio	0.000	0.000	0.000	0.000	0.000	0.621
Smoke			$\mu\text{g cm}^{-2}$	3.268	0.000	0.543	0.000	0.000	0.000
Smoke			ratio	0.016	0.000	0.006	0.000	0.000	0.000

Element			Unit	Halls Creek	Halls Creek	Halls Creek	Brisbane	Charleville	Charleville
				2007.10	2007.12	2008.1	2008.1	2008.1 (1/2)	2008.1 (2/2)
Na	nssNa	minNa	$\mu\text{g cm}^{-2}$	0.062	0.000	0.525	0.000	0.000	0.000
		tsNa	$\mu\text{g cm}^{-2}$	0.000	0.000	0.393	0.000	0.000	0.000
	ssNa		$\mu\text{g cm}^{-2}$	0.000	0.000	2.132	0.000	0.000	0.000
Ca	nssCa		$\mu\text{g cm}^{-2}$	1.093	1.237	1.639	0.008	0.000	0.550
	ssCa		$\mu\text{g cm}^{-2}$	0.000	0.000	0.081	0.000	0.000	0.000
Total			$\mu\text{g cm}^{-2}$	74.139	16.611	23.208	1.596	1.633	3.137
Soil			$\mu\text{g cm}^{-2}$	91.264	19.445	17.238	0.000	0.000	0.000
Soil			ratio	1.231	1.171	0.743	0.000	0.000	0.000
ts			$\mu\text{g cm}^{-2}$	0.000	0.000	0.998	0.000	0.000	0.000
ts			ratio	0.000	0.000	0.043	0.000	0.000	0.000
ss			$\mu\text{g cm}^{-2}$	0.000	0.000	5.416	0.000	0.000	0.000
ss			ratio	0.000	0.000	0.233	0.000	0.000	0.000
Smoke			$\mu\text{g cm}^{-2}$	0.000	0.000	0.557	0.000	0.000	0.000
Smoke			ratio	0.000	0.000	0.024	0.000	0.000	0.000

Element			Unit	Townsville	Townsville	Townsville	Townsville	Mt Isa	Mt Isa
				2007.10	2007.12	2008.1 (1/2)	2008.2 (2/2)	2007.10	2007.12
Na	nssNa	minNa	$\mu\text{g cm}^{-2}$	0.066	0.000	0.000	0.060	0.221	0.048
		tsNa	$\mu\text{g cm}^{-2}$	0.508	0.000	0.000	0.055	0.000	0.000
	ssNa		$\mu\text{g cm}^{-2}$	24.675	0.000	0.000	3.934	0.000	0.075
Ca	nssCa		$\mu\text{g cm}^{-2}$	1.026	0.000	0.000	0.206	2.424	0.086
	ssCa		$\mu\text{g cm}^{-2}$	0.938	0.000	0.000	0.150	0.000	0.003
Total			$\mu\text{g cm}^{-2}$	65.129	1.275	4.113	12.442	45.074	39.000
Soil			$\mu\text{g cm}^{-2}$	0.000	0.000	0.000	0.000	51.587	43.702
Soil			ratio	0.000	0.000	0.000	0.000	1.145	1.121
ts			$\mu\text{g cm}^{-2}$	1.291	0.000	0.000	0.140	0.000	0.000
ts			ratio	0.020	0.000	0.000	0.011	0.000	0.000
ss			$\mu\text{g cm}^{-2}$	62.675	0.000	0.000	9.993	0.000	0.000
ss			ratio	0.962	0.000	0.000	0.803	0.000	0.000
Smoke			$\mu\text{g cm}^{-2}$	1.090	0.010	0.000	0.000	0.000	0.000
Smoke			ratio	0.017	0.008	0.000	0.000	0.000	0.000

Appendix A-2: IBA Results 2

IBA results and the calculated values for CSIRO samples for which only insoluble material was analysed

		Cobar	Cobar	Cobar	Cobar	Cobar	Cobar
Element	Unit	2007.9	2007.10	2007.11	2007.12	2008.1	2008.2
F	$\mu\text{g cm}^{-2}$	0.000	0.388	0.000	0.059	0.000	0.000
Na	$\mu\text{g cm}^{-2}$	0.000	0.463	0.000	0.000	0.000	0.000
Al	$\mu\text{g cm}^{-2}$	0.000	12.339	2.478	0.054	0.067	1.135
Si	$\mu\text{g cm}^{-2}$	0.327	41.188	8.605	0.951	0.734	5.823
P	$\mu\text{g cm}^{-2}$	0.011	0.000	0.000	0.041	0.047	0.062
S	$\mu\text{g cm}^{-2}$	0.000	0.289	0.081	0.039	0.040	0.048
Cl	$\mu\text{g cm}^{-2}$	0.000	0.000	0.000	0.000	0.000	0.000
K	$\mu\text{g cm}^{-2}$	0.021	5.277	0.709	0.160	0.153	0.463
Ca	$\mu\text{g cm}^{-2}$	0.027	0.505	0.000	0.027	0.027	0.000
Ti	$\mu\text{g cm}^{-2}$	0.006	1.768	0.267	0.053	0.022	0.296
V	$\mu\text{g cm}^{-2}$	0.000	0.156	0.000	0.000	0.000	0.000
Cr	$\mu\text{g cm}^{-2}$	0.000	0.047	0.018	0.000	0.000	0.000
Mn	$\mu\text{g cm}^{-2}$	0.000	0.043	0.032	0.000	0.000	0.015
Fe	$\mu\text{g cm}^{-2}$	0.088	19.141	2.557	0.580	0.225	1.507
Co	$\mu\text{g cm}^{-2}$	0.000	0.475	0.000	0.000	0.000	0.000
Ni	$\mu\text{g cm}^{-2}$	0.000	0.366	0.008	0.000	0.000	0.000
Cu	$\mu\text{g cm}^{-2}$	0.000	0.998	0.032	0.016	0.004	0.013
Zn	$\mu\text{g cm}^{-2}$	0.002	0.286	0.013	0.008	0.007	0.012
Br	$\mu\text{g cm}^{-2}$	0.007	0.045	0.002	0.014	0.000	0.000
Sr	$\mu\text{g cm}^{-2}$	0.000	0.050	0.000	0.000	0.000	0.000
Pb	$\mu\text{g cm}^{-2}$	0.000	0.253	0.000	0.000	0.000	0.000
minNa	$\mu\text{g cm}^{-2}$	0.000	0.279	0.000	0.000	0.000	0.000
tsNa	$\mu\text{g cm}^{-2}$	0.000	0.000	0.000	0.000	0.000	0.000
ssNa	$\mu\text{g cm}^{-2}$	0.000	0.184	0.000	0.000	0.000	0.000
nssCa	$\mu\text{g cm}^{-2}$	0.027	0.498	0.000	0.027	0.027	0.000
ssCa	$\mu\text{g cm}^{-2}$	0.000	0.007	0.000	0.000	0.000	0.000
Total	$\mu\text{g cm}^{-2}$	0.912	151.077	28.017	3.410	2.349	17.830
Soil	$\mu\text{g cm}^{-2}$	0.000	180.267	0.000	4.037	2.606	0.000
Soil	ratio	0.000	1.193	0.000	1.184	1.109	0.000
ts	$\mu\text{g cm}^{-2}$	0.000	0.000	0.000	0.000	0.000	0.000
ts	ratio	0.000	0.000	0.000	0.000	0.000	0.000
ss	$\mu\text{g cm}^{-2}$	0.000	0.000	0.000	0.000	0.000	0.000
ss	ratio	0.000	0.000	0.000	0.000	0.000	0.000
Smoke	$\mu\text{g cm}^{-2}$	0.000	0.000	0.000	0.000	0.018	0.000
Smoke	ratio	0.000	0.000	0.000	0.000	0.008	0.000

		Cobar	Sydney	Sydney	Sydney	Sydney	Wagga Wagga
Element	Unit	2008.3	2007.9	2007.10	2007.12	2008.1	2007.6
F	µg cm ⁻²	0.300	0.032	0.023	0.013	0.013	0.000
Na	µg cm ⁻²	0.474	0.302	0.159	0.000	0.149	0.000
Al	µg cm ⁻²	16.941	1.584	1.376	0.087	0.127	0.000
Si	µg cm ⁻²	61.109	6.553	5.628	0.944	1.175	0.542
P	µg cm ⁻²	0.058	0.000	0.000	0.000	0.000	0.019
S	µg cm ⁻²	0.396	0.481	0.169	0.074	0.054	0.042
Cl	µg cm ⁻²	0.000	0.000	0.000	0.000	0.102	0.000
K	µg cm ⁻²	5.844	0.529	0.460	0.092	0.105	0.033
Ca	µg cm ⁻²	0.043	0.562	0.280	0.012	0.041	0.011
Ti	µg cm ⁻²	2.226	0.282	0.185	0.028	0.037	0.005
V	µg cm ⁻²	0.195	0.000	0.000	0.000	0.000	0.000
Cr	µg cm ⁻²	0.000	0.011	0.075	0.005	0.019	0.004
Mn	µg cm ⁻²	0.135	0.048	0.012	0.000	0.004	0.006
Fe	µg cm ⁻²	12.150	3.085	2.434	0.521	0.701	0.244
Co	µg cm ⁻²	0.042	0.023	0.016	0.000	0.000	0.000
Ni	µg cm ⁻²	0.134	0.000	0.000	0.000	0.000	0.000
Cu	µg cm ⁻²	0.764	0.105	0.048	0.006	0.007	0.000
Zn	µg cm ⁻²	0.168	0.234	0.025	0.007	0.007	0.009
Br	µg cm ⁻²	0.000	0.025	0.000	0.017	0.023	0.000
Sr	µg cm ⁻²	0.020	0.008	0.000	0.000	0.000	0.000
Pb	µg cm ⁻²	0.057	0.024	0.013	0.000	0.007	0.000
minNa	µg cm ⁻²	0.014	0.302	0.157	0.000	0.020	0.000
tsNa	µg cm ⁻²	0.000	0.000	0.000	0.000	0.000	0.000
ssNa	µg cm ⁻²	0.460	0.000	0.002	0.000	0.129	0.000
nssCa	µg cm ⁻²	0.026	0.562	0.280	0.012	0.036	0.011
ssCa	µg cm ⁻²	0.017	0.000	0.000	0.000	0.005	0.000
Total	µg cm ⁻²	192.511	24.470	19.774	3.183	4.336	1.633
Soil	µg cm ⁻²	223.195	28.731	23.746	3.877	5.032	0.000
Soil	ratio	1.159	1.174	1.201	1.218	1.161	0.000
ts	µg cm ⁻²	0.000	0.000	0.000	0.000	0.000	0.000
ts	ratio	0.000	0.000	0.000	0.000	0.000	0.000
ss	µg cm ⁻²	0.000	0.000	0.000	0.000	0.327	0.000
ss	ratio	0.000	0.000	0.000	0.000	0.075	0.000
Smoke	µg cm ⁻²	0.000	0.000	0.000	0.000	0.000	0.000
Smoke	ratio	0.000	0.000	0.000	0.000	0.000	0.000

		Wagga Wagga	Wagga Wagga	Wagga Wagga	Melbourne	Melbourne	Melbourne
Element	Unit	2007.9	2007.10	2007.11	2007.9	2007.10	2007.12
F	$\mu\text{g cm}^{-2}$	0.214	0.141	0.004	0.000	0.000	0.070
Na	$\mu\text{g cm}^{-2}$	0.522	0.470	0.064	0.000	0.018	0.687
Al	$\mu\text{g cm}^{-2}$	4.911	8.521	2.012	0.000	0.000	5.658
Si	$\mu\text{g cm}^{-2}$	19.506	32.477	7.380	0.178	0.661	26.399
P	$\mu\text{g cm}^{-2}$	0.000	0.000	0.073	0.000	0.012	0.000
S	$\mu\text{g cm}^{-2}$	0.555	0.220	0.058	0.046	0.023	0.236
Cl	$\mu\text{g cm}^{-2}$	0.000	0.000	0.000	0.000	0.000	0.000
K	$\mu\text{g cm}^{-2}$	2.955	3.166	0.671	0.023	0.068	1.763
Ca	$\mu\text{g cm}^{-2}$	0.668	0.380	0.013	0.026	0.058	0.773
Ti	$\mu\text{g cm}^{-2}$	0.975	1.127	0.293	0.000	0.037	1.080
V	$\mu\text{g cm}^{-2}$	0.033	0.064	0.000	0.000	0.000	0.000
Cr	$\mu\text{g cm}^{-2}$	0.043	0.025	0.005	0.000	0.001	0.065
Mn	$\mu\text{g cm}^{-2}$	0.109	0.097	0.022	0.000	0.000	0.028
Fe	$\mu\text{g cm}^{-2}$	9.157	9.034	1.312	0.066	0.267	7.781
Co	$\mu\text{g cm}^{-2}$	0.121	0.151	0.000	0.000	0.000	0.114
Ni	$\mu\text{g cm}^{-2}$	0.049	0.076	0.000	0.000	0.000	0.056
Cu	$\mu\text{g cm}^{-2}$	0.252	0.292	0.011	0.003	0.000	0.227
Zn	$\mu\text{g cm}^{-2}$	0.188	0.154	0.019	0.005	0.005	0.073
Br	$\mu\text{g cm}^{-2}$	0.044	0.049	0.000	0.000	0.000	0.021
Sr	$\mu\text{g cm}^{-2}$	0.000	0.034	0.000	0.000	0.000	0.023
Pb	$\mu\text{g cm}^{-2}$	0.081	0.054	0.000	0.000	0.000	0.052
minNa	$\mu\text{g cm}^{-2}$	0.371	0.207	0.006	0.000	0.018	0.427
tsNa	$\mu\text{g cm}^{-2}$	0.000	0.000	0.000	0.000	0.000	0.000
ssNa	$\mu\text{g cm}^{-2}$	0.151	0.263	0.058	0.000	0.000	0.260
nssCa	$\mu\text{g cm}^{-2}$	0.662	0.370	0.011	0.026	0.058	0.763
ssCa	$\mu\text{g cm}^{-2}$	0.006	0.010	0.002	0.000	0.000	0.010
Total	$\mu\text{g cm}^{-2}$	71.719	105.810	22.913	0.587	2.063	84.475
Soil	$\mu\text{g cm}^{-2}$	84.505	124.266	26.564	0.000	0.000	100.350
Soil	ratio	1.178	1.174	1.159	0.000	0.000	1.188
ts	$\mu\text{g cm}^{-2}$	0.000	0.000	0.000	0.000	0.000	0.000
ts	ratio	0.000	0.000	0.000	0.000	0.000	0.000
ss	$\mu\text{g cm}^{-2}$	0.000	0.000	0.000	0.000	0.000	0.000
ss	ratio	0.000	0.000	0.000	0.000	0.000	0.000
Smoke	$\mu\text{g cm}^{-2}$	0.000	0.000	0.000	0.000	0.000	0.000
Smoke	ratio	0.000	0.000	0.000	0.000	0.000	0.000

		Melbourne	Mildura	Mildura	Mildura	Mildura	Cape Grim
Element	Unit	2008.1	2007.8	2007.9	2007.11	2007.12	2007.9
F	$\mu\text{g cm}^{-2}$	0.088	0.000	0.395	0.353	0.069	0.130
Na	$\mu\text{g cm}^{-2}$	0.409	0.024	0.736	1.260	0.090	1.087
Al	$\mu\text{g cm}^{-2}$	1.740	0.638	6.815	18.552	2.506	3.561
Si	$\mu\text{g cm}^{-2}$	11.417	2.432	31.587	61.253	11.168	15.385
P	$\mu\text{g cm}^{-2}$	0.537	0.048	0.000	0.000	0.218	0.000
S	$\mu\text{g cm}^{-2}$	0.287	0.090	0.363	0.366	0.331	0.150
Cl	$\mu\text{g cm}^{-2}$	0.000	0.053	0.000	0.000	0.000	0.186
K	$\mu\text{g cm}^{-2}$	1.498	0.365	7.231	7.698	1.339	0.654
Ca	$\mu\text{g cm}^{-2}$	0.505	0.437	3.503	2.318	0.560	2.281
Ti	$\mu\text{g cm}^{-2}$	0.659	0.085	2.406	2.555	0.446	2.648
V	$\mu\text{g cm}^{-2}$	0.000	0.000	0.094	0.264	0.000	0.000
Cr	$\mu\text{g cm}^{-2}$	0.033	0.041	0.172	0.111	0.020	0.044
Mn	$\mu\text{g cm}^{-2}$	0.020	0.044	0.384	0.342	0.024	0.177
Fe	$\mu\text{g cm}^{-2}$	3.333	1.193	26.925	24.358	4.639	21.392
Co	$\mu\text{g cm}^{-2}$	0.034	0.000	0.495	0.112	0.042	0.295
Ni	$\mu\text{g cm}^{-2}$	0.000	0.019	0.314	0.291	0.000	0.090
Cu	$\mu\text{g cm}^{-2}$	0.062	0.006	0.738	1.372	0.065	0.325
Zn	$\mu\text{g cm}^{-2}$	0.036	0.090	0.495	0.430	0.090	0.069
Br	$\mu\text{g cm}^{-2}$	0.000	0.000	0.055	0.000	0.027	0.049
Sr	$\mu\text{g cm}^{-2}$	0.008	0.000	0.079	0.062	0.000	0.056
Pb	$\mu\text{g cm}^{-2}$	0.026	0.000	0.239	0.102	0.016	0.190
minNa	$\mu\text{g cm}^{-2}$	0.280	0.024	0.736	1.260	0.090	1.087
tsNa	$\mu\text{g cm}^{-2}$	0.000	0.000	0.000	0.000	0.000	0.000
ssNa	$\mu\text{g cm}^{-2}$	0.129	0.000	0.000	0.000	0.000	0.000
nssCa	$\mu\text{g cm}^{-2}$	0.500	0.437	3.503	2.318	0.560	2.281
ssCa	$\mu\text{g cm}^{-2}$	0.005	0.000	0.000	0.000	0.000	0.000
Total	$\mu\text{g cm}^{-2}$	37.398	9.622	138.950	221.009	39.015	80.294
Soil	$\mu\text{g cm}^{-2}$	42.416	11.224	169.181	261.016	46.326	106.767
Soil	ratio	1.134	1.166	1.218	1.181	1.187	1.330
ts	$\mu\text{g cm}^{-2}$	0.000	0.000	0.000	0.000	0.000	0.000
ts	ratio	0.000	0.000	0.000	0.000	0.000	0.000
ss	$\mu\text{g cm}^{-2}$	0.000	0.000	0.000	0.000	0.000	0.000
ss	ratio	0.000	0.000	0.000	0.000	0.000	0.000
Smoke	$\mu\text{g cm}^{-2}$	0.000	0.000	0.000	0.000	0.000	0.000
Smoke	ratio	0.000	0.000	0.000	0.000	0.000	0.000

		Cape Grim	Cape Grim	Adelaide	Adelaide	Adelaide	Adelaide
Element	Unit	2007.10	2007.12	2007.7	2007.10	2007.11	2007.12
F	$\mu\text{g cm}^{-2}$	0.152	0.049	0.012	0.045	0.000	0.000
Na	$\mu\text{g cm}^{-2}$	2.385	0.490	0.281	0.051	0.000	0.033
Al	$\mu\text{g cm}^{-2}$	4.529	1.250	1.988	1.169	1.174	0.960
Si	$\mu\text{g cm}^{-2}$	20.653	6.644	7.086	4.210	3.924	4.170
P	$\mu\text{g cm}^{-2}$	0.000	0.000	0.000	0.000	0.104	0.000
S	$\mu\text{g cm}^{-2}$	0.161	0.163	0.080	0.058	0.136	0.075
Cl	$\mu\text{g cm}^{-2}$	0.289	0.000	0.045	0.000	0.000	0.000
K	$\mu\text{g cm}^{-2}$	0.755	0.257	0.678	0.376	0.398	0.415
Ca	$\mu\text{g cm}^{-2}$	4.006	1.493	0.128	0.057	0.030	0.049
Ti	$\mu\text{g cm}^{-2}$	3.330	1.119	0.218	0.109	0.111	0.127
V	$\mu\text{g cm}^{-2}$	0.000	0.000	0.000	0.000	0.000	0.000
Cr	$\mu\text{g cm}^{-2}$	0.080	0.009	0.053	0.030	0.005	0.032
Mn	$\mu\text{g cm}^{-2}$	0.234	0.140	0.019	0.007	0.016	0.006
Fe	$\mu\text{g cm}^{-2}$	31.760	12.038	2.495	1.489	1.342	1.473
Co	$\mu\text{g cm}^{-2}$	0.566	0.131	0.025	0.000	0.000	0.000
Ni	$\mu\text{g cm}^{-2}$	0.247	0.019	0.012	0.008	0.000	0.007
Cu	$\mu\text{g cm}^{-2}$	0.655	0.077	0.045	0.021	0.016	0.019
Zn	$\mu\text{g cm}^{-2}$	0.158	0.064	0.073	0.032	0.017	0.027
Br	$\mu\text{g cm}^{-2}$	0.063	0.033	0.004	0.000	0.000	0.018
Sr	$\mu\text{g cm}^{-2}$	0.096	0.036	0.000	0.000	0.000	0.000
Pb	$\mu\text{g cm}^{-2}$	0.456	0.072	0.017	0.006	0.007	0.008
minNa	$\mu\text{g cm}^{-2}$	2.240	0.490	0.067	0.032	0.000	0.027
tsNa	$\mu\text{g cm}^{-2}$	0.000	0.000	0.000	0.000	0.000	0.000
ssNa	$\mu\text{g cm}^{-2}$	0.145	0.000	0.214	0.019	0.000	0.006
nssCa	$\mu\text{g cm}^{-2}$	4.001	1.493	0.120	0.056	0.030	0.049
ssCa	$\mu\text{g cm}^{-2}$	0.005	0.000	0.008	0.001	0.000	0.000
Total	$\mu\text{g cm}^{-2}$	114.239	38.633	24.316	14.203	13.422	13.729
Soil	$\mu\text{g cm}^{-2}$	151.230	53.030	28.674	16.961	15.865	16.386
Soil	ratio	1.324	1.373	1.179	1.194	1.182	1.194
ts	$\mu\text{g cm}^{-2}$	0.000	0.000	0.000	0.000	0.000	0.000
ts	ratio	0.000	0.000	0.000	0.000	0.000	0.000
ss	$\mu\text{g cm}^{-2}$	0.368	0.000	0.543	0.000	0.000	0.000
ss	ratio	0.003	0.000	0.022	0.000	0.000	0.000
Smoke	$\mu\text{g cm}^{-2}$	0.000	0.000	0.000	0.000	0.000	0.000
Smoke	ratio	0.000	0.000	0.000	0.000	0.000	0.000

		Adelaide	Woomera	Woomera	Woomera	Woomera
Element	Unit	2008.1	2007.9	2007.10	2008.1	2008.3
F	µg cm ⁻²	0.049	0.146	0.032	0.000	0.000
Na	µg cm ⁻²	0.067	0.192	0.082	0.000	0.174
Al	µg cm ⁻²	0.620	4.563	3.155	0.000	0.647
Si	µg cm ⁻²	3.273	15.302	11.383	0.122	3.041
P	µg cm ⁻²	0.020	0.000	0.049	0.023	0.033
S	µg cm ⁻²	0.053	0.120	0.121	0.007	0.109
Cl	µg cm ⁻²	0.000	0.000	0.000	0.000	0.284
K	µg cm ⁻²	0.332	1.619	1.100	0.011	0.448
Ca	µg cm ⁻²	0.088	0.544	0.152	0.010	1.109
Ti	µg cm ⁻²	0.095	0.595	0.377	0.000	0.127
V	µg cm ⁻²	0.000	0.015	0.000	0.000	0.000
Cr	µg cm ⁻²	0.025	0.011	0.010	0.000	0.002
Mn	µg cm ⁻²	0.007	0.029	0.013	0.000	0.052
Fe	µg cm ⁻²	0.995	5.392	4.334	0.044	2.249
Co	µg cm ⁻²	0.000	0.070	0.049	0.000	0.000
Ni	µg cm ⁻²	0.016	0.014	0.000	0.003	0.000
Cu	µg cm ⁻²	0.014	0.090	0.057	0.000	0.009
Zn	µg cm ⁻²	0.030	0.070	0.054	0.004	0.022
Br	µg cm ⁻²	0.004	0.006	0.004	0.000	0.000
Sr	µg cm ⁻²	0.000	0.019	0.009	0.000	0.000
Pb	µg cm ⁻²	0.000	0.034	0.027	0.000	0.008
minNa	µg cm ⁻²	0.049	0.192	0.082	0.000	0.174
tsNa	µg cm ⁻²	0.000	0.000	0.000	0.000	0.000
ssNa	µg cm ⁻²	0.018	0.000	0.000	0.000	0.000
nssCa	µg cm ⁻²	0.087	0.544	0.152	0.010	1.109
ssCa	µg cm ⁻²	0.001	0.000	0.000	0.000	0.000
Total	µg cm ⁻²	10.491	53.181	38.845	0.384	13.812
Soil	µg cm ⁻²	12.248	63.230	46.752	0.000	16.492
Soil	ratio	1.167	1.189	1.204	0.000	1.194
ts	µg cm ⁻²	0.000	0.000	0.000	0.000	0.000
ts	ratio	0.000	0.000	0.000	0.000	0.000
ss	µg cm ⁻²	0.000	0.000	0.000	0.000	0.000
ss	ratio	0.000	0.000	0.000	0.000	0.000
Smoke	µg cm ⁻²	0.000	0.000	0.000	0.000	0.000
Smoke	ratio	0.000	0.000	0.000	0.000	0.000

Appendix A-3: IBA Results 3

IBA results and the calculated values for Cowra samples in pellets

Element	Unit	Month						
		2006.10	2006.11	2007.1	2007.2	2007.3	2007.4	2007.5
F	mg kg ⁻¹	457	659	552	663	2140	699	1304
Na	mg kg ⁻¹	10007	7230	8915	14274	20500	19515	17205
Al	mg kg ⁻¹	76838	135070	0	116041	0	84551	76626
Si	mg kg ⁻¹	264133	535993	386804	491072	333813	345630	331491
P	mg kg ⁻¹	0	0	2723	0	0	3380	0
S	mg kg ⁻¹	7512	1724	8829	3127	17542	7070	22279
Cl	mg kg ⁻¹	16788	2837	7776	13289	30090	26208	12978
K	mg kg ⁻¹	17779	17029	21204	22234	27225	30120	24151
Ca	mg kg ⁻¹	9601	6164	7836	11131	25624	14888	12702
Ti	mg kg ⁻¹	11611	5928	4688	5034	5242	5742	4898
V	mg kg ⁻¹	0	95	0	103	0	0	100
Cr	mg kg ⁻¹	0	0	0	42	56	64	50
Mn	mg kg ⁻¹	586	732	715	906	907	891	828
Fe	mg kg ⁻¹	17624	24821	17909	25947	27856	33736	26346
Co	mg kg ⁻¹	167	253	184	251	281	271	222
Ni	mg kg ⁻¹	613	806	762	673	988	654	832
Cu	mg kg ⁻¹	118	81	66	84	159	76	176
Zn	mg kg ⁻¹	492	794	514	394	1170	329	792
Br	mg kg ⁻¹	24	38	57	22	133	49	127
Rb	mg kg ⁻¹	41	0	58	93	90	74	78
Sr	mg kg ⁻¹	79	72	58	102	129	127	96
Y	mg kg ⁻¹	23	0	48	22	36	34	42
Zr	mg kg ⁻¹	174	272	289	299	153	196	268
Pb	mg kg ⁻¹	32	324	98	80	125	70	95
minNa	mg kg ⁻¹	5276	3370	4290	6059	9833	8094	6894
tsNa	mg kg ⁻¹	0	0	0	0	4383	0	0
ssNa	mg kg ⁻¹	4731	3860	4625	8215	6284	11421	10311
nssCa	mg kg ⁻¹	9421	6017	7660	10819	25385	14454	12310
ssCa	mg kg ⁻¹	180	147	176	312	239	434	392
Total	mg kg ⁻¹	826692	1492039	928834	1392050	906128	1072717	1003614
Soil	mg kg ⁻¹	907267	1713152	0	1568252	0	1162972	1087315
Soil *1	ratio	0.907	1.713	0.000	1.568	0.000	1.163	1.087
ts	mg kg ⁻¹	0	0	0	0	11132	0	0
ts *1	ratio	0.000	0.000	0.000	0.000	0.011	0.000	0.000
ts *2	ratio	0.000	0.000	0.000	0.000	0.012	0.000	0.000
ss	mg kg ⁻¹	12017	9805	11748	20867	15962	29009	26191
ss *1	ratio	0.012	0.010	0.012	0.021	0.016	0.029	0.026
Smoke	mg kg ⁻¹	7205	2136	10459	6666	10511	9878	8343
Smoke	ratio	0.007	0.002	0.010	0.007	0.011	0.010	0.008

*1: Ratios calculated without using estimated total

*2: Ratios calculated using estimated total

		Month					
Element	Unit	2007.6	2007.7	2007.8	2007.11	2007.12	2008.1 – 2008.2
F	mg kg ⁻¹	907	826	339	715	2276	893
Na	mg kg ⁻¹	13183	15816	6851	12701	37513	12681
Al	mg kg ⁻¹	0	89722	83831	119940	0	95910
Si	mg kg ⁻¹	308405	265581	375423	459726	239935	369690
P	mg kg ⁻¹	0	0	0	0	0	0
S	mg kg ⁻¹	14160	3700	5644	6921	22169	7682
Cl	mg kg ⁻¹	18703	13022	5394	9381	84041	4428
K	mg kg ⁻¹	27475	15938	18761	27224	40002	22508
Ca	mg kg ⁻¹	23612	8585	8312	9767	18123	11918
Ti	mg kg ⁻¹	4051	4100	10651	5442	3592	5784
V	mg kg ⁻¹	0	111	119	108	0	108
Cr	mg kg ⁻¹	0	0	56	62	47	69
Mn	mg kg ⁻¹	614	637	769	945	678	875
Fe	mg kg ⁻¹	17346	20819	21599	26633	17011	28931
Co	mg kg ⁻¹	201	174	184	219	201	241
Ni	mg kg ⁻¹	847	576	507	653	793	718
Cu	mg kg ⁻¹	104	193	91	45	131	168
Zn	mg kg ⁻¹	524	467	445	554	925	651
Br	mg kg ⁻¹	87	43	15	63	183	32
Rb	mg kg ⁻¹	43	70	61	99	59	67
Sr	mg kg ⁻¹	109	82	81	100	125	106
Y	mg kg ⁻¹	0	16	19	23	0	25
Zr	mg kg ⁻¹	109	308	194	280	159	172
Pb	mg kg ⁻¹	81	50	41	107	105	82
minNa	mg kg ⁻¹	6123	4568	4607	5312	6005	6543
tsNa	mg kg ⁻¹	7060	0	0	0	3549	0
ssNa	mg kg ⁻¹	0	11248	2244	7389	27959	6138
nssCa	mg kg ⁻¹	23612	8158	8227	9486	17061	11685
ssCa	mg kg ⁻¹	0	427	85	281	1062	233
Total	mg kg ⁻¹	806876	841092	1064975	1335855	764586	1095404
Soil	mg kg ⁻¹	0	930318	1205574	1499058	0	1231810
Soil *1	ratio	0.000	0.930	1.206	1.499	0.000	1.232
ts	mg kg ⁻¹	17932	0	0	0	9015	0
ts *1	ratio	0.018	0.000	0.000	0.000	0.009	0.000
ts *2	ratio	0.022	0.000	0.000	0.000	0.012	0.000
ss	mg kg ⁻¹	0	28569	5700	18767	71016	15589
ss *1	ratio	0.000	0.029	0.006	0.019	0.071	0.016
Smoke	mg kg ⁻¹	17067	3447	5802	11244	29795	5149
Smoke	ratio	0.017	0.003	0.006	0.011	0.030	0.005

*1: Ratios calculated without using estimated total

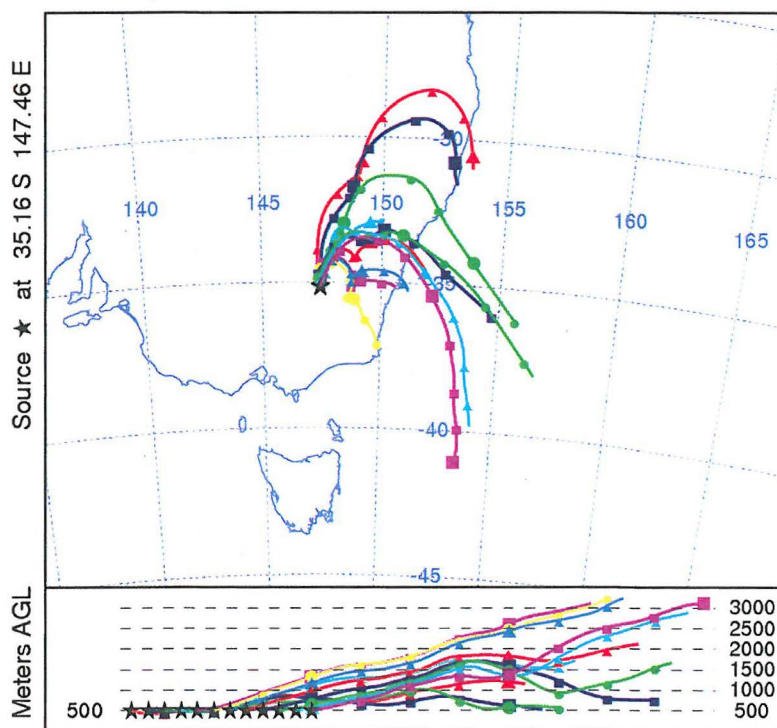
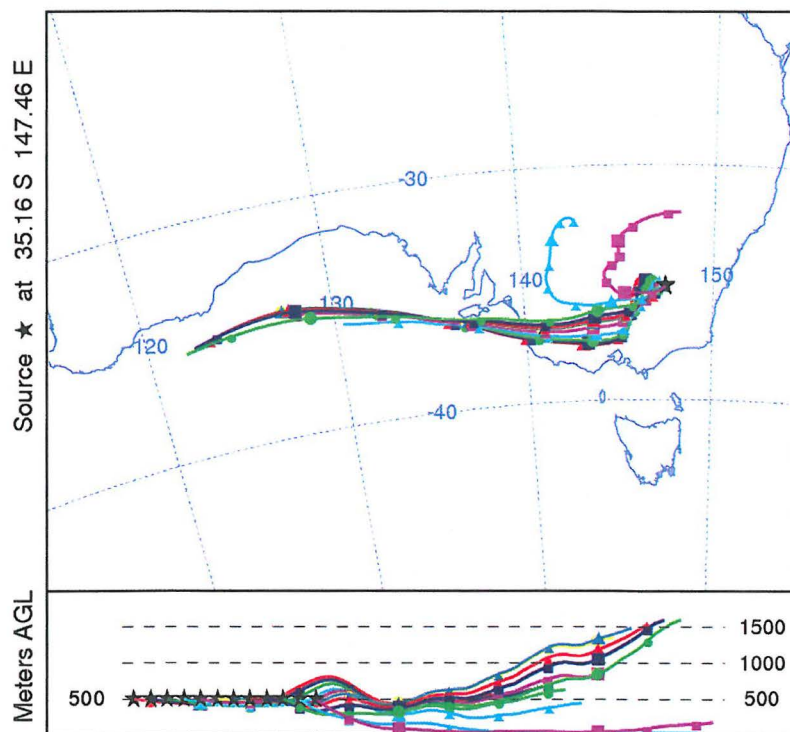
*2: Ratios calculated using estimated total

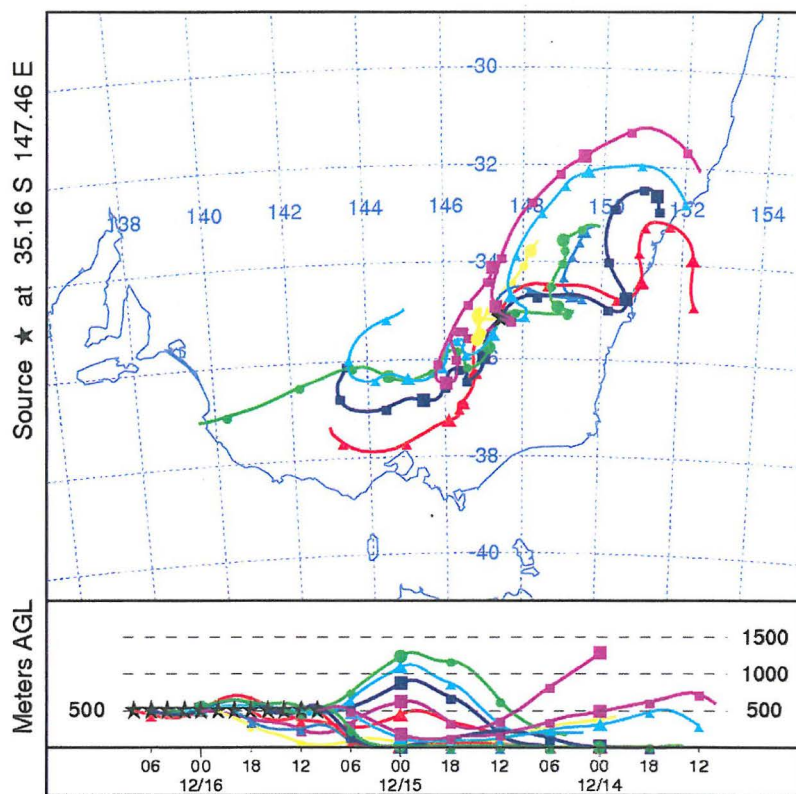
Appendix A-4: IBA Results 4

IBA results and the calculated values for Cowra samples on Teflon filters

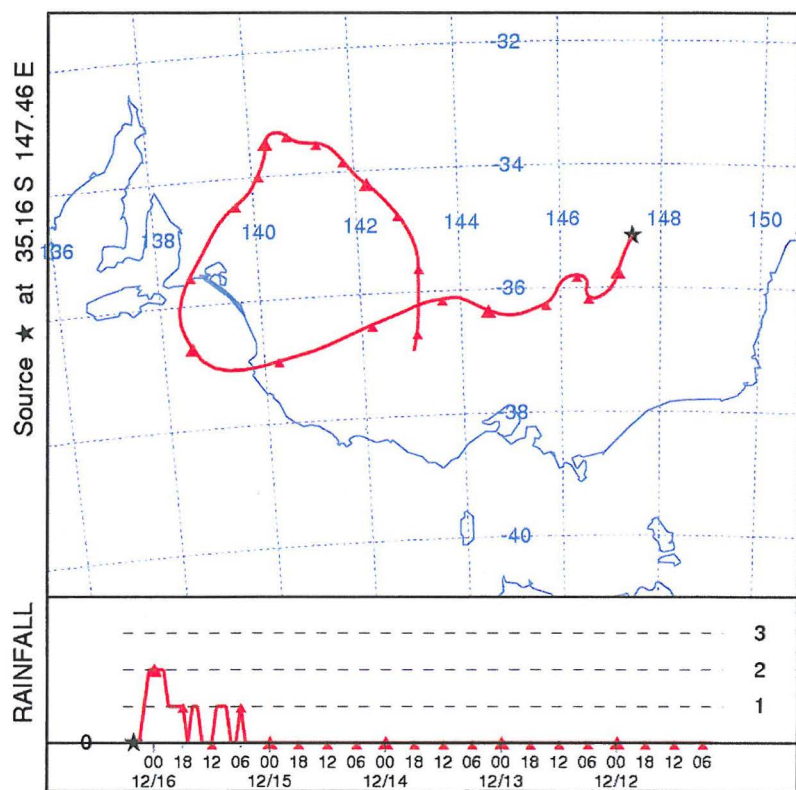
Element	Unit	Month						
		2006.12	2007.9	2007.10	2008.3	2008.4	2008.5	2008.6
F	$\mu\text{g cm}^{-2}$	495.724	338.951	320.767	287.318	333.105	220.932	252.726
Na	$\mu\text{g cm}^{-2}$	0.000	11.448	5.268	3.001	0.000	3.145	3.014
Al	$\mu\text{g cm}^{-2}$	10.726	6.716	20.740	22.400	27.617	20.927	10.622
Si	$\mu\text{g cm}^{-2}$	41.947	31.858	77.106	69.758	65.865	59.631	27.840
P	$\mu\text{g cm}^{-2}$	0.130	0.000	0.163	0.000	0.000	0.220	0.000
S	$\mu\text{g cm}^{-2}$	0.791	7.865	3.283	0.810	0.344	1.598	0.957
Cl	$\mu\text{g cm}^{-2}$	0.693	40.964	13.886	2.603	0.933	4.262	4.960
K	$\mu\text{g cm}^{-2}$	3.744	9.693	12.246	7.797	8.093	8.610	3.678
Ca	$\mu\text{g cm}^{-2}$	2.191	7.898	7.332	3.171	3.295	8.072	3.035
Ti	$\mu\text{g cm}^{-2}$	4.808	0.704	2.489	2.302	2.390	2.300	1.056
V	$\mu\text{g cm}^{-2}$	0.000	0.059	0.146	0.000	0.000	0.000	0.000
Cr	$\mu\text{g cm}^{-2}$	0.000	0.000	0.000	0.000	0.000	0.058	0.000
Mn	$\mu\text{g cm}^{-2}$	0.156	0.254	0.340	0.461	0.495	0.449	0.215
Fe	$\mu\text{g cm}^{-2}$	8.153	6.774	18.017	14.977	18.733	14.735	6.712
Co	$\mu\text{g cm}^{-2}$	0.000	0.000	0.184	0.000	0.000	0.000	0.000
Ni	$\mu\text{g cm}^{-2}$	0.000	0.083	0.000	0.000	0.000	0.000	0.000
Cu	$\mu\text{g cm}^{-2}$	0.085	0.115	0.248	0.133	0.141	0.182	0.039
Zn	$\mu\text{g cm}^{-2}$	0.136	0.667	0.659	0.250	0.117	0.215	0.140
Br	$\mu\text{g cm}^{-2}$	0.000	0.183	0.000	0.000	0.000	0.000	0.000
Sr	$\mu\text{g cm}^{-2}$	0.000	0.000	0.000	0.000	0.000	0.000	0.000
Pb	$\mu\text{g cm}^{-2}$	0.000	0.000	0.151	0.000	0.000	0.000	0.000
minNa	$\mu\text{g cm}^{-2}$	0.000	2.391	4.081	1.749	0.000	3.145	1.671
tsNa	$\mu\text{g cm}^{-2}$	0.000	1.879	0.000	0.000	0.000	0.000	0.000
ssNa	$\mu\text{g cm}^{-2}$	0.000	7.178	1.187	1.252	0.000	0.000	1.343
nssCa	$\mu\text{g cm}^{-2}$	2.191	7.625	7.287	3.123	3.295	8.072	2.984
ssCa	$\mu\text{g cm}^{-2}$	0.000	0.273	0.045	0.048	0.000	0.000	0.051
Total	$\mu\text{g cm}^{-2}$	634.212	514.574	603.517	524.317	571.548	444.266	361.58155
Soil	$\mu\text{g cm}^{-2}$	160.674	124.290	297.929	268.779	280.103	247.799	115.846
Soil	ratio	0.253	0.242	0.494	0.513	0.490	0.558	0.320
ts	$\mu\text{g cm}^{-2}$	0.000	4.772	0.000	0.000	0.000	0.000	0.000
ts	ratio	0.000	0.009	0.000	0.000	0.000	0.000	0.000
ss	$\mu\text{g cm}^{-2}$	0.000	18.232	3.016	3.180	0.000	0.000	3.411
ss	ratio	0.000	0.035	0.005	0.006	0.000	0.000	0.009
Smoke	$\mu\text{g cm}^{-2}$	0.000	5.629	1.436	0.000	0.000	0.000	0.000
Smoke	ratio	0.000	0.011	0.002	0.000	0.000	0.000	0.000

Appendix B: Back Trajectories

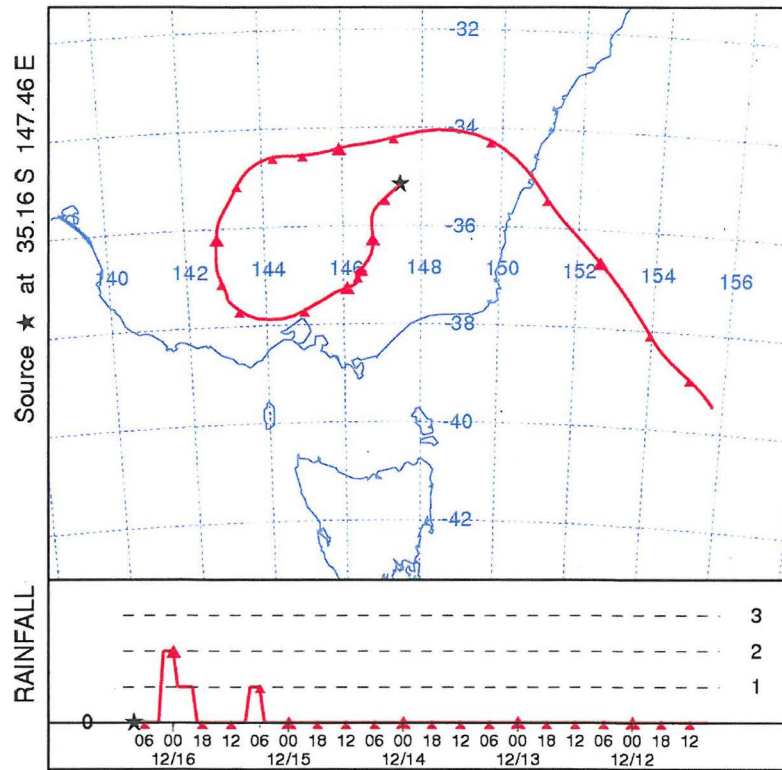




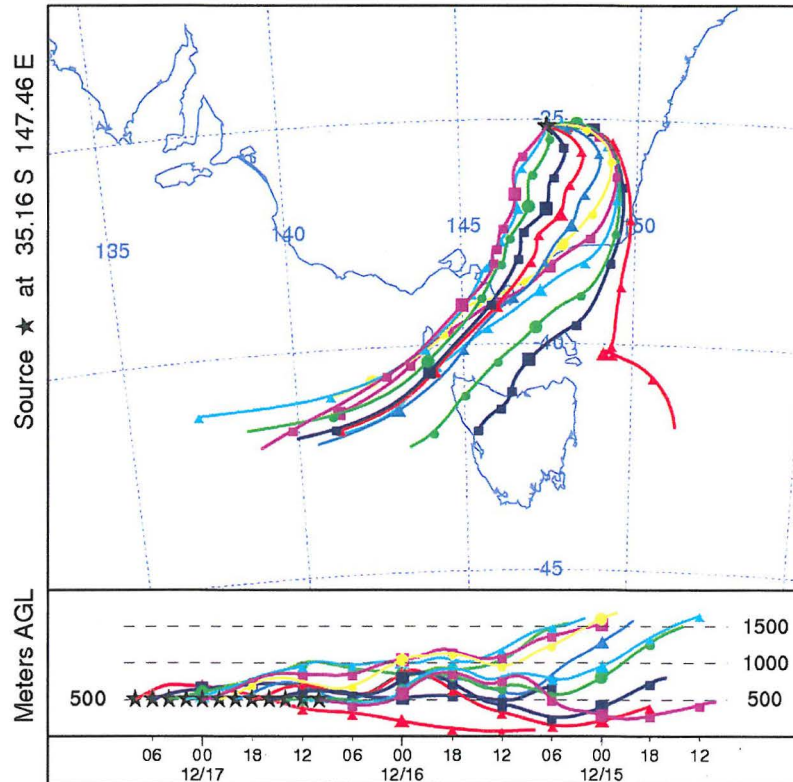
12 trajectories for Wagga Wagga December 16th



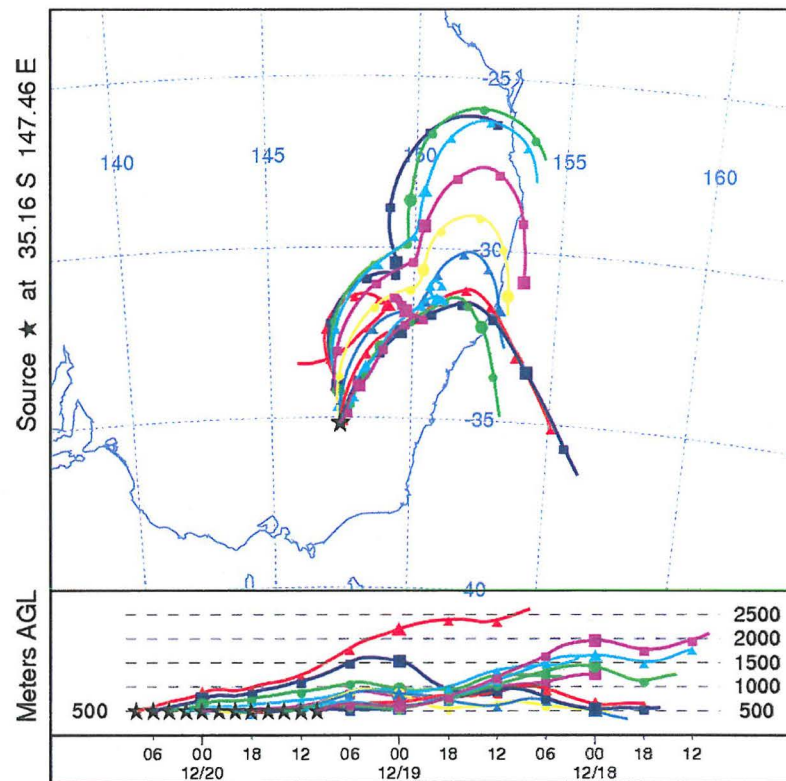
A 120 hours trajectory of Wagga Wagga December 16th at 04hrs



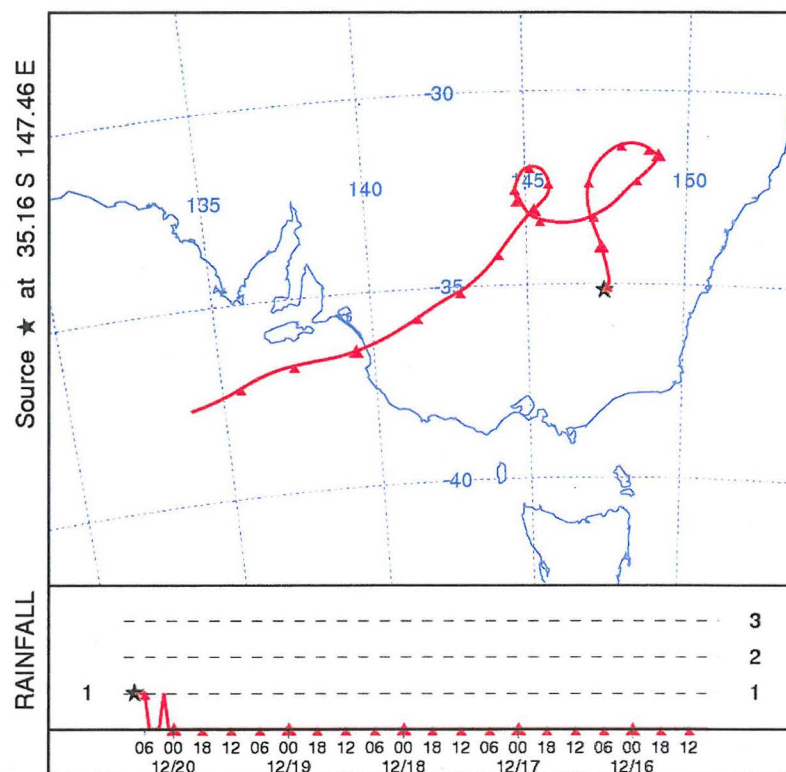
A 120 hours trajectory of Wagga Wagga December 16th at 08hrs



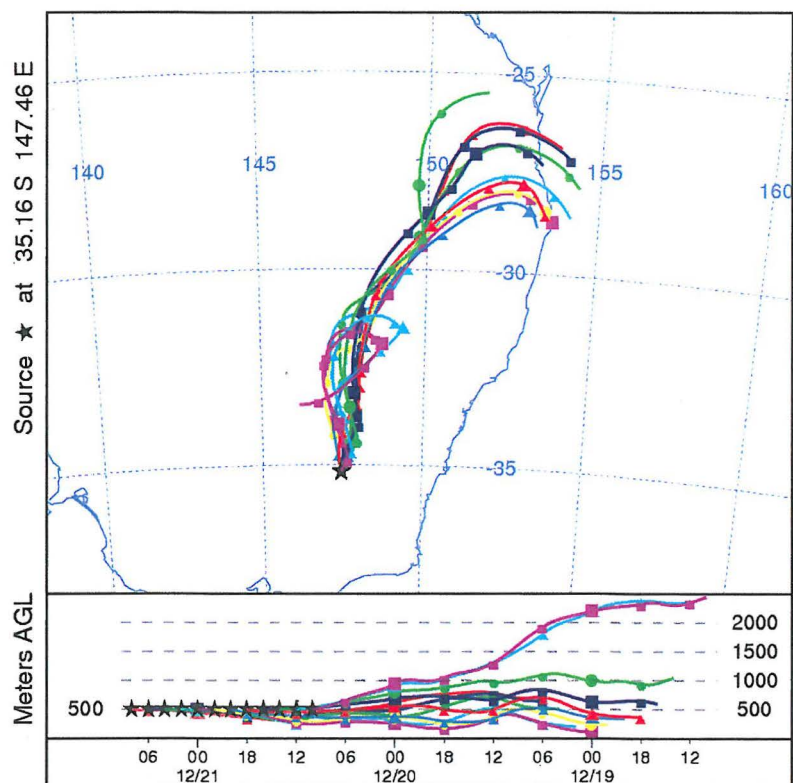
12 trajectories for Wagga Wagga December 17th



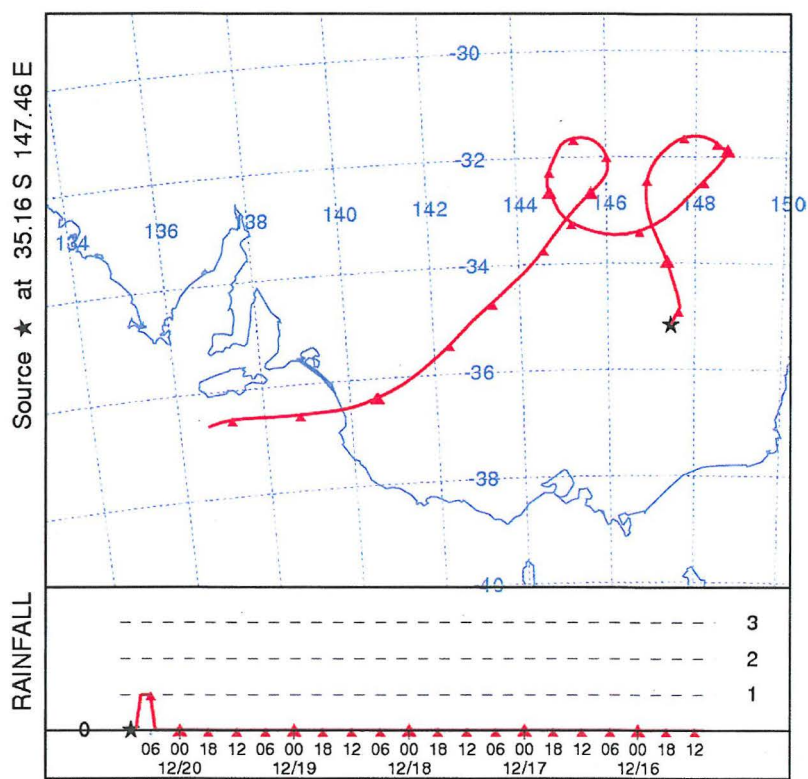
12 trajectories for Wagga Wagga December 20th



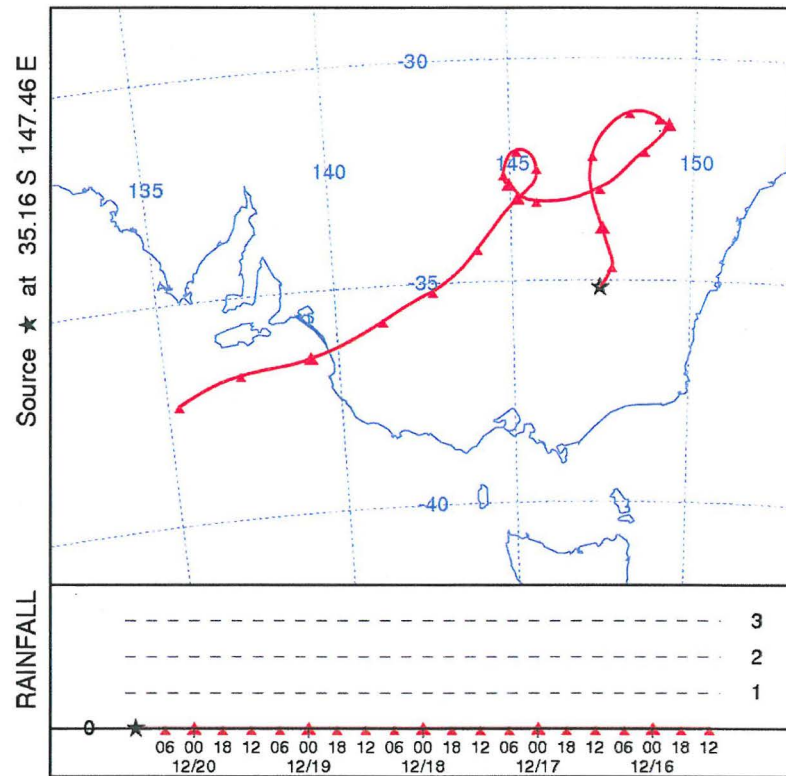
A 120 hours trajectory of Wagga Wagga December 20th at 08hrs



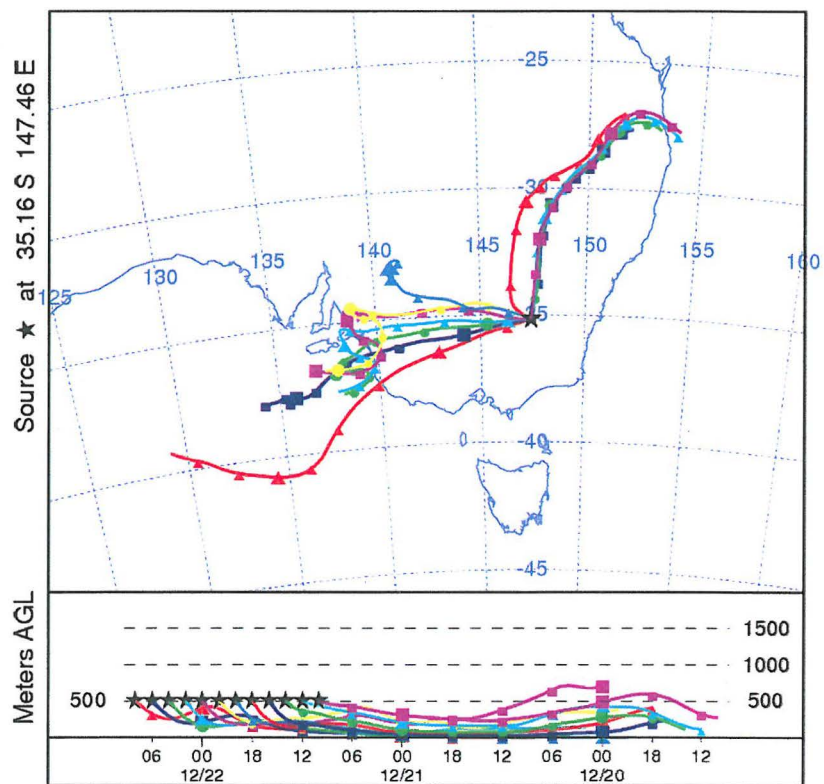
12 trajectories for Wagga Wagga December 21st



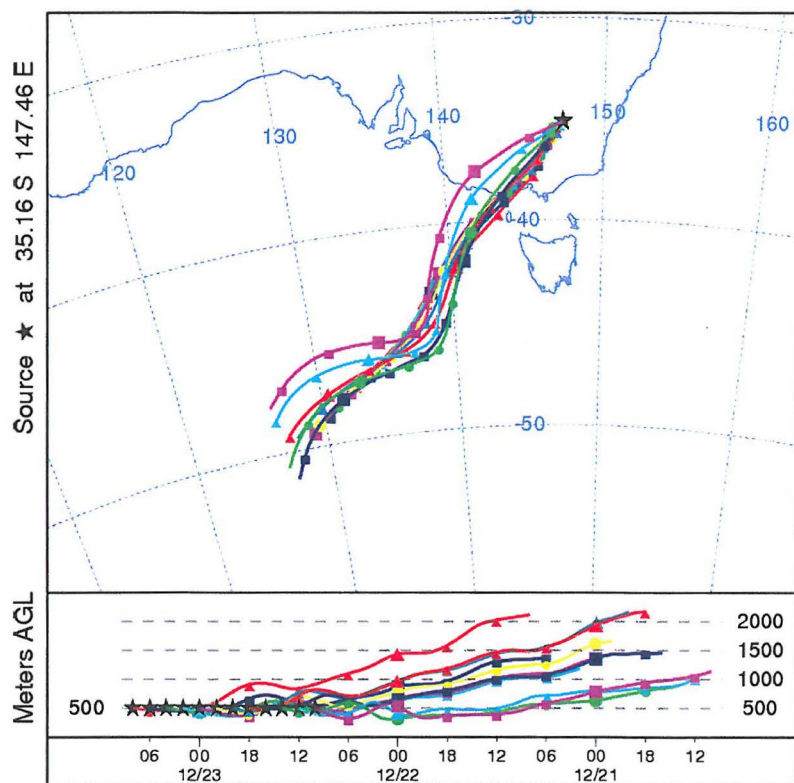
A 120 hours trajectory of Wagga Wagga December 20th at 10hrs



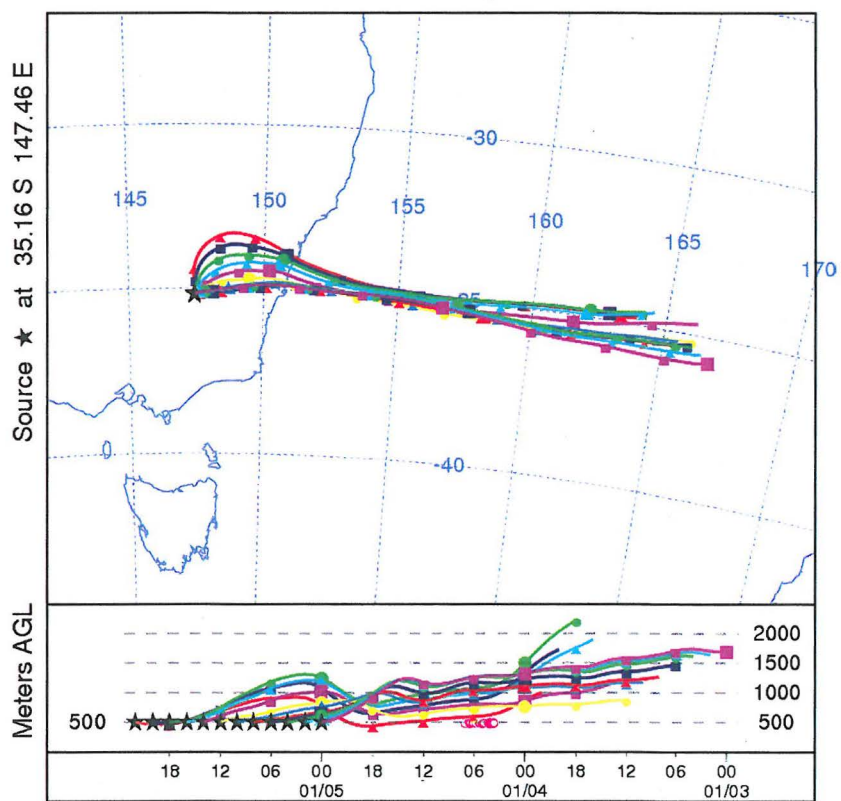
A 120 hours trajectory of Wagga Wagga December 20th at 12hrs



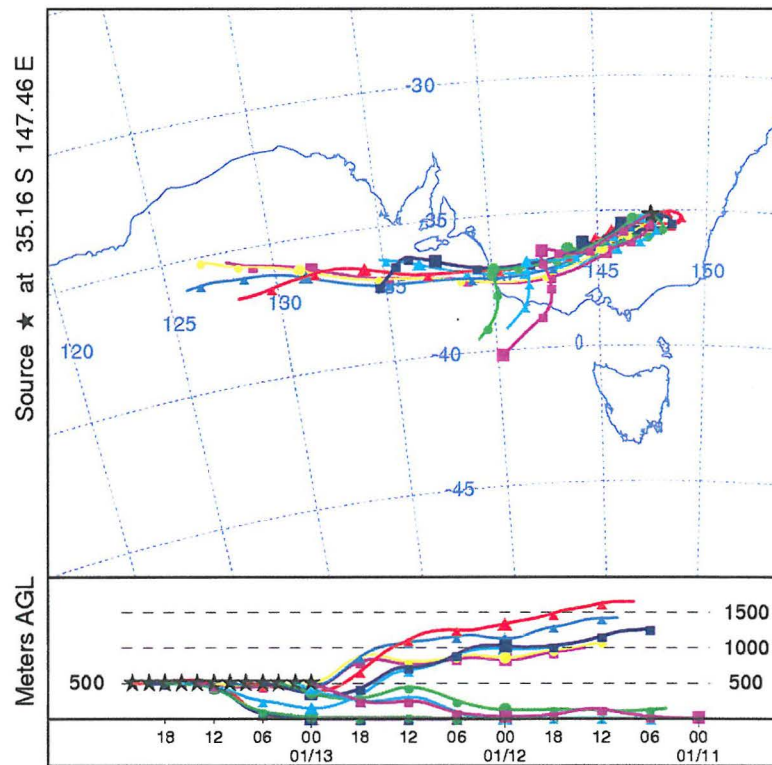
12 trajectories for Wagga Wagga December 22nd



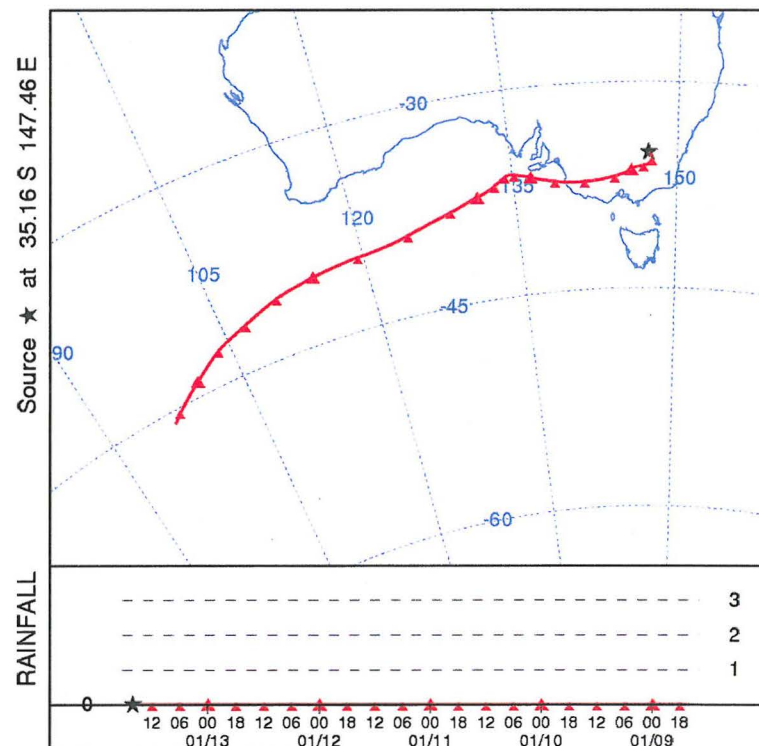
12 trajectories for Wagga Wagga December 23th



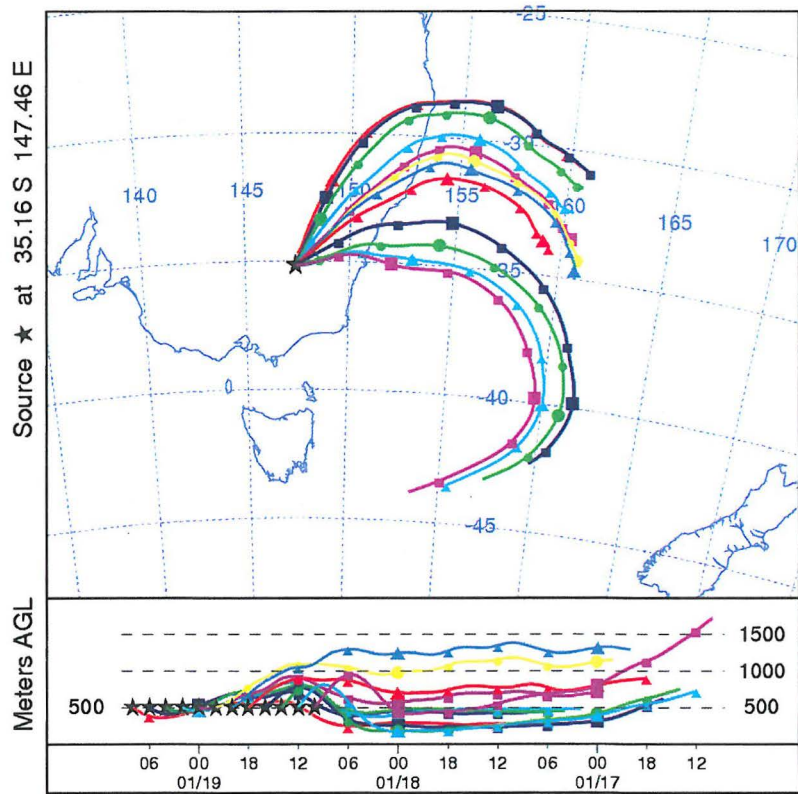
12 trajectories for Wagga Wagga January 5th



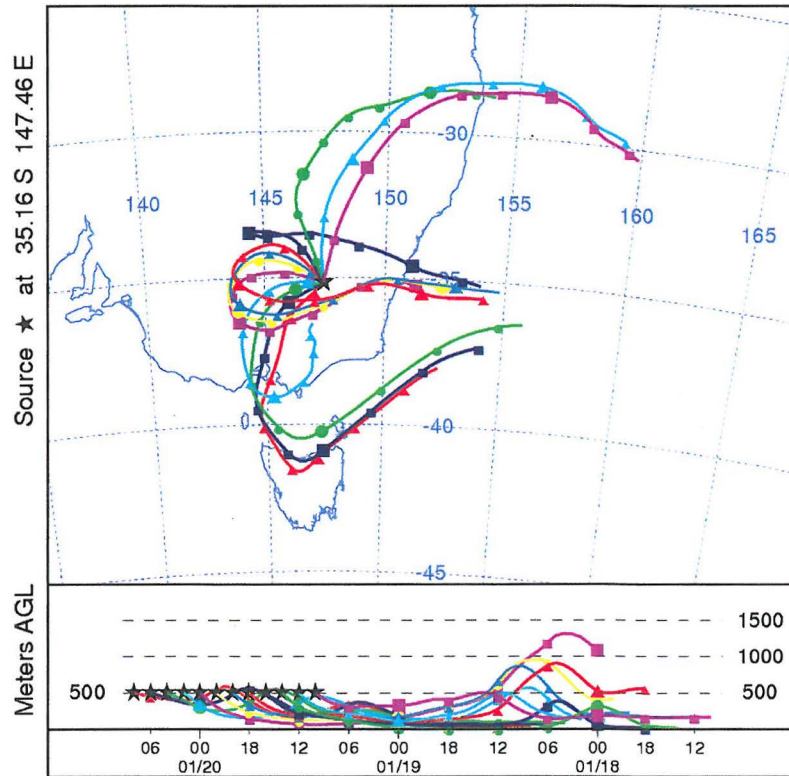
12 trajectories for Wagga Wagga January 13th



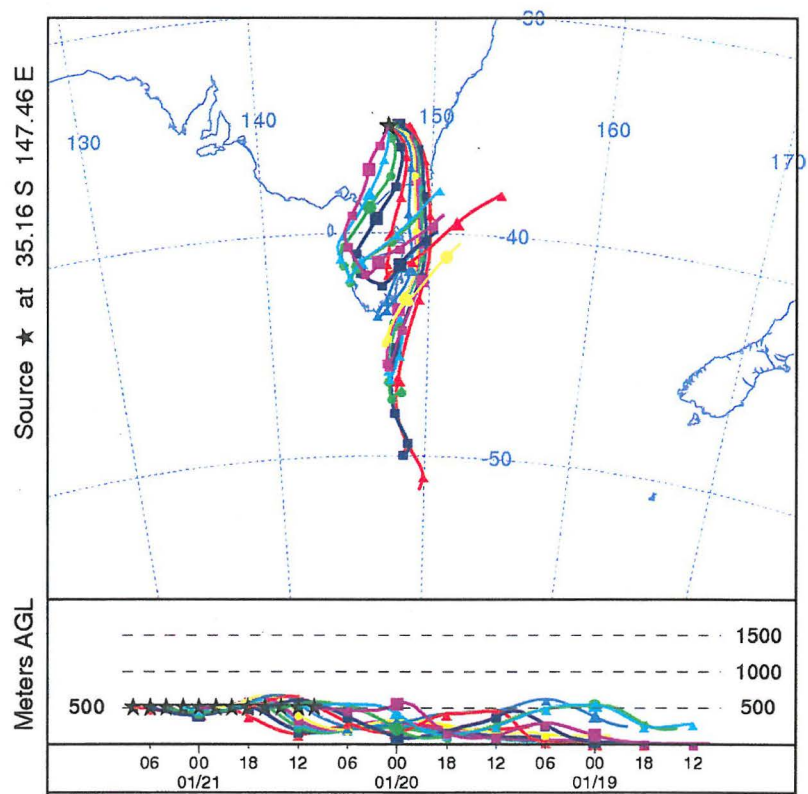
A 120 hours trajectory of Wagga Wagga January 13th at 16hrs



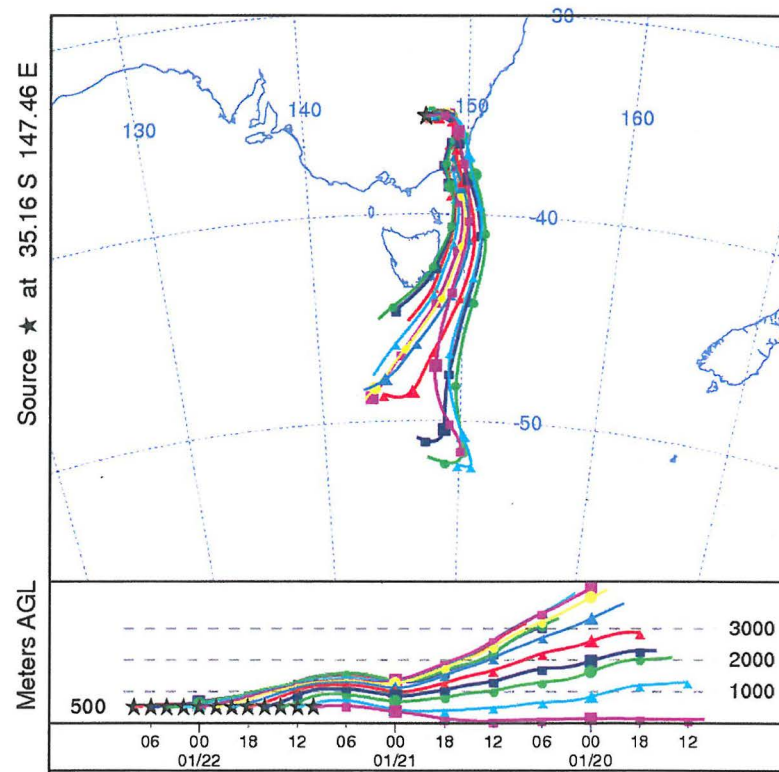
12 trajectories for Wagga Wagga January 19th



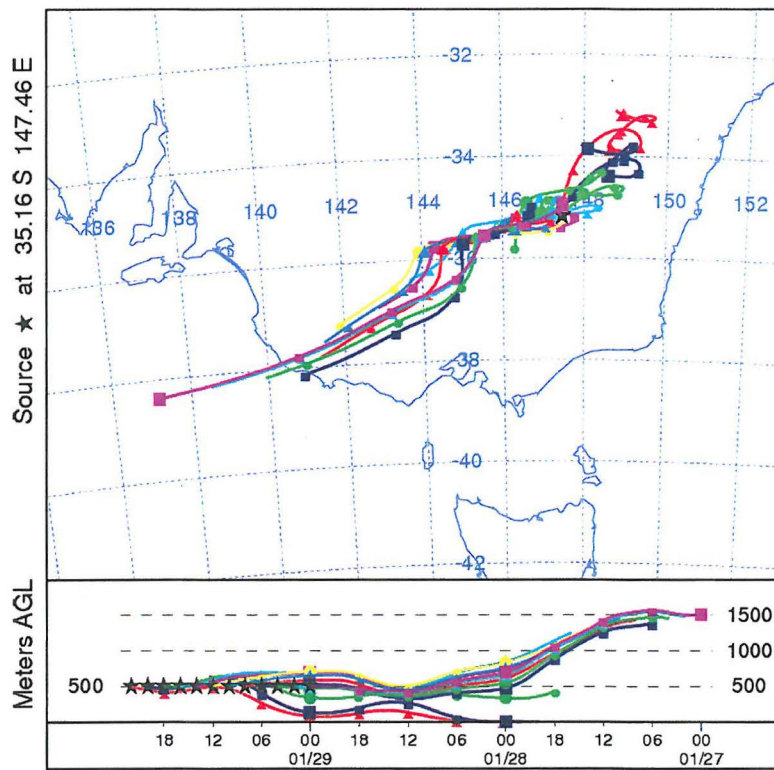
12 trajectories for Wagga Wagga January 20th



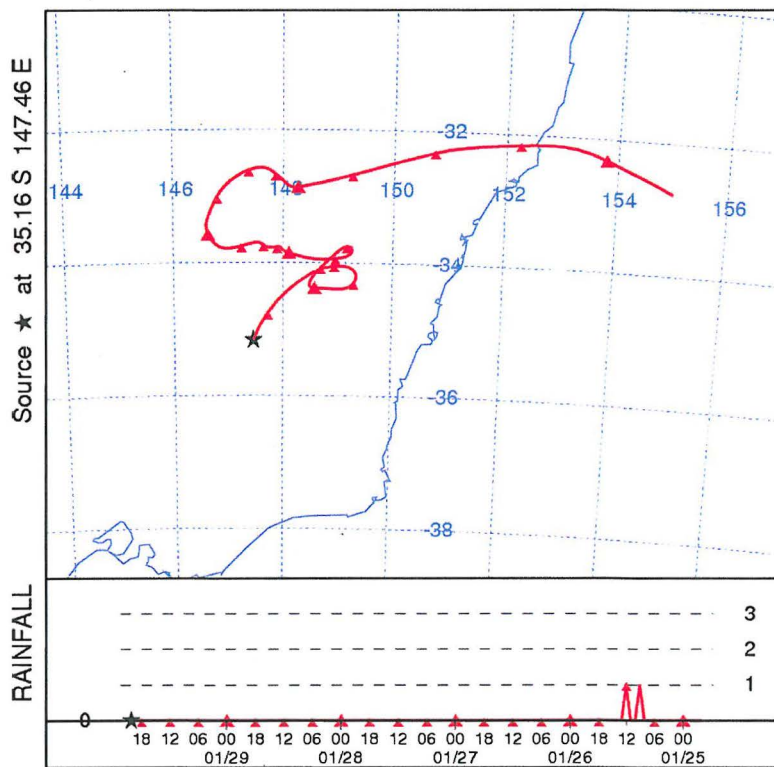
12 trajectories for Wagga Wagga January 21st



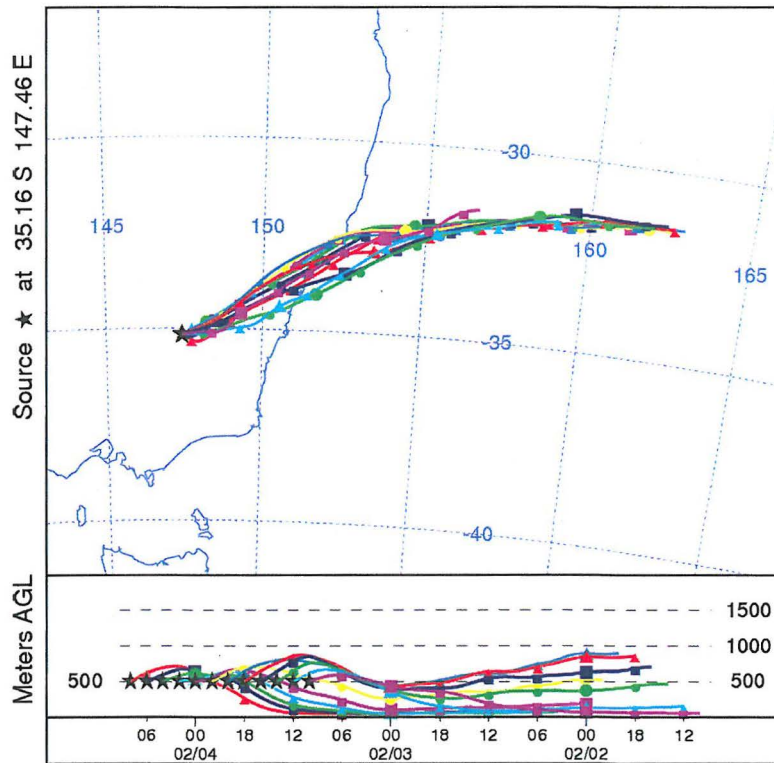
12 trajectories for Wagga Wagga January 22nd



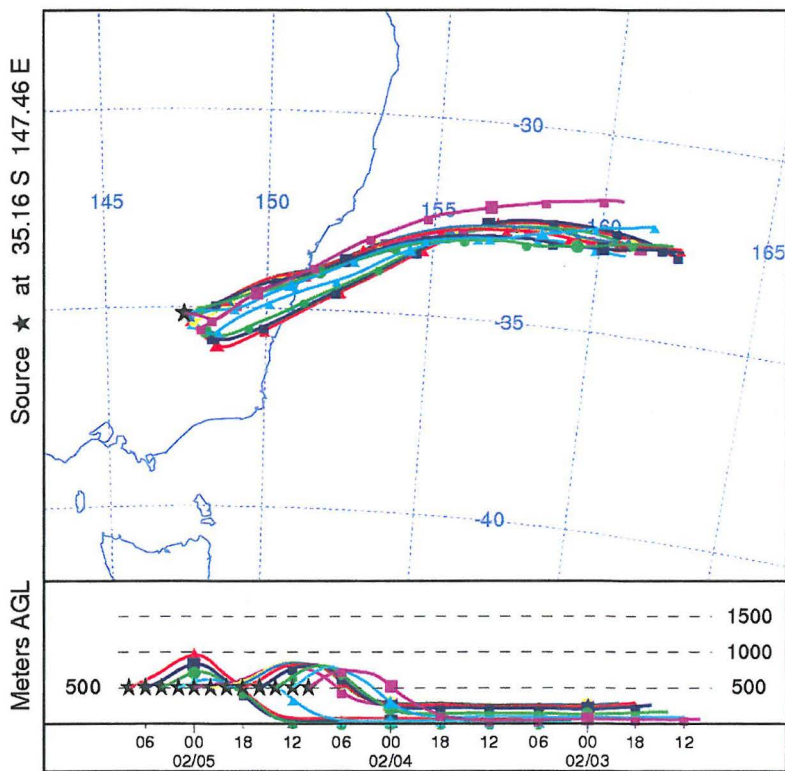
12 trajectories for Wagga Wagga January 29th



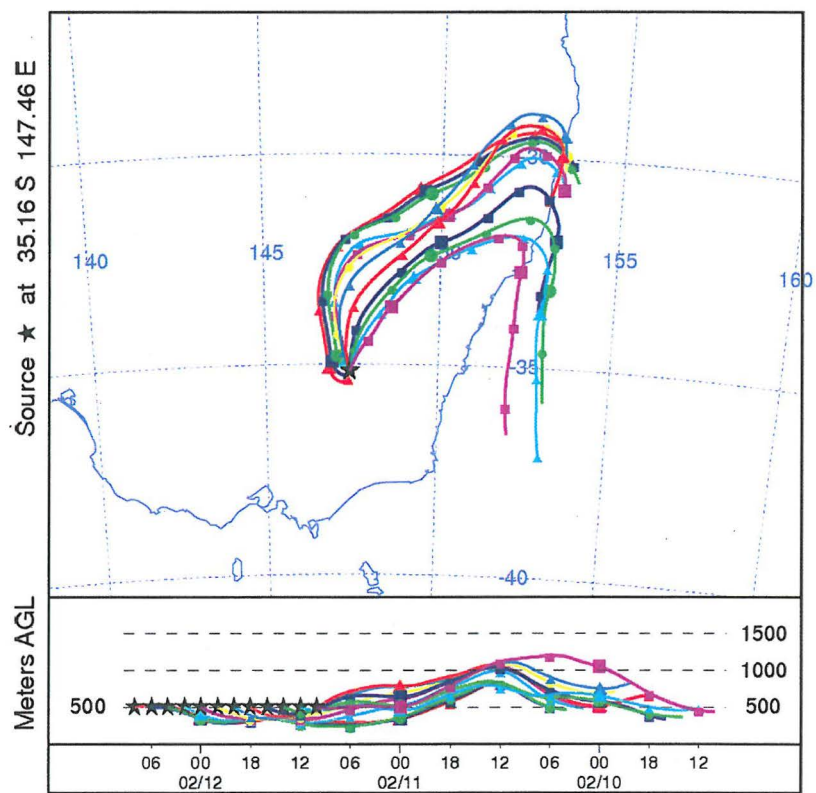
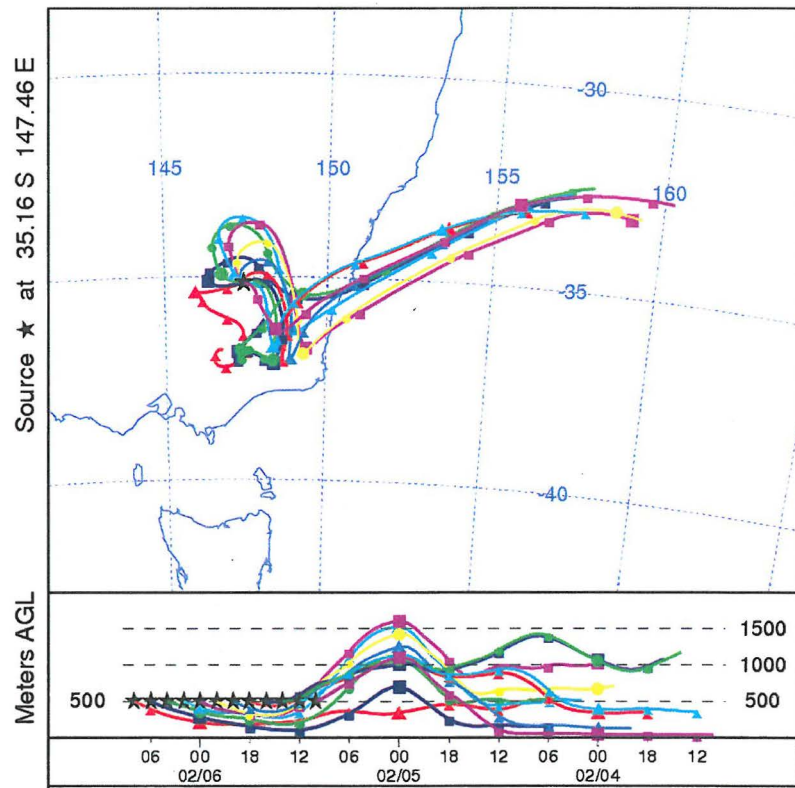
A 120 hours trajectory of Wagga Wagga January 29th at 20hrs

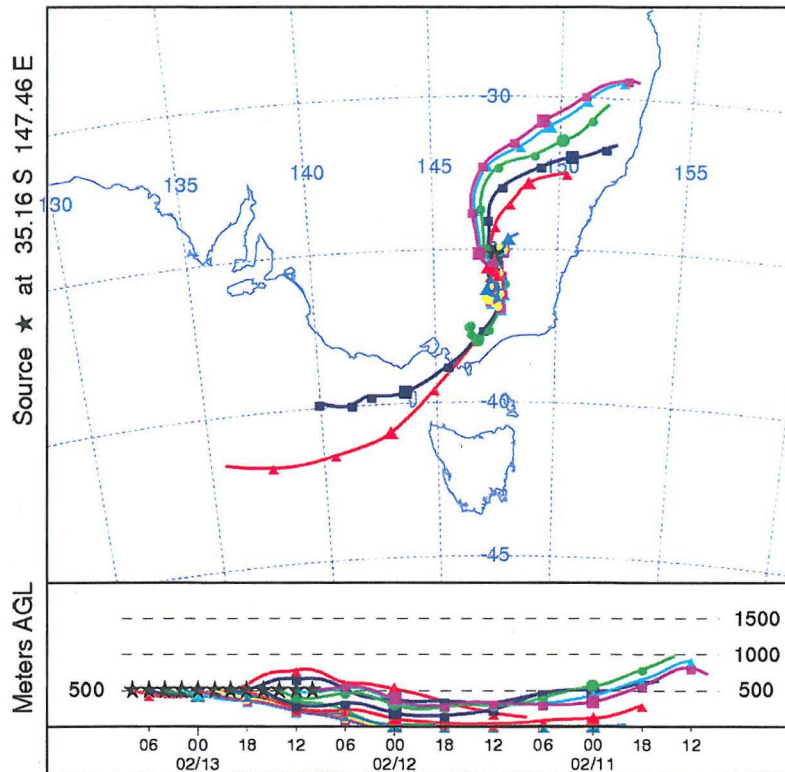


12 trajectories for Wagga Wagga February 4th

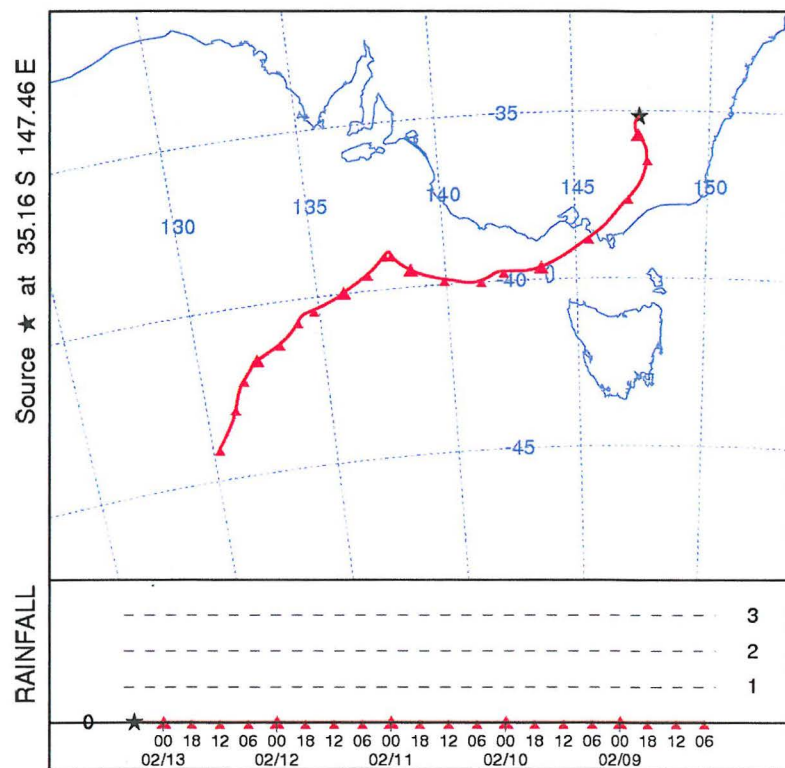


12 trajectories for Wagga Wagga February 5st

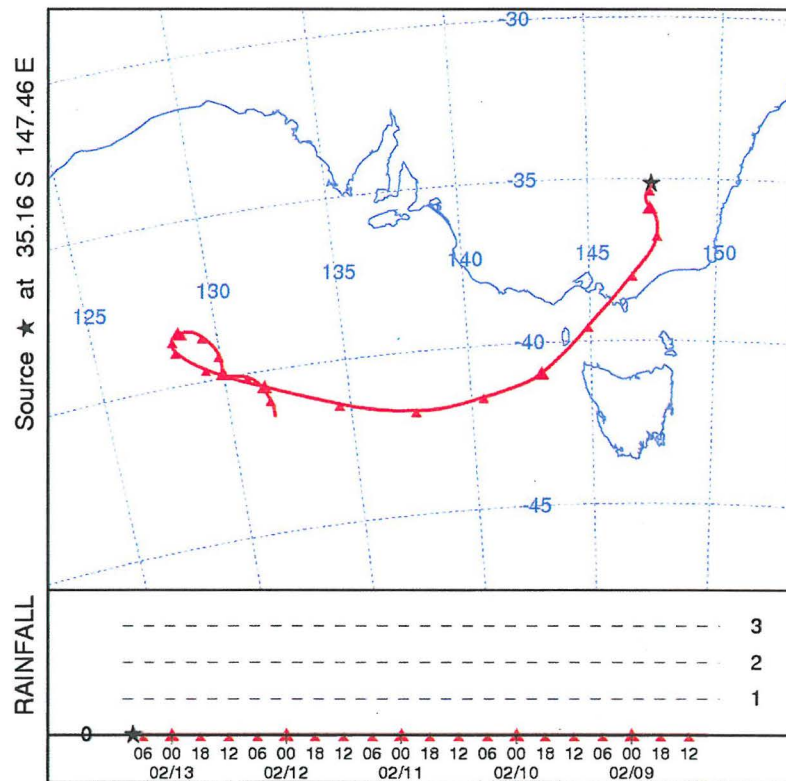




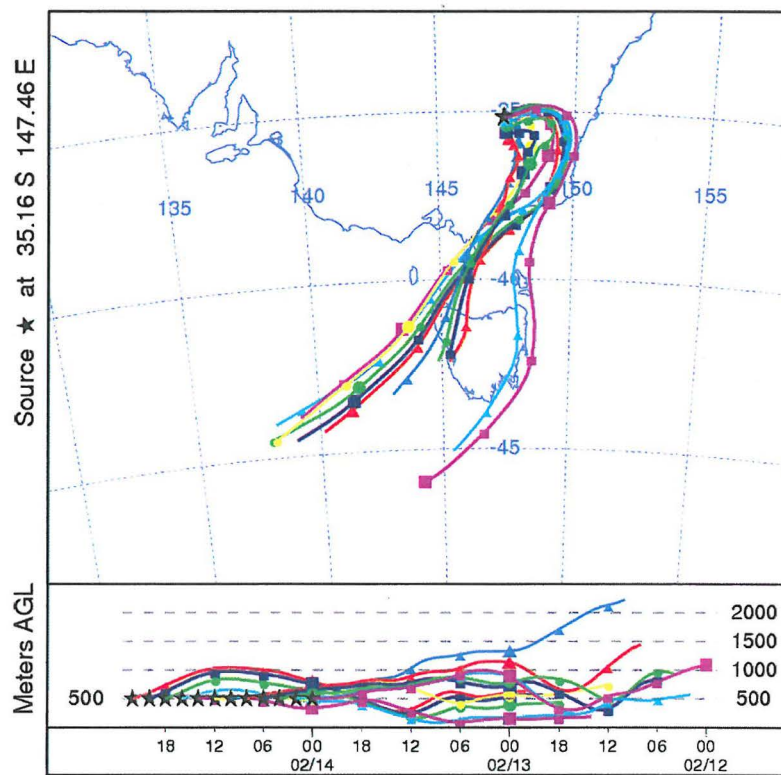
12 trajectories for Wagga Wagga February 13th



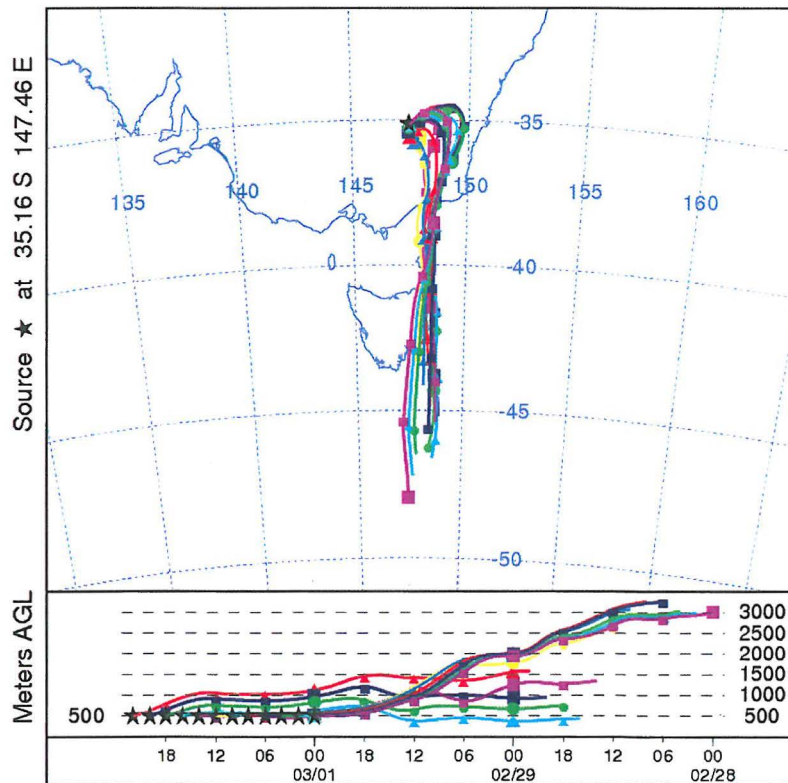
A 120 hours trajectory of Wagga Wagga February 13th at 06hrs



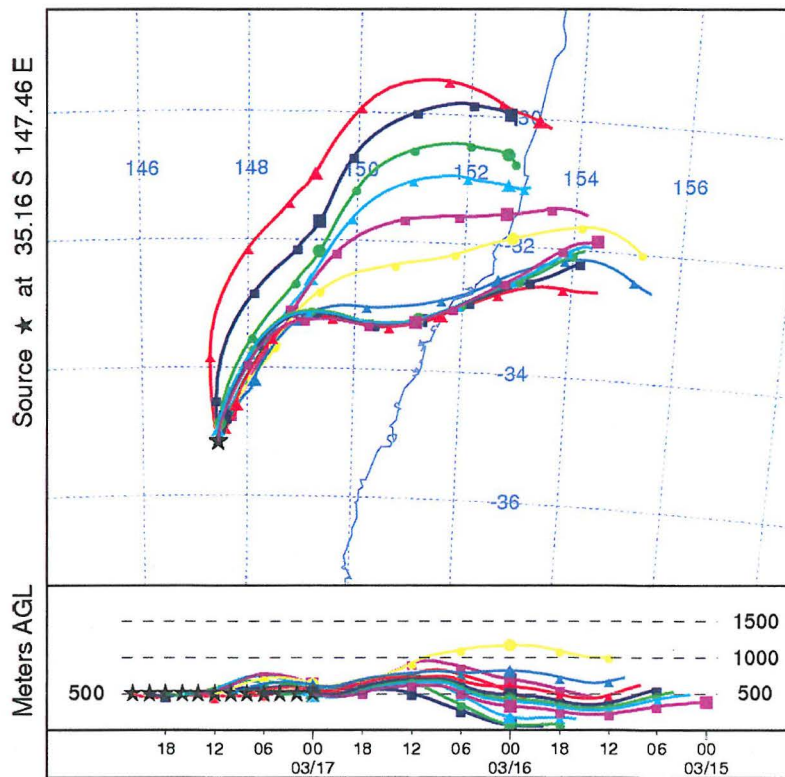
A 120 hours trajectory of Wagga Wagga February 13th at 08hrs



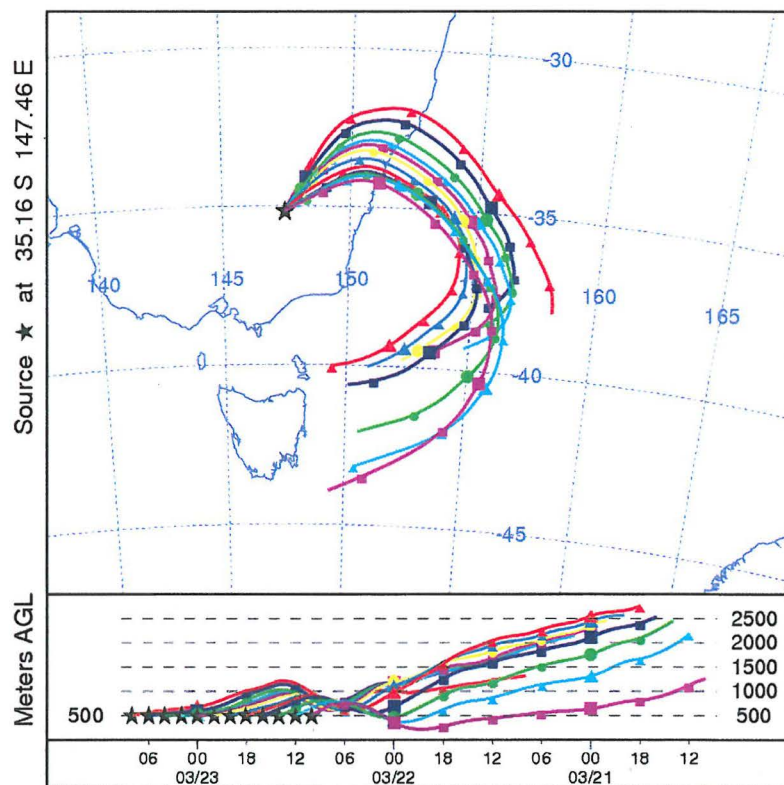
12 trajectories for Wagga Wagga February 14th



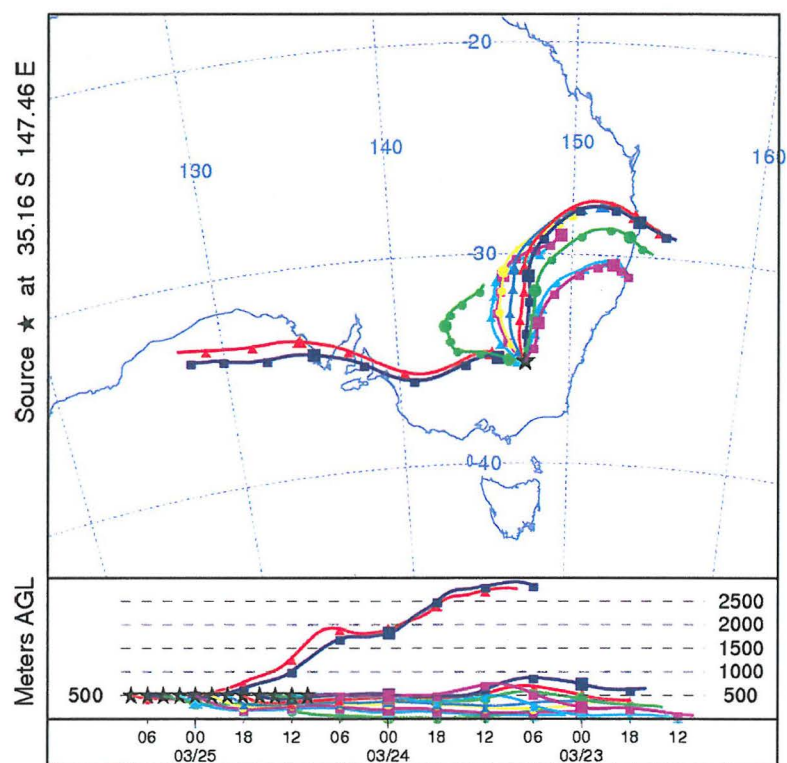
12 trajectories for Wagga Wagga March 1st



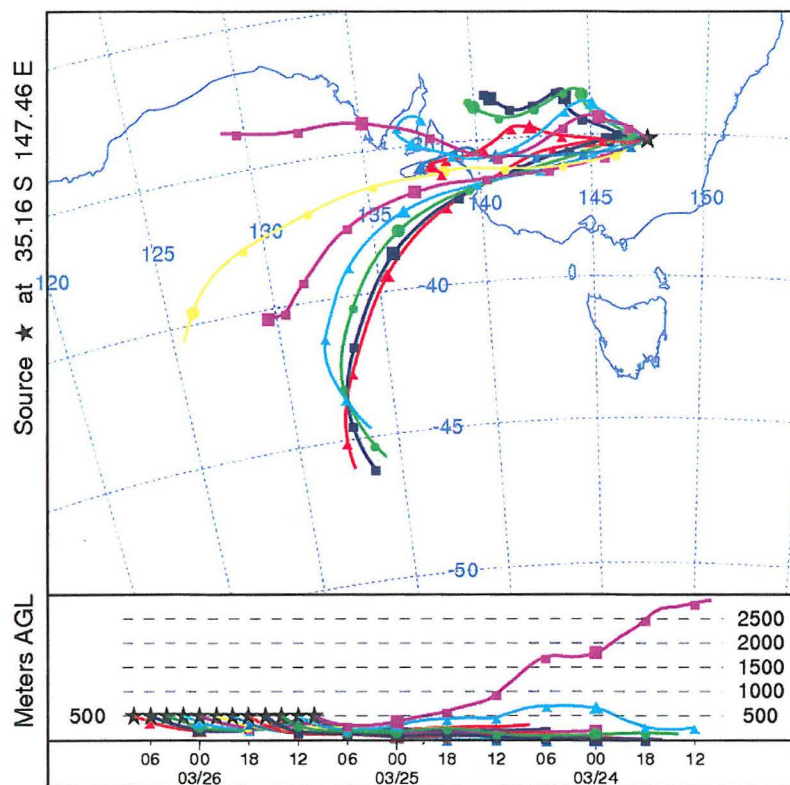
12 trajectories for Wagga Wagga March 17th



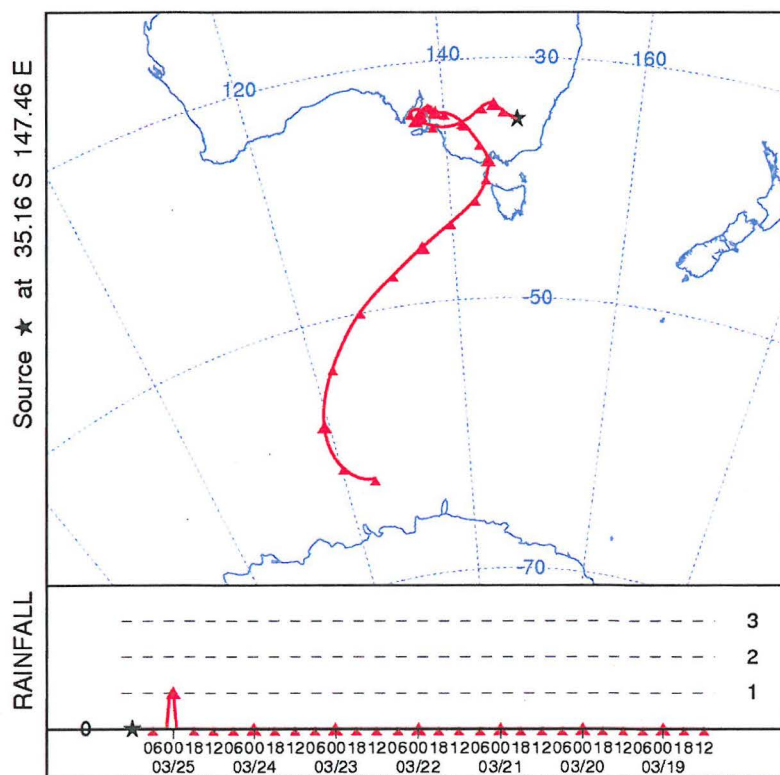
12 trajectories for Wagga Wagga March 23rd



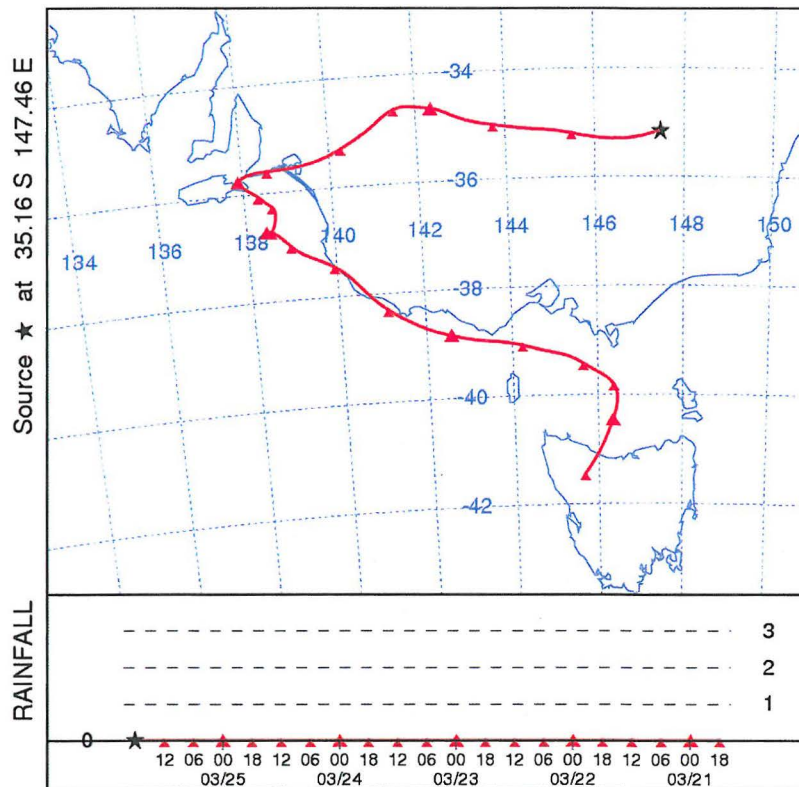
12 trajectories for Wagga Wagga March 25th



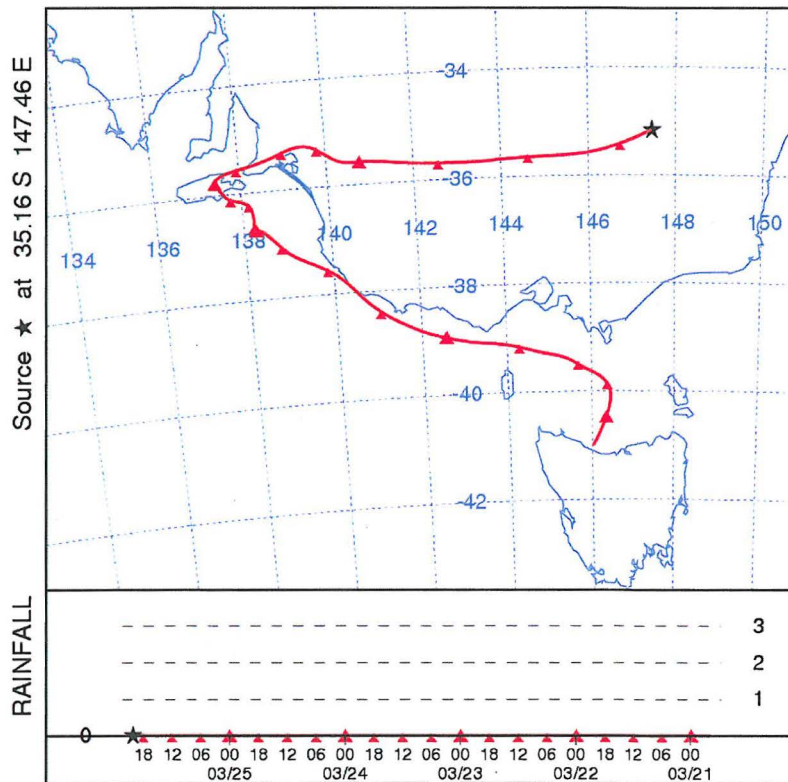
12 trajectories for Wagga Wagga March 26th



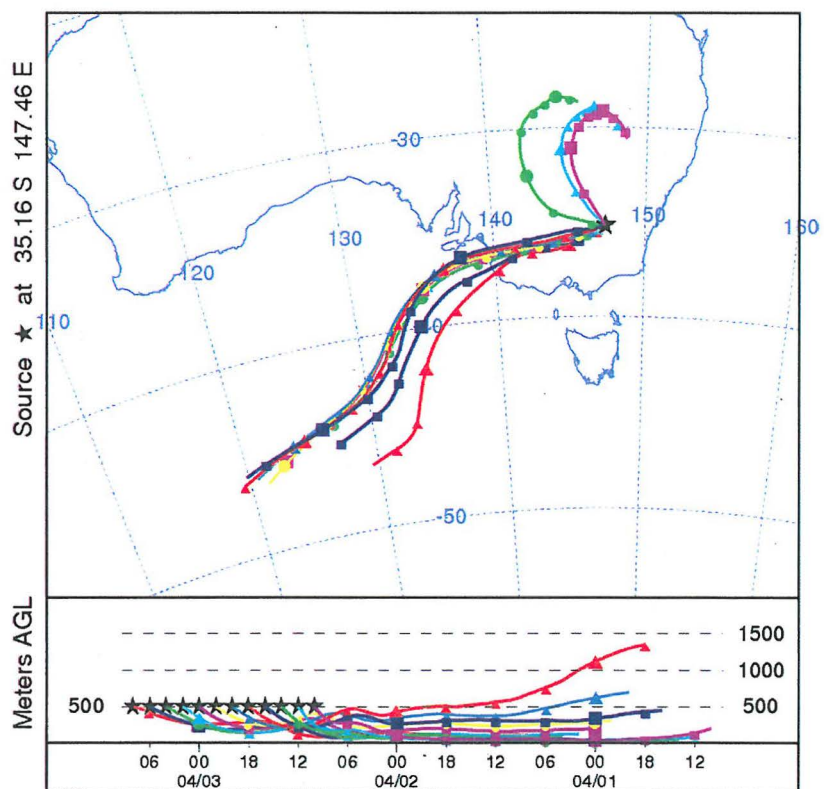
A 168 hours trajectory of Wagga Wagga March 25th at 12hrs



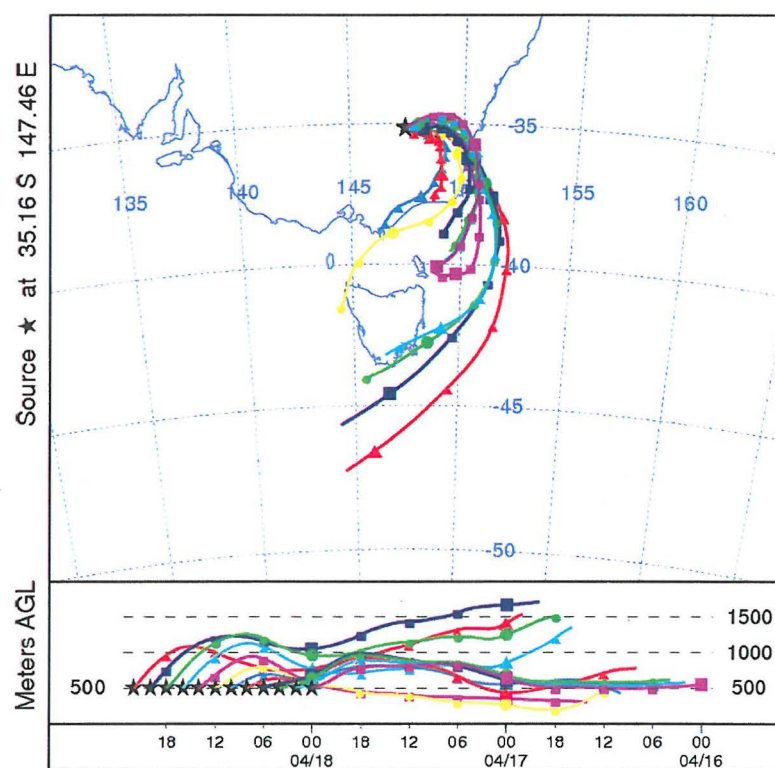
A 168 hours trajectory of Wagga Wagga March 25th at 18hrs



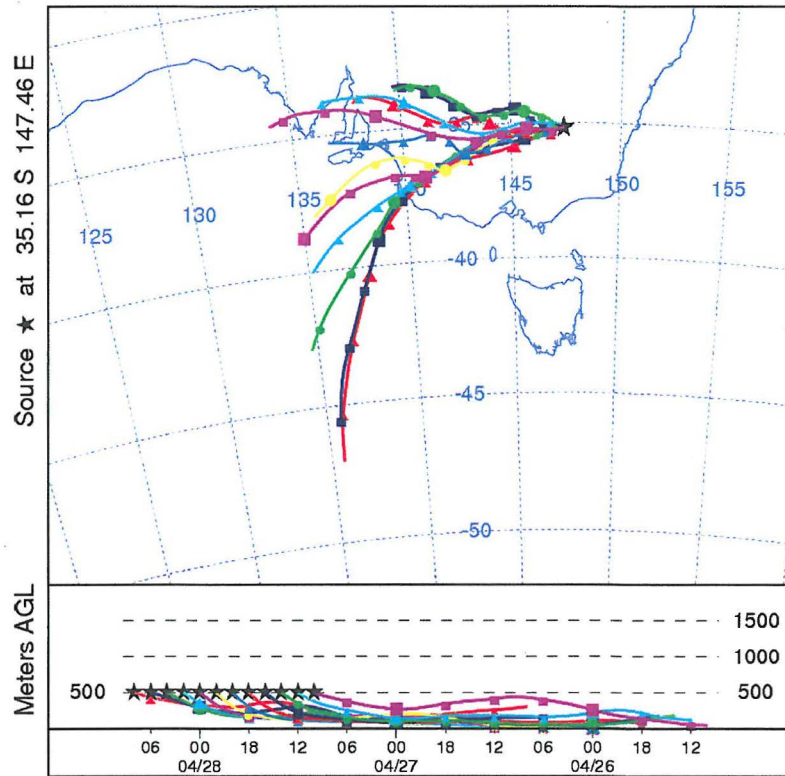
A 168 hours trajectory of Wagga Wagga March 25th at 20hrs



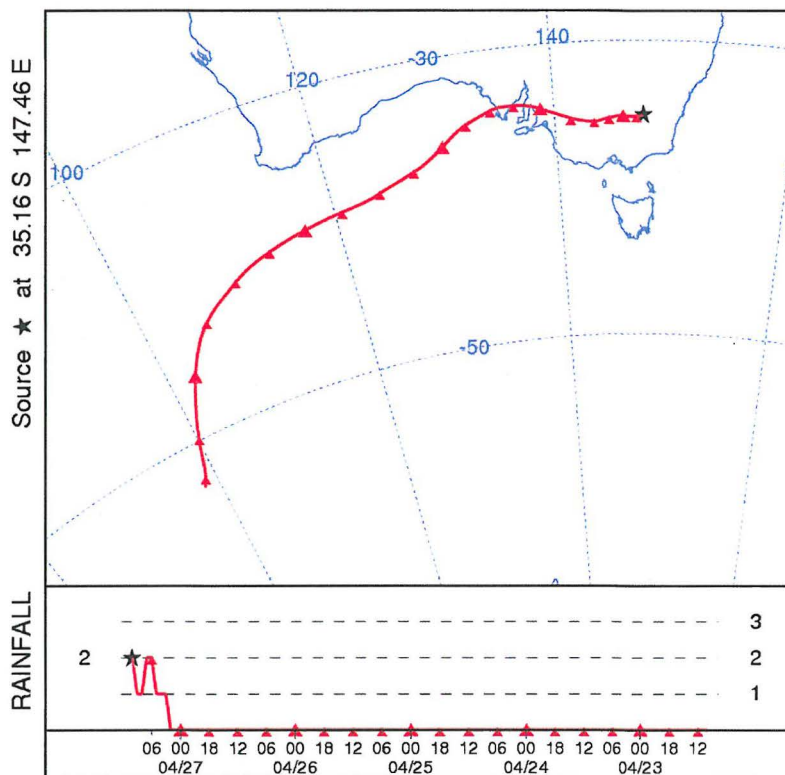
12 trajectories for Wagga Wagga April 3rd



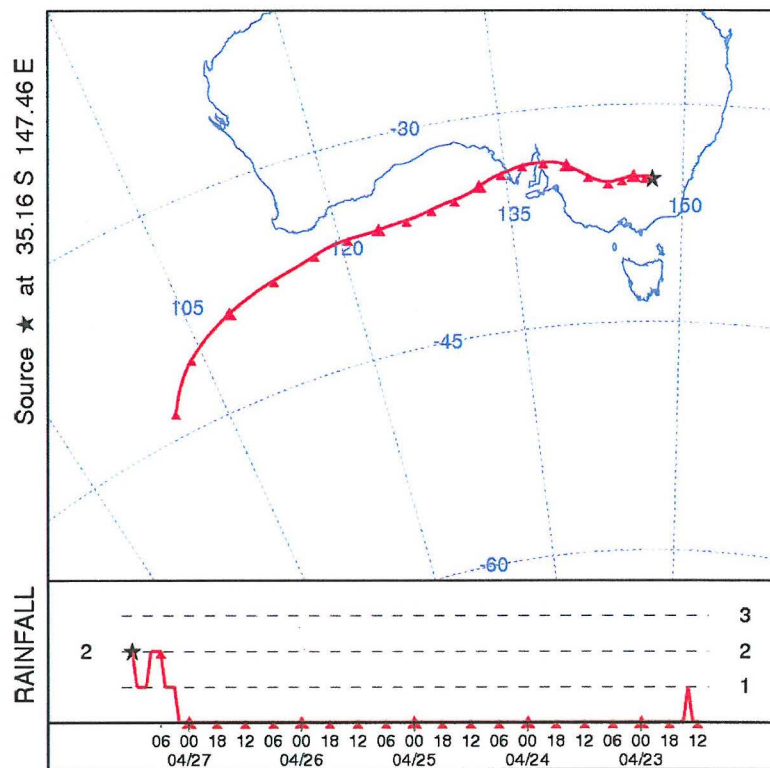
12 trajectories for Wagga Wagga April 18th



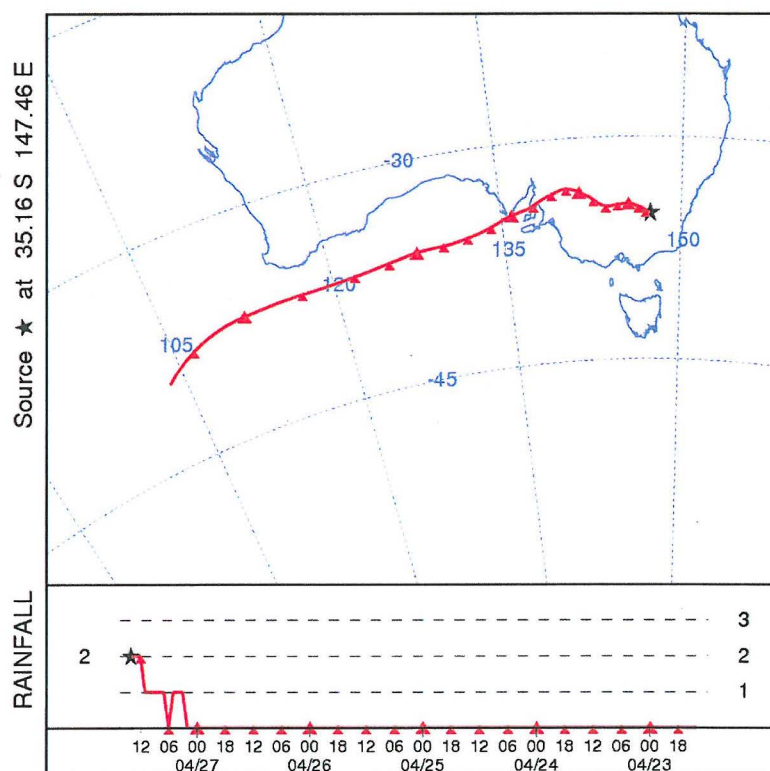
12 trajectories for Wagga Wagga April 28th



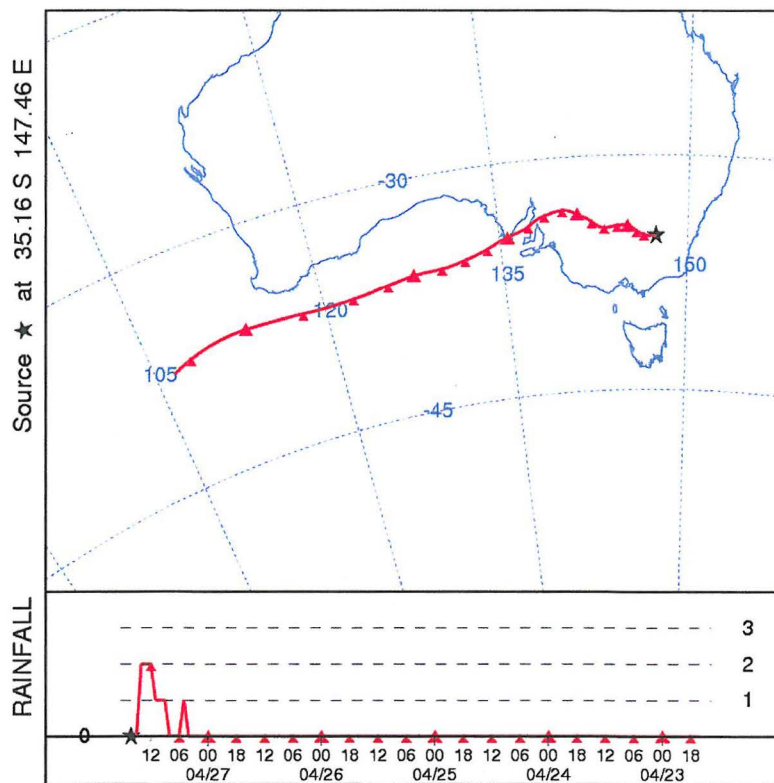
A 120 hours trajectory of Wagga Wagga April 27th at 10hrs



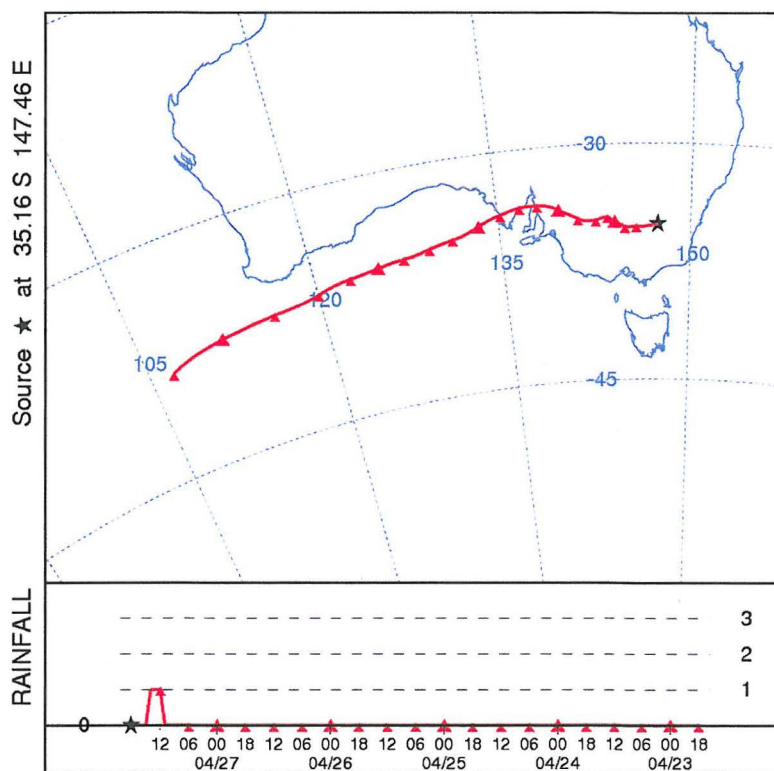
A 120 hours trajectory of Wagga Wagga April 27th at 12hrs



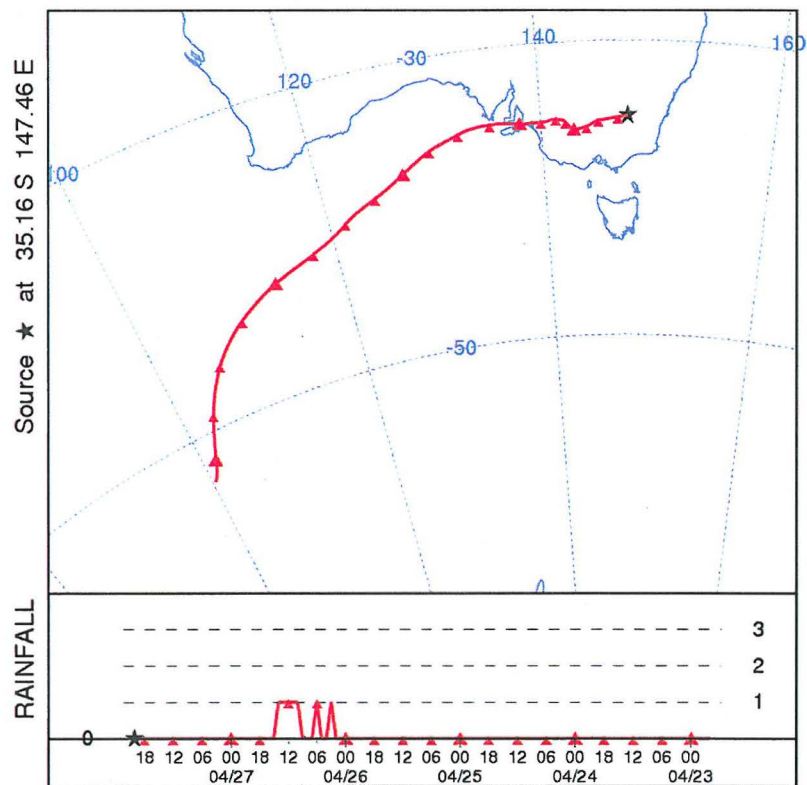
A 120 hours trajectory of Wagga Wagga April 27th at 14hrs



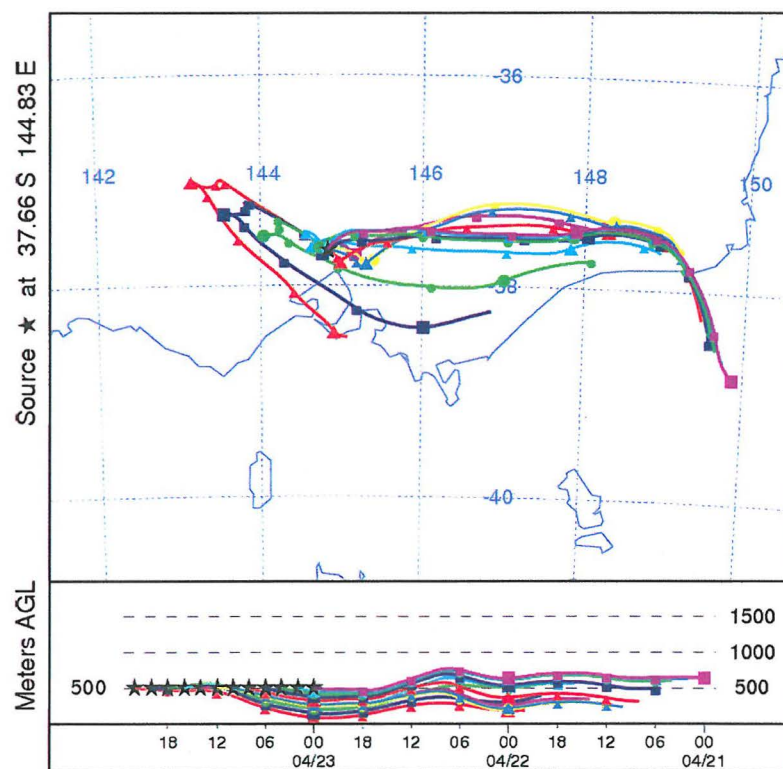
A 120 hours trajectory of Wagga Wagga April 27th at 16hrs



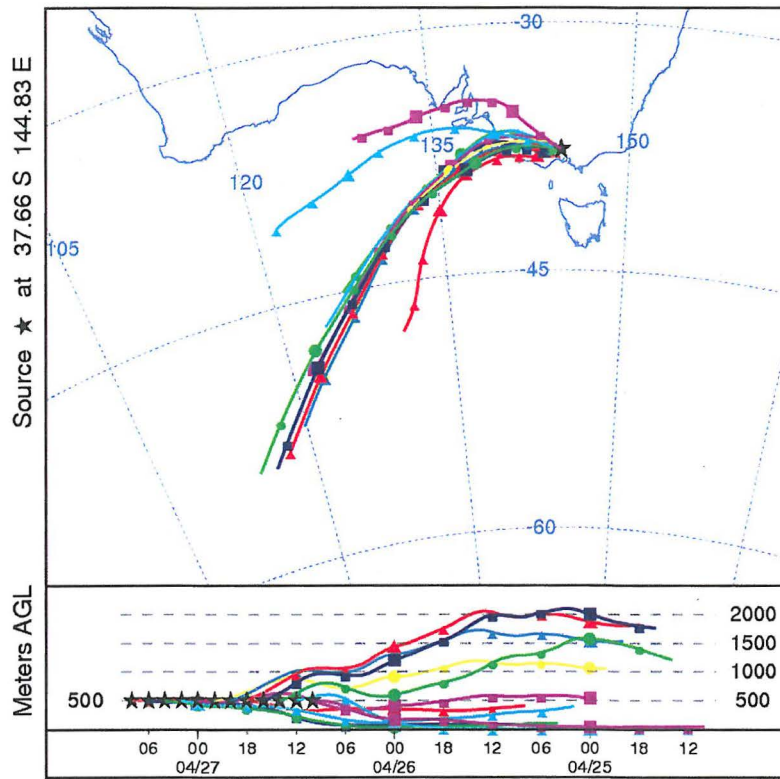
A 120 hours trajectory of Wagga Wagga April 27th at 18hrs



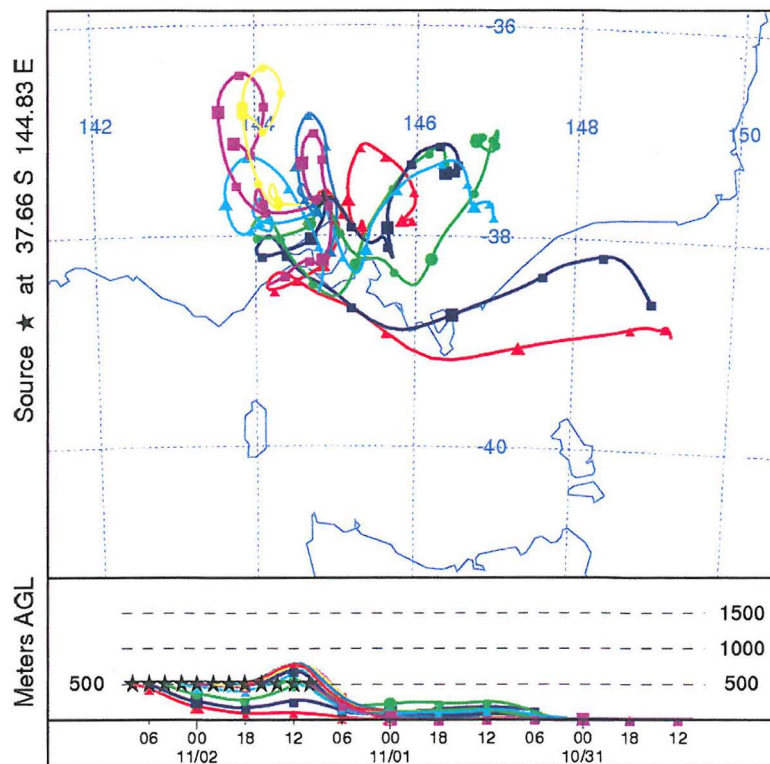
A 120 hours trajectory of Wagga Wagga April 27th at 20hrs



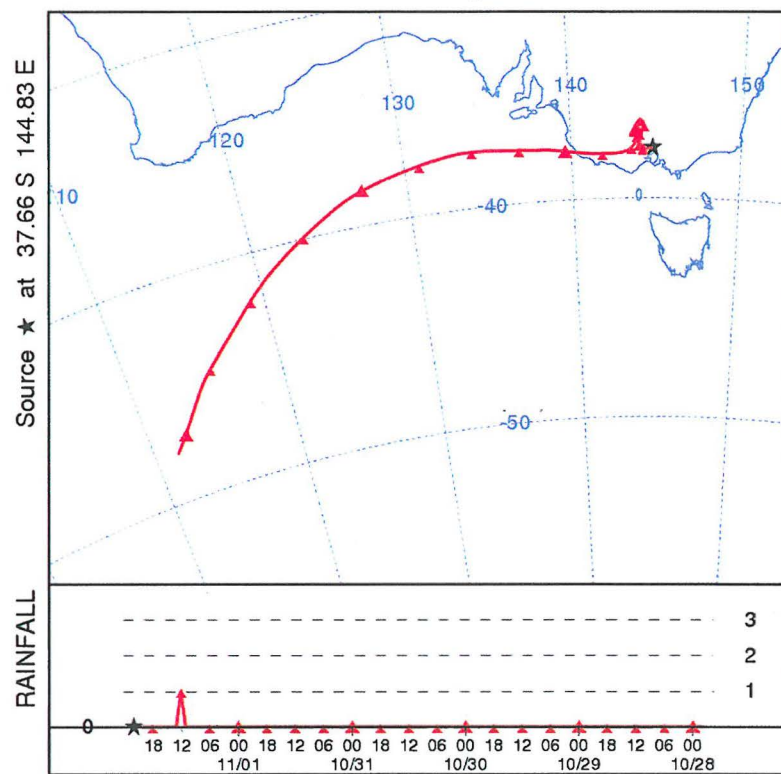
12 trajectories for Melbourne April 23rd



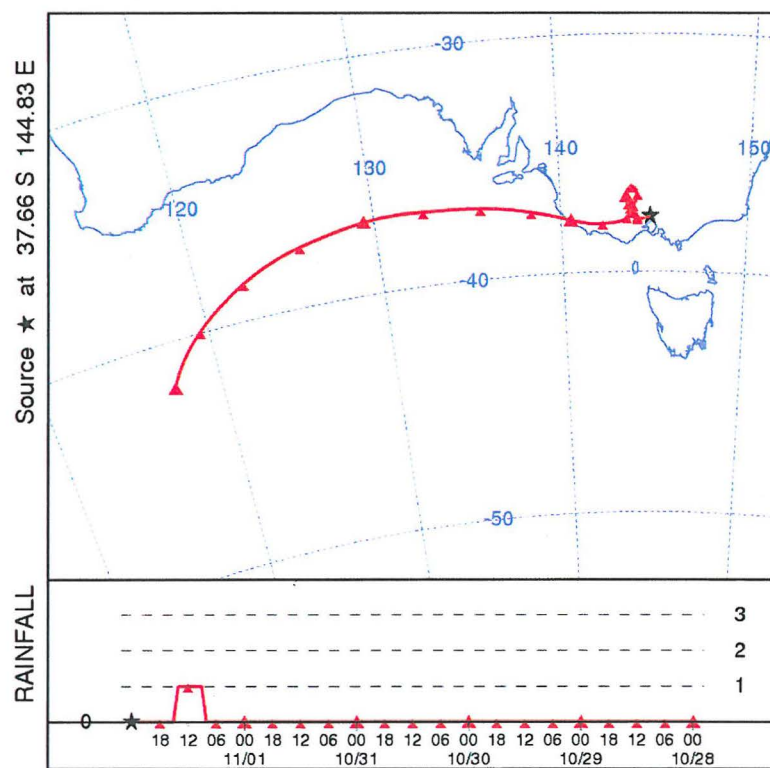
12 trajectories for Melbourne April 27th



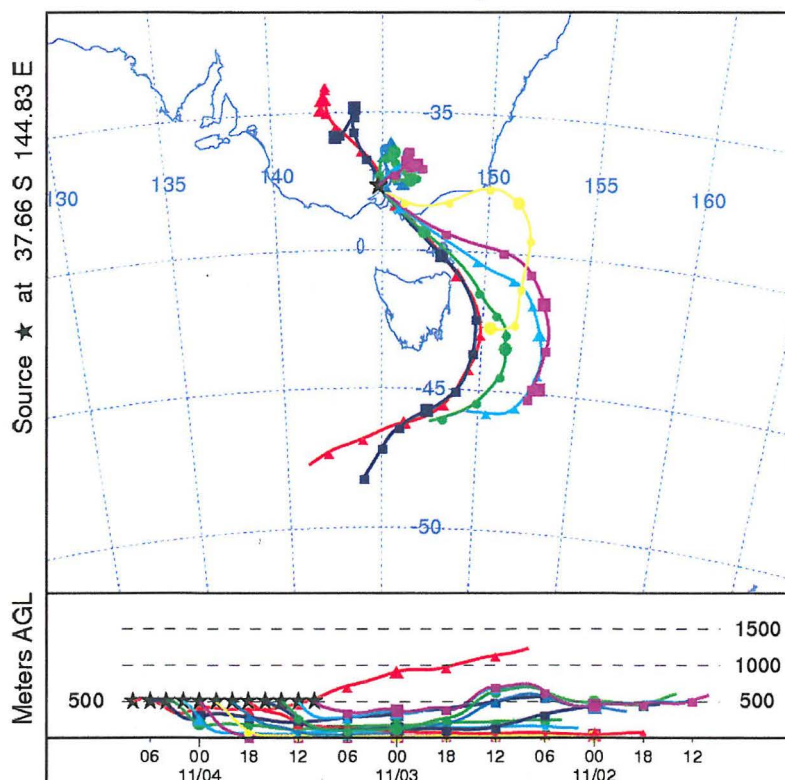
12 trajectories for Melbourne November 2nd



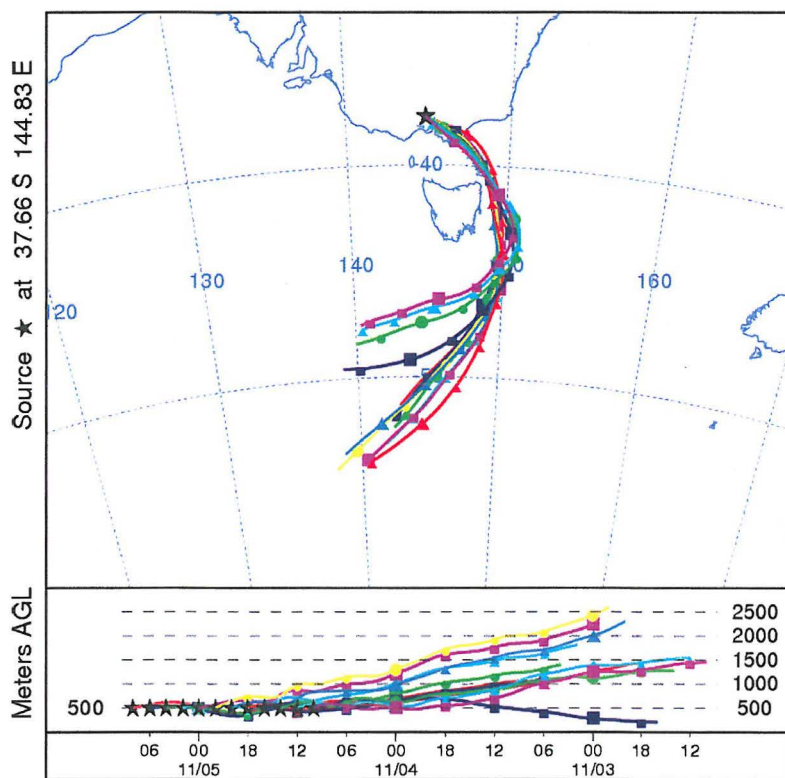
A 120 hours trajectory of Melbourne November 1st at 22hrs



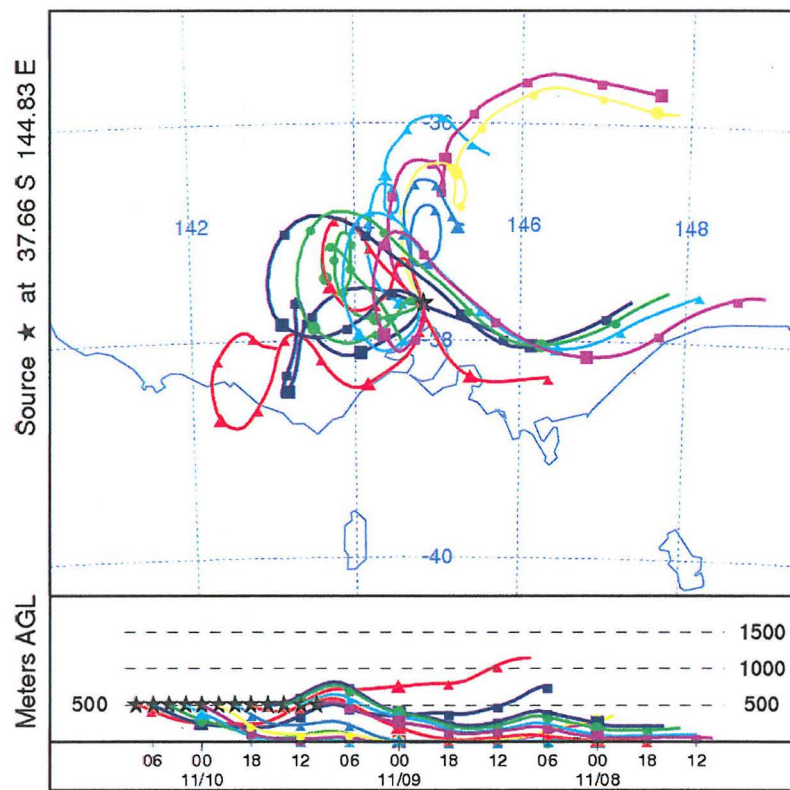
A 120 hours trajectory of Melbourne November 2nd at 00hrs



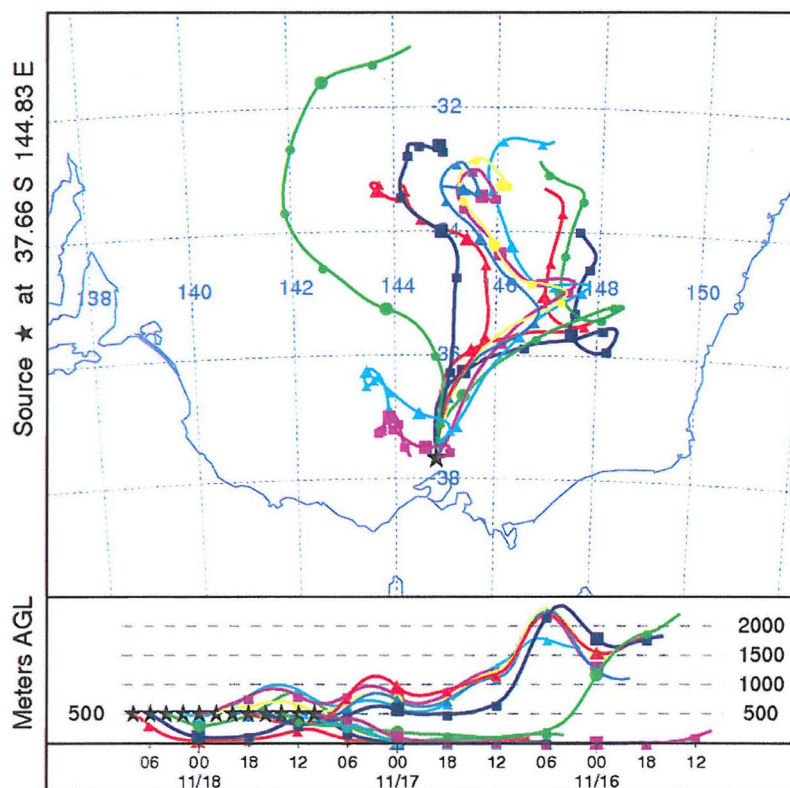
12 trajectories for Melbourne November 4th



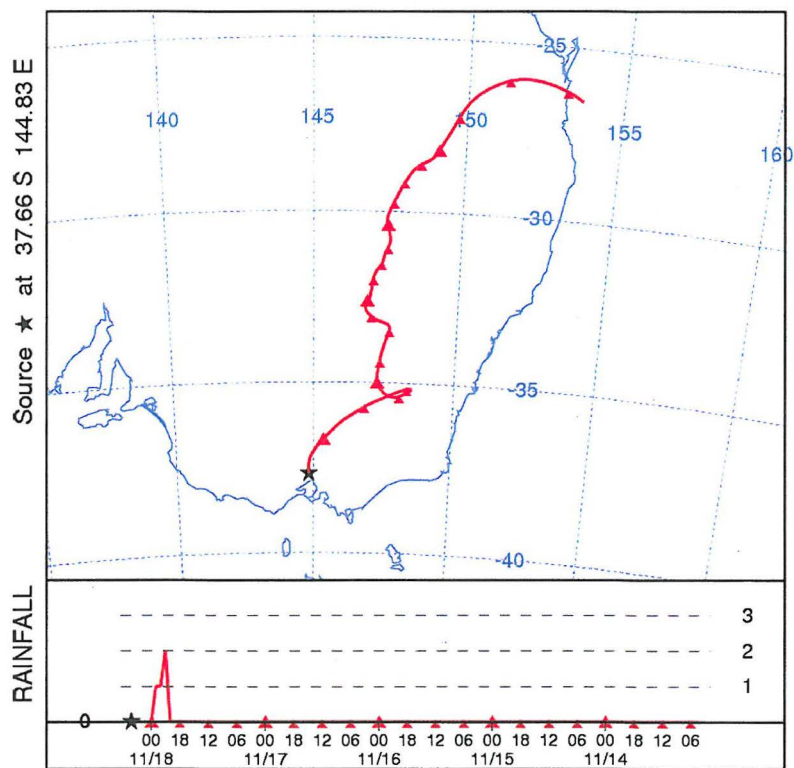
12 trajectories for Melbourne November 5th



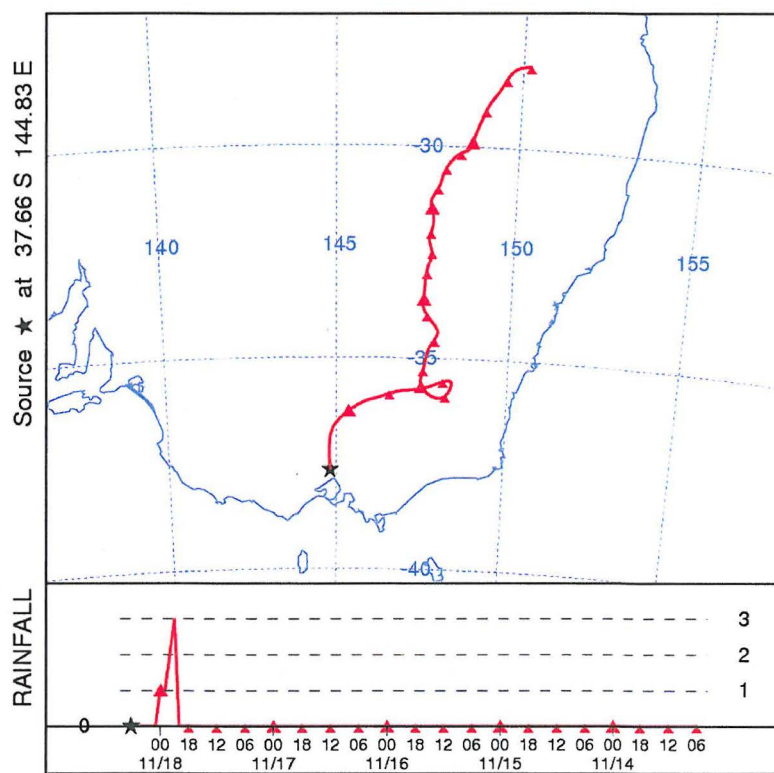
12 trajectories for Melbourne November 10th



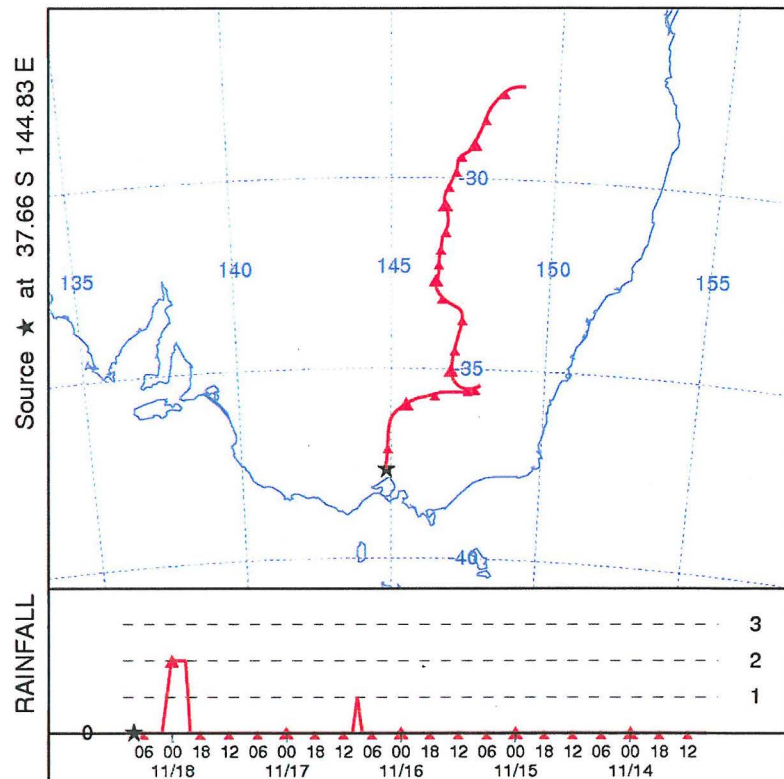
12 trajectories of Melbourne November 18th



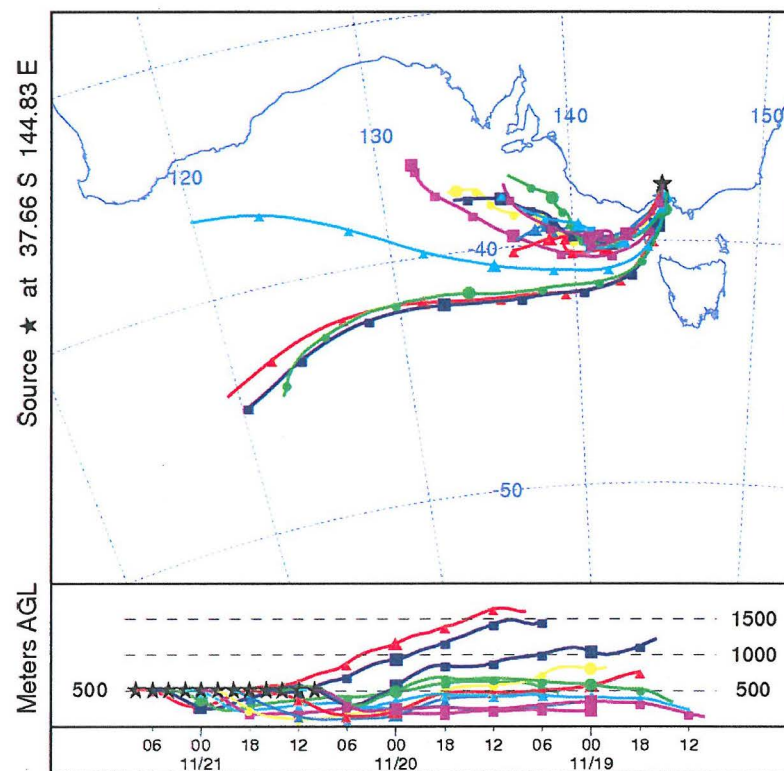
A 120 hours trajectory of Melbourne November 18th at 04hrs



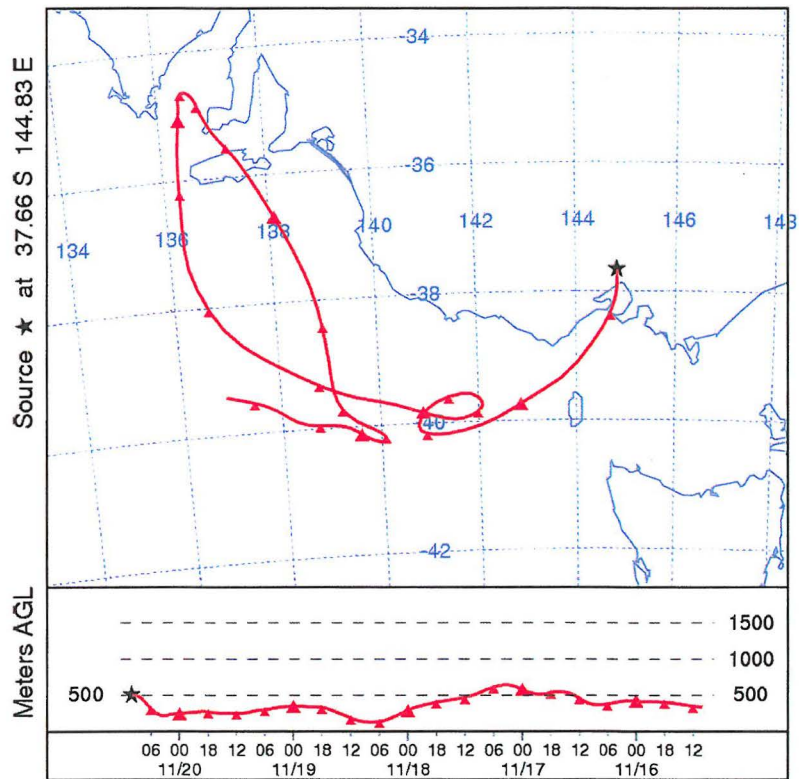
A 120 hours trajectory of Melbourne November 18th at 06hrs



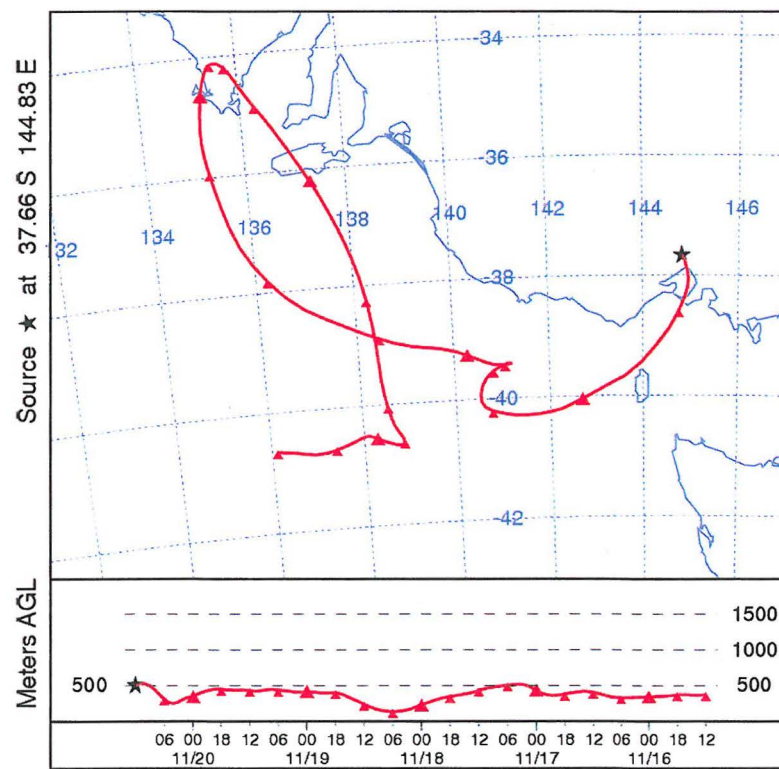
A 120 hours trajectory of Melbourne November 18th at 08 hrs



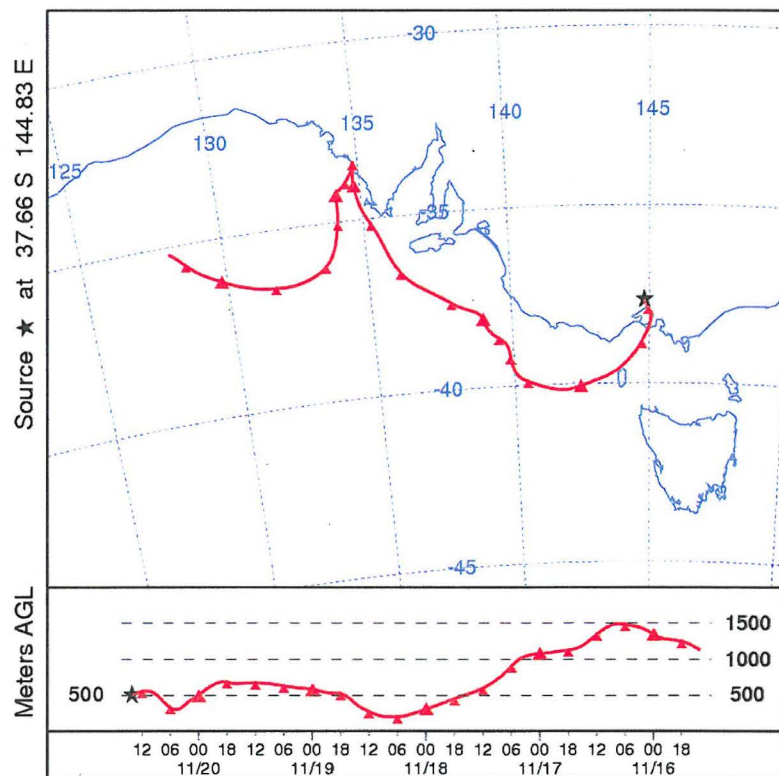
12 trajectories of Melbourne November 21st



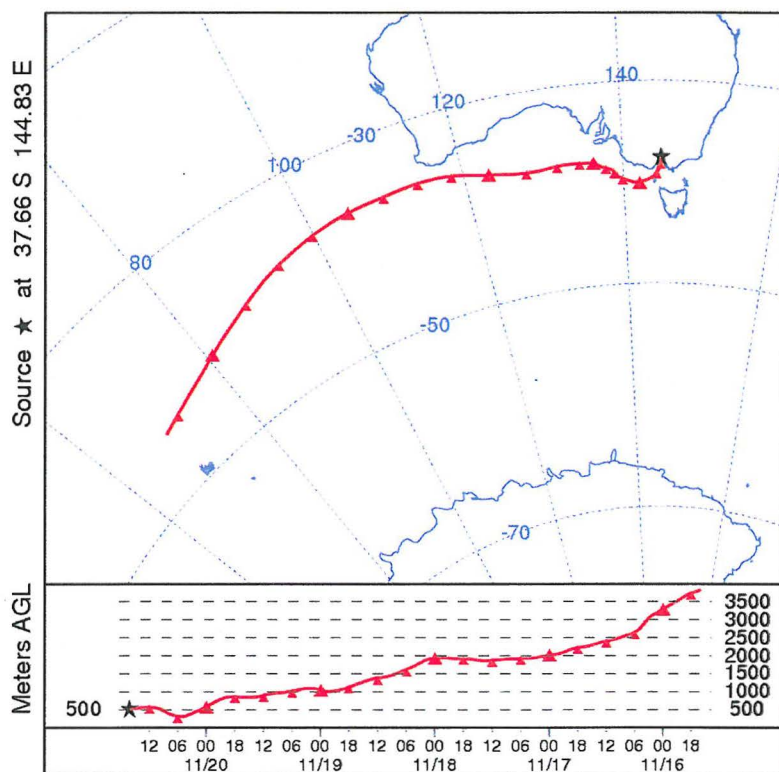
A 120 hours trajectory of Melbourne November 20th at 10hrs



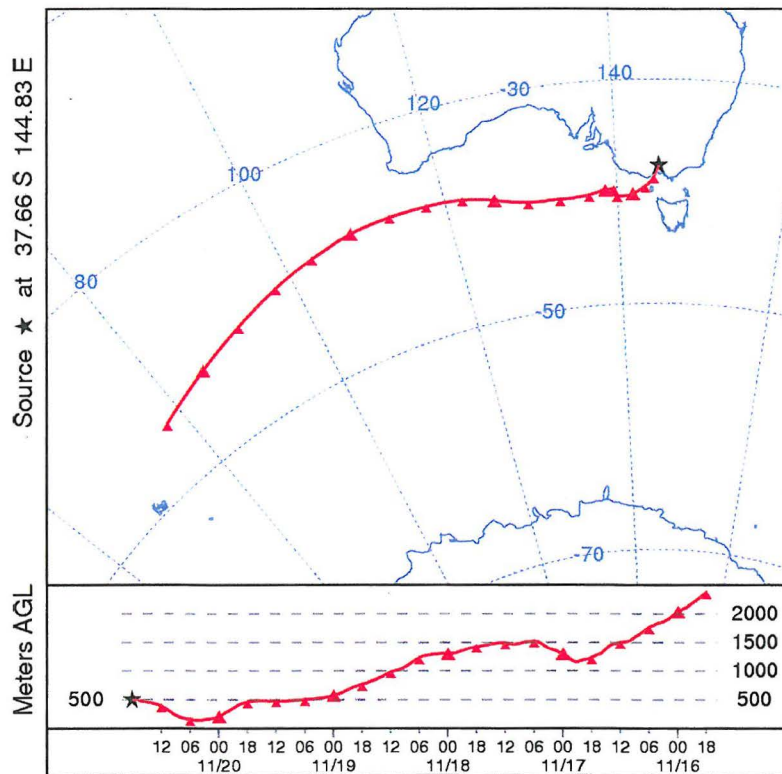
A 120 hours trajectory of Melbourne November 20th at 12hrs



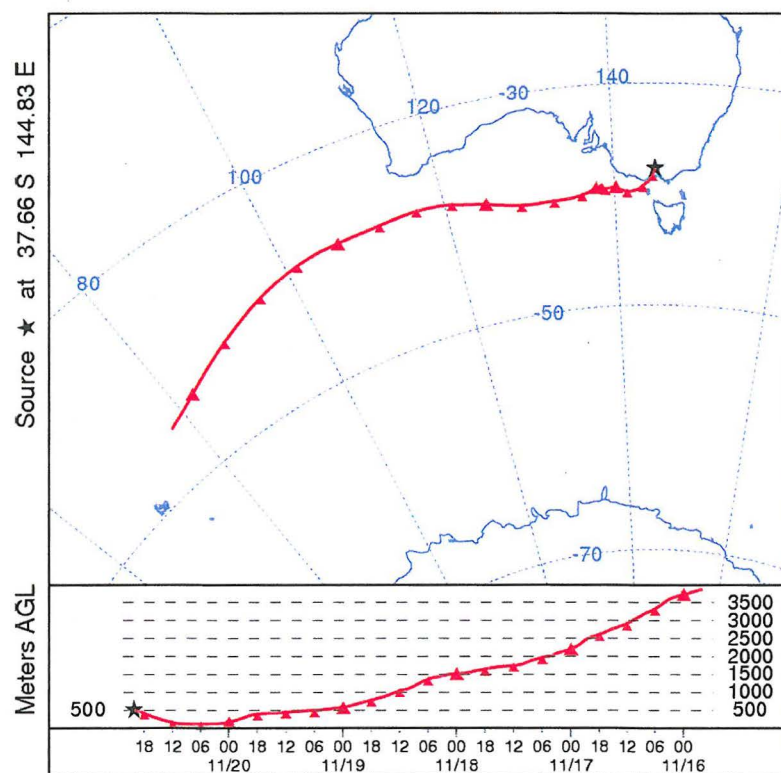
A 120 hours trajectory of Melbourne November 20th at 14hrs



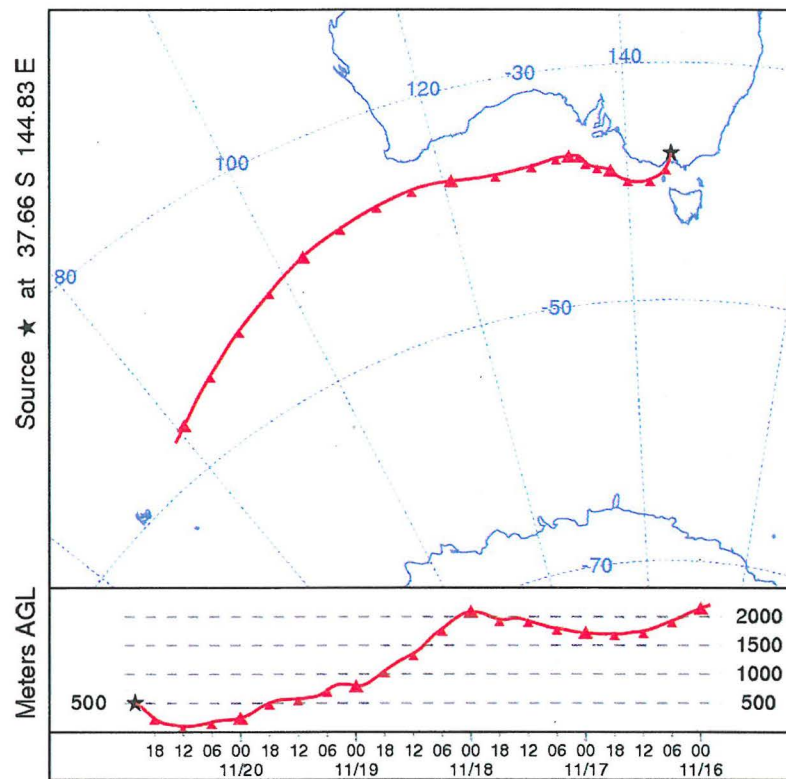
A 120 hours trajectory of Melbourne November 20th at 16hrs



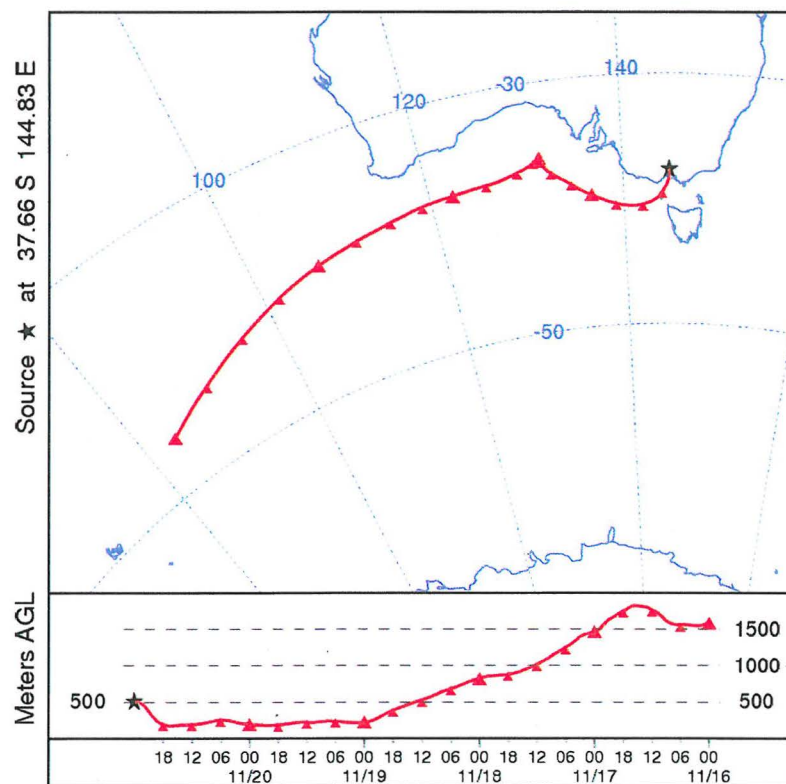
A 120 hours trajectory of Melbourne November 20th at 18hrs



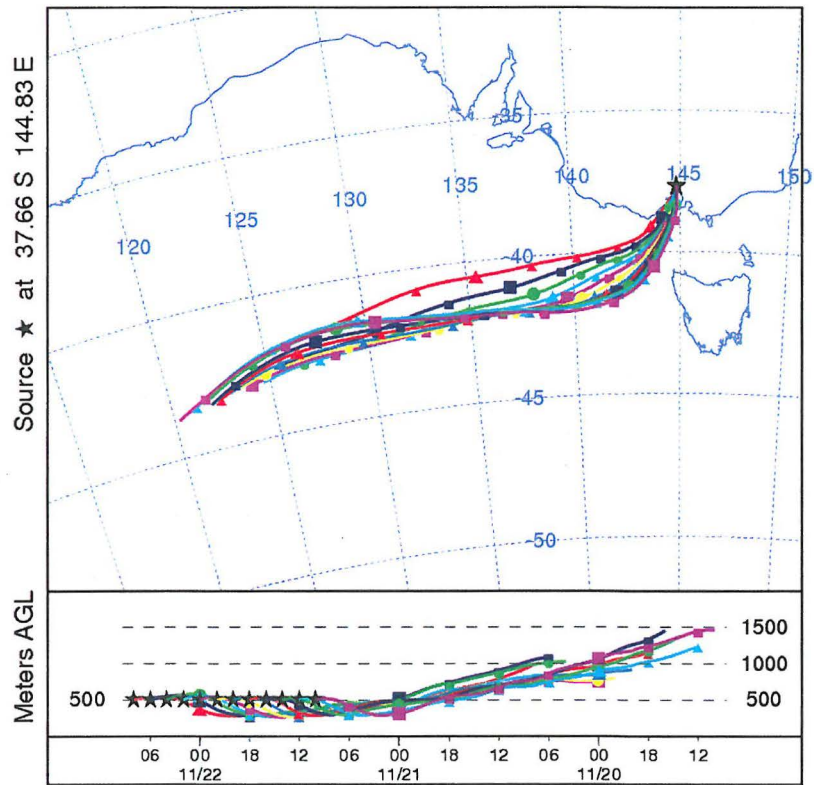
A 120 hours trajectory of Melbourne November 20th at 20hrs



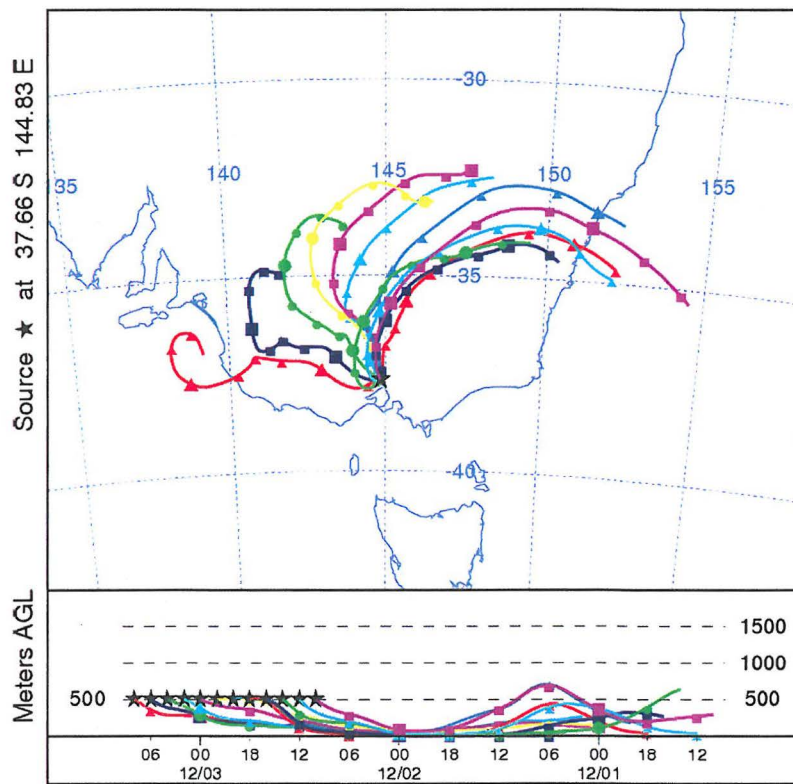
A 120 hours trajectory of Melbourne November 20th at 22hrs



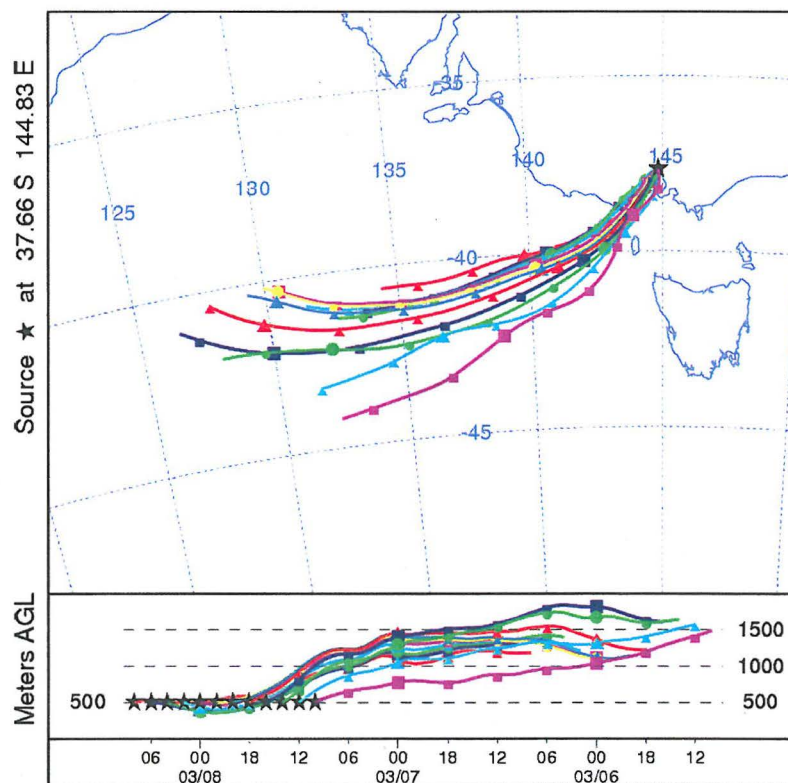
A 120 hours trajectory of Melbourne November 21st at 00hrs



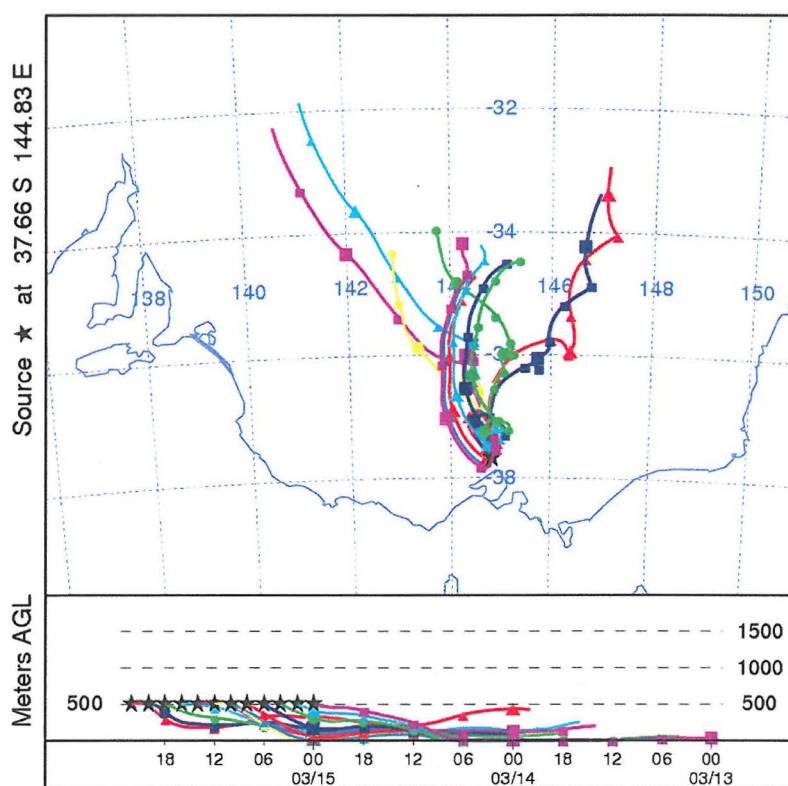
12 trajectories of Melbourne November 22nd



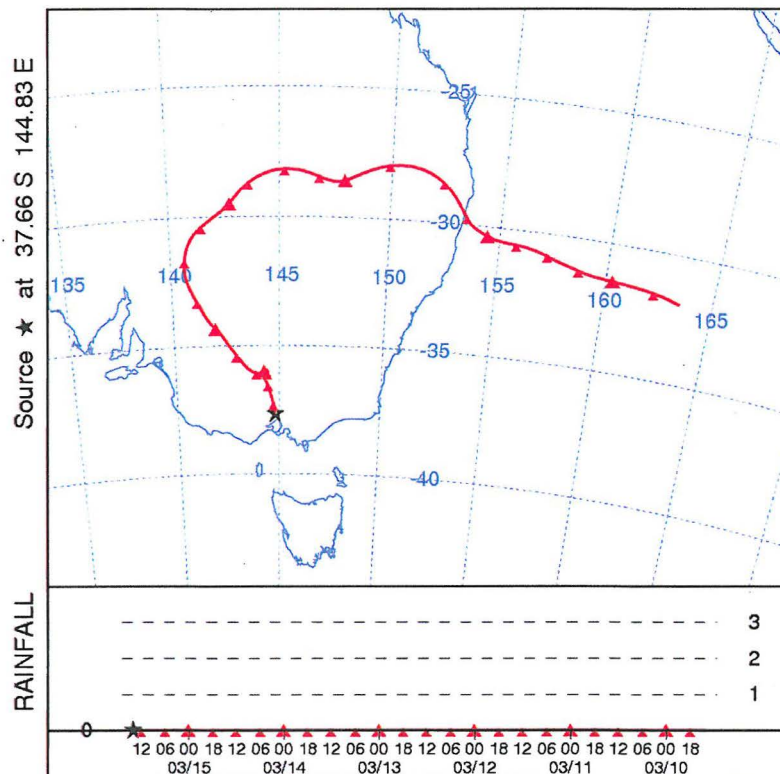
12 trajectories of Melbourne December 3rd



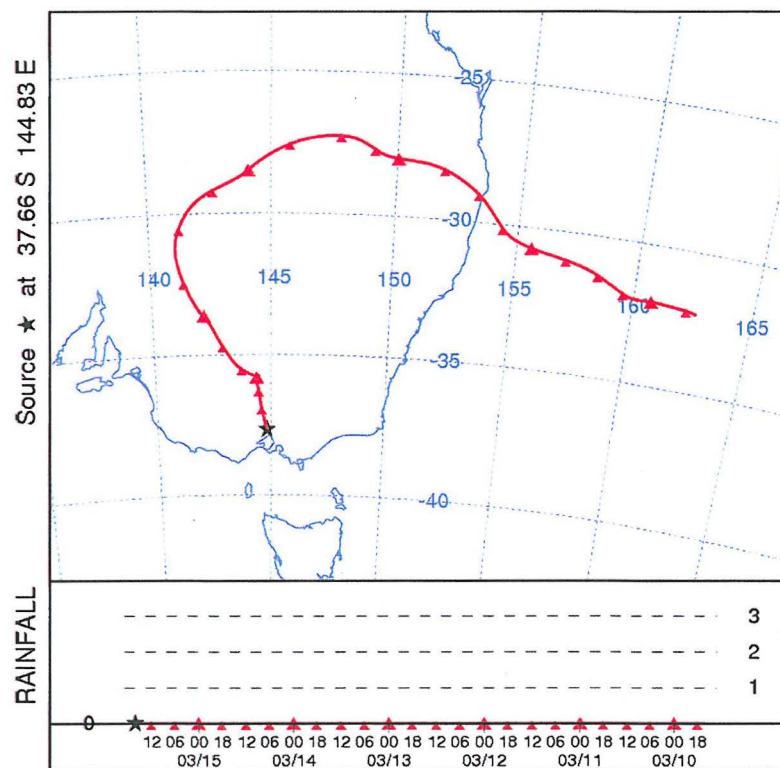
12 trajectories of Melbourne March 8th



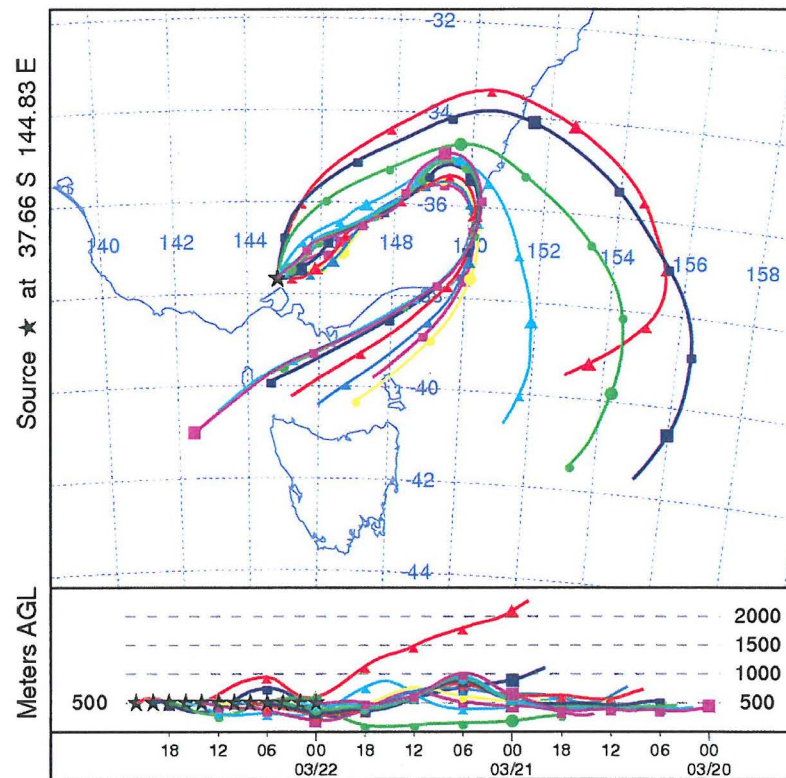
12 trajectories of Melbourne March 15th



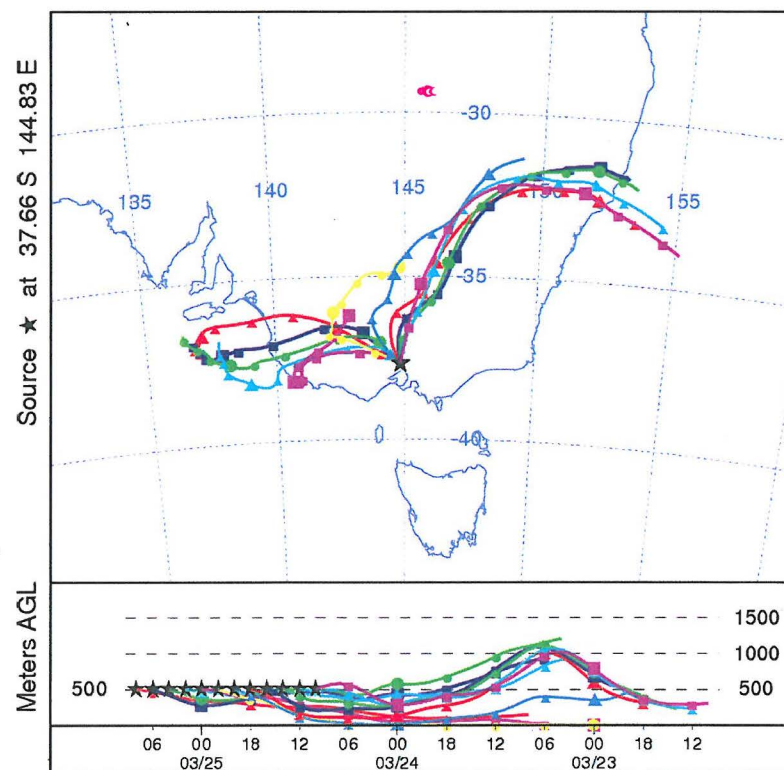
A 144 hours trajectory of Melbourne March 15th at 14hrs



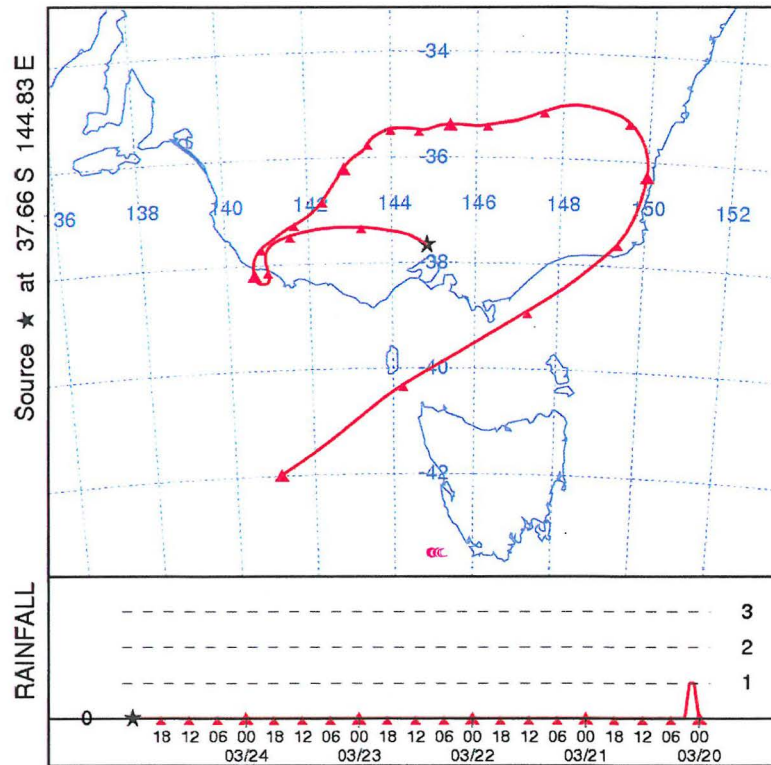
A 144 hours trajectory of Melbourne March 15th at 16hrs



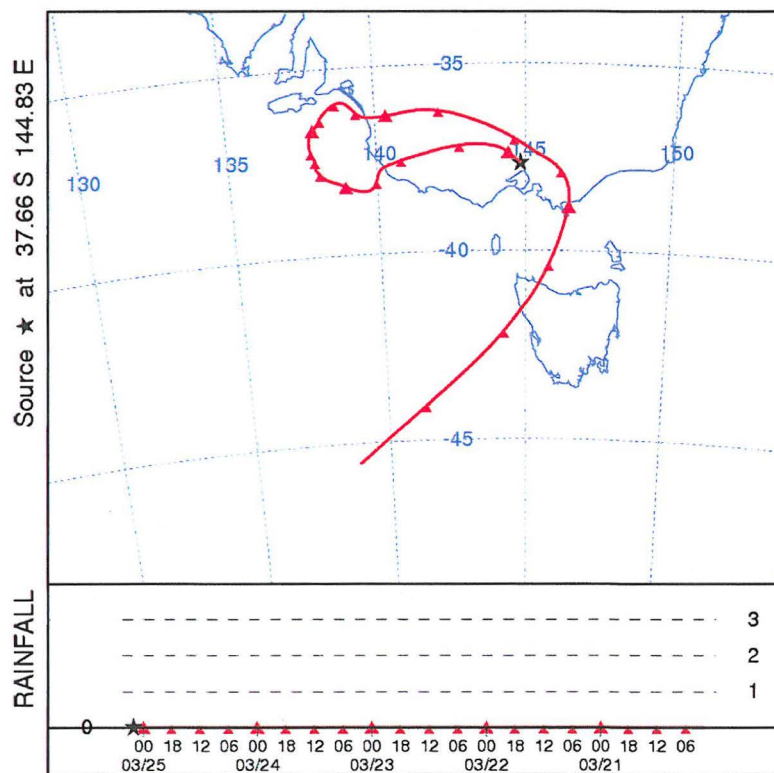
12 trajectories of Melbourne March 22nd



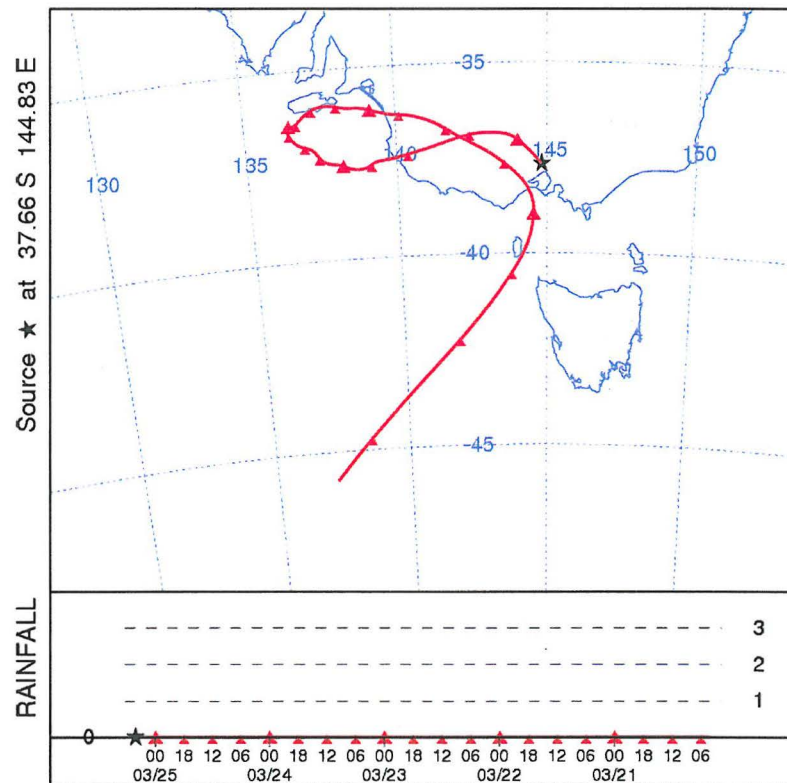
12 trajectories of Melbourne March 25th



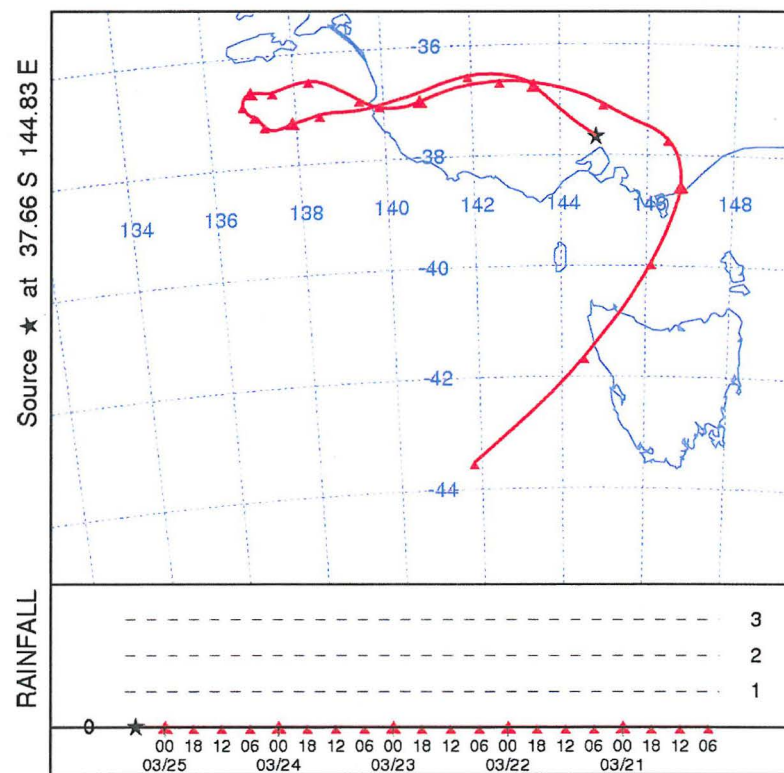
A 120 hours trajectory of Melbourne March 25th at 00hrs



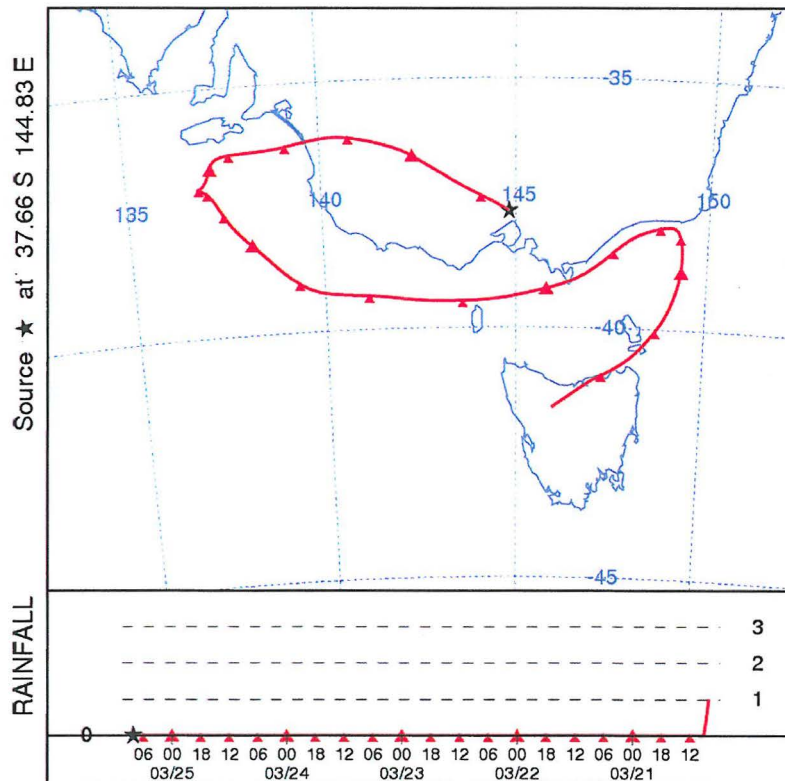
A 120 hours trajectory of Melbourne March 25th at 02hrs



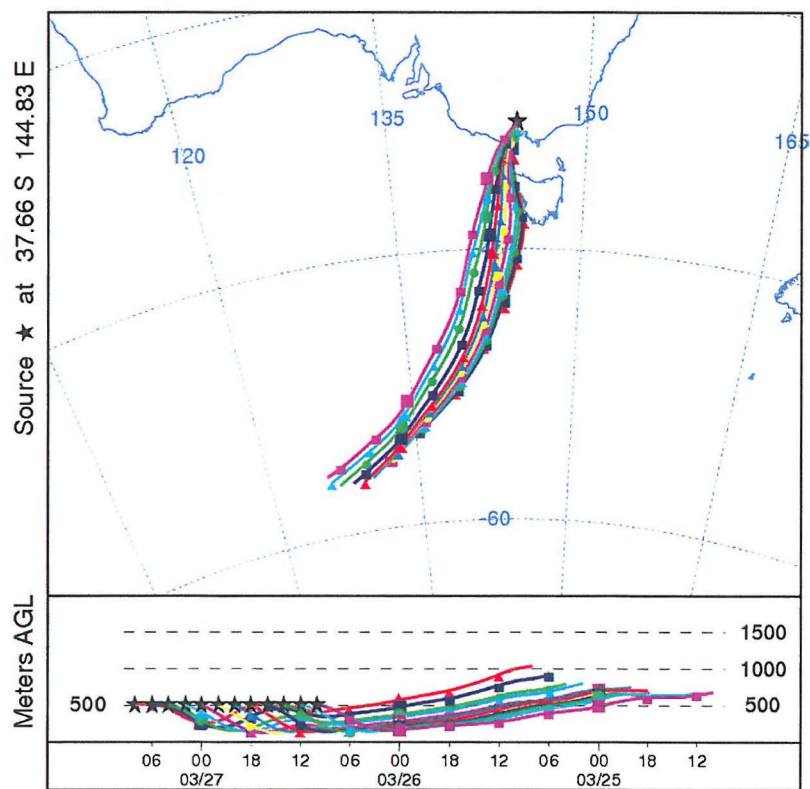
A 120 hours trajectory of Melbourne March 25th at 04hrs



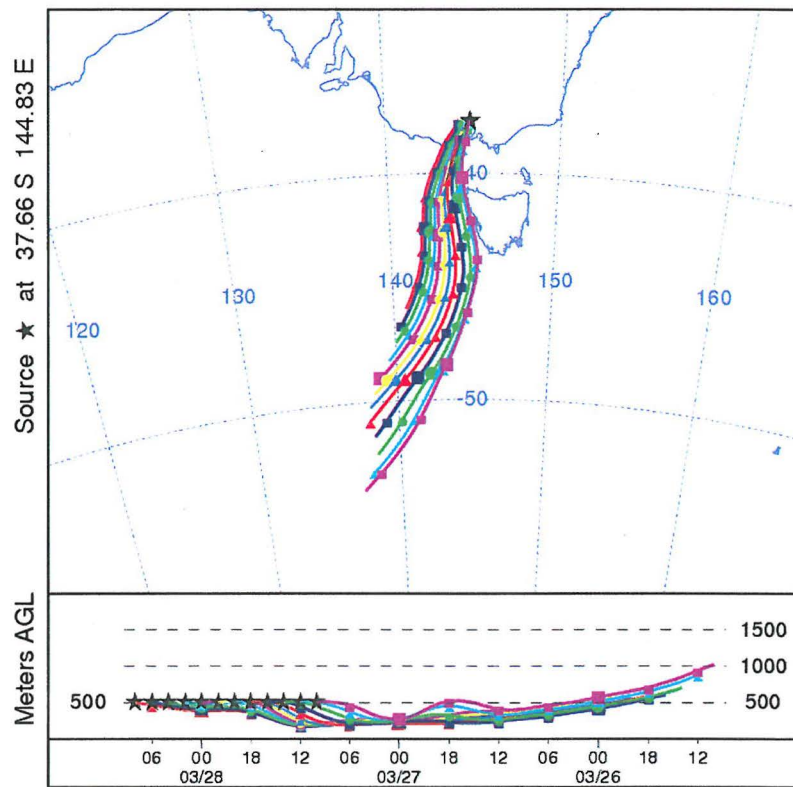
A 120 hours trajectory of Melbourne March 25th at 06hrs



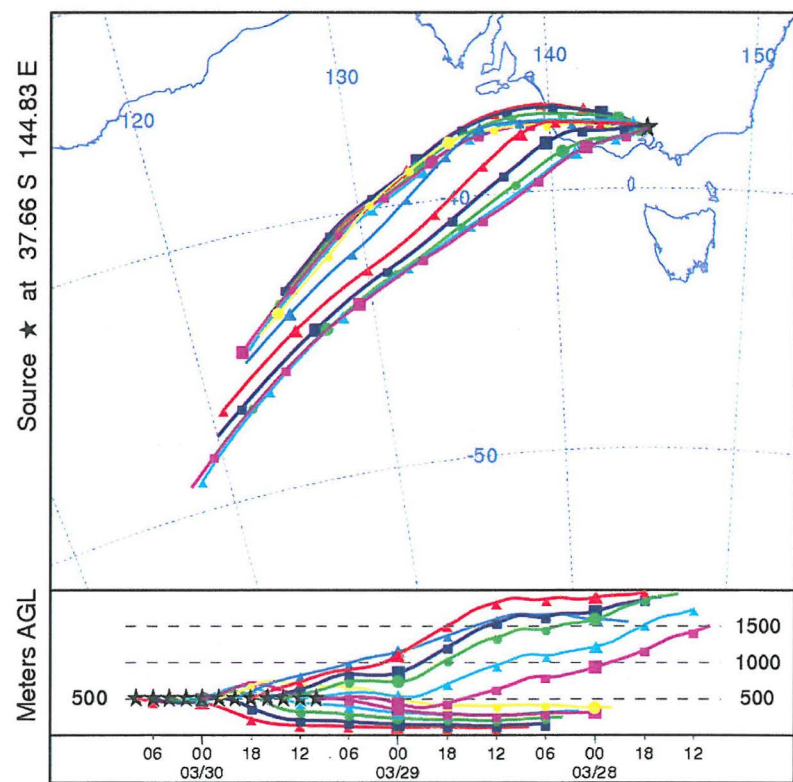
A 120 hours trajectory of Melbourne March 25th at 08hrs



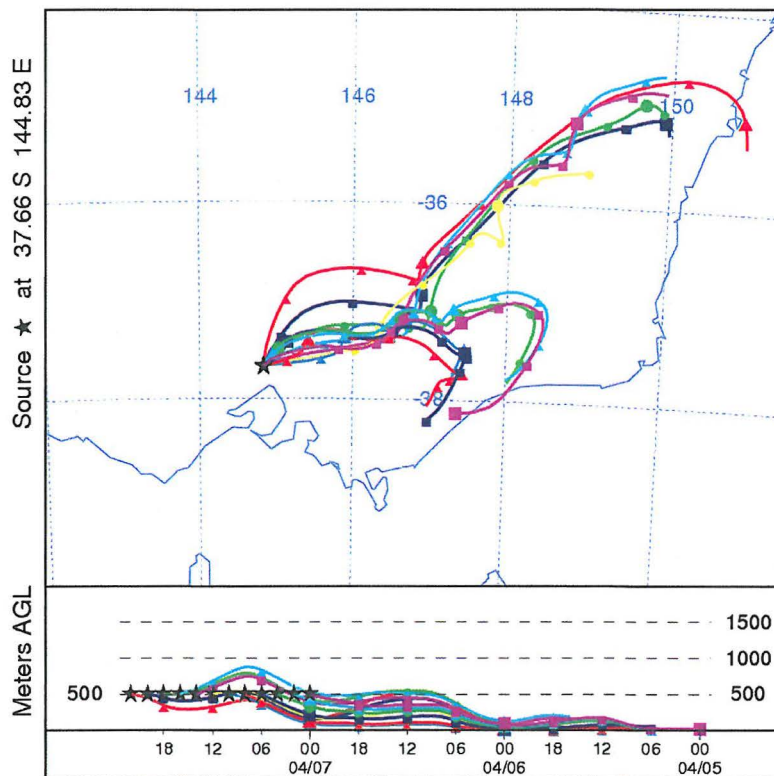
12 trajectories of Melbourne March 27th



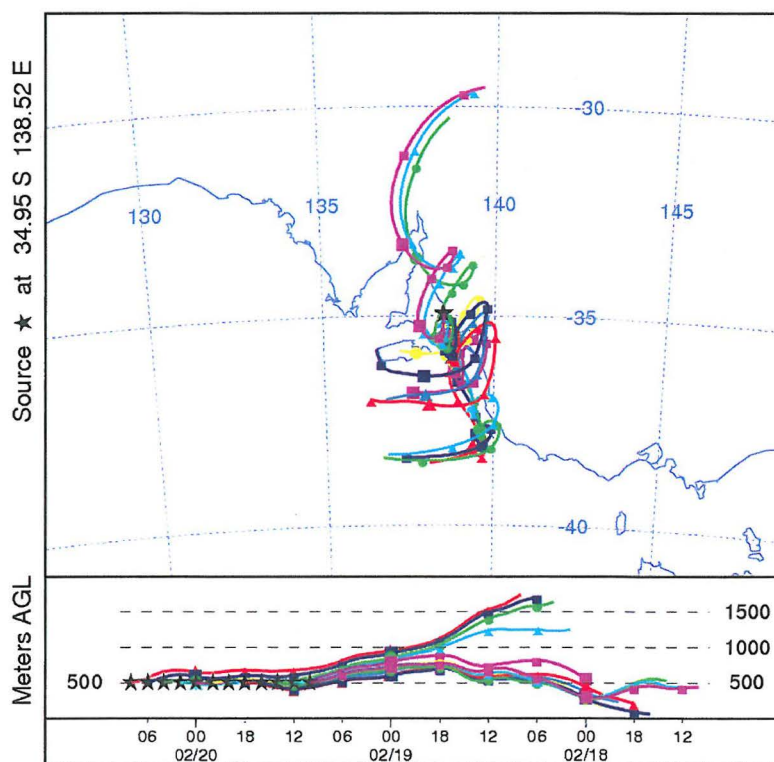
12 trajectories of Melbourne March 28th



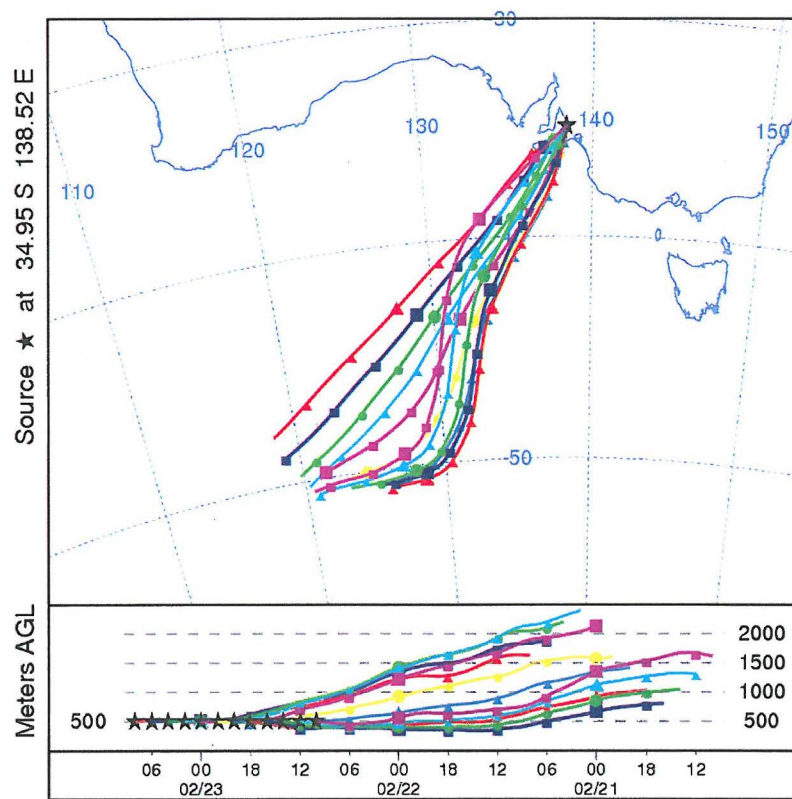
12 trajectories of Melbourne March 30th



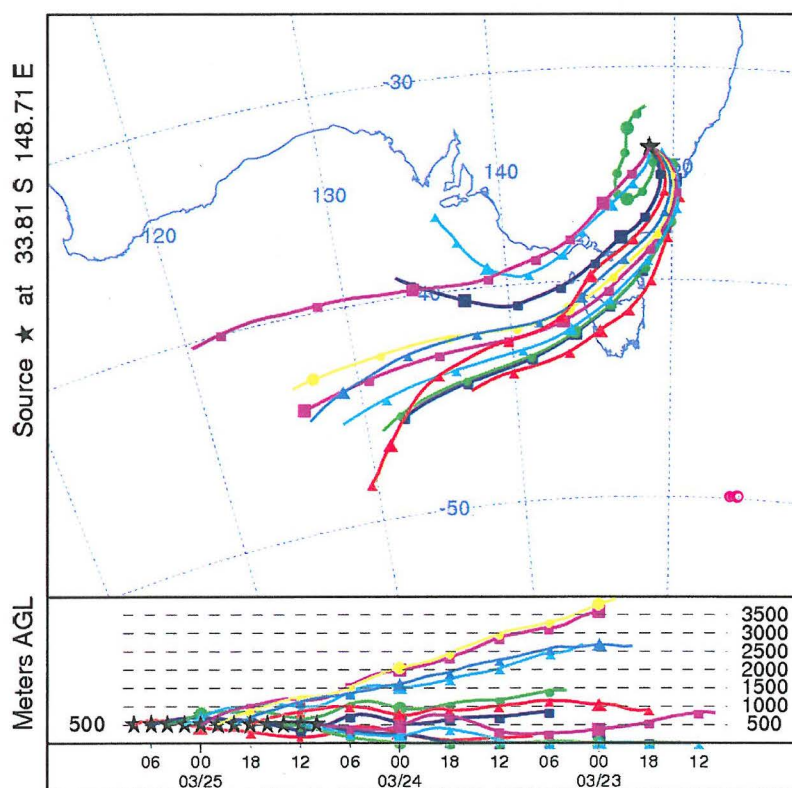
12 trajectories for Melbourne April 7th



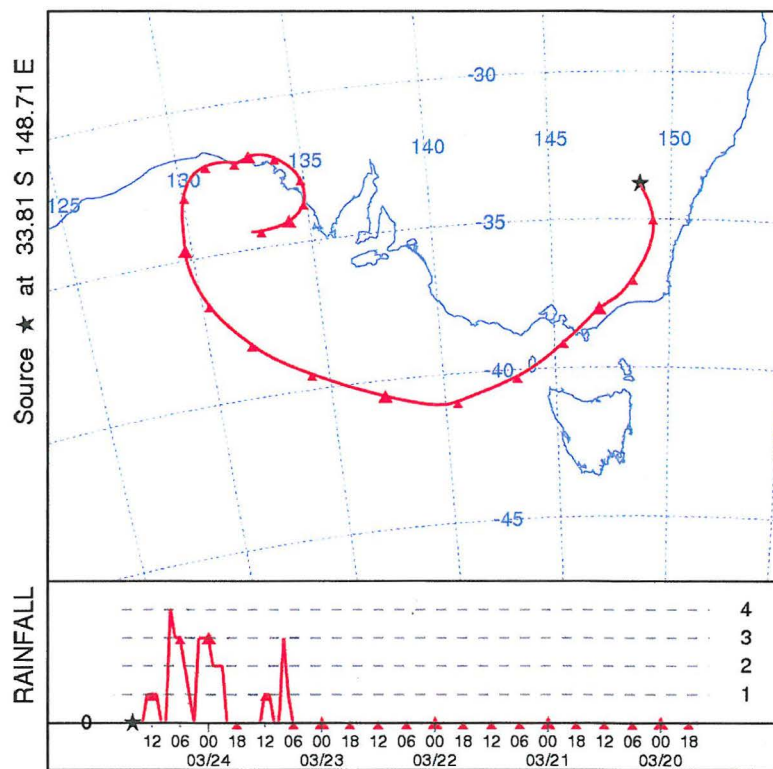
12 trajectories for Adelaide February 20th



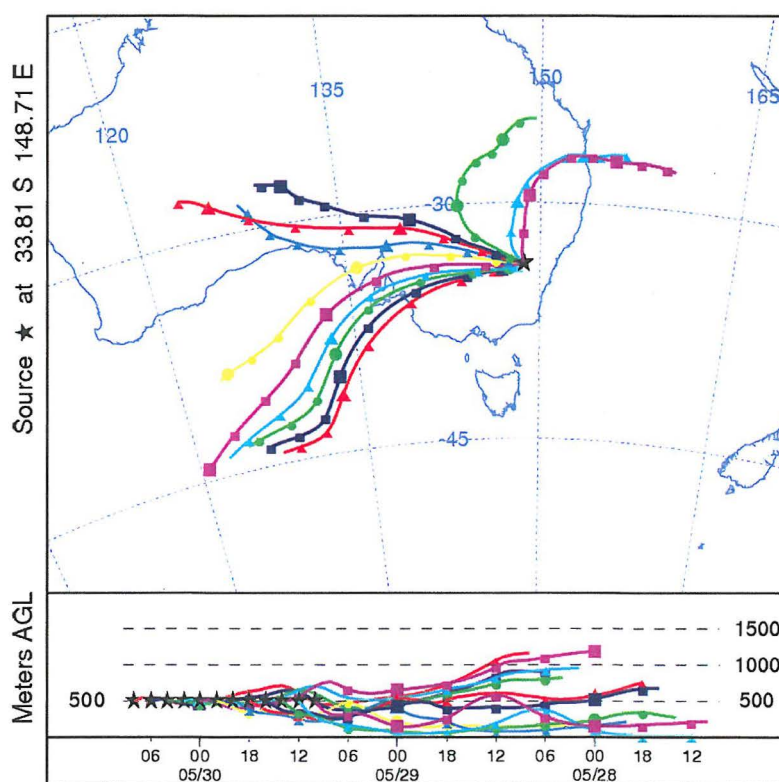
12 trajectories for Adelaide February 23rd



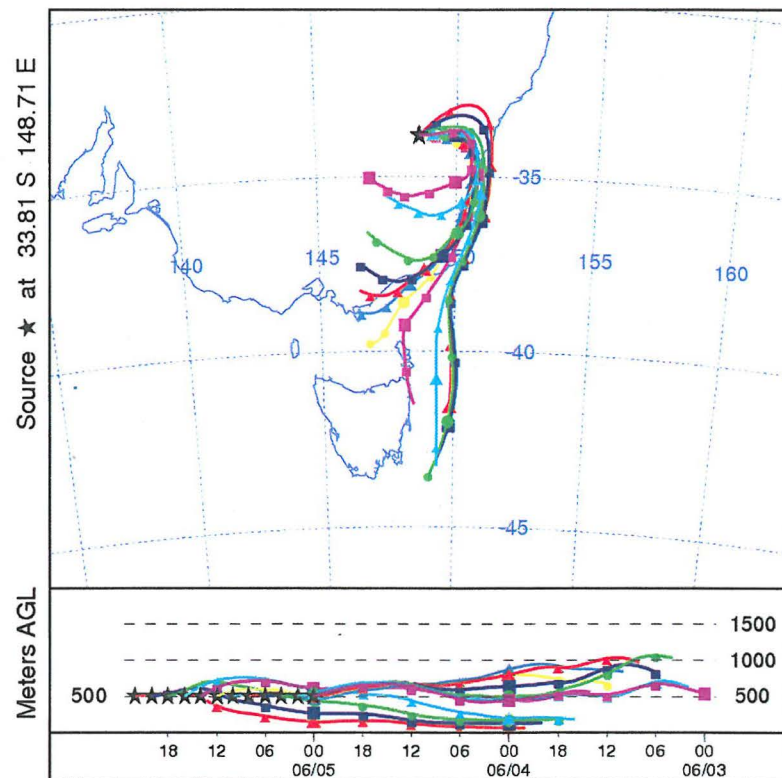
12 trajectories for CRS 2007 March 25th



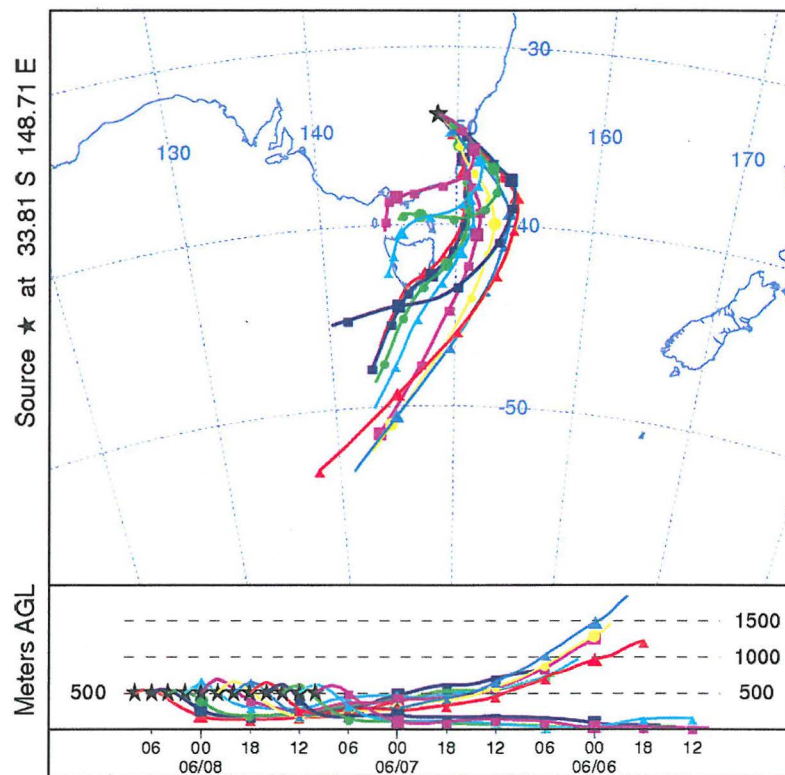
A 120 hours trajectory of CRS 2007 March 24th at 16hrs



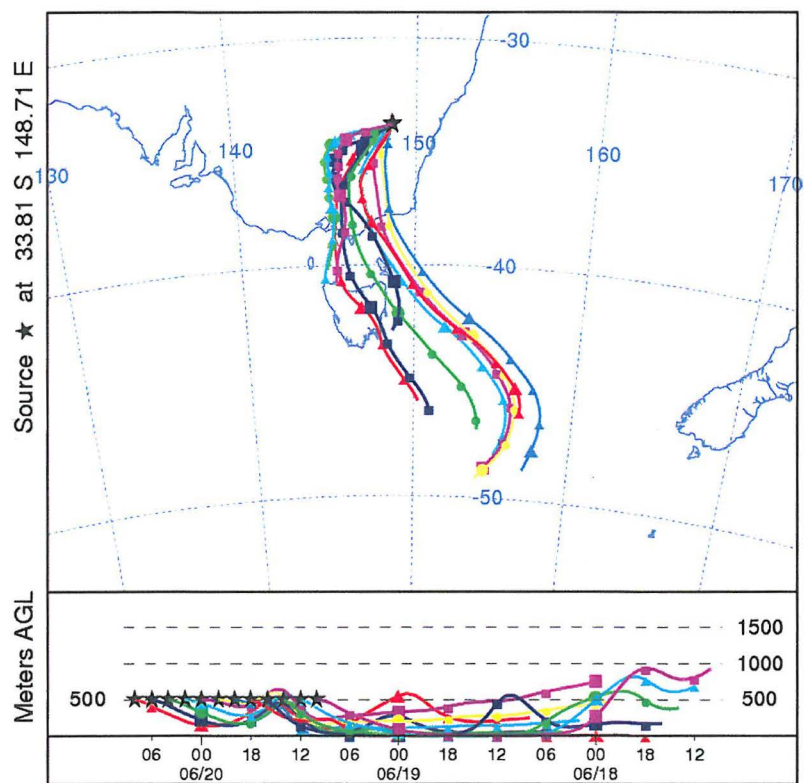
12 trajectories for CRS 2007 May 30th



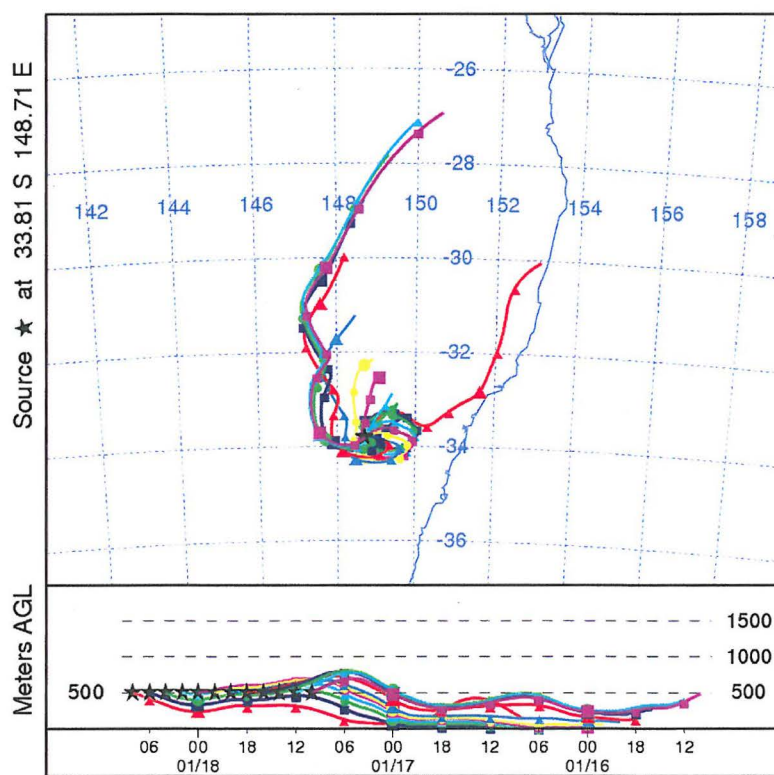
12 trajectories for CRS 2007 June 5th



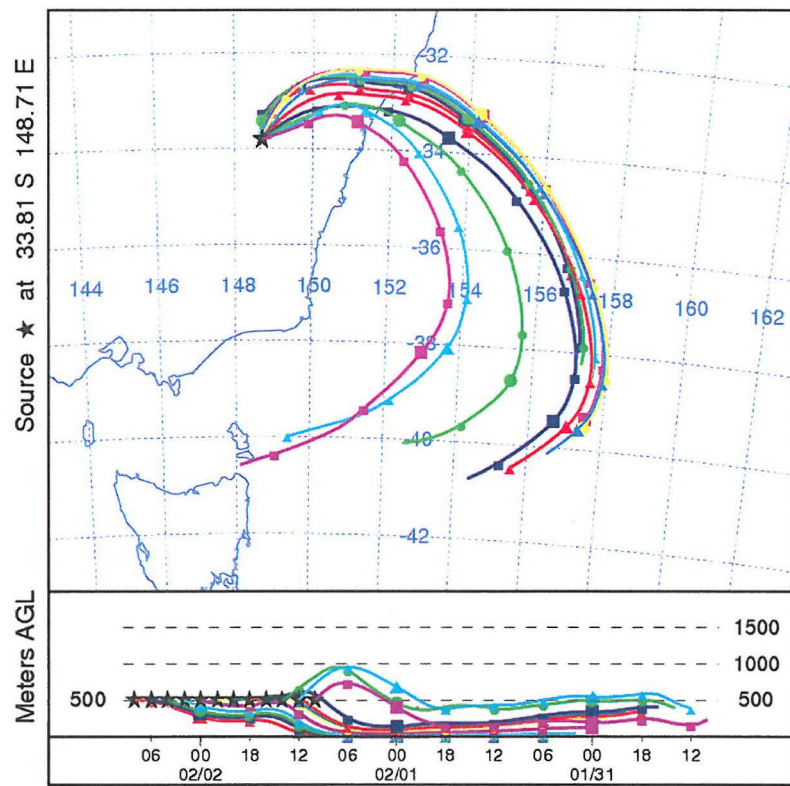
12 trajectories for CRS 2007 June 8th



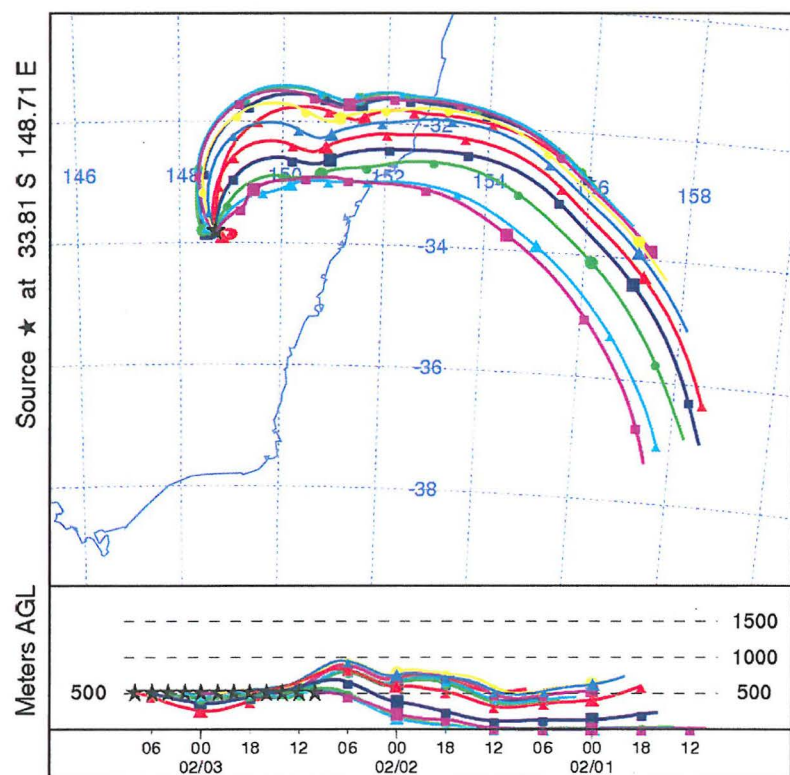
12 trajectories for CRS 2007 June 20th



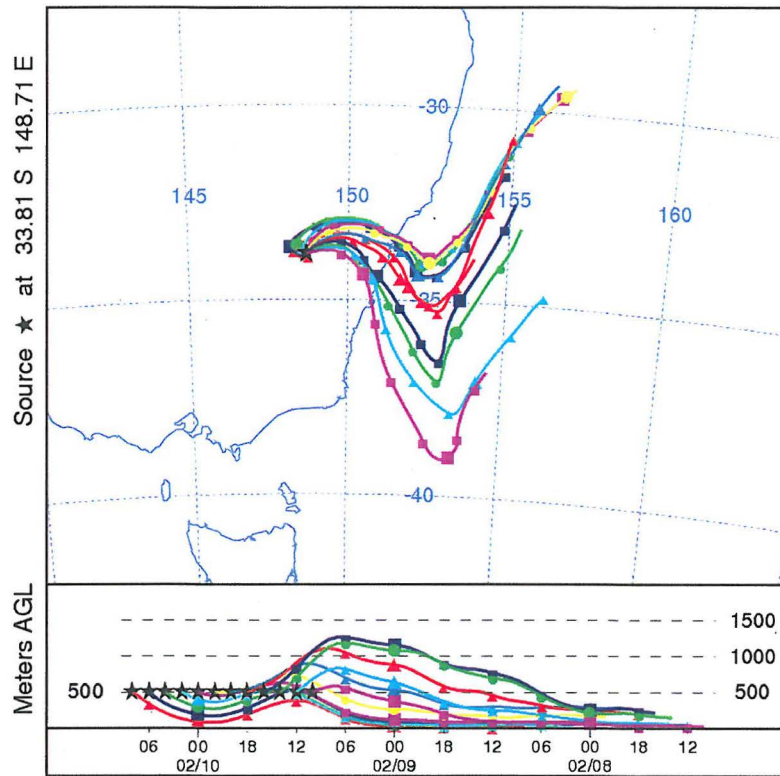
12 trajectories for CRS 2007 January 18th



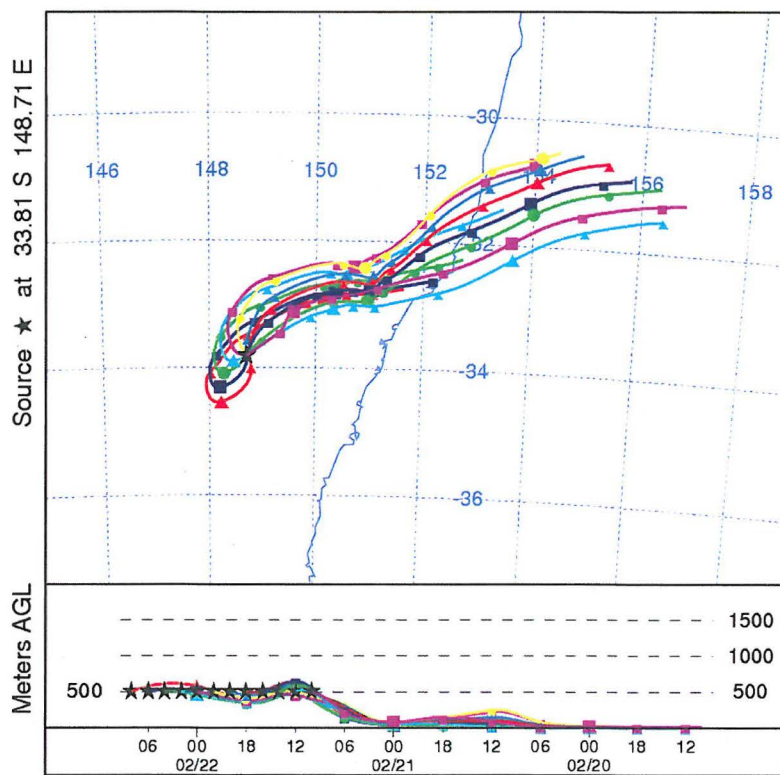
12 trajectories for CRS 2007 February 2nd



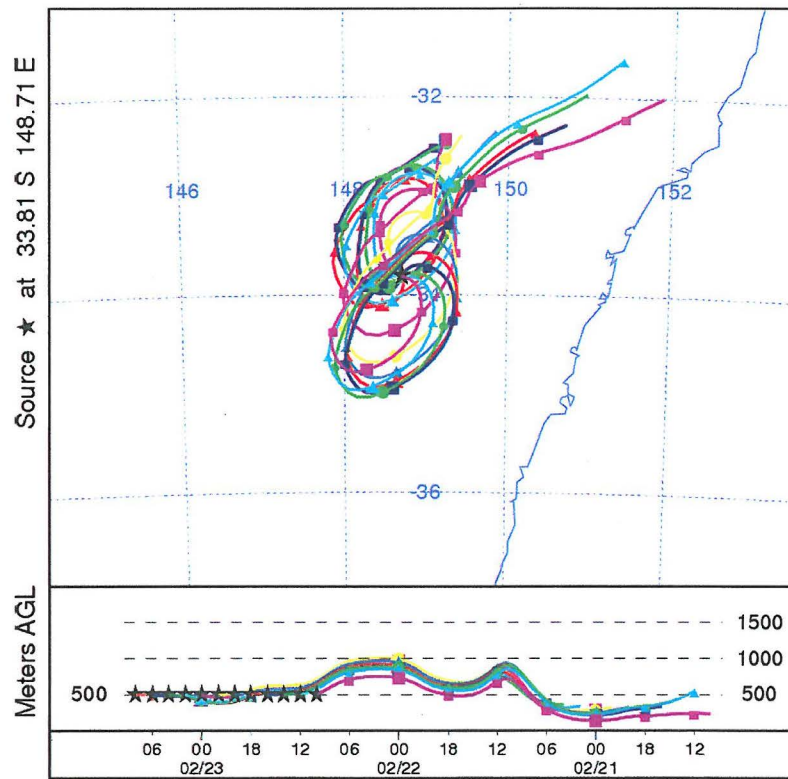
12 trajectories for CRS 2007 February 3rd



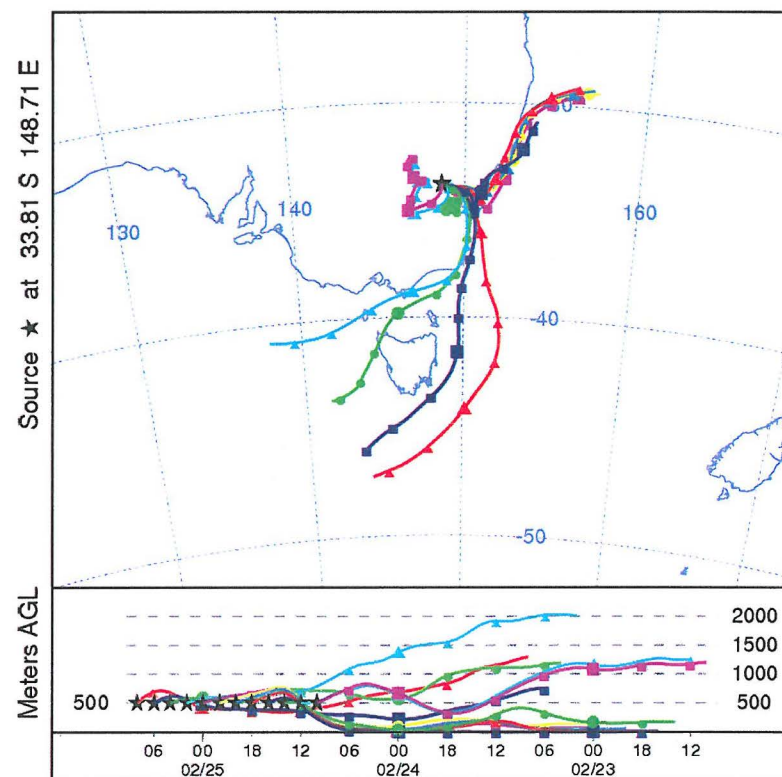
12 trajectories for CRS 2007 February 10th



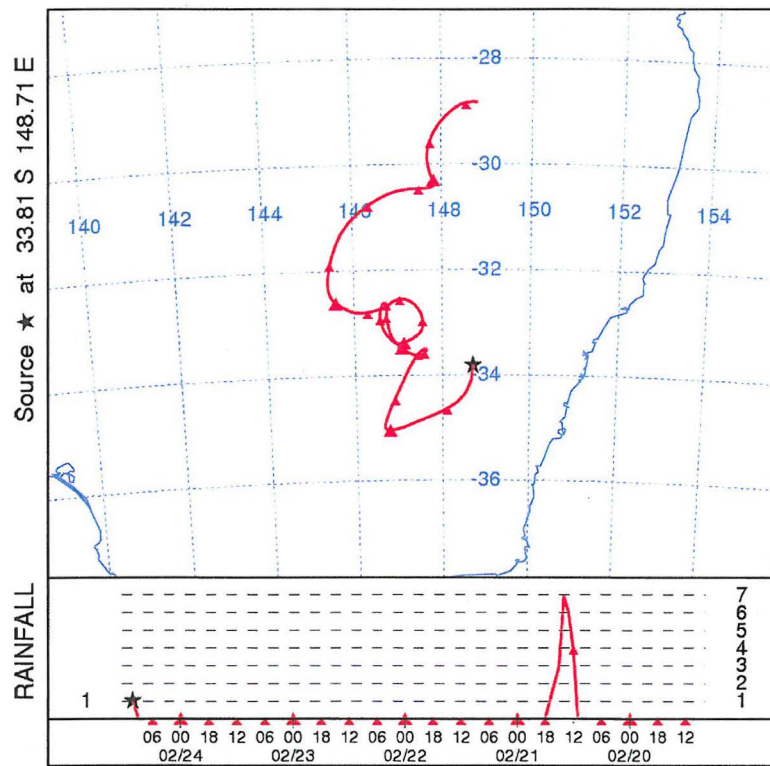
12 trajectories for CRS 2007 February 22nd



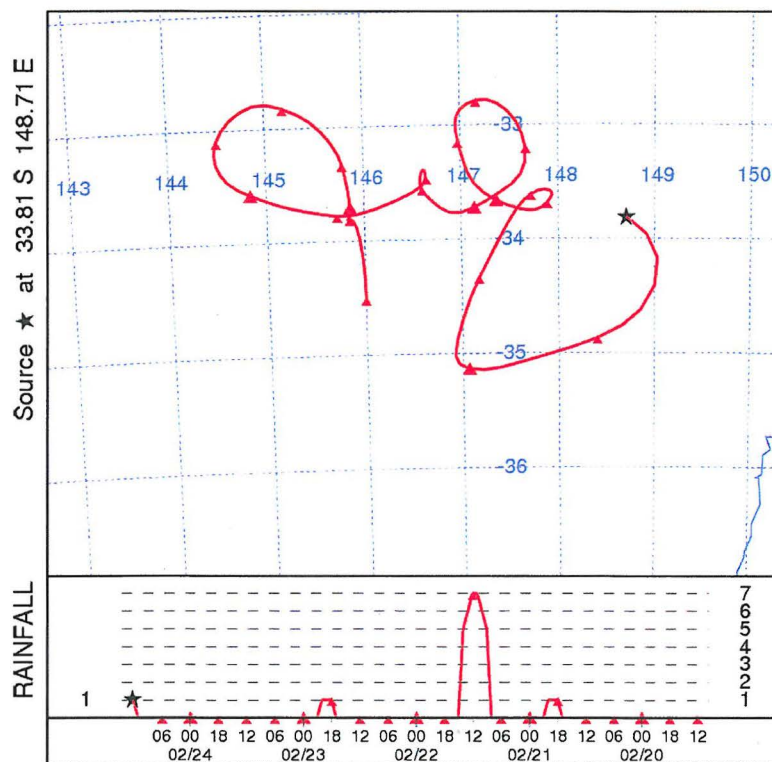
12 trajectories for CRS 2007 February 23rd



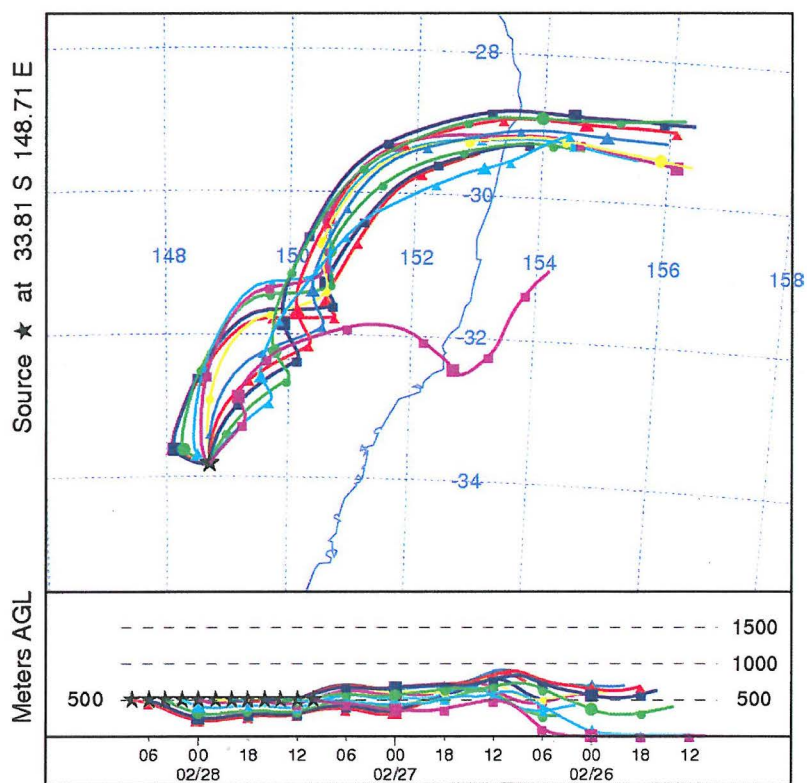
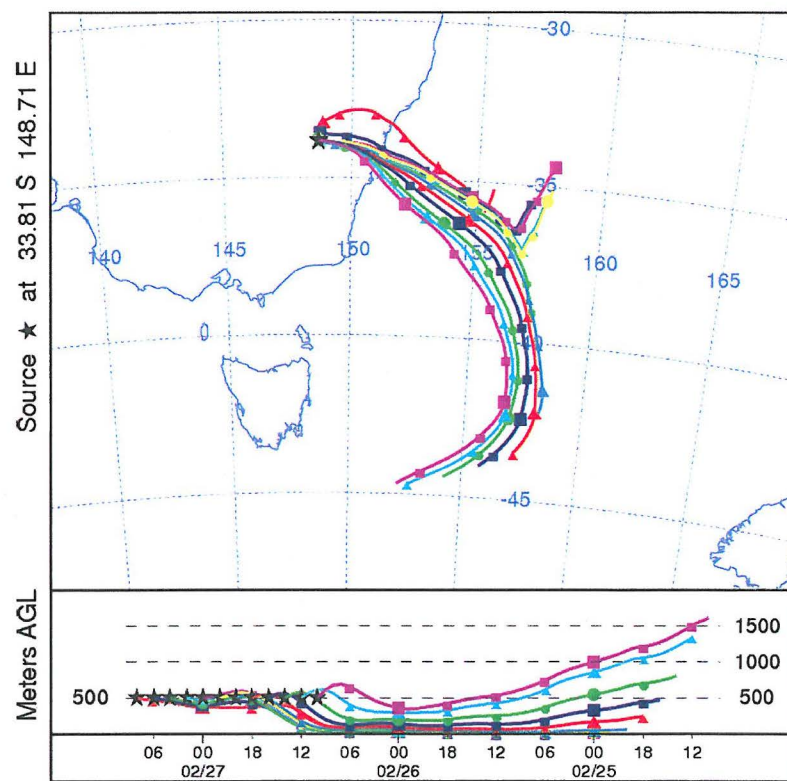
12 trajectories for CRS 2007 February 25th

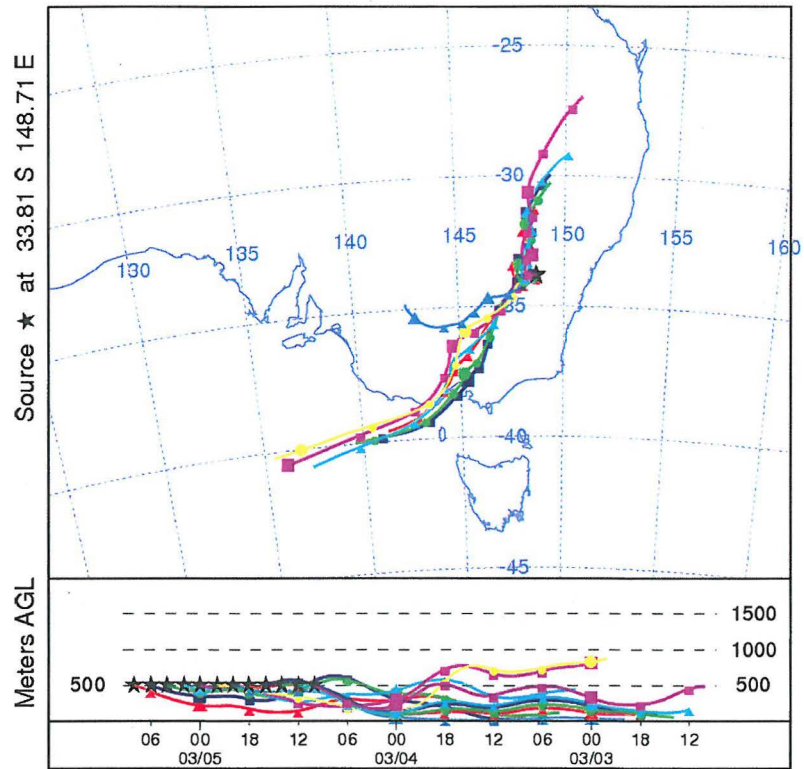


A 120 hours trajectory of CRS 2007 February 24th at 10hrs

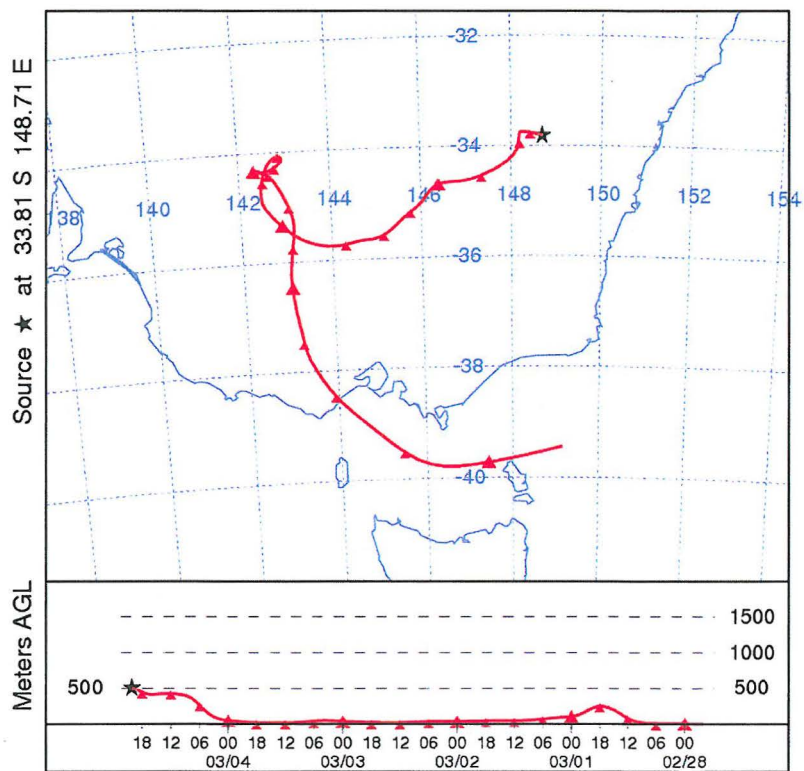


A 120 hours trajectory of CRS 2007 February 24th at 12hrs

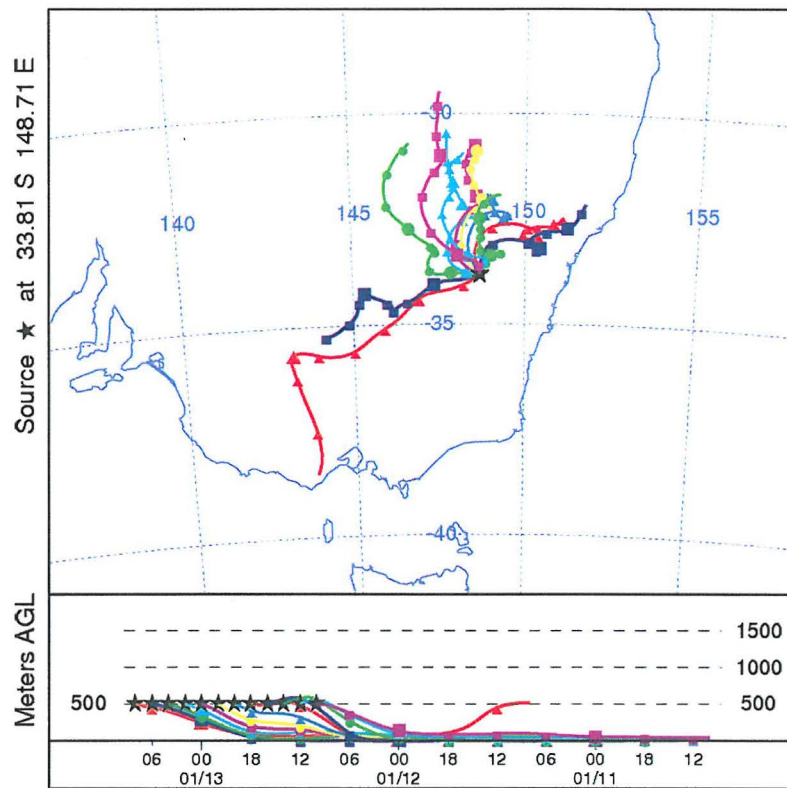




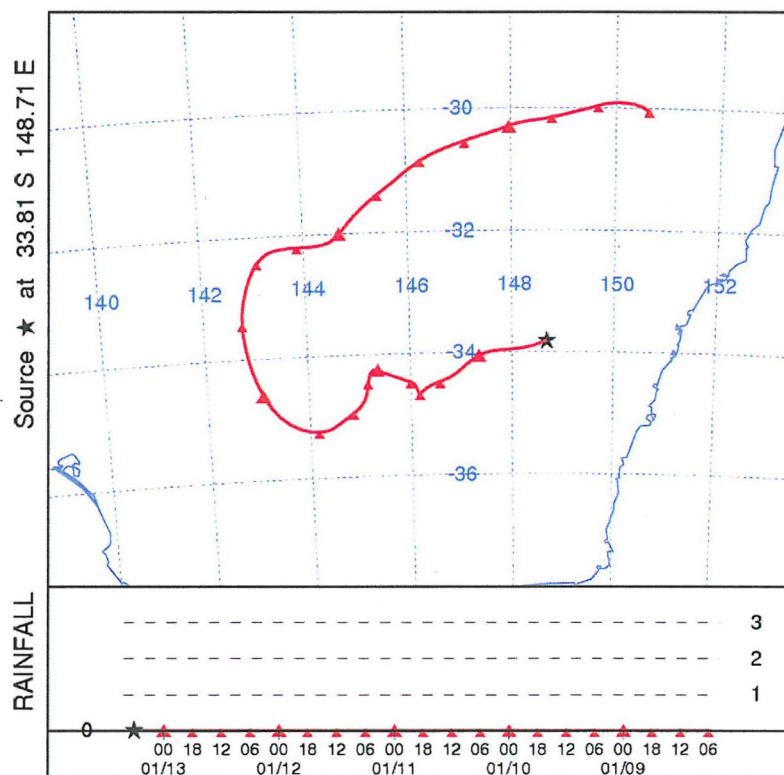
12 trajectories for CRS 2007 March 5th



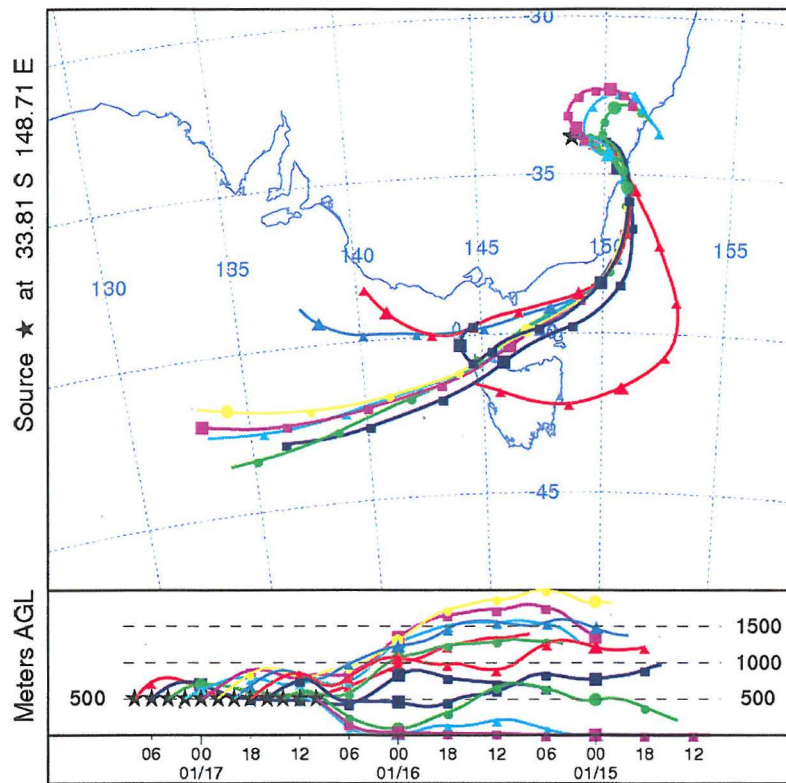
A 120 hours trajectory of CRS 2007 March 4th at 20hrs



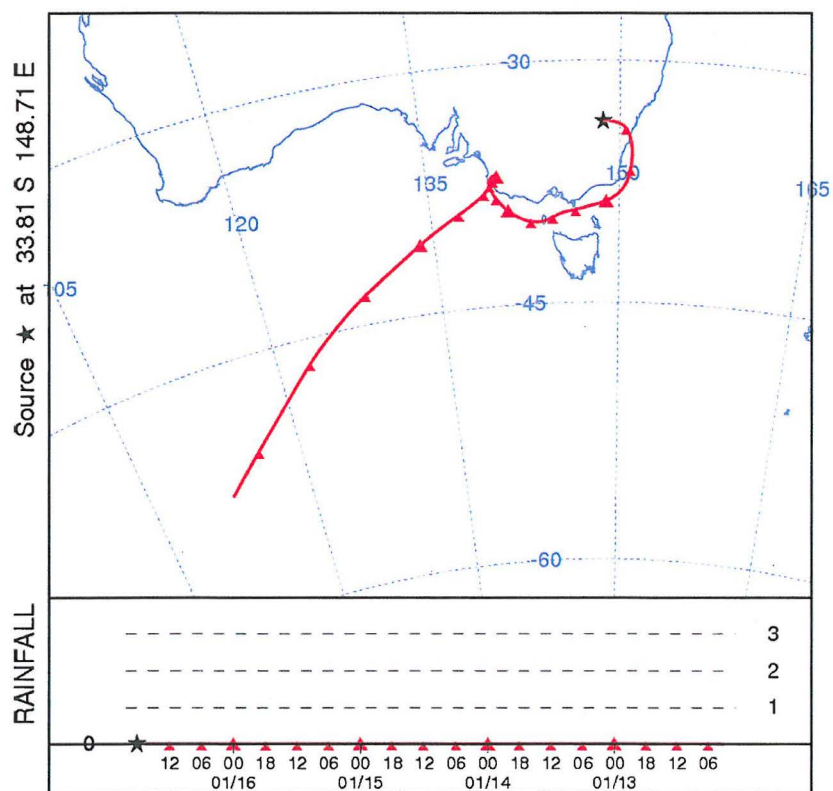
12 trajectories for CRS 2008 January 13th



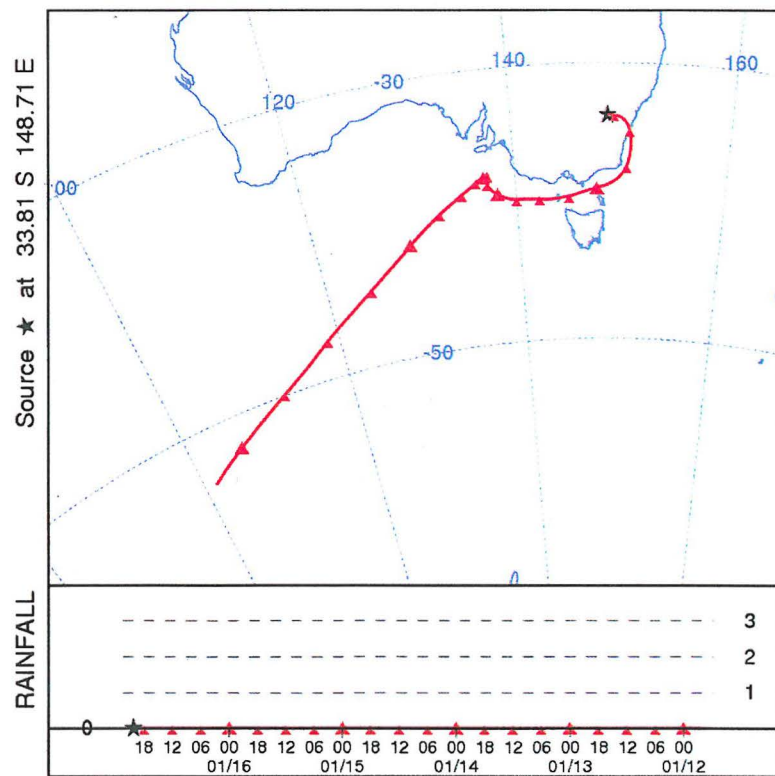
A 120 hours trajectory of CRS 2008 January 13th at 06hrs



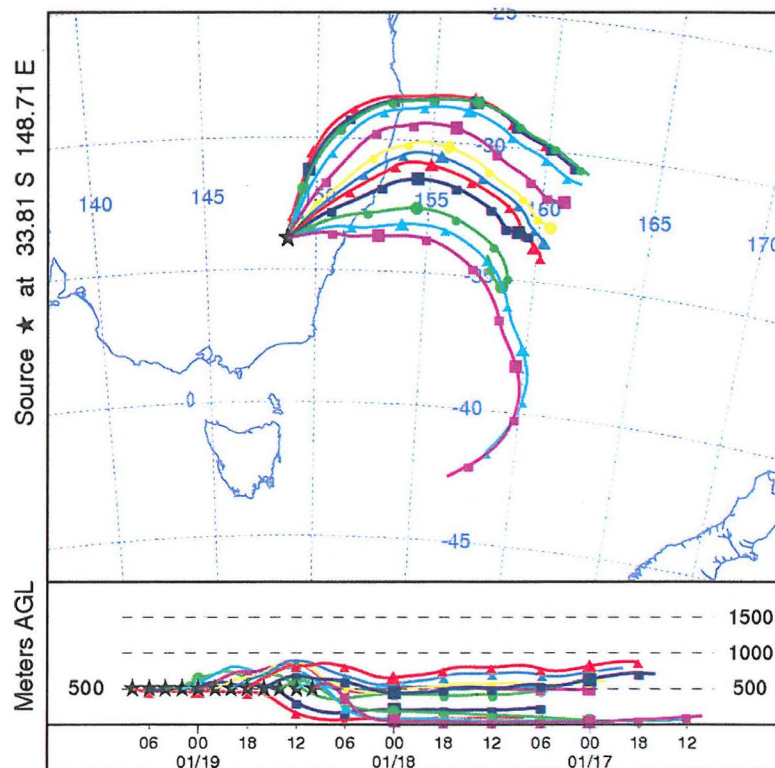
12 trajectories for CRS 2008 January 17th



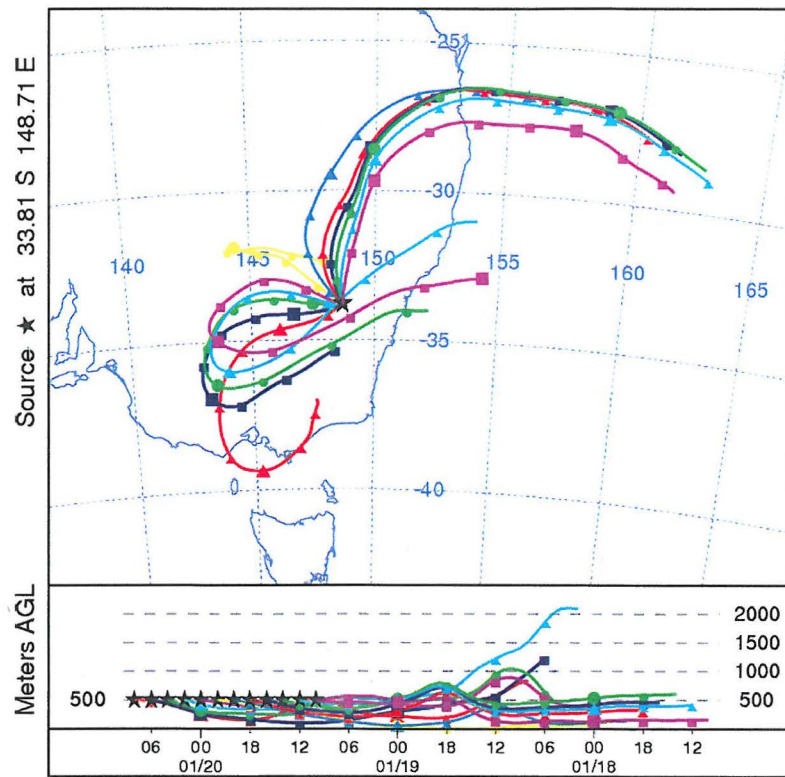
A 120 hours trajectory of CRS 2008 January 16th at 18hrs



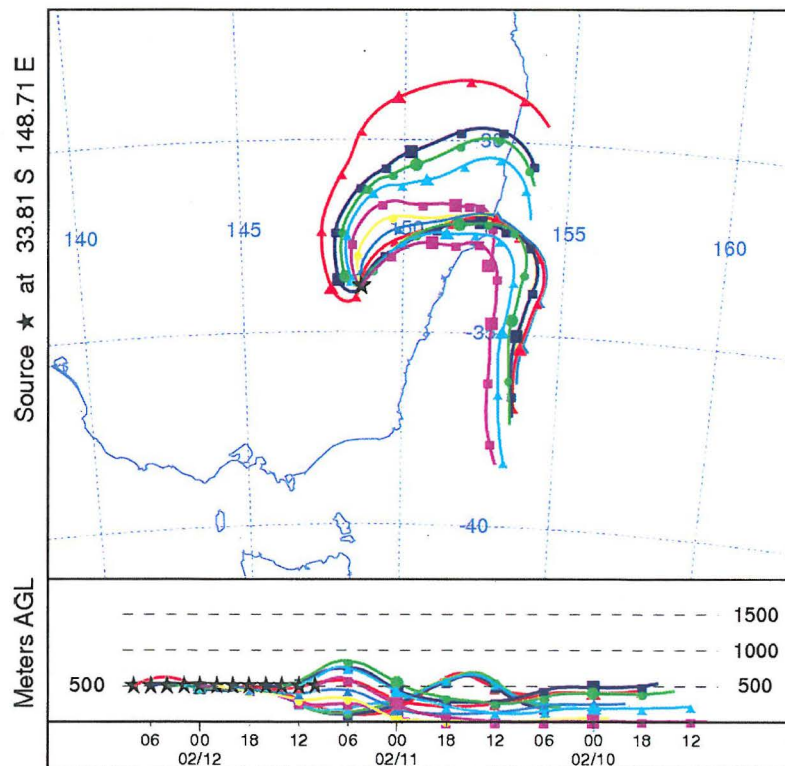
A 120 hours trajectory of CRS 2008 January 16th at 20hrs



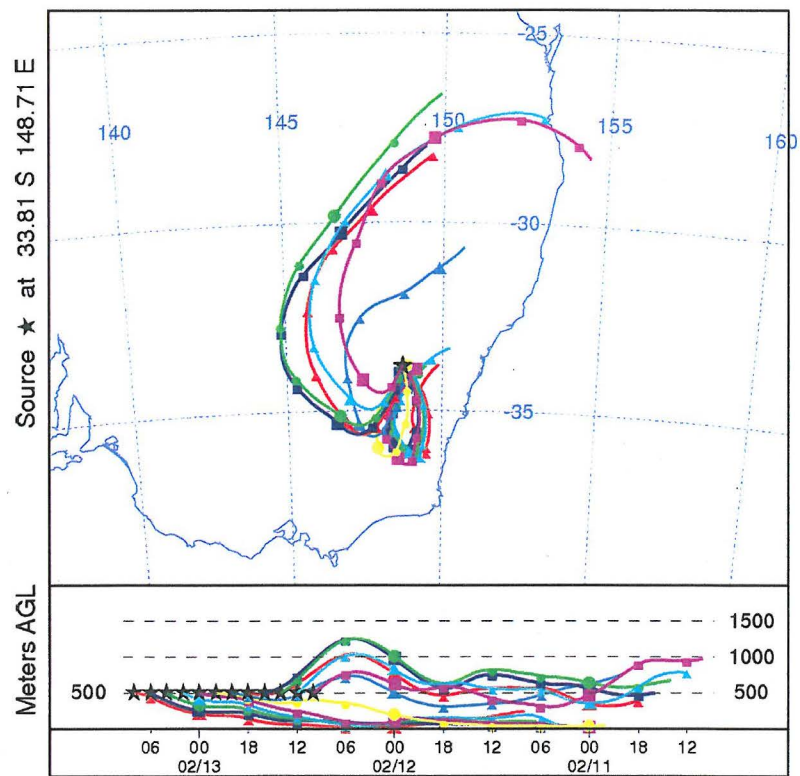
12 trajectories for CRS 2008 January 19th



12 trajectories for CRS 2008 January 20th

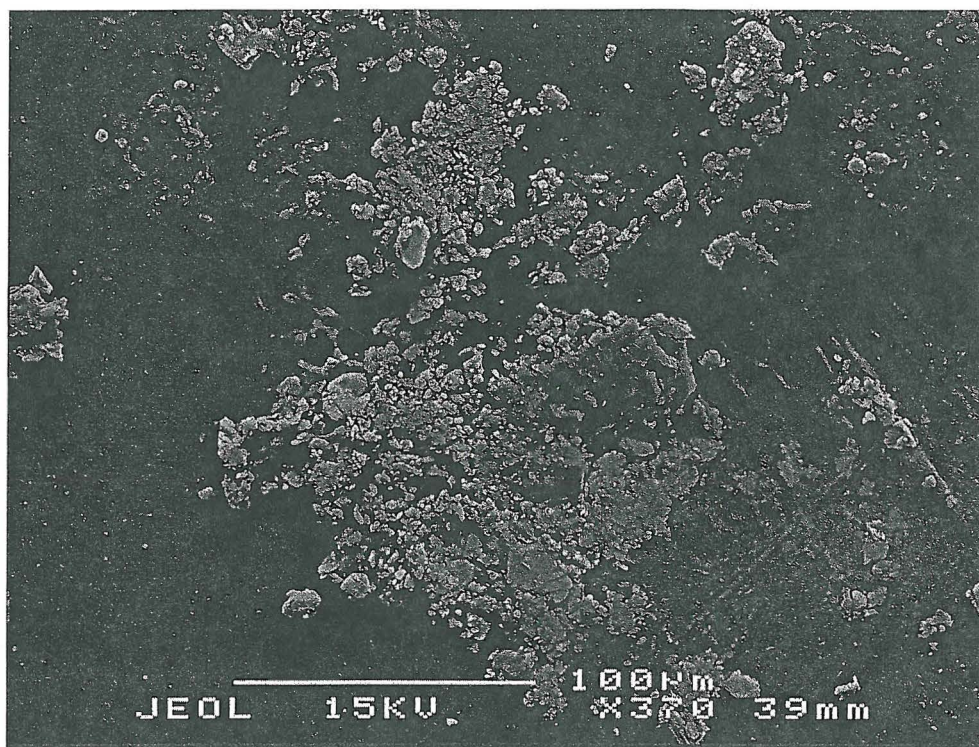


12 trajectories for CRS 2008 February 12th

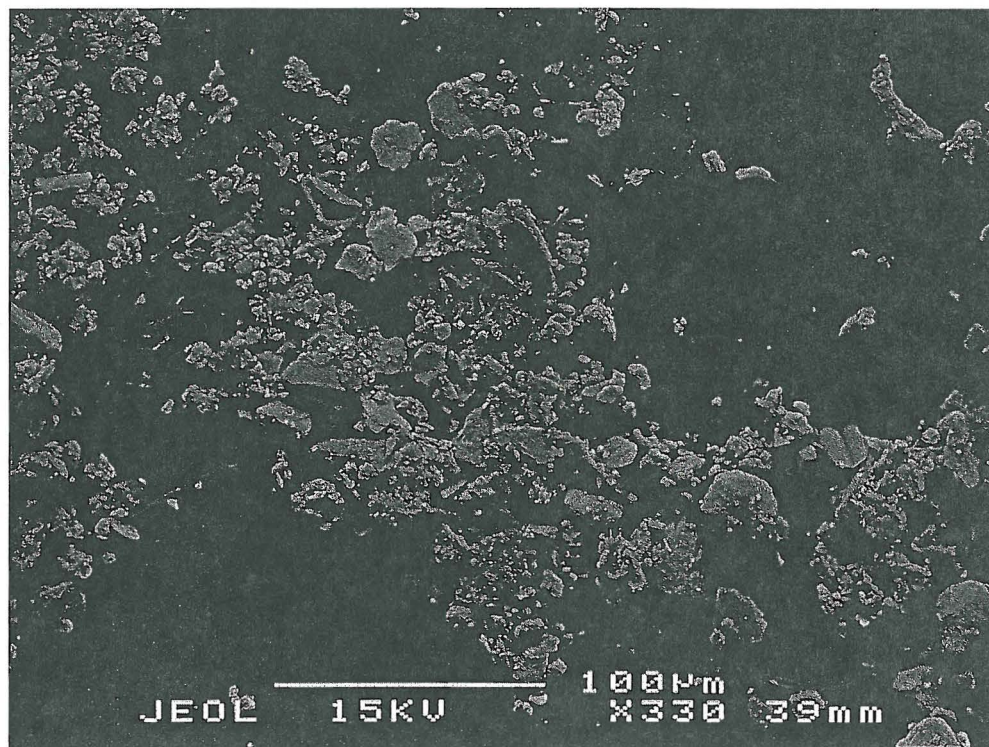


12 trajectories for CRS 2008 February 13th

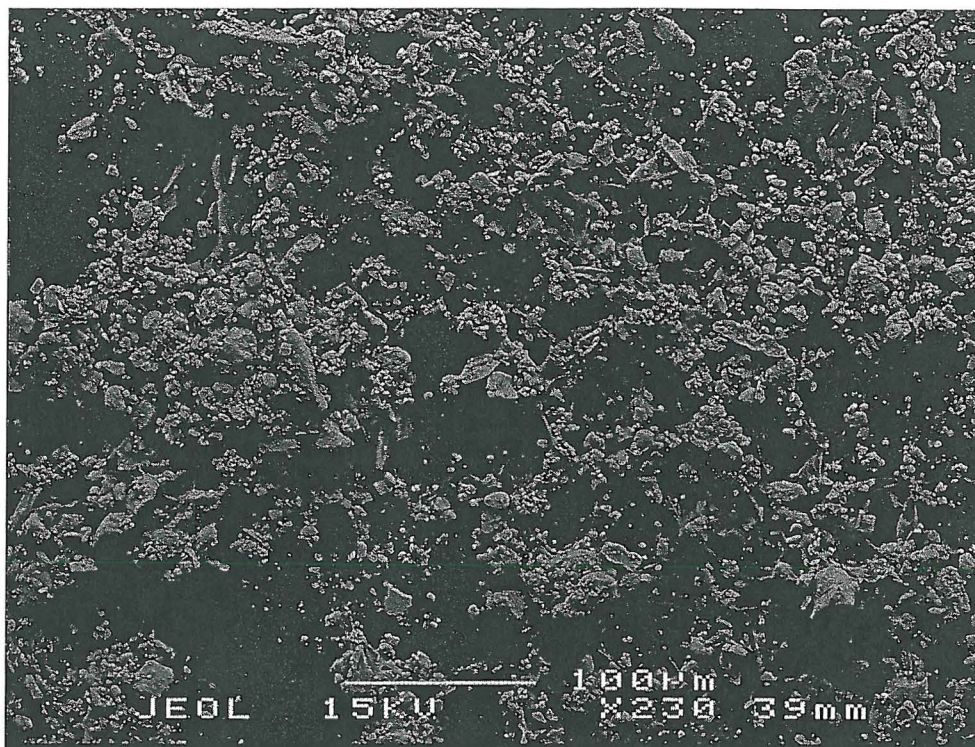
Appendix C: SEM Images



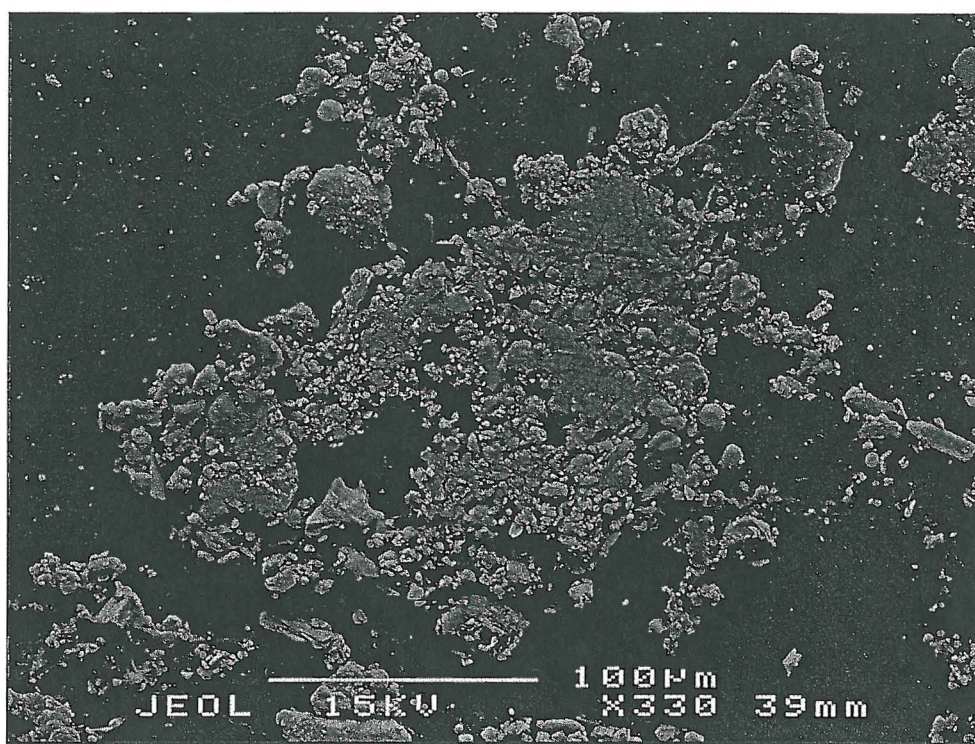
SEM image of Wagga Wagga January 2008 sample



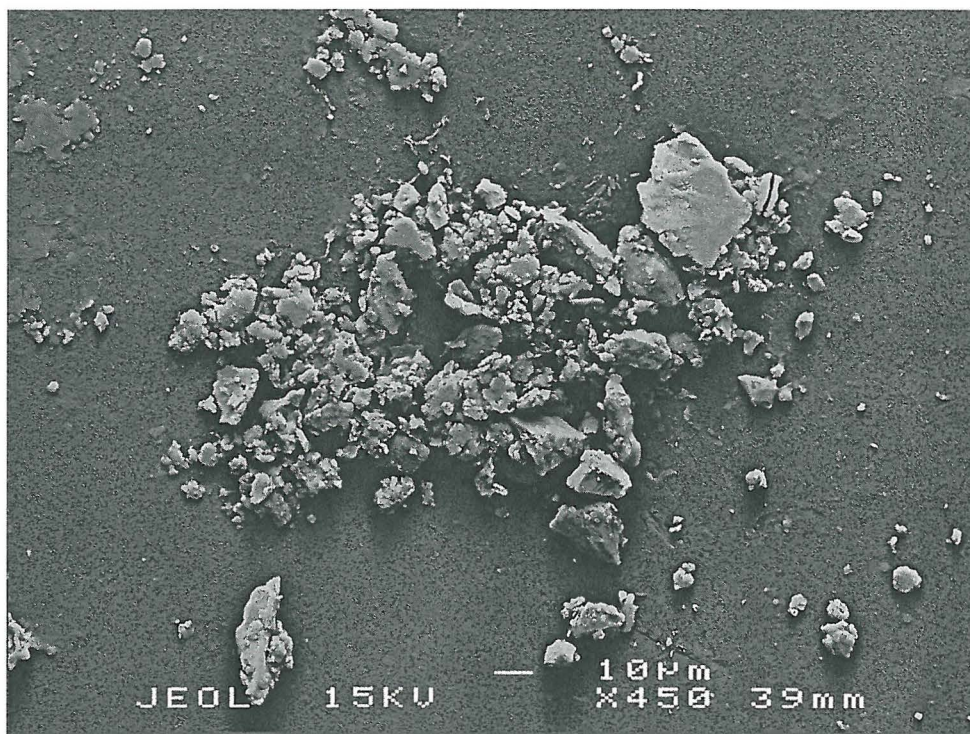
SEM image of Wagga Wagga February 2008 sample



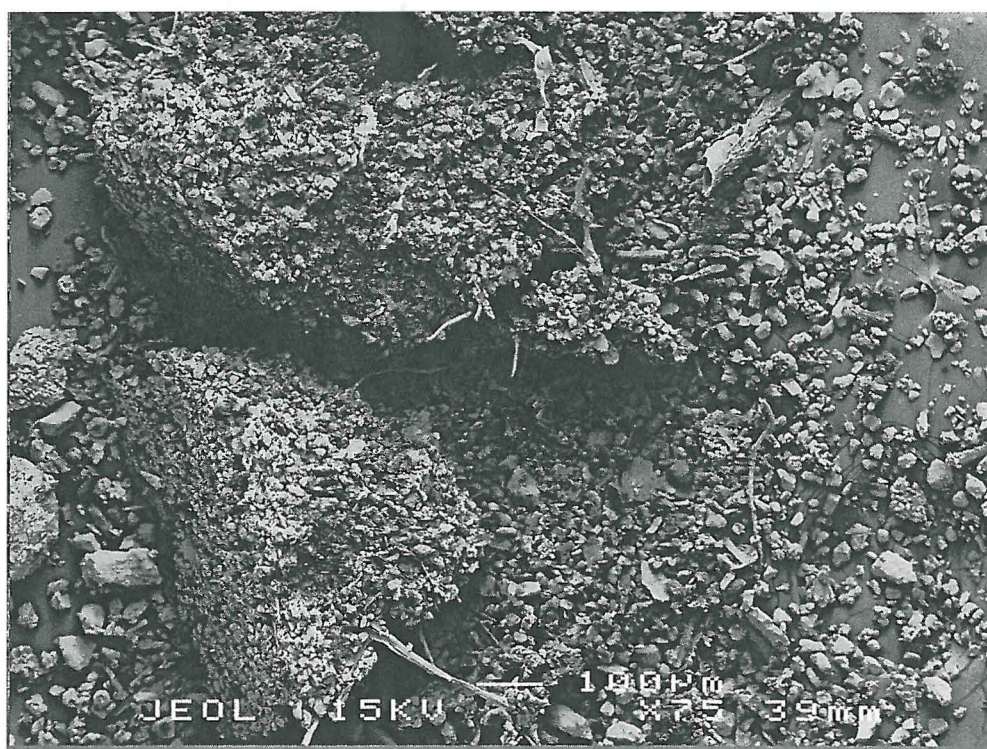
SEM image of Wagga Wagga March 2008 sample



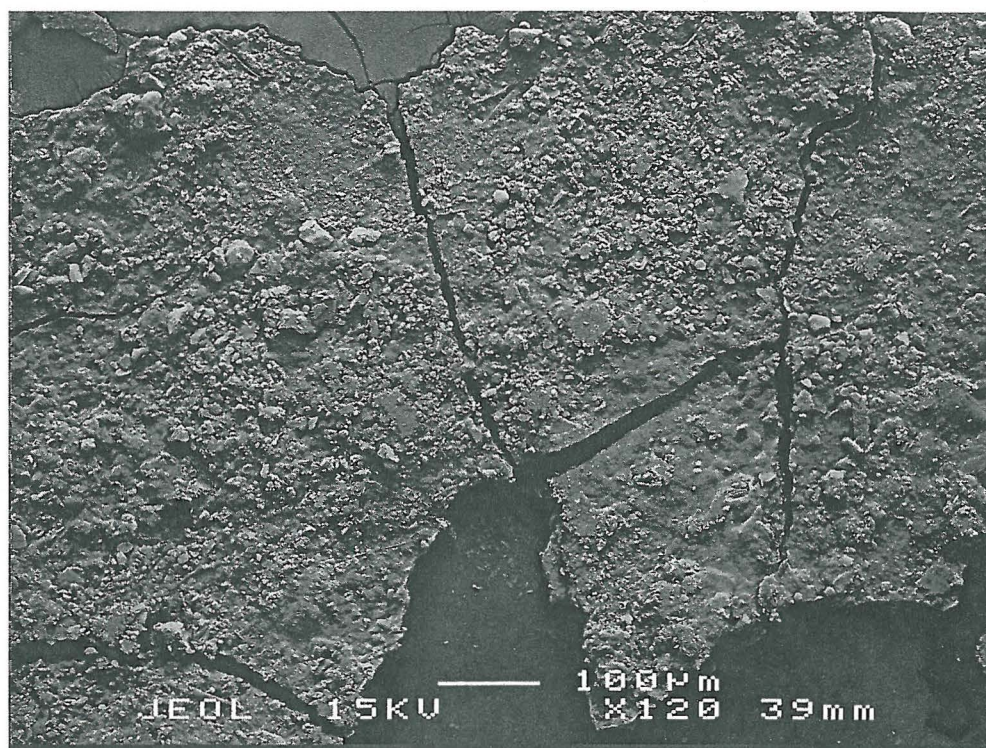
SEM image of Wagga Wagga April 2008 sample



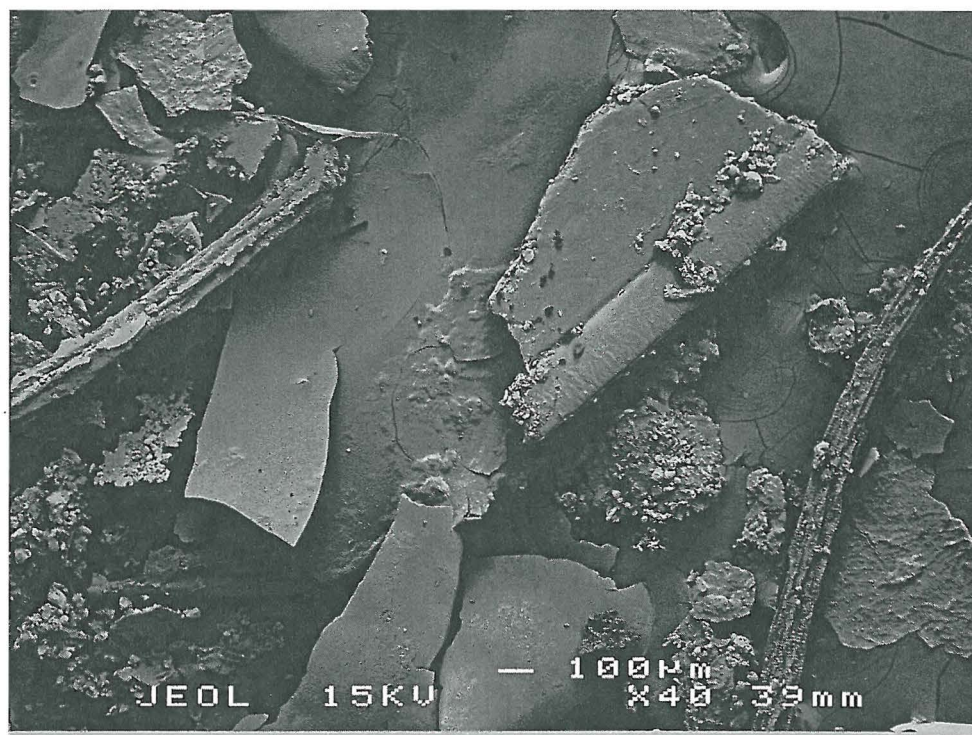
SEM image of Melbourne March 2008 sample



SEM image of CRS January 2007 sample



SEM image of CRS February 2007 sample



SEM image of CRS Januray – February 2008 sample